The role of cytochrome P450 1B1 and its associated metabolites in the pathogenesis of cardiac hypertrophy and drug-induced heart failure

by

Zaid Hussein Alma'ayah

A thesis submitted in partial fulfillment of the requirements for the degree of

Doctor of Philosophy

In
Pharmaceutical Sciences

Faculty of Pharmacy and Pharmaceutical Sciences
University of Alberta

Abstract

Heart failure (HF) is one of the most widespread and lethal forms of heart disease worldwide. Most HF patients have a history of hypertension and left ventricular hypertrophy in addition to drug-induced cardiotoxicity. Mechanisms regulating cardiac hypertrophy and drug-induced HF have been the focus of intense investigation in recent years. Among these mechanisms, cytochrome P450 (CYP) enzymes have been shown to play an important role in the regression or the progression of cardiac hypertrophy through the oxidation of arachidonic acid (AA) into cardioprotective epoxyeicosatrienoic acid (EETs) and cardiotoxic hydroxyeicosatetraenoic acids (HETEs). Of particular interest, numerous experimental studies have demonstrated a role for CYP1B1 and its associated mid-chain hydroxyeicosatetraenoic acids (mid-chain HETEs) metabolite in the development of cardiovascular diseases. Therefore, the objective of the present work was to investigate the role of CYP1B1 and its associated metabolites in the pathogenesis of cardiac hypertrophy and doxorubicin (DOX)-induced cardiotoxicity. Our results demonstrated that CYP1B1 AA metabolites, mid-chain HETEs, induced cellular hypertrophy in the human cardiomyocytes RL-14 cell line as evidenced by the induction of cardiac hypertrophic markers in addition to the increase in cell surface area. Moreover, mid-chain HETEs were able to induce cellular hypertrophy through MAPK- and NF-κB-dependent mechanisms. Interestingly, inhibition of CYP1B1 and its associated mid-chain HETE metabolites using 2,3',4,5'-tetramethoxystilbene (TMS), a selective CYP1B1 inhibitor, protected against DOX-induced cardiotoxicity and isoproterenol (ISO)-induced cardiac hypertrophy. Mechanistically, the protective effect of TMS was mediated through

the inhibition of MAPK and NF-κB signaling pathways. Of interest, overexpression of CYP1B1 significantly induced cellular hypertrophy and mid-chain HETE metabolites. In contrast to the negative effects of the cardiotoxic metabolites generated by CYP1B1, CYP1B1 also has an important role in the formation of a cardioprotective metabolite, 2-methoxyestradiol, 2ME. Therefore, we have investigated whether 2ME would prevent cardiac hypertrophy induced by abdominal aortic constriction (AAC). Our results showed that 2ME significantly inhibited AAC-induced left ventricular hypertrophy. The antihypertrophic effect of 2ME was associated with a significant inhibition of CYP1B1 and its associated mid-chain HETE metabolites. Based on proteomics data, the protective effect of 2ME is linked to the induction of antioxidant and anti-inflammatory proteins in addition to the modulation of proteins involved in myocardial energy metabolism. In vitro, 2ME has shown a direct antihypertrophic effect through the modulation of MAPK and NF-κB signaling pathways. In conclusion, our findings may shed light on the role of CYP1B1 in the development of cardiac hypertrophy and indicate that CYP1B1 can serve as a novel target for the treatment of heart diseases. Such observations will raise the potential of having selective inhibitors of this enzyme, such as 2ME and TMS, to be used clinically in the treatment of cardiovascular diseases.

Preface

This thesis is an original work done by Mr. Zaid Almaayah. All experimental animal procedures were approved by the University of Alberta Health Sciences Animal Policy and Welfare Committee. Section 1.5 of this thesis has been published as a review article: Maayah ZH, El-Kadi AO. The role of mid-chain hydroxyeicosatetraenoic acids in the pathogenesis of hypertension and cardiac hypertrophy. Arch Toxicol. 2016 Jan;90(1):119-36. doi: 10.1007/s00204-015-1620-8. I was responsible for collecting and summarizing data from the literature and writing the manuscript. A. O. El-Kadi was the supervisory author and was involved with concept formation and manuscript composition. Sections 3.1 and 4.1 of this thesis have been published as Maayah ZH, Elshenawy OH, Althurwi HN, Abdelhamid G, El-Kadi AO. Human fetal ventricular cardiomyocyte, RL-14 cell line, is a promising model to study drug metabolizing enzymes and their associated arachidonic acid metabolites. J Pharmacol Toxicol Methods. 71:33-41. doi: 10.1016/j.vascn.2014.11.005. I was responsible for designing the research, conducting experiments and data analysis as well as the manuscript composition. Elshenawy OH, Althurwi HN and Abdelhamid G assisted with the analysis and contributed to manuscript edits. El-Kadi AO was the supervisory author and was involved with concept formation and manuscript composition. Sections 3.2 and 4.2 of this thesis have been published as two articles: Maayah ZH, El-Kadi AO. 5-, 12- and 15-Hydroxyeicosatetraenoic acids induce cellular hypertrophy in the human ventricular cardiomyocyte, RL-14 cell line, through MAPK- and NF-κB-dependent mechanism. Arch Toxicol. 90(2):359-73. doi: 10.1007/s00204-014-1419-z and Maayah ZH, Abdelhamid G, El-Kadi AO. Development of cellular hypertrophy by 8-hydroxyeicosatetraenoic acid in the human ventricular cardiomyocyte, RL-14 cell line, is implicated by MAPK and NF-κB. Cell Biol Toxicol. 2015 Oct;31(4-5):241-59. I was responsible for designing the research, conducting experiments, and analysis as well as the manuscript composition. Abdelhamid G assisted with the analysis and contributed to manuscript edits. El-Kadi AO was the supervisory author and was involved with concept formation and manuscript composition. Section 3.3 and 4.3 has been published Maayah ZH, Althurwi HN, Abdelhamid G, Lesyk G, Jurasz P, El-Kadi AO. CYP1B1 inhibition

iv

attenuates doxorubicin-induced cardiotoxicity through a mid-chain HETEs-dependent mechanism. Pharmacol Res. 2016 Mar;105:28-43. doi: 10.1016/j.phrs.2015.12.016. I was responsible for designing the research, conducting experiments and data analysis as well as the manuscript composition. Althurwi HN, Abdelhamid G and Lesyk G assisted with conducting experiments. Jurasz P assisted with the analysis and contributed to manuscript edits. El-Kadi AO was the supervisory author and was involved with concept formation and manuscript composition. Sections 3.3 and 4.3 have been published as Maayah ZH, Althurwi HN, El-Sherbeni AA, Abdelhamid G, Siraki AG, El-Kadi AO. The role of cytochrome P450 1B1 and its associated mid-chain hydroxyeicosatetraenoic acid metabolites in the development of cardiac hypertrophy induced by ISO. Mol Cell Biochem. 2017 May;429(1-2):151-165. doi: 10.1007/s11010-017-2943-y. I was responsible for designing the research, conducting experiments and data analysis as well as the manuscript composition. Althurwi HN, El-Sherbeni AA and Abdelhamid G assisted with conducting experiments and contributed to manuscript edits. Siraki AG assisted with the analysis and contributed to manuscript edits. El-Kadi AO was the supervisory author and was involved with concept formation and manuscript composition. Section 3.4 and 4.4 of this thesis has been published as Maayah, Z.H., Levasseur J, Piragasam RS, Abdelhamid, G., Dyck JR , Fahlman RP, Siraki, A.G. and El-Kadi, A.O.(2017). 2-Methoxyestradiol protects against pressure overload-induced left ventricular hypertrophy. Scientific reports. 2018 Feb 9;8(1):2780. doi: 10.1038/s41598-018-20613-9. I was responsible for designing the research, conducting experiments and data analysis as well as the manuscript composition. Levasseur J, Piragasam RS and Abdelhamid, G assisted with conducting experiments. Dyck JR , Fahlman RP and Siraki, A.G. assisted with the analysis and contributed to manuscript edits. El-Kadi AO was the supervisory author and was involved with concept formation and manuscript composition.

This work is dedicated

to my parents, fiancée, sisters and brothers

Thank you

ACKNOWLEDGEMENTS

TABLE OF CONTENTS

LIST OF TABLES

LIST OF FIGURES

LIST OF ABBREVIATIONS

2ME	2-methoxyestradiol
3-MC	3-methylcholanthrene
AA	Arachidonic acid
AAC	Abdominal aortic constriction
AC	Adenylate cyclase
AhR	Aryl hydrocarbon receptor
ANOVA	Analysis of Variance
ANP	Atrial Natriuretic Peptide
Ang II	Angiotensin II
ATP	Adenosine-5'-triphosphate
ARNT	AhR nuclear translocator
BNP	B-type natriuretic peptide
BaP	Benzo(a)pyrene
CaMK	Ca2+/calmodulin-dependent kinase
c-AMP	Cyclic adenosine monophosphate
CAR	Androstane receptor
COX	Cyclooxygenase
CVD	Cardiovascular Disease
DAC	Descending aortic constriction
DEPC	Diethylpyrocarbonate
DHE	Dihydroethidium
DMSO	Dimethyl Sulfoxide
DMEM	Dulbecco's modified Eagle's medium
DHET	Dihydroxyeicosatrienoic acid
DOX	Doxorubicin
EDHF	Endothelium-derived Hyperpolarizing Factor
EET	Epoxyeicosatrienoic acid

ERK	Extracellular-signal regulated kinase
EROD	7-Ethoxyresorufin O-deethylation
Gapdh	Glyceraldehyde-3-phosphate dehydrogenase
GPCR	G protein-coupled receptor
GSK	Glycogen Synthase Kinase-3
HETE	Hydroxyeicosatetraenoic acid
HF	Heart Failure
h	Hours
HMCa	Adult human primary cardiomyocytes
HMC	Fetal human primary cardiomyocytes
HW/BW	Heart weight/body weight
HW/TL	Heart weight/tibia length
IL-6	Interleukin-6
i.p.	Intraperitoneal
JNK	c-Jun NH_2-terminal kinase
LC-ESI-MS	Liquid Chromatography-Electrospray Ionization-Mass Spectromerty
LOX	Lipoxygenase
LV	Left ventricular
LPS	Lipopolysaccharide
MAPK	Mitogen-activated protein kinases
MEF2	Myocyte Enhancer Factor-2
mTOR	Mammalian Target of Rapamycin
MTT	3-(4,5-Dimethylthiazol-2-yl)-2,5-diphenyltetrazolium bromide
MROD	Methoxyresorufin O-deethylase
NADPH	Nicotinamide adenine dinucleotide phosphate tetrasodium
NFAT	Nuclear factor of activated T cells

NF-κB	Nuclear factor-κB
PAGE	Polyacrylamide gel electrophoresis
PAHs	Polycyclic aromatic hydrocarbons
PCR	Polymerase Chain Reaction
PG	Prostaglandin
PI3K	Phosphoinositide 3-kinase
PKA	Protein kinase A
PKC	Protein kinase C
PPARα	Peroxisome proliferator-activated receptor α
PXR	Pregnane X receptor
ROS	Reactive oxygen species
SD	Sprague Dawley
SDS	Sodium dodecyl sulfate
sEH	Soluble epoxide hydrolase
SHR	Spontaneously hypertensive rat
STAT	Signal transducer and activator of transcription
tAUCB	Trans-4-[4-(3-adamantan-1-yl-ureido)-cyclohexyloxyl]-benzoic acid
TCDD	2,3,7,8-Tetrachlorodibenzo-p-dioxin
TEMED	N,N,N',N'-Tetramethylethylenediamine
TNF-α	Tumor necrosis factor-α
TGF-1	Transforming growth factor-1
VSMC	Vascular Smooth Muscle Cell
α-MHC	α-Myosin heavy chain
β-MHC	β- Myosin heavy chain

CHAPTER-1. INTRODUCTION

Portions of this chapter has been published in:

1-Maayah ZH, Abdelhamid G, El-Kadi AO (2015a). Development of cellular hypertrophy by 8-hydroxyeicosatetraenoic acid in the human ventricular cardiomyocyte, RL-14 cell line, is implicated by MAPK and NF-kappaB. *Cell biology and toxicology* **31**(4-5)**:** 241-259.

2-Maayah ZH, Althurwi HN, Abdelhamid G, Lesyk G, Jurasz P, El-Kadi AO (2016a). CYP1B1 inhibition attenuates doxorubicin-induced cardiotoxicity through a mid-chain HETEs-dependent mechanism. *Pharmacolgical Research* **105:** 28-43.

3-Maayah ZH, Althurwi HN, El-Sherbeni AA, Abdelhamid G, Siraki AG, El-Kadi AO (2017). The role of cytochrome P450 1B1 and its associated mid-chain hydroxyeicosatetraenoic acid metabolites in the development of cardiac hypertrophy induced by isoproterenol. *Molecular and Cellular Biochemistry* **429**(1-2)**:** 151-165.

4-Maayah ZH, El-Kadi AO (2016b). 5-, 12- and 15-Hydroxyeicosatetraenoic acids induce cellular hypertrophy in the human ventricular cardiomyocyte, RL-14 cell line, through MAPK- and NF-kappaB-dependent mechanism. *Archives of Toxicology* **90**(2)**:** 359-373.

5-Maayah ZH, El-Kadi AO (2016c). The role of mid-chain hydroxyeicosatetraenoic acids in the pathogenesis of hypertension and cardiac hypertrophy. *Archives of Toxicology* **90**(1)**:** 119-136.

6-Maayah ZH, Elshenawy OH, Althurwi HN, Abdelhamid G, El-Kadi AO (2015b). Human fetal ventricular cardiomyocyte, RL-14 cell line, is a promising model to study drug metabolizing enzymes and their associated arachidonic acid metabolites. *Journal of Pharmacological and Toxicological Methods* **71:** 33-41.

7-Maayah ZH, Levasseur J, Siva Piragasam R, Abdelhamid G, Dyck JRB, Fahlman RP*, et al.* (2018). 2-Methoxyestradiol protects against pressure overload-induced left ventricular hypertrophy. *Scientific Reports* **8**(1)**:** 2780.

1.1. Heart failure (HF)

HF is a complex clinical syndrome where the ventricle is unable to effectively fill or eject sufficient blood to meet the body organs demand (Hunt *et al.*, 2005). HF is one of the most widespread and lethal forms of heart disease worldwide (Roger, 2013). In Canada, it is estimated that 600,000 Canadians are living with HF and 50,000 new cases are diagnosed every year (Tran *et al.*, 2016). Due to high hospital readmission rates, HF costs more than 500 million dollars annually for inpatient care alone (Tran *et al.*, 2016). Despite early diagnosis and aggressive medical management, HF patients still have a poor prognosis, with an average annual mortality rate of 33% (Roger, 2013).

1.2.1 Etiology of HF

The etiology of HF is complex, and traditionally, HF has been described as either ischemic or nonischemic idiopathic HF, with ischemic HF being predominant (>52% of cases) (Fox *et al.*, 2001). Ischemic HF occurs as a result of chronic coronary artery disease or after myocardial infarction (MI), whereas nonischemic idiopathic HF may be due to chronic hypertension, aortic or mitral stenosis, and several cardiomyopathies including familial cardiomyopathy and diabetic cardiomyopathy (Johnson, 2014). Another important nonischemic idiopathic HF causes are drug-induced cardiomyopathy. Cardiotoxic agents include several widely used anti-neoplastic agents such as doxorubicin (DOX), trastuzumab, arsenic trioxide and sunitinib, selective cyclooxygenase-2 (COX-2) inhibitor (Rofecoxib), antiviral compound azidothymidine (Zidovudine), several oral antidiabetics (e.g., rosiglitazone), methamphetamine, synthetic cannabinoids and cocaine (Varga *et al.*, 2015).

1.2.2. Pathophysiology of HF

HF pathophysiology includes: neurohormonal activation, an increased oxidative stress in several organs in addition to stimulation of the immune system and inflammatory responses (Anker *et al.*, 1997). Neurohormonal regulation is largely responsible for homeostatic regulation of cardiac function. The acute decrease in cardiac output stimulates baroreceptor-mediated adrenergic system activity which initially compensates for an

acutely reduced cardiac output by increasing inotropy (Dube *et al.*, 2011). However, high sympathetic activity is associated with cardiac β-receptor desensitization in addition to the release of renin from the juxtaglomerular apparatus in the renal system. The activation of the renin-angiotensin-aldosterone system (RAAS) is considered as an important mediator of the pathophysiology of HF. Angiotensin II (Ang II), a peptide hormone, is derived from the precursor molecule angiotensinogen and responsible for vasoconstriction as well as the adrenal and posterior pituitary gland secretion of aldosterone and vasopressin, respectively, (Anker *et al.*, 1997). These peptide hormones increase sodium and water retention, edema and preload on a heart susceptible to hemodynamic injury and eventually lead to maladaptive hypertrophic remodeling and potentially heart failure (Gradman *et al.*, 2006). Most HF patients have a history of hypertension and left ventricular (LV) hypertrophy (Gradman *et al.*, 2006).

1.2.2.1. Forms of HF
Heart failure with preserved ejection fraction (HFpEF) is congestive heart failure with normal ejection fraction. Historically, HFpEF was named diastolic heart failure; however, recent studies suggest more complex pathophysiology (Owan *et al.*, 2006). HFpEF is characterized by an enlargement of the wall thickness and cardiac mass with relatively small cavities, reduced diastolic function, decreased heart rate and increased cardiac output, termed concentric hypertrophy (Grossman *et al.*, 1975). Alternatively, heart failure with reduced ejection fraction (HFrEF) is accompanied by an increase in the cardiac mass with large dilated cavities and relatively thin walls, defects in systolic function, ventricular tachyarrhythmia's in addition to an increase in end-diastolic volume termed eccentric hypertrophy (Grossman *et al.*, 1975).

1.2. Cardiac hypertrophy
Cardiac hypertrophy is an adaptive response to enhanced biomechanical stress, which results from acute events, such as myocardial infarction, or accompanying chronic insults such as hypertension (Vakili *et al.*, 2001). In response to this, the heart wall thickens in an attempt to normalize the diastolic and systolic function (Vakili *et al.*, 2001). However, prolonged cardiac hypertrophy can become maladaptive and eventually lead to dilated

cardiomyopathy, HF, malignant arrhythmia and even sudden death (Berenji *et al.*, 2005). Understanding the molecular basis of cardiac hypertrophy is an often ignored but significant facet for identifying the best treatment of the HF. This is because cardiomyocyte hypertrophy and fibrosis are prerequisites for the development of HF and cardiomyopathy (Gradman *et al.*, 2006).

The heart consists of cardiac myocytes, non-myocytes such as vascular smooth muscle cells, fibroblasts, and surrounding extracellular matrix (Gregorio *et al.*, 2000). Cardiac myocytes are surrounded by collagen fiber to provide structural and biochemical support and composed of bundles of myofibrils. Each myofibrills has basic contractile units of the cardiac muscle known as sarcomeres (Gregorio *et al.*, 2000). Hypertrophy of the cardiac muscle cell is defined as a growth of existing cardiac myocytes in contrast to hyperplasia, which belongs to an increase in the number of myocardial cells by mitotic division (Frey *et al.*, 2004). An increase in cell volume, enhanced protein synthesis, and heightened organization of the sarcomere are the most charateritic features of cardiomyocyte hypertrophy (Frey *et al.*, 2004).

1.2.1. Classification of cardiac hypertrophy

Cardiac hypertrophy is classified into either physiological or pathological. Both kinds of cardiac hypertrophy occur in response to diverse stimuli are functionally distinct, and are accompanied by different structural and molecular phenotypes (Kaplan *et al.*, 1994; Iemitsu *et al.*, 2001). Physiological and pathological hypertrophy can be further sub-classified as concentric or eccentric based on changes in shape that are dependent on the initiating cause.

1.2.1.1. Physiological hypertrophy

Physiological hypertrophy occurs during postnatal growth, pregnancy, regular physical activity or chronic exercise training (Fagard, 1997). Physiological hypertrophy does not progress into dilated cardiomyopathy and is characterized by normal or improved cardiac function with no changes in the fetal gene expression pattern in addition to enhanced glucose and fatty acid oxidation (Pluim *et al.*, 2000; Dyck *et al.*, 2006). Strength training

such as weight lifting includes developing muscular tension against resistance with little movement. Pressure overload on the cardiac muscle results from reflex and mechanical changes. This causes physiological concentric hypertrophy (Pluim *et al.*, 2000). In contrast, endurance exercise, such as running, cycling and swimming, includes large muscle groups' activity. This produces vasodilatation of the vascular skeletal muscle, and thereby eccentric hypertrophy occurs as a result of the increasing venous return to the cardiac muscle and volume overload (Fagard, 1997).

1.2.1.2. Pathological hypertrophy

Pathological cardiac hypertrophy may develop in response to different disease settings, such as myocardial infarction, hypertension, and valvular heart disease (Levy *et al.*, 1988). Pressure overload, caused by hypertension or aortic stenosis, increases systolic left ventricular wall stress (Kannel, 1974) and thereby results in an enlargement of the wall thickness and cardiac mass with relatively small cavities. This is known as concentric hypertrophy (Grossman *et al.*, 1975). Alternatively, volume overload due to aortic regurgitation or arteriovenous fistulas increases diastolic left ventricular wall stress and results in eccentric hypertrophy. An increase in the cardiac mass with large dilated cavities and relatively thin walls are the most characteristic features of eccentric hypertrophy (Grossman *et al.*, 1975). Although the hypertrophy of cardiac myocytes and the formation of new sarcomeres in response to pathological insult fairly normalize cardiac function, prolonged cardiac hypertrophy may eventually decompensate, leading to dilated cardiomyopathy and heart failure (Berenji *et al.*, 2005). This is usually associated with disproportional accumulation of cardiac fibroblasts and collagen and eventually result in interstitial fibrosis (Shimizu *et al.*, 2016).

At the molecular level, pathological hypertrophy is often associated with the re-induction of the cardiac fetal gene expression including, atrial natriuretic peptide (ANP), B-type natriuretic peptide (BNP) and β-myosin heavy chain (β-MHC), and suppression of genes typically expressed at greater level in the adult than in the developing heart, such α-MHC (Barry *et al.*, 2008).

MHC isoform switching from α-MHC to β-MHC decreases the myosin ATPase enzyme velocity and depletes the intracellular energy level, thereby disrupting myocardial twitch kinetics. This detrimentally affects the systolic function and decreases contractile performances of the cardiomyocytes that significantly contributes to the progression of heart failure (Fatkin *et al.*, 2000; Kiriazis *et al.*, 2000; Locher *et al.*, 2011).

On the other hand, natriuretic peptides, such as ANP and BNP are considered as potent endogenous inhibitors of hypertrophy and they are released from cardiomyocytes in response to increased ventricular wall stress (Maayah *et al.*, 2016b). BNP has been considered as a good predictor of heart failure (Maayah *et al.*, 2016c) whereas ANP may serve as a marker of cardiac stress but is not essentially a hypertrophic marker, especially on an organ level (Maayah *et al.*, 2015a).

1.2.2. Signaling pathways in cardiac hypertrophy

The process of cardiac hypertrophy and myopathy is complex and involves multiple cross-regulated signaling pathways (Frey *et al.*, 2003) that culminate in massive alterations in myocardial architecture (Fard *et al.*, 2000). These molecular mechanisms have not been fully elucidated, and no precise cellular mechanisms have yet been identified. Importantly, some potential pathways, such as phosphoinositide 3-kinases (PI3Ks), protein kinase C (PKC), mitogen activated protein kinases (MAPK) and nuclear factor-κB (NF-κB) that may stimulate cellular growth and hypertrophy have been explored. PKC, MAPK and NF-kB are pivotal to this process as central mediators of cardiac remodeling in response to injury and/or cardiac wall stress (Figure 1.1).
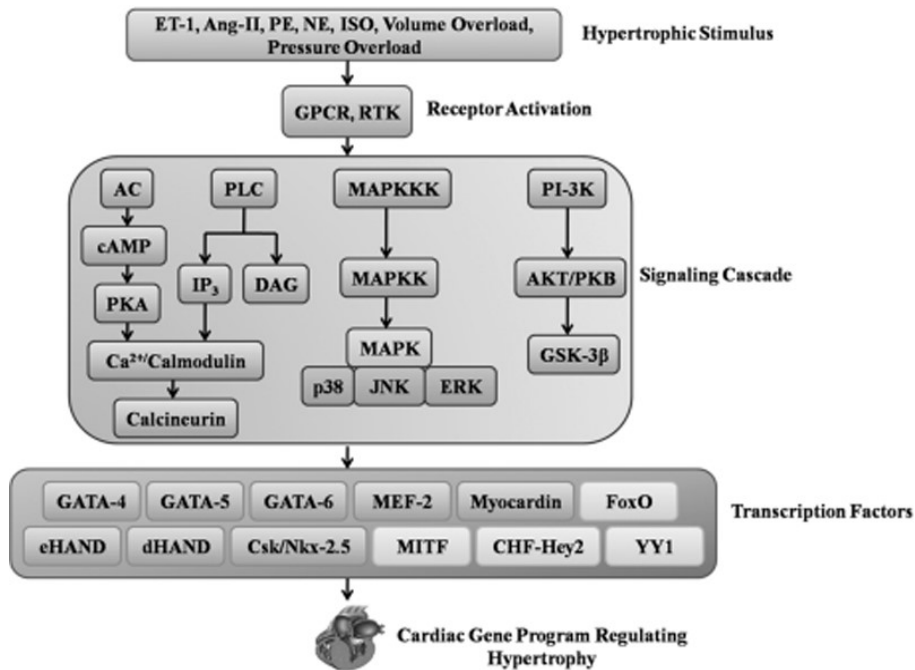
Figure 1.1. Schematic diagram of possible intracellular signaling pathways involved in cardiac hypertrophy.

Phosphoinositide 3-kinases (PI3Ks), PKC, mitogen activated protein kinases (MAPK), nuclear factor- κB (NF-κB). Reprinted from (Kohli *et al.*, 2011) with permission from Bentham Science Publishers.

1.2.2.1 PI3K/Akt/Glycogen Synthase Kinase-3

PI3Ks have been involved in the regulation of many cellular physiological and pathophysiological functions, e.g. cell development, survival, and proliferation (Cantley, 2002). The PI3K, p110α isoform, is regulated physiologically through the coupling of insulin-like growth factor (IGF-1) to cell surface receptor tyrosine kinases and pathologically by the activation of G protein coupled receptors (GPCRs) (Schlessinger, 2000). The involvement of PI3K in the development of cardiac hypertrophy was supported by the finding that overexpression of PI3K increased cardiac size whereas genetic inhibition of PI3K significantly reduced heart size (Shioi *et al.*, 2000). Although the induction of PI3K has been reported in pressure overload induced cardiac hypertrophy, suppression of PI3K was shown to attenuate hypertrophy in response to swim training but not pressure overload, suggesting PI3K as a physiological but not pathological signaling pathway. Important downstream targets of PI3K signaling are the serine/threonine kinase Akt, mammalian target of rapamycin (mTOR) and glycogen synthase kinase-3 (GSK-3).

mTOR enhances protein translation through the activation of key protein translation mediators such as p70S6 kinase and 4EBP1/eIF4E. Inhibition of mTOR activity by rapamycin, an immunosuppressant agent, was shown to inhibit cardiac hypertrophy induced by Ang-II (Sadoshima *et al.*, 1995). Phosphorylation of GSK-3 promotes translocation of many transcription factors such as nuclear factor of activated T-cells (NFAT) and NF-κB. ISO, endothelin-1 (ET-1), and phenylephrine has been demonstrated to induce cardiac hypertrophy through PI3K/GSK-3-dependent mechanism.

1.2.2.2. PKC and G_q-protein coupled receptor

The PKC is a family of multifunctional isoenzymes expressed in different tissues which plays a pivotal role in apoptosis, migration, adhesion, tumorgenesis, cardiac hypertrophy, angiogenesis, platelet function and inflammation (Newton, 2001). PKC, discovered by Inoue et al. in 1977, was originally named PKM since it was hypothesized that magnesium ion is essential for its activation (Inoue *et al.*, 1977). However, after understanding the crucial role of calcium and phospholipids for its activation, the protein was renamed as PKC. PKC has three isoforms, α, β and γ, which differ in their composition of the 50 amino acids at the C-terminal end. They are expressed in various organs of the body and this specificity is associated with their physiological functions. Of importance, PKCα is found in almost all organs, especially in the heart (Wetsel *et al.*, 1992). PKCα contributes to cardiac contractility and heart failure in a manner different from what is observed with PKCβ and PKCγ. Overexpression of PKCα has demonstrated a decrease in cardiac output and left ventricular hypertrophy, implicating PKCα as a detrimental signaling pathway to the cardiac muscle (Hahn *et al.*, 2003; Braz *et al.*, 2004; Liu *et al.*, 2009). Inhibition of PKCα protects against cardiac hypertrophy induced by Ang-II (Yan *et al.*, 2010). PKCα is regulated by G_q-protein coupled receptor in which the activation of G_q-protein coupled receptor stimulates the effector enzyme phospholipase C (PLC). PLC cleaves phosphoinositol bisphosphate (PIP2) in the membrane to yield diacylglycerol (DAG) and inositol trisphosphate. DAG remains in the membrane and activates PKC (Hahn *et al.*, 2003).

1.2.2.3. Ca^{2+} Calcineurin/NFAT

Calcineurin, a calmodulin-dependent Ca^{2+}-activated phosphatase, is an effector downstream of G_q-protein coupled receptors and PKC activation that dephosphorylates the NFAT transcription factor (Molkentin *et al.*, 1998). Upon activation by several mechanical and neurohormonal factors, NFAT translocates to the nucleus where it activates GATA-4 transcription factor leading to cardiac hypertrophy and heart failure (Molkentin *et al.*, 1998). Calcineurin deficiency in mice has been reported to ameliorate pressure overload-, Angiotensin-II (Ang-II)- or isoproterenol (ISO)-induced cardiac hypertrophy (Bueno *et al.*, 2002). Furthermore, cardiac overexpression of modulatory calcineurin-interacting protein (MCIP1) blunted hypertrophy mediated by ISO, exercise, or thoracic aortic banding suggesting an involvement of calcineurin/NFAT in both physiological and pathological hypertrophy (Rothermel *et al.*, 2001; Hill *et al.*, 2002).

1.2.2.4. MAPK

MAPK are serine/threonine specific protein kinases that are involved in the regulation of various cellular responses such as gene expression, mitosis, differentiation, proliferation and survival/apoptosis (Kayama *et al.*, 2009). MAPK were found to exert control over those genes that stimulate protein synthesis and initiate hypertrophy (Thorburn *et al.*, 1994). When hypertrophy stimulus is initiated at cell membrane, activated MAPK move through large pores on the nuclear membrane, translocating into the nucleus and activating transcription factors involved in cardiac hypertrophy (Pearson *et al.*, 2001). The MAPK signaling cascade consists of extracellular-regulated kinases (ERK), c-Jun NH2-terminal kinases (JNKs) and p38 MAPK (Sopontammarak *et al.*, 2005). Previous studies analyzing MAPK activities in cardiac hypertrophy and myopathy have demonstrated differential effect; in that persistent activation of p38 and JNK can promote apoptosis, resulting in cardiac dilation and dysfunction (Pearson *et al.*, 2001), whereas ERK1/2 has been proposed to regulate smooth muscle contraction and to promote cellular hypertrophy (Pearson *et al.*, 2001; Sopontammarak *et al.*, 2005; Modesti *et al.*, 2008).

1.2.2.5. NF-κB

Cardiac hypertrophy and myopathy are also regulated by several transcription factors such as NF-κB, myocyte enhancer factor 2 (MEF2), and homeobox transcription factors Csx/Nkx 2-5 (Akazawa *et al.*, 2003). Among these transcription factors, NF-κB is involved in a wide range of physiological and pathophysiological functions, such as B cell proliferation, cell cycle control, carcinogenesis and cardiac hypertrophy and myopathy (Grabellus *et al.*, 2002).

Biochemical analysis has established that the major form of NF-κB has two distinct polypeptides of 50 and 65 kDa, termed as p50 and p65 NF-κB, respectively. Upon activation by inflammatory mediators and hypertrophy agonists, NF-κB binds to its responsive element sequences, κB, to initiate target gene transcription that is involved in cardiac hypertrophy (Leychenko *et al.*, 2011). NF-κB has been shown to be activated in the failing human heart (Grabellus *et al.*, 2002). Genetic NF-κB inhibition attenuates Ang II-induced hypertrophy, suggesting an important role of NF-κB in cardiac hypertrophy (Esposito *et al.*, 2002). Furthermore, it has been demonstrated that blockade of NF-κB ameliorates myocardial hypertrophy in response to aortic banding and chronic infusion of Ang II, suggesting an important role of NF-κB as a signaling pathway in the regulation of cardiac hypertrophy (Kawano *et al.*, 2005).

Chronic pressure overload and HF are usually associated with excessive fibrosis and inflammation and they are predictors of poor prognosis (Shimizu *et al.*, 1988). Several studies have linked the inflammation and fibrosis to the activation of NF-κB (Wong *et al.*, 1998; Grabellus *et al.*, 2002). NF-κB has crucial role in the regulation of inflammatory response through the induction of pro-inflammatory cytokines genes such tumor necrosis factor α (TNFα) and interleukin 6 (IL-6) in addition to chemokines (Testa *et al.*, 1996; Lawrence, 2009). NF-κB was shown to activate circulating monocyte during HF (Frantz *et al.*, 2004) and it promotes T cells differentiation and activation (Tak *et al.*, 2001).

1.2.2.6. Oxidative stress

The consumption of oxygen produces potentially toxic metabolites called reactive oxygen species (ROS). These ROS are kept at low level, by naturally occurring antioxidant, in normal situations, and some of these ROS even exert physiological roles. Examples of ROS include hydrogen peroxide, superoxide, hydroxyl radical, nitric oxide, and peroxynitrite. When there is an overproduction of ROS and/or deficiency in antioxidant mechanisms, a damaging event called oxidative stress ensues. Cardiomyocytes are more susceptible to ROS-dependent toxicity because they have low expression levels of the antioxidant enzymes. Furthermore, mitochondria, a source of as well as a target for ROS, comprise about 50% of the cardiomyocyte mass (Lemieux *et al.*, 2009).

Superoxide anion was shown to be implicated in the hypertrophy process through the increase of proto-oncogene factors, such as c-my and c-fos, mediating the linkage of Na$^+$/K$^+$ ATPase to hypertrophy and modulating the activity of MAPK (Xie *et al.*, 1999; Wassmann *et al.*, 2001). Treatment with antioxidants inhibited the hypertrophic response of cardiomyocytes to superoxides (Nakamura *et al.*, 1998; Tanaka *et al.*, 2001). Overexpression of superoxide dismutase or NADPH oxidase knockdown blunted hypertrophic responses to Ang-II (Welch, 2008). On the other hand, superoxide dismutase deficiency was shown to aggravate pressure overload-induced cardiac hypertrophy (Lu *et al.*, 2008b). The above information suggests the contribution of superoxide in the development of left ventricular hypertrophy.

1.2.2.7. Peroxisome proliferator activated receptors (PPARs)

PPARs, typified by PPARα, PPARβ and PPARγ, are ligand-activated nuclear hormone receptor transcription factors that affect lipid metabolism by modulating the expression of enzymes involved in fatty acid oxidation (Wahli *et al.*, 1995). Heart, skeletal muscle and liver have high expression levels of PPARα and the latter is activated by various ligands, including unsaturated fatty acids and drugs such as fibrates (Gilde *et al.*, 2003). Although cardiac overexpression of PPARα results in cardiomyopathy with contractile dysfunction (Finck *et al.*, 2002), fibrates have been demonstrated to protect against Ang-II-induced cardiac hypertrophy (Zou *et al.*, 2013). This is because fibrates activate peripheral fatty

acid β-oxidation and decrease free fatty acids in the circulation, thereby decreasing myocardial exposure to circulating free fatty acids, ultimately reducing the cardiac fatty acid β-oxidation at the expense of glucose oxidation (Yue *et al.*, 2003; Lopaschuk *et al.*, 2010). This shift protects cardiac muscle by decreasing myocardial oxygen consumption per mole of ATP generated. With regard to PPARγ, it has been demonstrated that induction of cardiac hypertrophy in response to aortic construction was blunted by thiazolidinedione, PPARγ agonists (Asakawa *et al.*, 2002). Although previous studies have linked myocardial infarction and death to rosiglitazone administration (Lindenfeld *et al.*, 2007; Nissen *et al.*, 2007), a recent study has demonstrated that rosiglitazone use was not associated with increased risk of myocardial infarction (Florez *et al.*, 2015).

1.2.2.8. Other signaling pathways

The Na+/H+ exchanger, β1-adrenergic receptor kinase (βARK) in addition to microRNAs (miRNAs) have been also implicated in cardiac hypertrophy.

The increase in cardiac Na^+/H^+-exchanger (NHE) activity has been demonstrated in several in vivo and in vitro models of cardiac hypertrophy (Takewaki *et al.*, 1995). Enhanced NHE activity diminishes transmembrane Na^+, activates the Na^+/Ca^{2+}-exchanger and thereby increases intracellular Ca^{2+} level which may trigger several signaling cascades involved in cardiac hypertrophy (Yoshida *et al.*, 2000). Of particular interest, cariporide, a specific NHE inhibitor, was shown to protect mice overexpressing β1-recptor against cardiac remodeling and fibrosis (Engelhardt *et al.*, 2002).

β1-receptor, a G_s heterotrimeric GTP-binding protein coupled receptor, is the most dominant adrenergic receptor in the cardiac tissue. Short term activation of β1-receptor may initially improve contractile function but prolonged hyperadrenergic drive may result in the overexpression of βARK and desensitization of β1-receptors and eventually lead to progressive deterioration of cardiac performance and cardiac hypertrophy (Engelhardt *et al.*, 1999; Bisognano *et al.*, 2000). Inhibition of βARK activity, a kinase implicated in receptor desensitization, genetically or pharmacologically has been demonstrated to

preserve membrane density of β1-receptors, restoring the integrity of the β1-adrenergic system in hypertrophic cardiac muscle (Rockman *et al.*, 1998; Harding *et al.*, 2001).

MicroRNAs (miRNAs) are short (= 22 nucleotide long) non-coding RNAs that pair in a sequence-specific manner to binding sites present in the 3'untranslated region of target messenger RNAs (mRNAs) (Ambros, 2003). Binding with miRNAs, in the cytoplasm, is responsible for negative regulation of the target either through degradation of the bound mRNA or by inhibition of its translation. Up-regulation of miRNAs, therefore, leads to decreased gene expression (Farh *et al.*, 2005). Of interest, miRNAs have been implicated in the development of cardiac remodeling. For instance, hypertrophied heart has low expression level of miR-133, miR-1, miR-29, and miR-30. Furthermore, upregulation of miR-133 has been shown to minimize cardiac hypertrophy and fibrosis-induced by Ang-II (Li *et al.*, 2016), whereas downregulation of miR-133 was sufficient to induce cardiomegaly (Care *et al.*, 2007).

1.3. Doxorubicin

1.3.1. History

In 1950s, a new strain of *Streptomyces peucetius* was isolated from a soil sample in the area nearby the Castel del Monte, a 13th-century castle, by farmitalia research laboratories (Weiss, 1992). These bacteria produce a red pigment antibiotic that has a potent anticancer activity in different animal models (Baruffa, 1966). Simultaneously, the same antibiotic was discovered by a team of French researchers. Both groups had agreed to name the discovered antibiotic daunorubicin. This name combines the word Dauni, a pre-Roman tribe that colonized the region of Italy where the antibiotic was extracted, with the French word for ruby, rubis, describing its color. In 1960s, daunorubicin was successfully used to treat patients with acute leukemia and lymphoma. Unfortunately, by 1967, clinical usefulness of daunorubicin was badly compromised by its fatal cardiotoxicity (Tan *et al.*, 1967). Immediately, N-nitroso-N-methyl urethane was used to mutate a strain of *Streptomyces* producing a different, red-colored antibiotic, doxorubicin (DOX), which was also named Adriamycin, after the Adriatic Sea, (Di Marco *et al.*, 1969). Although DOX

has shown a potent antitumor activity against solid tumors and a wide therapeutic index, the cardiotoxicity remains the main adverse effect.

1.3.2. DOX-induced cardiotoxicity

DOX is a broad-spectrum anthracycline antibiotic widely used to treat various types of human neoplastic disease, including lymphoblastic, hematopoietic and a wide range of solid tumors, such as lung, breast and thyroid cancer (Minotti *et al.*, 2004). Although DOX has improved survival rates in cancer patients, cardiotoxicity has been reported as a significant side effect (Horenstein *et al.*, 2000). Two types of cardiomyopathies may occur as a result of DOX treatment, an acute form which is characterized by abnormal electrocardiographic changes, including ST- and T-wave alterations and arrhythmias. The second type results from chronic, cumulative dose-related toxicity ($\geq$550 mg/m^2), which may progress to congestive heart failure. A steady decrease in left ventricular ejection fraction may be observed over the first four cycles of therapy (Felker *et al.*, 2000). Dilatation of all chambers, myofibrillar loss and vacuolar degeneration are the three diagnostic features of DOX's cardiotoxicity (Chatterjee *et al.*, 2010).

1.3.2.1. Possible mechanisms of DOX-induced cardiotoxicity

Though the specific mechanisms mediating the cardiotoxic effect of DOX are still controversial, several reports illustrated that modulation of topoisomerase II, oxidative stress, mitochondrial damage and apoptosis could play a role in DOX-induced cardiotoxicity (Minotti *et al.*, 2004; Takemura *et al.*, 2007; Deng *et al.*, 2014). The toxicity is irreversible, cumulative, dose-dependent and may occur within a month or years after the treatment initiation.

1.3.2.1.1. Oxidative stress

DOX has quinone and hydroquinone moieties on adjacent rings that permit the gain and loss of electrons and favors superoxide generation after being reduced by NADPH-cytochrome P450 reductase to an unstable semiquinone intermediate (Ravi *et al.*, 2004). The formation of superoxide is significantly increased by the interaction of reduced DOX with iron (Yang *et al.*, 2014a). Furthermore, DOX could generate H_2O_2 which may interact

with free iron forming highly toxic hydroxyl radicals through a reaction known as Haber-Weiss reaction (Xu *et al.*, 2005).

Although the DOX-induced cardiotoxicity was alleviated by overexpressing antioxidant enzymes such as manganese superoxide dismutase and catalase (Kang *et al.*, 1996; Yen *et al.*, 1996), the effectiveness of using antioxidants to prevent DOX-induced cardiac injury is still controversial. In that, several antioxidant agents such as vitamin E or N-acetylcysteine were not able to attenuate DOX-induced cardiotoxicity at chronic stages (Ladas *et al.*, 2004). Nevertheless, carvedilol, a combined β- and α-receptor blocker with potent antioxidant properties, was shown to prevent and delay DOX-induced cardiomyopathy (Kalay *et al.*, 2006). Furthermore, dexrazoxane, a free iron chelator, has been approved by FDA to alleviate DOX-induced cardiac injury (Lipshultz *et al.*, 2004; Lebrecht *et al.*, 2007). However, dexrazoxane was shown to reduce the anticancer activity of DOX when administered in conjunction (Tebbi *et al.*, 2007).

1.3.2.1.2. Stabilization of the mitochondrial topoisomerase IIβ

Topoisomerase II is an ATP-dependent enzyme that binds to DNA and produces double-strand breaks at the 3′-phosphate backbone, allowing strand passage and uncoiling of super-coiled DNA. Following strand passage, topoisomerase II religates the DNA strands. This enzymatic function is crucial for DNA replication and repair. DOX forms a tripartite complex with it and blocks the religation of the broken DNA strands and eventually leads to apoptosis (Low *et al.*, 2003). Cardiac tissue has three forms of topoisomerase II proteins namely, nuclear topoisomerase IIα, IIβ and the mitochondrial topoisomerase IIβ (Wang *et al.*, 2002). Although DOX exerts its cytotoxic activity through the inhibition of nuclear topoisomerase IIα and β, it has been reported that DOX may induce cardiotoxicity through the stabilization of the mitochondrial topoisomerase IIβ (Swift *et al.*, 2008). DOX stimulates DNA response genes and initiates cardiomyocyte apoptosis in the presence of topoisomerase IIβ. This was supported by the finding that genetic inhibition of mitochondrial topoisomerase IIβ attenuates DOX-induced cardiac injury in mice (Zhang *et al.*, 2012a). Furthermore, dexrazoxane was shown to exert a cardioportective effect through the inhibition of topoisomerase IIβ (Deng *et al.*, 2014).

1.3.2.1.3. Apoptosis and mitochondrial dysfunction

Doxorubicinol, a DOX metabolite, can activate the ryanodine receptor, leading to an increase in the release of calcium from the sarcoplasmic reticulum (Zhou *et al.*, 2001). The high level of calcium may elicit a mitochondrial transition pore which results in the release of cytochrome c and eventually initiate apoptosis through the activation caspase cascade (Phaneuf *et al.*, 2002; Octavia *et al.*, 2012). DOX may also increase the release of cytochrome c by disrupting the mitochondrial electron transport chain (Thorn *et al.*, 2011). In addition, upregulation of the tumor suppressor gene p53 and the pro-apoptotic, Bax, has been implicated in DOX-induced cardiomyocyte apoptosis (Yoshida *et al.*, 2009). Of interest, genetic deletion of p53 was shown to protect cardiomyocytes against DOX-induced apoptosis (Shizukuda *et al.*, 2005).

1.4. Cytochrome P450

The oxidative metabolism of a vast majority of endogenous compounds and xenobiotics is mediated by single polypeptide membrane-bound hemeproteins known as cytochrome P450s (CYPs) (Nebert *et al.*, 2002). CYPs are mainly located in the cellular microsome and have a hydrophobic transmembrane helix at the N-terminus of the protein to attach to the cellular membrane (Aguiar *et al.*, 2005). Structurally, CYPs have 45-60 kDa molecular size since they have approximately 500 amino acids in addition to a single heme group coordinated with a cysteine molecule (Poulos, 2005). CYPs are expressed in the liver as well as extrahepatic tissues such as kidneys, lungs and heart.

1.4.1. Classification of CYPs and their expression in the cardiovascular system

The classification of CYPs into families and subfamilies depends on the primary amino acid sequences of the purified CYP enzyme (Nelson, 2006; Sim *et al.*, 2006). Members of the same family should have greater than 40% amino acid sequence homology, whereas members in a gene subfamily should have more than 55% amino acid sequence homology. Generally, an Arabic number and a capital letter are usually used to designate the family and subfamily, respectively (Nelson, 2006; Sim *et al.*, 2006). The metabolism of xenobiotics such as pharmacological agents in mammalian tissues are known to be

mediated by CYP1, 2, and 3 families. Many other families of CYPs contribute to the oxidative metabolism of endogenous molecules such as eicosanoids, fatty acids and steroids (Barouki *et al.*, 2001). CYP enzymes have been detected in the cardiovascular tissue and their specific isoforms have been detected in rat heart (Imaoka *et al.*, 2005) and in different regions of human heart (Roman, 2002; Delozier *et al.*, 2007). Several lines of evidence support the role of CYP metabolites in the maintenance of cardiovascular health, including the regulation of vascular tone, extracellular fluid volume, and heart contractility (Roman, 2002).

1.4.1.1. CYP1 family

CYP1A1, CYP1A2 and CYP1B1 are the only members of the human CYP1 family currently detected. CYP1A2 is mainly expressed in liver while CYP1A1 and CYP1B1 are predominantly expressed in extrahepatic tissues such as heart (Monostory *et al.*, 2009). Procarcinogenic polycyclic aromatic hydrocarbons (PAHs) are mainly metabolized by CYP1A1, whereas CYP1A2 is responsible for the metabolism of many pharmacological agents such as theophylline, imipramine and fluvoxamine (Shimada *et al.*, 1996; Danielson, 2002; Hu *et al.*, 2007).

The CYP1A1 mRNA has been detected in explanted human hearts, healthy cardiac tissue and human cardiac fibroblasts in addition to the left atrium of patients with dilated cardiomyopathy (Thum *et al.*, 2000a; Dubey *et al.*, 2005; Bieche *et al.*, 2007). CYP1A2 has been found in coronary vessels and the endothelium of the endocardium (Minamiyama *et al.*, 1999; Thum *et al.*, 2000a). Generally, it has been shown that CYP1 expression in fetal cardiomyocytes cells is higher than that in adult cardiomyocytes (Aragon *et al.*, 2008). Benzo(a)pyrene (BaP), 2,3,7,8-tetrachloro-dibenzodioxin (TCDD), 3-methylcholanthrene (3MC) and are well-known inducers of CYP1A1 (Korashy *et al.*, 2006). CYP1B1 will be discussed in section 1.5.3 of this thesis.

1.4.1.2. CYP2 family

CYP2A, CYP2B, CYP2C, CYP2D, CYP2E and CYP2J are the main members of CYP2 family (Lewis, 2004). These enzymes are accountable for the metabolism of both

endogenous compounds such as arachidonic acid and xenobiotics such as halothane (CYP2A6), cyclophosphamide (CY2B6), clopidogrel (CYP2C19), mirtazapine (CYP2D6), acetaminophen (CYP2E1) and terfenadine (CYP2J2) (Manyike *et al.*, 2000; Minoda *et al.*, 2001; Xie *et al.*, 2003; Kirchheiner *et al.*, 2004; Lee *et al.*, 2010). CYP2A6 and CYP2C are considered the most abundant CYP2 isoform in the hepatic tissue (Goldstein *et al.*, 1994; Su *et al.*, 2004). CYP2B6 and CYP2D6 represent just 1% and 2% of the total liver CYP content, respectively, though they are involved in the metabolism of many different pharmacological agents (Danielson, 2002). CYP2E1 is not detected during the human neonatal period, whereas it is the main CYP implicated in the metabolism of ethanol in adult liver (Vieira *et al.*, 1996; Lu *et al.*, 2008a). In contrast to all CYP2 isoforms, CYP2J2 is mainly expressed in the extrahepatic tissues (Lieber, 1997).

While CYP2A6, CYP2B6, CYP2C8, CYP2D6 and CYP2E1 were detected in human cardiac tissue, CYP2J2 is considered the most predominant CYP isoform in human left ventricles (Thum *et al.*, 2000a; Bieche *et al.*, 2007; Michaud *et al.*, 2010). Previous studies have shown that CYP2E1 is basally expressed in both atria and ventricles, whereas CYP2B6 and CYP2D6 are found only in the right ventricles (Thum *et al.*, 2000b; Imaoka *et al.*, 2005). Of interest, the alteration in the expression level of CYP2 enzymes has been illustrated in cardiac ischemia and hypertrophy in addition to failing hearts of both humans and rats (Imaoka *et al.*, 2005; Ishihara *et al.*, 2012).

1.4.1.3. CYP3 family

CYP3A4, CYP3A5, CYP3A7 and CYP3A43 are the main members of CYP3A subfamily (Gellner *et al.*, 2001). CP3A4 comprises up to 60% of the total hepatic CYP content and is involved in the metabolism of greater than 30% of clinically used pharmacological agents (Anzenbacher *et al.*, 2001). In addition to hepatic tissue, CYP3A4 is expressed in intestinal tissue (Granvil *et al.*, 2003). However, the expression of the CYP3A subfamily has not been detected in the heart of humans or rats. Nevertheless, CYP3A4 was found in the endothelium, endocardium and coronary vessels (Minamiyama *et al.*, 1999).

1.4.1.4. CYP4 family

CYP4A and CYP4F are the most important members of CYP4 family and they are responsible for the fatty acid omega-hydroxylation (Okita *et al.*, 2001). CYP4A and CYP4F are expressed predominantly in kidneys but there in very little if any in the hepatic tissue (Theken *et al.*, 2011). With respect to the expression of CYP4 family in the cardiovascular system, it has been demonstrated that CYP4 is mainly expressed in freshly isolated cardiomyocytes of control animals and adult human cardiomyocytes (Simpson, 1997; Thum *et al.*, 2000a; Chaudhary *et al.*, 2009). In addition, human, dog and rodent cardiac tissues have shown a high expression level of CYP4A and CYP4F enzymes (Thum *et al.*, 2000a; Nithipatikom *et al.*, 2004). Furthermore, CYP4A and CYP4F were found in the failing human heart whereas, CYP4A has been shown to be induced in hypertrophied human hearts (Thum *et al.*, 2002; Elbekai *et al.*, 2006).

1.4.1.5. Other CYP families

Synthesis and degradation of many endogenous compounds are mediated through other CYP families. For instance, thromboxane A2 (TxA2) synthase, CYP5A1, is incriminated in the synthesis of platelet aggregation factor, TxA2, (Elbekai *et al.*, 2006). Furthermore, CYP8A1 and CYP27B1 mediate the biosynthesis of prostaglandin I2 and lα,25-dihydroxyvitamin D3 from prostaglandin H2 and 25-hydroxyvitamin D3, respectively (Inouye *et al.*, 2001; Elbekai *et al.*, 2006). CYP11A has been detected in normal and failing human heart while CYP11B1 and CYP11B2 are not expressed in normal human heart (Silvestre *et al.*, 1998).

1.4.2. Transcriptional regulation of CYPs

Activation of CYP genes begins with binding of xenobiotics or endobiotics to specific nuclear receptors leading to the initiation of the transcription process (Barouki *et al.*, 2001). At least four nuclear receptor mechanisms are crucially involved in the transcriptional activation of most CYPs: the aryl hydrocarbon receptor (AhR) for CYP1A1, CYP1A2, CYP1B1, and CYP2S1; the constitutive androstane receptor (CAR) for the CYP2 family; the pregnane X receptor (PXR) for the CYP3 family; and the PPARα for the CYP4 family (Ramana *et al.*, 1998).

1.4.2.1. AhR

AhR is a cytosolic ligand-activated transcriptional factor that is involved in regulation of cell differentiation and proliferation (Whitelaw *et al.*, 1993; Kerzee *et al.*, 2001). AhR nuclear translocator (ARNT) protein, the *Drosophila* neurogenic protein single-minded (Sim) and the *Drosophila* circadian rhythm protein period (Per) are the main members of the AhR family (Schmidt *et al.*, 1996a; Schmidt *et al.*, 1996b). The N-terminal half of AhR consists of bHLH and PAS domains which are vital for activation and heterodimerization. Furthermore, the NH_2-terminal region is composed of nuclear localization and export signals (NLS and NES) that play roles in AhR shuttling between the cytoplasm and the nucleus (Ikuta *et al.*, 1998). Upon binding with its ligand, AhR dissociates from its inhibitory protein, heat shock protein 90 (HSP90) (Denison *et al.*, 1986) allowing it to translocate to the nucleus, where it heterodimerizes with the nuclear transcription factor protein, called ARNT (Whitelaw *et al.*, 1994). The heterodimeric AhR-ARNT complex then binds to specific DNA recognition sequences, GCGTG, within the xenobiotic responsive element (XRE) located in the promoter region of CYP1 family gene (Nebert *et al.*, 2004; Korashy *et al.*, 2006a).

Cardiac tissue has shown a higher AhR expression level which is further induced during ischemic and dilative cardiomyopathies (Korashy *et al.*, 2006). Of interest, it has been previously reported that the AhR ligands, BaP, and 3-MC, cause significant cardiac hypertrophy in vivo in rats. On the other hand, treatment with benzo(e)pyrene, an isomer of BaP with less affinity to AhR, did not induce cardiac hypertrophy (Aboutabl *et al.*, 2009). Furthermore, several cardiotoxic chemotherapeutic agents such as DOX and sunitinib have been demonstrated to activate AhR signaling pathway both in vivo and in rat cardiomyocytes (Volkova *et al.*, 2011; Maayah *et al.*, 2014).

1.4.2.2. Constitutive Androstane Receptor (CAR)

CAR is a nuclear ligand-activated transcriptional factor that is involved in the regulation of several genes involved in the metabolism of xenobiotics and endobiotics including CYP2B6, CYP2C8 and CYP3A4 (Ueda *et al.*, 2002; Yang *et al.*, 2014b). Upon activation

either directly by binding with its ligand or indirectly by dephosphorylating it through protein phosphatase 2, CAR dissociates from its inhibitory proteins, hsp90, allowing it to translocate to the nucleus, where it heterodimerizes with a nuclear transcription factor protein called retinoid X receptor (RXR) (Kawamoto *et al.*, 1999; Kodama *et al.*, 2006). The heterodimeric CAR-PXR complex then binds to the phenobarbital-responsive enhancer module (PBREM) located in the distal enhancer region of CYP2B and CYP3A family genes (Honkakoski *et al.*, 1998; Sueyoshi *et al.*, 1999; Makinen *et al.*, 2002). CAR is dominantly expressed in the hepatic and intestinal tissues, but a minor constitutive expression level is also identified in the cardiac tissues (Shmueli *et al.*, 2003). Furthermore, CAR splice variants have been detected in human heart (Lamba *et al.*, 2004).

CYP2B and CYP3A genes may be regulated by pregnane X receptor (PXR), also known as the steroid nuclear receptor (SXR) (Bertilsson *et al.*, 1998; Kliewer *et al.*, 2002). PXR is activated by steroids, e.g. dexamethasone, in addition to antibiotics, e.g. rifampicin, and inhibited by ketoconazole (Li *et al.*, 2013). Similar to CAR, PXR is predominantly expressed in the in hepatic and intestinal tissues (Beigneux *et al.*, 2002; Li *et al.*, 2012).

1.4.2.3. PPAR

Initially, the name of PPAR was chosen because it induces the proliferation of peroxisome in the ˣenopus frogs (Dreyer *et al.*, 1992). Later, PPAR became a molecular target for fibrates and thiazolidinedione agents in the early 1980s and late1990s, respectively (Issemann *et al.*, 1990). PPAR, mainly the α-isoform, is a nuclear ligand-activated transcriptional factor that is involved in regulation of CYP4 genes. Upon binding with its ligand, e.g. clofibrate, PPAR heterodimerizes with RXR and then the heterodimeric PPAR-PXR complex binds to specific DNA recognition sequences, AGGTCANAGGTCA, within the peroxisome proliferator hormone response elements (PPREs) located in the promoter region of the CYP4 family gene (Yu *et al.*, 2007).

1.5. CYP-mediated arachidonic acid metabolism

Arachidonic acid (AA) is a nonessential polyunsaturated fatty acid that is released following activation of phospholipase A_2 and subsequent metabolism by COX, lipoxygenase (LOX) and CYP pathways. These enzymes insert oxygen at different positions in AA to generate a major family of biologically active mediators called eicosanoids (Capdevila *et al.*, 1981). COX, a prostaglandin-endoperoxide synthase, is implicated in the formation of prostaglandin G_2 and H_2 (Picot *et al.*, 1994) whereas LOX, a non-heme iron dioxygenase enzyme, oxygenates AA and catalyzes the formation of hydroxyperoxyeicosatetraenoic acid, which is then subsequently converted into hydroxyeicosatetraenoic acids (HETEs) and leukotrienes (Kuhn *et al.*, 2015). CYP, cysteinato-heme mixed function mono-oxygenases enzymes oxidize AA into epoxyeicosatrienoic acids (EETs) and HETEs which play a crucial role in the maintenance of cardiovascular health (Roman, 2002; Zordoky *et al.*, 2010c).
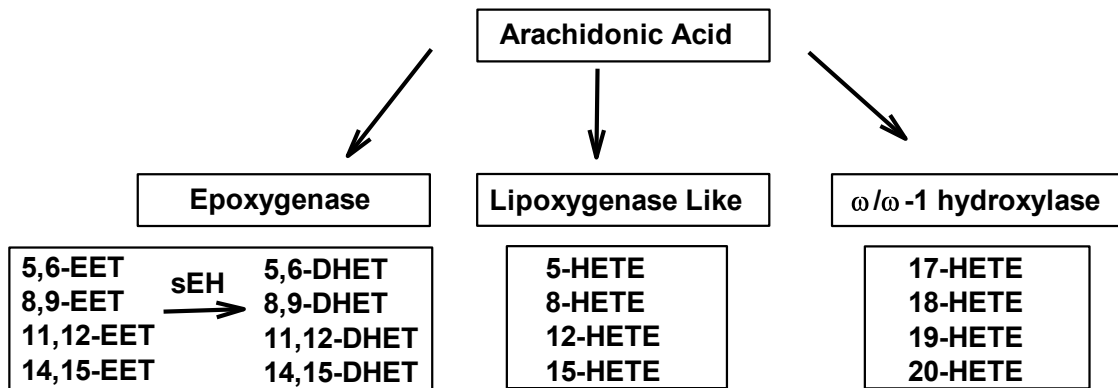
Figure 1.2. CYP-mediated arachidonic acid metabolism.
Arachidonic acid is released following activation of phospholipase A_2 and subsequent metabolism by CYP pathways. These enzymes insert oxygen at different positions in AA to generate a major family of biologically active mediators called eicosanoids.

1.5.1. EETs

CYP epoxygenases, mainly CYP2B, CYP2C and CYP2J subfamilies, metabolize AA into four regioisomers of cardioprotective EETs namely, 14,15-EET, 11,12-EET, 8,9-EET and 5,6-EET metabolites (Roman, 2002). EETs, which are endothelium derived hyperpolarizing factors (EDHFs) and vasodilators, have potent anti-inflammatory and antiapoptotic effects and reduce vascular smooth muscle cell proliferation (Tacconelli *et al.*, 2014).

EETs are considered potent vasodilators as they induce vascular smooth muscle cell membrane hyperpolarization through the activation of the large-conductance calcium-activated potassium channels (Kca) (Imig, 2012). The anti-inflammatory action of EETs is due to the inhibition of NF-κB mediated induction of cytokines and leukocytes adhesion (Node *et al.*, 1999) whereas the antiproliferative effect has been reported to be mediated by PI3K/Akt, MAPK, and cAMP/PKA signaling pathways (Spector *et al.*, 2007). EETs have also antithrombotic action through the inhibition of platelet aggregation and the activation of tissue-type plasminogen activator (tPA) gene expression (Fitzpatrick *et al.*, 1986; Node *et al.*, 2001; Krotz *et al.*, 2004).

The protective effect of EETs has been reported against cardiac hypertrophy and HF in addition to drug induced-cardiotoxicity (Wang *et al.*, 2014). For instance, EETs were shown to protect against ISO-induced cardiac hypertrophy and Ang II-induced HF (Wang *et al.*, 2014; Althurwi *et al.*, 2015). In addition, EETs protect against DOX and daunorubcin-induced cardiotoxicity (Zhang *et al.*, 2009a; Maayah *et al.*, 2017). Mechanistically, EETs exert their cardioprotective effects through the activation of ATP-sensitive potassium channels and p42/p44 MAPK pathway in addition to the inhibition of NF-κB (Seubert *et al.*, 2004; Lu *et al.*, 2006b).

EETs are known to be metabolized by soluble epoxide hydrolase (sEH) into their corresponding degradation products dihydroxyeicosatrienoic acids (DHETs) which diminishes their cardioprotective effects (Imig *et al.*, 2002). Importantly, hypertrophied heart induced by Ang-II and ISO has demonstrated a high mRNA and protein expression

level of sEH (Althurwi *et al.*, 2013; El-Sherbeni *et al.*, 2014c). On the other hand, sEH inhibitors have been reported to increase EET availability, thereby exerting an antihypertensive effect, improving endothelial function and reducing Ang-II- and ISO-induced cardiac hypertrophy (Althurwi *et al.*, 2013; Wang *et al.*, 2014; Althurwi *et al.*, 2015). Clinically, AR9281, a selective sEH inhibitor, has been evaluated in phase II clinical trials for the treatment of hypertension in patients with type II diabetes mellitus (Tacconelli *et al.*, 2014).

1.5.2. 20-HETE

CYP ω-hydroxylases, namely the CYP4 family, metabolize AA into its cardiotoxic form 20-HETE (Schwartzman *et al.*, 1996; Gross *et al.*, 2005; Zordoky *et al.*, 2008; Yousif *et al.*, 2009; Zordoky *et al.*, 2010a; Wu *et al.*, 2011b; Fava *et al.*, 2012; Anwar-Mohamed *et al.*, 2013; Elshenawy *et al.*, 2013). 20-HETE is considered a potent vasoconstrictor of coronary, renal, cerebral, mesenteric and skeletal muscle vessels (Alonso-Galicia *et al.*, 1999; Gebremedhin *et al.*, 2000; Kunert *et al.*, 2001; Wang *et al.*, 2001; Hoopes *et al.*, 2015). Mechanistically, 20-HETE blocks Kca in the vascular smooth muscle cells thereby activating voltage-gated calcium channels (Hoopes *et al.*, 2015). Furthermore, the vasoconstrictive action of 20-HETE has been reported to be mediated by PKC and MAPK signaling pathways (Muthalif *et al.*, 1998; Obara *et al.*, 2002). The formation of 20-HETE was increased in Ang II-, endothelin-1- and androgen-induced hypertension in addition to spontaneously hypertensive rats (Dunn *et al.*, 2008; Wu *et al.*, 2011a; Hoopes *et al.*, 2015). On the other hand, inhibition of 20-HETE formation protected against Ang-II-induced hypertension (Muthalif *et al.*, 1998; Alonso-Galicia *et al.*, 2002; Chabova *et al.*, 2007).

The cardiotoxic effect of 20-HETE may be mediated through a direct effect on the cardiac muscle in addition to the blood vessels (Elshenawy *et al.*, 2013). For instance, 20-HETE exerts a direct hypertophic effect on rat cardiomyoblasts, H9c2 cells, and promotes the apoptotic effect of Ang-II in primary cultured neonatal rat ventricular myocytes (Tse *et al.*, 2013). Moreover, the biosynthesis of 20-HETE was increased in several models of cardiac hypertrophy and xenobiotic-induced cardiotoxicity (Zordoky *et al.*, 2008; Aboutabl *et al.*, 2009; Alsaad *et al.*, 2012). Of interest, HET0016, an inhibitor of 20-HETE formation, was

shown to protect against BaP- and DOX-induced cardiotoxicty (Zordoky *et al.*, 2008; Aboutabl *et al.*, 2009; Alsaad *et al.*, 2012).

1.5.3. Mid-chain HETEs

Mid-chain HETEs, typified by 5-, 12-, and 15-HETE, are biologically active eicosanoids that result from the metabolism of AA by both LOX and CYP-catalyzed bis-allylic oxidation reaction (LOX-like reaction). On the other hand, 8-, 9-, and 11-HETE are considered non-LOX mid-chain HETE metabolites as they are produced by auto-oxidation reaction in addition to CYP1B1. Lipid peroxidation may have a LOX-like activity. Subsequent to the abstraction of hydrogen, the peroxide produced by oxygenation of the radical can be reduced to a corresponding HETE. In practice, non-enzymatic AA metabolism, like auto-oxidation due to ROS, generates 8-, 9-, and 11-HETE and isoprostanes which are useful biomarkers of oxidative stress in vivo (Guido *et al.*, 1993; Shishehbor *et al.*, 2006).

While 9- and 11-HETE have minimal or no physiological functions (Honn *et al.*, 1992), 8-HETE has been reported to have a proliferator and pro-inflammatory action. This is supported by a previous observation that 8-HETE directly stimulates human neutrophil chemotaxis in vitro (Hunter *et al.*, 1985). 8-HETE is formed as a minor metabolite in human neutrophils and human tracheal epithelial cells (Goetzl *et al.*, 1979; Hunter *et al.*, 1985). In rodents, 8-HETE was characterized as 8(S)-LOX-derived metabolite by identifying 8-hydroperoxy-5,9,11,14-eicosatetraenoic acid [8-H(P)ETE] as precursor product and 8-HETE as a pure S-enantiomer (Furstenberger *et al.*, 1991; Horenstein *et al.*, 2000). In humans, 8-HETE is most probably not the product of 8-LOX since this enzyme has not been detected in human tissues. Instead, 8-HETE may be either formed by non-enzymatic lipid peroxidation or by CYP1B1-catalyzed AA metabolism (Capdevila *et al.*, 1986; Guido *et al.*, 1993; Choudhary *et al.*, 2004). Currently, we will focus on LOX products of AA, namely 5-, 12- and 15-HETE, and we will discuss the role of them in the pathogenesis of hypertension and cardiac hypertrophy.

1.5.3.1. Biosynthesis of mid-chain HETEs

1.5.3.1.1. LOX

1.5.3.1.1.1. Regulation of LOXs enzymes

LOXs, non-heme iron dioxygenase enzymes, constitute a family of lipid-peroxidizing enzymes that insert molecular oxygen into free and esterified polyunsaturated fatty acids. The LOX enzymes are named in line with the specific carbon atoms of AA that are oxidized (Chen *et al.*, 1994). For instance, the 12-LOX oxygenates AA at C-12 and catalyzes the formation of 12-hydroxyperoxyeicosatetraenoic acid (12-HPETE), which then is subsequently converted into 12-hydroxyeicosaenoic acid (12-HETE) by glutathione peroxidase. The platelet-type 12-lipoxygenase was the first mammalian LOX to be cloned as a functionally distinct isoform and is expressed in leukocytes and epidermal cells (Yamamoto, 1992).

Interestingly, though some LOXs form exclusively one metabolite from AA, others are categorized as dual-specificity LOX [12-LOX (leukocyte type) and 15-LOX-1] because they form both 12-HETE and 15-HETE metabolites at the same time (Yamamoto, 1992). 15-LOX-1 has been shown to catalyze the metabolism of linoleic acid to synthesize hydroxy octadecadienoic acids. A second 15-LOX gene was discovered in humans in 1997 (Brash *et al.*, 1997). Based on the amino acid sequence, it seems that the murine homolog of 15-LOX-2 has primarily an 8-LOX like activity, while the rat homolog has not been characterized to date (Jisaka *et al.*, 2000).

Unlike other LOXs, 5-LOX requires the presence of 5-LOX activating protein (FLAP) for 5-HETE synthesis in vivo. FLAP is a member of the MAPEG (Membrane-Associated Proteins in Eicosanoid and Glutathione metabolism) superfamily, which is attached to the nuclear envelope. FLAP has been shown to exist as a trimer, creating a binding pocket that allows AA to laterally diffuse into the protein complex from the membrane (Ferguson *et al.*, 2007). The cytosolic loops of FLAP interact with the 5-LOX catalytic domain and transfer AA into the 5-LOX active site.

1.5.3.1.1.2. LOX expression in cardiovascular system

Although 12/15-LOX was initially extracted from porcine leukocytes (Yokoyama *et al.*, 1986), its tissue expression is relatively wide, including the adrenal gland, the brain, and the kidneys (Watanabe *et al.*, 1993; Gu *et al.*, 1994; Katoh *et al.*, 1994). Significant amounts of 12/15-LOX mRNA were also detected in rat spleen, aorta, lung and leukocytes (Hada *et al.*, 1994). In endothelial cells, the basal level of 12/15-LOX is required for serum-stimulated endothelial cell proliferation and for the binding of the minimally modified low-density lipoprotein-induced monocyte to endothelial cells (Tang *et al.*, 1995; Honda *et al.*, 1999). Although the expression of 12/15-LOX in heart tissue is relatively low compared with the blood vessels, the induced 12/15-LOX activities in heart were 4 times greater than that in reticulocytes, the previously known richest source of this enzyme (Bailey *et al.*, 1995). Furthermore, the 5-LOX mRNA content was significantly greater in the heart compared to the brain in mice (Dzitoyeva *et al.*, 2009). The induction of LOX has been shown to play a major role in the pathogenesis of cardiovascular diseases (CVDs) including hypertension and atherosclerosis. Furthermore, a nonsynonymous polymorphism in 12-LOX was shown to be associated with essential hypertension and urinary 12-HETE (Quintana *et al.*, 2006). Polymorphism of 5-LOX has been reported to be related to the vulnerability of the carotid atherosclerosis plaques (Jin *et al.*, 2010). The 5-LOX protein was prominantly expressed in arterial walls of patients burdened with various lesion stages of atherosclerosis (Spanbroek *et al.*, 2003).

1.5.3.1.2. CYP1B1

1.5.3.1.2.1. Regulation and physiologic role of CYP1B1 enzyme

CYP1B1, CYP-catalyzed bis-allylic oxidation (LOX-like reaction), also metabolizes AA to produce mid-chain HETEs (Choudhary *et al.*, 2004). CYP1B1 is a monooxygenase enzyme that is involved in a number of cellular functions such as metabolism of xenobiotics (Walisser *et al.*, 2005). The CYP1B1 gene was cloned in 1994 from tetrachloro-dibenzo-1/2-dioxin-treated human keratinocyte cells (Sutter *et al.*, 1994). CYP1B1 is a cancer-correlated form of CYP which is basally expressed in extrahepatic tissues and is noticeably overexpressed in a vast majority of primary cancer cells (McFadyen *et al.*, 2001a). The existence of CYP1B1 in cancer cells may be of importance

in the modulation of these cancers by chemotherapeutic agents (McFadyen *et al.*, 2001b; Murray *et al.*, 2001). In that, proteasomal degradation of the CYP1B1 enzyme may explain a high expression level of CYP1B1 in tumor tissues in comparison to normal tissue (Bandiera *et al.*, 2005). CYP1B1 has been shown to be responsible for the bioactivation of a variety of environmental carcinogens such as polycyclic aromatic hydrocarbons (PAHs) to epoxide and diol-epoxide intermediates (Shimada *et al.*, 2004). Besides a transcriptional mechanism, CYP1B1 expression has been shown to be controlled by post-translational mechanisms (Murray *et al.*, 2001). Several studies has shown that the basal and inducible forms of CYP1B1 mRNA do not associate with the expression of AhR mRNA. Moreover, the Cyp1b1 mRNA and protein were constitutively expressed in Arnt-deficient murine hepatoma cells compared to wild-type cells (Eltom *et al.*, 1999). These results proposed that perhaps other mechanisms are implicated in the regulation of CYP1B1, including an AhR-independent mechanism and/or post-transcriptional pathways. For instance, human CYP1B1 is post transcriptionally inhibited by miR-27b (Tsuchiya *et al.*, 2006; Chuturgoon *et al.*, 2014). Mechanistically, miR-27b suppresses the translation of CYP1B1 protein expression through a direct interaction of miR-27b miRNA-recognition elements within the 3′UTR of CYP1B1 mRNA (Tsuchiya *et al.*, 2006; Yu *et al.*, 2016). This interaction might explain a high expression level of CYP1B1 in AhR/ARNT-deficient tumor cells (Tsuchiya *et al.*, 2006). Furthermore, overexpression of miR-200c has been reported to down regulate CYP1B1 enzyme and overcome the underlying resistance of renal cell cancer cells to docetaxel (Chang *et al.*, 2015).

Physiologically, CYP1B1 was found to be involved in fetal development because genetic polymorphisms of CYP1B1 are associated with primary congenital glaucoma (Vasiliou *et al.*, 2008). This was supported by the finding that cyp1b1 knockout mice have demonstrated a structural defect in eyes suggesting a possible role of cyp1b1 in eye development (Libby *et al.*, 2003). Though the precise role of CYP1B1 in glaucoma is still ambiguous, it has been hypothesized that CYP1B1 generates metabolites crucial for the remission and the progression of glaucoma (Vasiliou *et al.*, 2008). For instance, CYP1B1 metabolizes estradiol into 2-hydroxyestradiol and 4-hydroxyestradiol which may reduce intraocular pressure by maintaining blood flow to the optic nerve (Jansson *et al.*, 2001;

Dewundara *et al.*, 2016). On the other hand, the metabolism of AA and testosterone into 12-HETE and 6β-hydroxytestosterone, respectively, may aggravate glaucoma through the increase in the intraocular pressure (Masferrer *et al.*, 1990; Jansson *et al.*, 2001; Vasiliou *et al.*, 2008). While CYP1B1 is known to cause congenital glaucoma due to a structural defect in eyes, it has been postulated that CYP1B1 inhibition acutely or chronically in adults may not result in high ocular pressure and glaucoma (Zhao *et al.*, 2015).

CYP1B1 is also predominantly expressed in breast, ovaries and uterus and preferentially oxidizes a variety of procarcinogens, including polycyclic aromatic hydrocarbons and 17β-estradiol (Sutter *et al.*, 1994; Shimada *et al.*, 1996). Oxidation of 17β-estradiol and estrone into 2/4-hydroxyestradiol, 2/4-hydroxyestrone, 16α-hydroxyestrone, and 16α-hydroxyestradiol metabolites by CYP1B1 promotes the progression of breast and endometrial tumors (Hayes *et al.*, 1996; Lee *et al.*, 2003). The formation of the aforementioned metabolites is associated with the generation of highly reactive quinones and semiquinones which are mutagenic and cause DNA damage (Han *et al.*, 1994; Newbold *et al.*, 2000). Since the expression of CYP1B1 is higher in tumor tissues in comparison to the normal one (Murray *et al.*, 1997), CYP1B1 has become a target for anticancer drugs (Gribben *et al.*, 2005). In that, ZYC300, an anti-CYP1B1 specific for T cells, was used in phase I clinical trial to treat aggressive forms of cancers such as progressive metastatic multiple myeloma (Gribben *et al.*, 2005).

1.5.3.1.2.2. CYP1B1 expression in cardiovascular system

CYP1B1 has been reported to be constitutively expressed in adult human heart at the mRNA level and in the human fetal ventricular cardiomyocyte, RL-14 cell line, at mRNA and protein levels (Choudhary *et al.*, 2005; Maayah *et al.*, 2015e). Furthermore, Cyp1b1 mRNA is significantly expressed in the heart of both AhR-WT and -null adult mice heart representing about 13% of the total cardiac CYPs (Choudhary *et al.*, 2003). In female NMRI mice heart, ethoxy resurofin O-deethylase (EROD) activity, the functional marker of Cyp1b1, was 8- and 180-fold lower than the lung and hepatic EROD activity, respectively (Granberg *et al.*, 2000).

CYP1B1 has been shown to be constitutively expressed in vascular smooth muscle cells, retinal endothelial cells and coronary artery smooth muscle cells (Dubey *et al.*, 2003; Conway *et al.*, 2009; Tang *et al.*, 2009). Although CYP1B1 is expressed in normal tissues and is constitutively active, the induction of CYP1B1 has been reported to play an important role in the pathogenesis of CVDs including ischemic heart diseases, myocardial infarction, hypertension, atherosclerosis, cardiac hypertrophy and heart failure (Korashy *et al.*, 2006; Malik *et al.*, 2012). Furthermore, CYP1B1 polymorphism was shown to play a role in the pathogenesis of heart diseases. In this regard, the hazard ratio for heart disease among non-smokers was 1.9 (95% confidence interval: 1.2-3.2) for CYP1B1*3 GG (19%) versus CC (32%) according to the Copenhagen City Heart Study (Kaur-Knudsen *et al.*, 2009) (Table 1.1).

Table 1.1. The expression of CYP1B1 in the cardiovascular system

Species	Tissue/Segemnt/Cell	CYP1B1	References
Human	Adult heart	mRNA Protein	(Choudhary *et al.*, 2005)
Mouse	WT adult heart AhR-null adult heart	mRNA	(Choudhary *et al.*, 2003)
Mouse	Female NMRI mice heart	EROD	(Granberg *et al.*, 2000)
Human	Coronary artery smooth muscle cells	Protein	(Dubey *et al.*, 2003)
Human	Vascular smooth muscle cells	mRNA Protein	(Conway et al. 2009)
Mouse	Retinal endothelial cells	mRNA	(Tang et al. 2009)

1.5.3.2. Metabolism of mid-chain HETEs

1.5.3.2.1. 5-HETE

5-HETE is metabolized by acyltransferase-dependent acylation into cellular phospholipids and glycerides (Stenson *et al.*, 1979; O'Flaherty *et al.*, 1986; Arai *et al.*, 1997). The enzyme 5-hydroxyicosanoid dehydrogenase (5-HEDH) converts 5-HETE into its 5-keto analog, 5-oxo-6E,8Z,11Z,14Z-eicosatetraenoate (5-oxo-ETE, 5-oxoETE) (Powell *et al.*, 1992). CYP4F2 and CYP4F3 oxidize 5-HETE to 5,20-dihydroxyETE (5,20-diHETE) (O'Flaherty *et al.*, 1986; Kikuta *et al.*, 1998; Kikuta *et al.*, 2000). 12-LOX metabolizes 5-HETE to 5,12-diHETE whereas, COX-2 further metabolizes 5-HETE into its corresponding degradation products, 5-(S),11(R)-diHETE and 5-(S),15(R)-diHETE (Borgeat *et al.*, 1981; Mulugeta *et al.*, 2010; Tejera *et al.*, 2012).

1.5.3.2.2. 12-HETE

12-HETE is metabolized to 12-oxo-ETE by microsomal NAD^+-dependent 12-hydroxyeicosanoid dehdrogenase in porcine polymophonuclear leukocytes (Powell *et al.*, 2015). 12-Oxo-ETE is further metabolized in porcine neutrophils by the NADH-dependent cytosolic enzyme, 12-oxoeicosanoid Δ10-reductase, to 12-oxo-6,8,14-eicosatrienoic acid (12-oxo-ETrE; i.e. 10,11-dihydro-12-oxo-ETE) (Powell *et al.*, 2015). CYP4F2 and CYP4F3 oxidize 12-HETE to 12,20-dihydroxyETE (12,20-diHETE) (Marcus *et al.*, 1984; Kikuta *et al.*, 1998; Kikuta *et al.*, 2000). Tetranor-12-HETE is the major β-oxidation product resulting from peroxisomal metabolism of 12-HETE in numerous tissues including vascular smooth muscle cells (Lacape *et al.*, 1992). 12-HETE released from platelets is converted into 5, 12-dihydroxy-(E,Z,E,Z)-6,8,10,14-eicosatetraenoic acid [5, 12-DHETE] by the 5-lipoxygenase in Ca^{2+}-ionophorestimulated neutrophils (Marcus *et al.*, 1982).

1.5.3.2.3. 15-HETE

15-HETE is oxidized into its keto analog, 15-oxo-ETE by NAD^+-dependent 15-hydroxyprostaglandin dehydrogenase. 15-oxo-ETE is similar to 15-HETE in that its product can be converted to 13-cysteinyl-glycyl-glutamyl and then 13-cysteinyl-glycine products (Bergholte *et al.*, 1987; Hammond *et al.*, 2012). 5-LOX oxidizes 15-HETE to form its 5,6-trans epoxide derivative which may then rearrange to the lipoxins (LX), LXA4

and LXB4 or to 5,15-dihydroperoxy-6E,8Z,11Z,13E-eicosatetraenoate (5,15-diHETE) (Serhan, 2005). 15-HETE may be also acylated into membrane phospholipids, particularly phosphatidylinositol and phosphatidylethanolamine (Brezinski *et al.*, 1990; Brinckmann *et al.*, 1998; Maskrey *et al.*, 2007; Thomas *et al.*, 2010). The phosphatidylethanolamine-bound 15-HETE may be then metabolized to phosphatidylethanolamine-bound 15-oxo-ETE (Hammond *et al.*, 2012).

1.5.3.3. Mid-chain HETEs and their role in cardiovascular diseases
1.5.3.3.1. The role of mid-chain HETEs in the vasculature

Prior to explaining the role of mid-chain HETEs in the pathogenesis of hypertension, it is imperative to discuss the vasoactive functions of these metabolites. Increased formation of mid-chain HETE metabolites by the biological agents involved in cardiovascular dysfunction has been reported in vascular smooth muscle cells, endothelial cells, and monocytes (Conrad *et al.*, 1992; Natarajan *et al.*, 1993; Natarajan *et al.*, 1996; Patricia *et al.*, 1999). Mid-chain HETEs have direct effects like chemotaxis, changes in vascular tone and production of vascular endothelial growth factor, a potent angiogenic agent (Nakao *et al.*, 1982; Stern *et al.*, 1989; Tang *et al.*, 1995; Honda *et al.*, 1999). Mid-chain HETEs have been shown to exhibit direct mitogenic effects and to increase the levels of the key extracellular matrix protein fibronectin in vascular smooth muscle cells (Natarajan *et al.*, 1994). Furthermore, they also mediate the hypertrophic effect of Ang II and have a direct hypertrophic effect on vascular smooth muscle cells (Reddy *et al.*, 2002; Zhang *et al.*, 2014).

The role of 5- and 15-HETEs as vasoactive monohydroxyeicosatetraenoic acids have been investigated on the pulmonary artery of isolated perfused lung (Burhop *et al.*, 1988). It has been shown that 5- and 15-HETEs were able to induce pulmonary vasoconstriction, lung vascular permeability and edema (Burhop *et al.*, 1988). 15-HETE mediates hypoxia-induced pulmonary vascular medial thickening, intimal endothelial cells migration and angiogenesis (Ma *et al.*, 2011; Shen *et al.*, 2013). Mechanistically, 15-HETE controlled the cell cycle progression from the G0/G1 phase to the G2/M$^+$S phase and induced the microtubule formation in cell nucleus (Ma *et al.*, 2011). The effect of 15-HETE was

mediated via Rho-kinase pathway (ROCK) (Ma *et al.*, 2010). The prominence of ROCK in chronic hypoxic pulmonary hypertension is emphasized because of its potential role in maintaining vasoconstriction and the vascular wall cell proliferation (Kroll *et al.*, 2009).

The vasoactive effects of 12-HETE have been investigated on isolated perfused canine renal arcuate arteries using videomicroscopy (Ma *et al.*, 1991). 12-HETE was found to act as a vasoconstrictor in small renal arteries since it reduced vascular diameter by 63 um (from 306 um), which was 37% of the maximal vasoconstrictor response to norepinephrine (Ma *et al.*, 1991; Yiu *et al.*, 2003). Mechanistically, the vasoconstrictor response induced by 12-HETE was associated with depolarization of vascular smooth muscles. In addition, 12-HETE is an inhibitor of the Na^+-K^+-ATPase in the corneal epithelium (Schwartzman *et al.*, 1987; Masferrer *et al.*, 1990) and the kidney (Masferrer *et al.*, 1990). Furthermore, the incubation of renal arteries obtained from ischemic kidneys with nordihydroguaiaretic acid (NDGA), a LOX inhibitor, showed no effect on the formation of 12-HETE suggesting that the 12-HETE formed by renal arteries may be produced by the LOX pathway-independent mechanism (Ma *et al.*, 1991). In agreement with this suggestion, it has been demonstrated that inhibitors of CYP diminish the myogenic echo of dog renal arcuate arteries (Kauser *et al.*, 1991). The L-type calcium channel may be also involved in 12-HETE-mediated vasoconstriction in renal blood vessels. In that, the vasoconstrictive effect of 12-HETE was abolished during L-type calcium channel inhibition (Yiu *et al.*, 2003). Renal myocyte Ca^{2+} response following exposure to 12-HETE was greatly reduced in the absence of extracellular Ca^{2+} or calcium channel blockade, implying it as an important mechanism responsible for the afferent arteriolar vasoconstriction stimulated by 12-HETE (Yiu *et al.*, 2003).

1.5.3.3.3. The role of mid-chain HETEs in the pathogenesis of hypertension

Hypertension is a powerful risk factor for heart disease in which the force of the blood against arterial walls is high enough to cause adverse effects, such as cardiac hypertrophy, acute myocardial infraction, stroke and coronary artery disease (Vakili *et al.*, 2001; Chaturvedi, 2004; DiNicolantonio *et al.*, 2015). Accumulating data provides convincing evidence that mid-chain HETEs are involved in the development of hypertension, in that,

the generation of mid-chain HETEs was shown to be increased in patients with essential hypertension (Gonzalez-Nunez *et al.*, 2001; Dolegowska *et al.*, 2009). This generation suggests a role for these metabolites in the pathogenesis of essential hypertension.

Experimentally, mice lacking macrophage 12/15-LOX have been reported to be resistant to both N(G)-nitro-L-arginine-methyl ester (L-NAME)- and deoxycorticosterone acetate/high-salt-induced hypertension (Kriska *et al.*, 2012). Furthermore, 12-HETE participates in Ang II-induced hypertension by the modulation of Ang II–induced aldosterone secretion. In this regards, BW755c, a non-selective LOX blocker, inhibited the Ang II-stimulated level of aldosterone in a dose-dependent manner (Nadler *et al.*, 1987). The specific role of 12-HETE is supported by the following findings, first; Ang II-induces 12-HETE production in adrenal glomerulosa cells; second: the inability of BW755c to block the binding of Ang II with its receptor, suggesting an AT-I receptor-independent mechanism; and third: the addition of 12-HETE and 12-HPETE restores the Ang II stimulatory effects during LOX inhibition (Nadler *et al.*, 1987).

The above observations support the fact that that the 12-HETE formation may be an obligatory step in Ang-II control of aldosterone secretion. Moreover, it raises a question of whether or not 12-HETE is a mediator of the Ang II effect in vascular tissue parallel to its effect in the adrenal cortex. This hypothesis was confirmed by a previous study which investigated the potential role of 12-HETE in the vasculature in an Ang II-dependent model of hypertension. In that, the two-kidney, one-clip (2K, lC) Goldblatt hypertensive rat was used as a model since it is primarily dependent on the renin-Ang system (Freeman *et al.*, 1977; DeForrest *et al.*, 1982). Acute and chronic administration of phenidone, a non-selective LOX inhibitor, prevents the development of hypertension in this model (Nozawa *et al.*, 1990). The antihypertensive effect of phenidone was accompanied by a suppression of 12-HETE formation produced by aortic segments in the 2K, 1C rats (Nozawa *et al.*, 1990). In agreement with the above findings, it has been shown that 12-HETE potentiates the Ang II-induced pressor response (Takai *et al.*, 2001). In addition, renal microvascular 12-HETE formation has been reported to be increased in response to Ang II-induced renal vasoconstriction (Yiu *et al.*, 2003). Inhibiting the formation of 12-HETE markedly

attenuated the in vitro contractile response to Ang II of femoral artery rings parallel with lowering the pressor effect in vivo (Stern *et al.*, 1989). The previous studies supported the fact that the formation of 12-HETE in vascular tissue may mediate, at least in part, the vasoconstrictor actions of Ang II.

The mechanism by which the inhibition of 12-HETE formation attenuates the rise in blood pressure produced by Ang II has been investigated by studying the changes in cytosolic calcium using the fluorescent dye fura-2 in cultured rat vascular smooth muscle cells (Saito *et al.*, 1992). In that model, baicalein and 5,8,11-eicosatriynoic acid, 12-LOX inhibitors, repressed Ang II-induced increase in cytosolic calcium in both normal and calcium-poor buffer (Saito *et al.*, 1992). The addition of 12-HETE alone to the cells had no acute effect on intracellular calcium concentration. However, the addition of 12-HETE restored the initial calcium response to Ang II in vascular smooth muscle cells pretreated with LOX inhibitors. 12-HETE, by increasing Ang II-induced cytosolic calcium in vascular tissue, may enhance pressor induced vascular reactivity (Sasaki *et al.*, 1997). Furthermore, 5,8,11-eicosatriynoic acid, a 12-HETE formation inhibitor, repressed vasopressin and endothelin-stimulated induction of the intracellular calcium (Saito *et al.*, 1992). Taken together, 12-HETE may participate in the contractile actions of Ang II through modulation of the intracellular calcium in vascular smooth muscle cells.

Spontaneously hypertensive rats (SHR), often with the Wistar Kyoto rat as the normotensive control, is the most commonly used model of hypertension, with over 5000 Pubmed references in the last 10 years. The importance of this model comes from the following factors; first, it is clinically relevant; second, it has uniform polygenetic disposition and excitatory factors; and third, it lacks inter-individual variation (Lindpaintner *et al.*, 1992). Accordingly, the modulation in the formation of mid-chain HETEs using this model would reflect, at least in part, their importance in the pathogenesis of essential hypertension.

The association between the formation of 12-HETE and intra-arterial blood pressure in SHR and Wistar-Kyoto rats has been investigated using both a cross-sectional analysis and

an acute pharmacological intervention (Stern *et al.*, 1996; Sasaki *et al.*, 1997). 12-HETE production was substantially induced in SHR compared with Wistar-Kyoto rats. An overall linear correlation between 12-HETE and systolic pressure suggested a positive relationship between systolic arterial pressure and the formation of 12-HETE (Stern *et al.*, 1996). This is consistent with the finding that specific 12-LOX inhibitors, cinnamyl-3,4-dihydroxycyanocinnamate and 5,8,11-eicosatriynoic acid, significantly provoked a noticeable hypotensive effect in SHR but not in Wistar-Kyoto rats (Stern *et al.*, 1996; Sasaki *et al.*, 1997). This reduction in arterial pressure was accompanied by a clear inhibition in 12-HETE formation in both serum and aortic smooth muscle, suggesting an important role of 12-HETE in the pathogenesis of elevated arterial blood pressure in SHR.

Both 5- and 15-HETEs have also been reported to play role in the development of hypertension. In that respect, the formation of 5- and 15-HETEs was markedly increased in SHR (Koeners *et al.*, 2011). Treatment of spontaneously hypertensive female rats with 12-(3-adamantan-1-yl-ureido)-dodecanoic acid during the perinatal phase was associated with a significant decrease in the formation of 5- and 15-HETE suggesting, an important role of these HETEs in the pathogenesis of hypertension (Koeners *et al.*, 2011). The importance of 15-HETE as a potential mediator of hypertension is highlighted by its high formation level in placentae from pregnancies complicated by pregnancy-induced hypertension compared with gestation-matched controls (Mitchell *et al.*, 1991). Mechanistically, 15-HETE and its hydroperoxy precursor inhibited prostacyclin biosynthesis, which may contribute to the pathological sequelae of pregnancy-induced hypertension (Mitchell *et al.*, 1991).

1.5.3.3.4. The role of mid-chain HETEs in the pathogenesis of cardiac hypertrophy

Several lines of evidence support the role of mid-chain HETEs in the development of cardiac hypertrophy, in that the formation of mid-chain HETEs was shown to increase during pressure overload-induced cardiac hypertrophy (El-Sherbeni *et al.*, 2014a). The importance of descending aortic constriction (DAC) as a model of cardiac hypertrophy is pronounced since it is more clinically relevant as the cardiac hypertrophy develops over a relatively longer period of time (Patten *et al.*, 2009). Of particular interest in the

aforementioned model, the generation of mid-chain HETEs was accompanied by the induction of CYP1B1 protein expression levels, implicating CYP1B1 enzyme as a crucial generator of mid-chain HETEs. The role of CYP1B1 in the formation of mid-chain HETEs was further confirmed by the ability of the recombinant CYP1B1 enzyme to catalyze the formation of mid-chain HETEs (Choudhary *et al.*, 2004; El-Sherbeni *et al.*, 2014a).

The overexpression of 12-LOX in cardiac fibroblast cells was used as a model to investigate the hypertrophic effect of 12-HETE (Wen *et al.*, 2003). The significance of this model lies in the fact that the growth of fibroblast cells and their concomitant deposition of extracellular matrix protein is one of the characteristic of cardiac fibrosis (Lal *et al.*, 2014). The previous detrimental effects account for the abnormal myocardial stiffness and ultimate ventricular dysfunction that is seen in many forms of pathogenic cardiac hypertrophy (Souders *et al.*, 2009). The expressed 12-LOX enzyme was functionally intact after transfection since overexpressed 12-LOX cardiac fibroblasts showed a higher level of 12-HETE in comparison to control cells. Overexpression of 12-LOX induced cell [(^{3})H]leucine and [(^{3})H]thymidine incorporation, cell protein content, fibronectin content, collagen protein expression and enlargement of cell size compared with that of mock-transfected cells (Wen *et al.*, 2001). 12-LOX overexpression leads to morphologic evidence of cellular hypertrophy in rat cardiac fibroblasts. This is supported by cell morphologic examination using hematoxylin and eosin (H & E) staining. This demonstrated that long axis of nuclei and the mean number of nucleoli of 12-LOX-transfected cells was significantly higher than mock-transfected cells (Wen *et al.*, 2001; Wen *et al.*, 2003).

15-HETE has been shown to increase the sensitivity of the ISO-mediated β-adrenergic response in cardiomyocytes and has been proposed to be implicated in heart failure by induction of cardiac fibrosis (Wallukat *et al.*, 1994; Levick *et al.*, 2007; Kayama *et al.*, 2009; Zhang *et al.*, 2014). Furthermore, it has been shown that norepinephrine induced its hypertrophic effect through the induction of 12- and 15-HETE (Parmentier *et al.*, 2001). Mechanistically, 15-HETE is markedly incorporated into the cellular phosphatidylinositol pool. The 15-HETE-containing phosphatidylinositols may then be converted to 15-HETE-

substituted diacylglycerol. This diacylglycerol species may in turn modulate a PKC (Wallukat *et al.*, 1994). 15-HETE also induced adventitia fibrosis and fibroblast phenotypic alterations which depended on signaling of the transforming growth factor-β1 (Zhang *et al.*, 2014). The above observation comes in agreement with a previous finding which illustrated that baicalein, a 12/15LOX inhibitor, attenuated myocardial fibrosis in spontaneously hypertensive rats (Kong *et al.*, 2011). Moreover, the 12/15 LOX inhibitors, baicalein and wogonin, have been reported to suppress collagen deposition in response to Ang II (Kong *et al.*, 2010).

5-HETE has been shown to participate in the pathogenesis of Ang-II-induced hypertrophy (Revermann *et al.*, 2011), in that LP105, a 5-LOX blocker, inhibited Ang-II-induced hypertrophy in ApoE-/- mice. This was manifested by the ability of LP105 to show a lower heart rate, a trend towards reduced heart to body weight ratio and it significant prevention of the increase in aortic weight and diameter mediated by Ang II (Revermann *et al.*, 2011). Furthermore, selenium was reported to reduce diabetic cardiac hypertrophy through down regulation of 5-LOX and its corresponding metabolite, 5-HETE (Dhanya *et al.*, 2014).

1.5.3.3.4. The role of mid-chain HETEs in the pathogenesis of Heart failure and Cardiomyopathy

The role of mid-chain HETEs is not restricted to cardiac hypertrophy but also involved in the development of cardiac dysfunction and heart failure. It has been reported that 12- and 15-HETEs were markedly up-regulated in heart failure (Kayama *et al.*, 2009). The role of 12- and 15-HETEs in the pathogenesis of heart failure was investigated in transgenic mice overexpressing 12/15-LOX in cardiomyocytes. The overexpression of 12/15-LOX and its corresponding 12- and 15-HETE metabolites was able to induce systolic dysfunction, infiltration of macrophages, up-regulation of monocyte chemoattractant protein 1 and cardiac fibrosis (Kayama *et al.*, 2009). In HL-1 mouse cardiac myocytes, 12-HETE increased intramitochondrial calcium and mitochondrial NO, and induced apoptosis (Nazarewicz *et al.*, 2007). Furthermore, treatment of cardiac fibroblasts and endothelial cells with 12-HETE significantly induced the expression of monocyte chemoattractant protein 1. On the other hand, disruption of 12/15-LOX significantly inhibited cardiac

monocyte chemoattractant protein 1 expression, macrophage infiltration and restored systolic dysfunction induced by chronic pressure overload (Kayama *et al.*, 2009).

12- and 15-HETE were also implicated in the development of diabetic cardiomyopathy. Treatment of mice with streptozotocin, a well-known diabetes inducer, up-regulated the expression of 5-LOX and 12/15-LOX and its corresponding AA metabolites, 12- and 15-HETEs as well as inducing cardiac dysfunction and fibrosis (Kumar *et al.*, 2013; Suzuki *et al.*, 2015). Interestingly, disruption of 12/15-LOX significantly inhibited the induction of TNF-α, nuclear factor kappa B (NF-κB), ROS and eventually attenuated streptozotocin-induced cardiac dysfunction and fibrosis (Suzuki *et al.*, 2015).

In vitro, neonatal cultured cardiomyocytes incubated with high glucose conditions illustrated a high expression of 12/15-LOX enzyme. The increase in the expression level of 12/15LOX was associated with an induction of TNF-α, NF-κB, and collagen markers. Of interest, 12/15-LOX inhibitor was able to reduce the induction of the aforementioned inflammatory markers implying the role of 12- and 15-HETE in the development of diabetic cardiomyopathy (Suzuki *et al.*, 2015). Tables 1.2 and 1.3 summarize the effect and the role of mid-chain HETEs in the development of CVDs.

Table 1.2. Pathological roles of mid-chain HETEs on CVS

Species	Tissue/Segemnt/Cell	HETE	Effect	References
Guinea Pig Rat	Isolated perfused lung Pulmonary artery smooth muscle	5-HETE 15-HETE	Vasoconstriction Hypertrophy	(Burhop *et al.*, 1988; Ma *et al.*, 2011; Shen *et al.*, 2013)
Dog Rat	Small renal arterties	12-HETE	Vasoconstriction	(Ma *et al.*, 1991; Yiu *et al.*, 2003)
Mouse	Cardiac fibroblast cells	12-HETE	hypertrophy	(Wen *et al.*, 2003)
Rat	Cardiomyocytes	15-HETE	Supersensitivity to β-adrenergic agonists	(Wallukat *et al.*, 1994)
Mouse	Cardiac fibroblast cells Endothelial cells	12-HETE	monocyte chemoattractant protein 1 induction	(Kayama *et al.*, 2009)
Rat	Adrenal glomerulosa cells	12-HETE	Ang-II induced aldosterone secretion	(Nadler *et al.*, 1987)

Table 1.3. The generation of mid-chain HETEs during hypertension and cardiac hypertrophy

Species	Disease	Model	HETE	References
Rat	Hypertension	Two-kidney, one-clip (2K, lC) Goldblatt	12-HETE	(Nozawa *et al.*, 1990)
Rat	Hypertension	Spontaneously hypertensive rats	5-HETE 12-HETE 15-HETE	(Stern *et al.*, 1996; Sasaki *et al.*, 1997; Koeners *et al.*, 2011)
Rat	Cardiac hypertrophy	Descending aortic constriction	5-HETE 12-HETE 15-HETE	(El-Sherbeni *et al.*, 2014a)
Mouse	Heart failure	Transgenic mice	12-HETE 15-HETE	(Kayama *et al.*, 2009)
Mouse	Diabetic cardiomyopathy	Streptozotocin	12-HETE 15-HETE	(Kumar *et al.*, 2013; Suzuki *et al.*, 2015)
Mouse	Hypertension-induced-renal dysfunction	Ang II	12-HETE	(Jennings *et al.*, 2012b)
Human	Essential hypertension	Patients	12-HETE 5-HETE	(Gonzalez-Nunez *et al.*, 2001; Dolegowska *et al.*, 2009)

41

1.5.3.4. Molecular mechanism of mid-chain HETEs action

Understanding the mechanism by which mid-chain HETEs are involved in cardiac hypertrophy and myopathy could be a critical issue in cardiac homeostasis. However, these molecular mechanisms have not been fully elucidated, and no precise cellular receptors for mid-chain HETEs have been identified yet. Importantly, some potential pathways, such as PKC, MAPK and NF-κB, by which these AA metabolites may stimulate cellular growth and hypertrophy have been explored. PKC, MAPK and NF-kB are pivotal to this process as central mediators of cardiac remodeling in response to injury and/or cardiac wall stress. Therefore, it is necessary to discuss the role of mid-chain HETEs on each pathways.
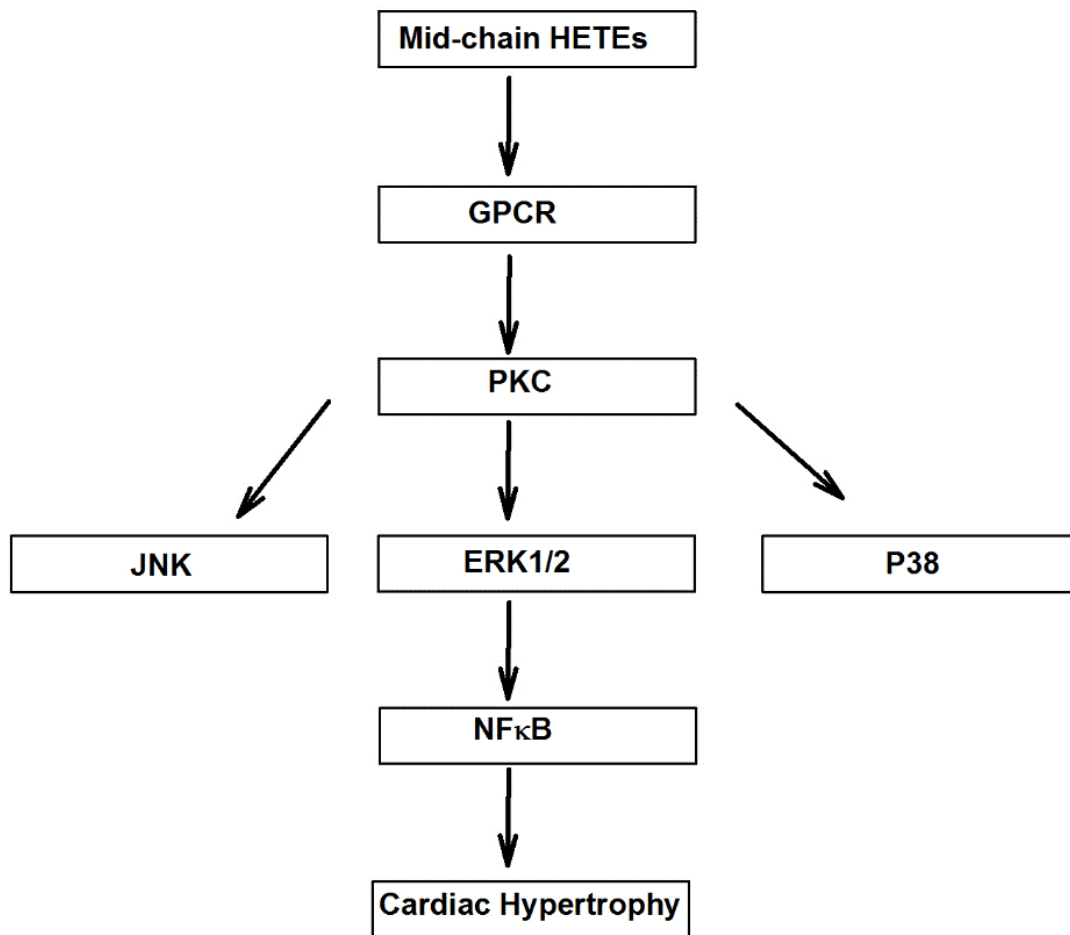
Figure 1.3. Molecular Mechanism of mid-chain HETEs. Mid-chain HETEs bind to G-protein coupled receptor 31 (GPCR), induce GTPγS coupling and activate PKC. The activated PKC phosphorylates MAPK signaling cascade components, ERK, JNKs and p38. Phosphorylated MAPK then stimulate NF-κB binding to its responsive element sequences, κB, to initiate target gene transcription that is involved in cardiac hypertrophy.

1.5.3.4.1. MAPK

Mid-chain HETEs were shown to induce cell growth in cancer and cardiac fibroblast cells through the ERK1/2 signaling pathway (Szekeres *et al.*, 2000; O'Flaherty *et al.*, 2002; Lu *et al.*, 2006a; Guo *et al.*, 2011a; Garcia-Verdugo *et al.*, 2012; Cabral *et al.*, 2013; Kang *et al.*, 2013; Song *et al.*, 2015b). Norepinephrine has been reported to stimulate cytosolic phospholipase A(2)-dependent phospholipase D(2) through mid-chain HETEs via the ERK pathway by a mechanism involving tyrosine phosphorylation of phospholipase D(2) in rabbit vascular smooth muscle (Parmentier *et al.*, 2001). Furthermore, it has been shown that Ang II induced cellular hypertrophy in H9c2 cells through ERK1/2 but not p38 or JNK (Zong *et al.*, 2013). Of particular interest in this study, baicalein, 12/15 LOX inhibitor, blocked the cellular hypertrophic effect of Ang-II through the ERK1/2 signaling pathway (Zong *et al.*, 2013). The effect of mid-chain HETEs is not restricted only to ERK1/2 but also involves the activation of the p38 pathway. In that, 12-HETE has been shown to induce hypertrophy in cardiac fibroblasts through the p38 signaling pathway (Wen *et al.*, 2003). Furthermore, treatment of porcine vascular smooth muscle cells with 12-HETE led to hypertrophy through the activation of Ras and p38 MAPK (Reddy *et al.*, 2002). Inhibition of p38 using SB202190 significantly blocked the hypertrophy induced by 12-HETE in both cardiac fibroblast and porcine vascular smooth muscle cells, suggesting an important role of p38 in 12-HETE induced cellular hypertrophy (Reddy *et al.*, 2002; Wen *et al.*, 2003). Ang II also induced protein synthesis and hypertrophy in rat vascular smooth muscle through mid-chain HETEs/p38 signaling pathways (Yaghini *et al.*, 2007). Moreover, 12- and 15-HETEs have been reported to augment AT-1 receptor and Ang II signaling through ERK and p38 signaling pathways (Xu *et al.*, 2008).

1.5.3.4.2. NF-κB

Mid-chain HETEs have been reported to induce cell growth and angiogenesis through the NF-κB signaling pathway (Stoltz *et al.*, 1996; Kandouz *et al.*, 2003; Prato *et al.*, 2010; Vonach *et al.*, 2011). Viral vector-mediated 12/15-LOX overexpression in vascular smooth muscle cells stimulated the expression of NF-κB (Dwarakanath *et al.*, 2008). Of particular interest in this study, mid-chain HETEs induced NF-κB through a MAPK dependent mechanism (Dwarakanath *et al.*, 2008; Guo *et al.*, 2011b). Inhibition of 12/15 LOX,

Baicalein, attenuates Ang II-Induced cardiac hypertrophy and fibrosis through the inhibition of ERK1/2 and NF-κB signaling pathways in mice (Wang *et al.*, 2015).

1.5.3.4.3. PKC

It has been demonstrated that 12-HETE activates PKCα through GPCR-mediated hydrolysis of inositol phospholipids (Liu *et al.*, 1995). Several studies also suggest that 12-HETE activates the PKCα/ERK1/2 axis via an unidentified plasma membrane GPCR (Szekeres *et al.*, 2000). Mechanistically, treatment with mid-chain HETEs, mainly 12-HETE, specifically induces GTPγS coupling in membrane fractions of GPCR31-transfected cells (Guo *et al.*, 2011b). Furthermore, 12-HETE stimulated ERK1/2 and NF-κB activation in GPR31-transfected cells. In contrast, there was no detectable ERK1/2 or NF-κB activation in 12-HETE-treated mock-transfected cells (Guo *et al.*, 2011b). Furthermore, it has been shown that 12-HETE stimulates PKCα/ NF-κB axis in freshly isolated aortic endothelial cells (Bolick *et al.*, 2005). 5- and 15-HETE has been shown to induce their pathological responses through a PKCα/MAPK signaling pathway (Rao *et al.*, 1994; Awasthi *et al.*, 2001; Guo *et al.*, 2009). In addition, 15-HETE specifically stimulates a signal transduction cascade leading to a supersensitivity of the cells toward β-adrenergic agonists, which involves the phosphatidylinositol cycle and a PKC (Wallukat *et al.*, 1994). Figure 1.3 summarize the molecular mechanism of action of mid-chain HETEs.

1.5.3.5. Mid-chain HETEs as promising drug targets

As suggested in the previous discussions, inhibiting the formation of mid-chain HETEs can be achieved by suppressing both LOXs and CYP1B1 enzymes. In contrast to receptor blockade, suppression of these enzymes directly results in decreasing the formation of fatty acid metabolites with concomitant dampening of the associated inflammatory and hypertrophy activities that contribute to the pathogenesis of cardiovascular diseases.

1.5.3.5.1 Flavonoids

Baicalein, a low molecular weight 5,6,7-trihydroxyflavone isolated from *Scutellaria baicalensis Georgy* roots, is a key component of Chinese herbal medicine *Scutellaria*

species, commonly used to treat bacterial and viral infections and cardiovascular diseases in China (Li-Weber, 2009). Early studies conducted on rat platelets showed that baicalein exert potent inhibitory activity against 12/15-LOX in addition to CYP1B1 (Chan *et al.*, 2002; Deschamps *et al.*, 2006). Baicalein exerts protective effects against I/R injury, hypertension and cardiac dysfunction in mouse or rat models (Li-Weber, 2009). Baicalein significantly attenuated Ang II-induced elevation of blood pressure, cardiac hypertrophy, and fibrosis. These beneficial effects were associated with inhibition of inflammation, oxidative stress, and multiple signaling pathways ERK1/2 and NF-κB (Wang *et al.*, 2015). In addition to baicalein, the flavonoid luteolin, 3′, 4′, 5, 7-tetrahydroxyflavone, and a naturally occurring furocoumarin, imperatorin, exhibit anti-inflammatory and antioxidant activities (Abad *et al.*, 2001; Lopez-Lazaro, 2009; Guo *et al.*, 2012). Luteolin and imperatorin exert an inhibitory effect against both LOXs and CYP1B1 at nanomolar concentrations (Abad *et al.*, 2001; Sadik *et al.*, 2003; Kim *et al.*, 2005; Mammen *et al.*, 2005). Recent study has demonstrated that luteolin protects against the progression of diabetes mellitus-induced cardiac dysfunction by the attenuation of myocardial oxidative stress (Wang *et al.*, 2012). Imperatorin can attenuate cardiac hypertrophy both in vivo and in vitro and the progression of cardiac hypertrophy to heart failure (Zhang *et al.*, 2012b). However, naturally occurring furocoumarin and flavonoid compounds are known to have poor bioavailability in that they are rapidly metabolized and excreted, which limits their uses clinically.

1.5.3.5.2. Zileuton

Zileuton [Leutrol, N-(1-benzo(b)-thien-2yl) ethyl-N-hydroxyurea] is a specific 5-LOX inhibitor that was developed by Abbott (Carter *et al.*, 1991). Zileuton apparently inhibits 5-LOX via iron chelation but is lacking of 12- and 15-LOX inhibitory activity. Furthermore, it has an inhibitory activity against the CYP1 family (Wang *et al.*, 2009). Of interest, the 5-HETE formation inhibitor, zileuton, has been shown to protect cardiomyocytes from H_2O_2-induced cytotoxicity which suggests its possible application as a potent therapeutic agent for the prevention of ischemia and heart failure (Kwak *et al.*, 2010).

Mid-chain HETEs probably produced by the CYP pathway might be involved in the mitogenesis and the regulation of cellular growth. This is supported by the finding that CYP inhibitors such as SKF-525A persuade a cell cycle delay and inhibit cellular hypertrophy whereas, LOX inhibitors such as NDGA have failed to produce such effects (Nieves *et al.*, 2006). The inhibition of cellular growth in response to SKF-525A was associated with CYP inhibition and the subsequent impairment of mid-chain HETEs synthesis. Interestingly, exogenous addition of mid-chain HETEs reversed the effects of SKF-525A confirming an important role of CYP in the regulation of mid-chain HETEs (Nieves *et al.*, 2006).

1.5.3.5.3. TMS

TMS, a methoxy derivative of resveratrol, is a potent and selective competitive inhibitor of CYP1B1 with an IC_{50} of 3 nM for ethoxyresorufin-O-deethylase and $\sim$90 nM for E2 4-hydroxylation. Compared to other potent inhibitors such as α-naphthoflavone and resveratrol which are known CYP1 family inhibitors with no selectivity between CYP1B1 and CYP1A2, TMS is $\sim$50- and 520-fold specific for inhibition of CYP1B1 in comparison to CYP1A1 and CYP1A2, respectively (Chun *et al.*, 2001). Accordingly, TMS may help as a chemical scalpel for dissecting CYP1B1 activity from the overall activity of CYP1 family members and LOX enzymes against the formation of mid-chain HETEs. In contrast to resveratrol, TMS is rapidly absorbed upon oral administration and has a long half-life, and high tissue distribution (Lin *et al.*, 2010) making TMS a promising candidate to be used clinically.

TMS and *Cyp1b1* gene disruption have been shown to reduce the formation of mid-chain HETEs induced by Ang II (Jennings *et al.*, 2012b). Of particular interest in this study, the levels of 12/15 LOX, Cyp4a, and Cyp4f protein were not changed in the Cyp1b1−/− mice suggesting a CYP1B1-specific production of mid-chain HETEs. TMS and Cyp1b1 gene disruption also exert protective effects against Ang II-induced hypertension and associated cardiac hypertrophy, fibrosis, and inflammation (Jennings *et al.*, 2010). Furthermore, they reversed deoxycorticosterone –salt-induced hypertension and cardiac and vascular hypertrophy and minimized renal dysfunction through the inhibition of reactive oxygen species (ROS) and MAPK (Sahan-Firat *et al.*, 2010). TMS displays an

antihypertensive effect and inhibits its associated cardiovascular events in spontaneously hypertensive rats, primarily by inhibiting ROS, pro-inflammatory cytokines, catecholamines and MAPK (Jennings *et al.*, 2014b). The cyp1b1 gene disruption was found to attenuate Ang-II-induced hypertension by inhibiting the formation of cyp1b1-dependent testosterone metabolites, 6β-hydroxytestosterone and 16α-hydroxytestosterone, in male mice (Pingili *et al.*, 2015; Pingili *et al.*, 2016).

1.6. 2-Methoxyestradiol

In contrast to the negative effects of the cardiotoxic metabolites generated by CYP1B1, CYP1B1 also has an important role in the formation of a cardioprotective metabolite, 2-methoxyestradiol (2ME) (Jennings *et al.*, 2014a). This is supported by a recent finding demonstrating that Ang-II caused oxidative stress, cardiovascular changes, endothelial dysfunction and enhanced vascular reactivity in cyp1b1(-/-) but not in cyp1b1(+/+) female mice (Jennings *et al.*, 2014a). Furthermore, the cardiovascular remodeling induced by Ang-II coincided with a dramatic diminution in the formation of 2ME in cyp1b1(-/-) mice establishing a 2ME-dependent mechanism. Moreover, when these mice were treated with 2ME, the typical increase in blood pressure in cyp1b1(-/-) mice did not occur, suggesting that not only 2ME restored these knockout mice to normal levels, but also that 2ME may be a physiologically substantial metabolite at naturally occurring titers (Figure 1.4).

2ME is an endogenous metabolite of estradiol resulting from the sequential metabolism of estradiol to 2-hydroxyestradiol (2-HE) and 2-ME by CYP1B1 and catechol-O-methyltransferase (COMT), respectively. Historically 2ME was contemplated an inactive metabolite and the effect of COMT was assumed to be an alternative pathway of estrogen elimination. Later, several studies have demonstrated that 2ME possesses cardioprotective activity by inhibiting vascular smooth muscle reactivity, reducing endothelin-1 levels, upregulating COX-2 and its associated prostacyclin production and inhibiting cardiac fibroblast migration and proliferation (Barchiesi *et al.*, 2002; Barchiesi *et al.*, 2010). In various animal models, these effects have resulted in a substantial decrease in the vascular hypertrophy and right ventricular remodeling, resulting in reduced disease progression and improved survival (Tofovic *et al.*, 2010).
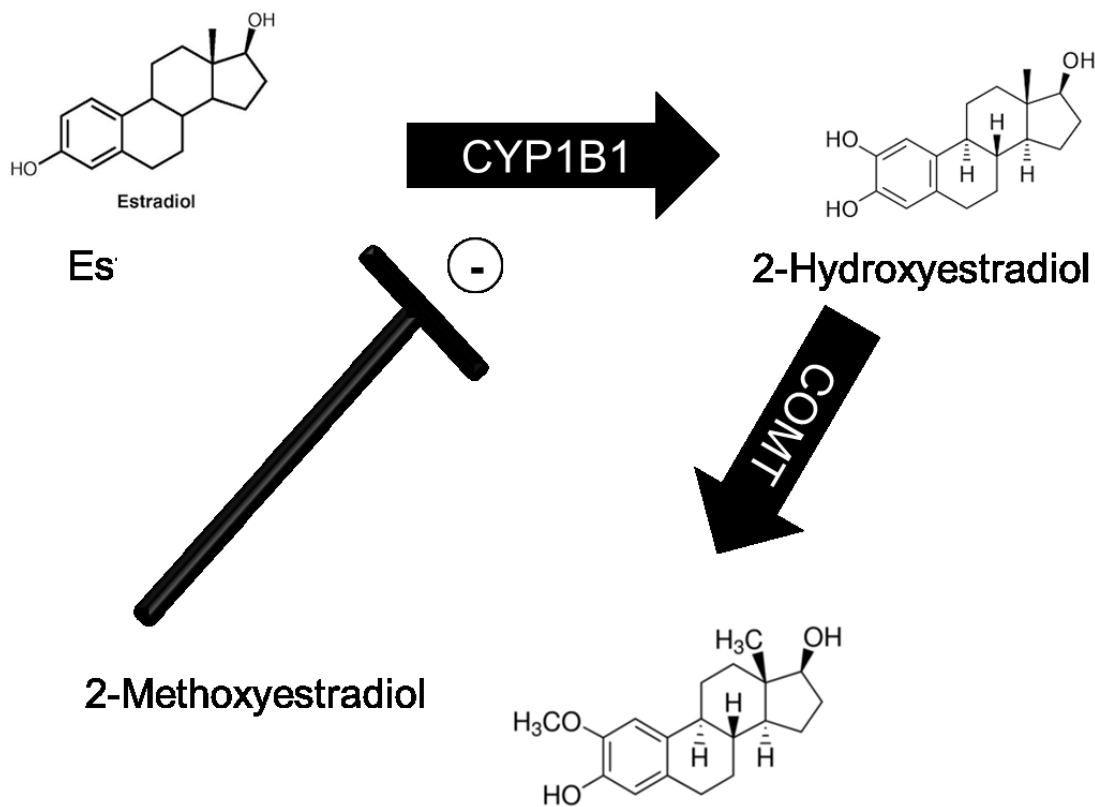
Figure 1.4. Formation of 2ME metabolite.
2-ME results from the sequential metabolism of estradiol to 2-hydroxyestradiol (2-HE) and 2-ME by CYP1B1 and catechol-O-methyltransferase (COMT), respectively.

Furthermore, 2ME displayed antihypertensive effects and inhibited its associated cardiovascular events such as coronary vascular remodeling in spontaneously hypertensive rats, obese ZSF1 rats and DOCA-induced hypertension (Tofovic *et al.*, 2001; Bonacasa *et al.*, 2008; Dubey *et al.*, 2009; Yuan *et al.*, 2013). Clinically, patients with preeclampsia have shown lower circulating levels of 2ME in comparison to controls. Of interest, the level of 2ME was inversely correlated with the value of blood pressure in these patients (Pertegal *et al.*, 2015).

Interestingly, 2ME was shown to exert a negative feedback effect on CYP1B1 catalytic activity (Dawling *et al.*, 2003) and to inhibit the generation of highly reactive quinones and semiquinones associated with CYP1B1-mediated oxidation of 17β-estradiol (Dubey *et al.*,

2009). Furthermore, 2ME attenuates TCDD-mediated oxidative stress through the inhibition of CYP1B1 and its associated reactive metabolites (Lavigne *et al.*, 2001). Unlike TMS 2ME protects against Ang II-induced hypertension and oxidative stress in female mice (Jennings *et al.*, 2014a). Furthermore, beneficial effects of 2ME seem to be equal in males and females alike as it has few or no feminizing effects (Dantas *et al.*, 2006).

The antimitogenic effect of estradiol in left ventricular cardiac fibroblast and coronary artery smooth muscle cells is credited to its metabolism by CYP1B1 to hydroxyestradiol followed by the conversion of hydroxyestradiol to more potent cardioprotective metabolite 2ME by COMT (Dubey *et al.*, 2003; Dubey *et al.*, 2005). This finding was further reinforced by the observation that estradiol-mediated cardioprotection was abrogated by pyrene and OR486, a selective CYP1B1 and COMT inhibitor, respectively, while further augmented by 3-methylcholantherene, CYP1B1 inducer (Dubey *et al.*, 2003; Dubey *et al.*, 2005). Exogenous and endogenous 2ME override the deleterious effects resulting from the oxidative metabolism of estrogen by CYP1B1 and its associated pathological consequences such as pulmonary hypertension and renal disease (Zhu *et al.*, 1998; Dubey *et al.*, 2009; Lindsey, 2014; Hood *et al.*, 2016). Randomized clinical trial did not support the notion that estrogen depicts a protective effect against cardiovascular disease in postmenopausal women though animal observations have shown an opposite concept (Alhurani *et al.*, 2016). This discrepancy is because 17β-estradiol is normally metabolized by CYP1B1 into beneficial and deleterious metabolites. Moreover, the observed protective effects of 17β-estradiol in animal models may not be translated in humans since animals are housed under controlled conditions while the human CYP1B1 enzyme could be affected by many factors such as, dietary factors, pollutants, drugs and smoking, which may disturb the ying-yang balance between the protective and toxic metabolites. In contrast to 2ME, the use of estrogen therapy is associated with the risk of cancer suggesting 2ME a good candidate for treating cardiovascular disease in postmenopausal women (Zhu *et al.*, 1998). The previous observations raise the question of whether or not 2ME could be used as an alternative for estrogen therapy. Since there is no report yet exploring the role of 2ME on postmenopausal symptoms, such as hot flushes, night sweats and urogenital dryness,

2ME cannot be considered a substitute for estrogen therapy. However, 2ME might have a beneficial effect when it is combined with existing estrogen therapy.

1.6.1. Molecular mechanism of action of 2ME

The molecular mechanisms by which 2ME exert its antiproliferative, anti-inflammatory and cardioprotective actions have not been fully elucidated and no precise cellular receptors for 2ME have yet been identified. However, some potential signaling pathways have been previously explored. Reportedly, 2ME suppresses hypoxia-inducible factor-1α nuclear accumulation and its associated transcriptional activity through the interaction with colchicine binding site and thereby disrupts and depolarizes microtubules which are required for hypoxia-inducible factor-1α transcriptional activity and cell proliferation (Mabjeesh *et al.*, 2003). 2ME may act as agonist to G-protein–coupled estrogen receptor-30 (GPR30) which modulates adenylate cyclase and cAMP in addition to down regulating Ang type 1 receptor (AT1 receptor) expression through a MAPK-dependent mechanism (Koganti *et al.*, 2012; Broselid *et al.*, 2014). Because 2ME has a structure similar to that of rosiglitazone, it may act as a PPARγ ligand (Chen *et al.*, 2015). The previous notion is supported by the finding that silencing PPARγ blunted 2ME induced endothelial nitric oxide synthase (eNOS) and protein kinase B and it associated endothelial relaxation (Chen *et al.*, 2015).

1.6.2. Biotransformation of 2ME

Phase I and II clinical trials have demonstrated negligible toxicities of 2ME even upon administration of large doses, suggesting 2ME is a well-tolerated compound (Sweeney *et al.*, 2005; Dahut *et al.*, 2006; James *et al.*, 2007; Rajkumar *et al.*, 2007). However, detrimental pharmacokinetic properties, i.e. its poor oral bioavailability and short half-life, are the key challenges in development of 2ME as a valuable medication (Verenich *et al.*, 2010). The low oral bioavailability of 2ME is due to extensive metabolic transformations rather than its poor absorption (Lakhani *et al.*, 2007; Verenich *et al.*, 2010). Structurally, 2ME has two hydroxyl groups at the positions C-3 and C-17 and consequently, it is a likely substrate for UDP-glucuronosyltransferases (UGTs) which is believed to be major pathway of 2ME elimination (Ritter *et al.*, 1990; Gall *et al.*, 1999; Basu *et al.*, 2004). Being a

substrate for ABC efflux transporters is not also excluded due to a structural similarity with estrogen (Schinkel *et al.*, 2003). However, this could be overridden by diffusional permeability (Imai *et al.*, 2002; Schinkel *et al.*, 2003).

The undesirable pharmacokinetic properties of 2ME might be overcome by developing 2ME analogs or altering 2ME delivery. Several approaches have been reported previously including improved formulations e.g. nanocrystal dispersion of 2ME (Tevaarwerk *et al.*, 2009). A sustained-release injection indicated for the treatment for pulmonary arterial hypertension has been recently developed as non-oral route of administration to reduce difficulties with the extensive first pass metabolism of 2ME (Dubey *et al.*, 2007). Hydroxyl groups at the sites C-3 and C-17 of 2ME may be protected by combining 2ME with UGT inhibitors or glucuronidase activators (Murdter *et al.*, 1997). Another approach that might be useful to improve the pharmacokinetic properties of 2ME is to replace the hydroxyl groups at the locations C-3 and C-17 with amine (NH2) groups or synthesize 2ME analogs. However, the development of more potent and stable 2ME analogs requires extensive efforts to recognize its precise functional receptor and transporters.

1.7. Rationale, hypotheses and objectives

1.7.1. Rationale

HF is one of the most widespread and lethal forms of heart disease worldwide (Roger, 2013). In Canada, it is estimated that 600,000 Canadians are living with HF and 50,000 new cases are diagnosed every year (Tran *et al.*, 2016). Despite early diagnosis and aggressive medical management, HF patients still have a poor prognosis, with an average annual mortality rate of 33% (Roger, 2013). Most HF patients have a history of hypertension and LV hypertrophy in addition to drug-induced cardiomyopathy (Gradman *et al.*, 2006). Understanding the molecular basis of cardiac hypertrophy and drug-induced cardiomyopathy is an often ignored but significant facet for identifying the best treatment of the HF since cardiomyocyte hypertrophy and fibrosis are prerequisites for the development of HF and cardiomyopathy (Gradman *et al.*, 2006).

Mechanisms regulating cardiac hypertrophy and drug-induced cardiomayopathy have been the focus of intense investigation in recent years. Among these mechanisms, CYP enzymes

have been shown to play an important role in the regression or the progression of cardiac hypertrophy through the oxidation of AA into cardioprotective EETs and cardiotoxic HETEs (Zordoky *et al.*, 2008). Of particular interest in the current study, CYP1B1 has been reported to contribute to the pathogenesis of cardiovascular diseases such as ischemic heart diseases, myocardial infarction, hypertension, atherosclerosis, cardiac hypertrophy, and heart failure (Korashy *et al.*, 2006; Malik *et al.*, 2012).

The cardiotoxic role of CYP1B1 might be mediated through the metabolism of AA into mid-chain HETEs (Choudhary *et al.*, 2004). Several studies have established the role of mid-chain HETEs, typified by 5-, 8-, 12-, and 15-HETE, in the development of cardiovascular diseases (Nozawa *et al.*, 1990; Cyrus *et al.*, 1999; Jenkins *et al.*, 2009). 5- and 12-HETEs possess a broad spectrum of biological actions with potent effects on recruitment and activation of inflammatory effectors and the induction of cellular hypertrophy (Burhop *et al.*, 1988; Wen *et al.*, 2001; Wen *et al.*, 2003). 15-HETE has been shown to increase the sensitivity to the ISO-mediated β-adrenergic response in cardiomyocytes and has been proposed to be implicated in heart failure by induction of cardiac fibrosis (Wallukat *et al.*, 1994; Kayama *et al.*, 2009). However, most of these previous studies were conducted on vascular smooth muscle, and none of them have utilized in vitro human cardiomyocytes to study the cardiac hypertrophic effect of mid-chain HETEs.

An important nonischemic idiopathic HF cause is drug-induced cardiomyopathy. DOX is a broad-spectrum anthracycline antibiotic widely used to treat various types of human neoplastic disease (Minotti *et al.*, 2004). Unfortunately, clinical usefulness of DOX is badly compromised by its cumulative cardiotoxicity leading to irreversible cardiomyopathy and congestive heart failure. The exact mechanism of DOX-induced cardiotoxicity and its progression to HF has not been fully elucidated yet and the role of mid-chain HETEs in DOX-induced cardiotoxicity has never been reported before and could not be ruled out.

Cardiac hypertrophy is a well characterized predisposing factor to HF. ISO-induced cardiac hypertrophy is a reliable, reproducible, and well-characterized model as it mimics the

sustained sympathetic activation during maladaptive cardiac hypertrophy (Meszaros *et al.*, 1990; Althurwi *et al.*, 2015; Maayah *et al.*, 2015e). Several lines of evidence support the role of CYP1B1 and its associated mid-chain HETE metabolites in the development of cardiovascular diseases (Korashy *et al.*, 2006; Malik *et al.*, 2012). For example, the expression of CYP1B1 protein and the formation of mid-chain HETE metabolites were shown to be increased during pressure overload-induced cardiac hypertrophy (El-Sherbeni *et al.*, 2014a). In addition, the induction of CYP1B1 has been demonstrated in the rat heart exposed to ISO and Ang-II and in the left ventricular tissue of spontaneously hypertensive rats (Thum *et al.*, 2002; Zordoky *et al.*, 2008; Jennings *et al.*, 2012b). Taken together, the possibility that the inhibition of CYP1B1 and its associated mid-chain HETE metabolites would protect against cardiac hypertrophy induced by ISO has never been investigated before and could not be ruled out.

In contrast to the negative effects of the cardiotoxic metabolites generated by CYP1B1, CYP1B1 also has an important role in the formation of cardioprotective metabolites, 2-methoxyestradiol (2ME) (Jennings *et al.*, 2014a). This is supported by a recent finding demonstrating that Ang-II caused oxidative stress, cardiovascular changes, endothelial dysfunction and enhanced vascular reactivity in Cyp1b1(-/-) but not in Cyp1b1(+/+) female mice (Jennings *et al.*, 2014a). Interestingly, 2ME was shown to exert a negative feedback effect on CYP1B1 catalytic activity (Dawling *et al.*, 2003). However, whether 2ME would inhibit the formation of mid-chain HETEs and subsequently protect against left ventricular hypertrophy have never been examined before and needs further investigations (Tevaarwerk *et al.*, 2009).

1.7.2. Hypotheses

1- The human ventricular cardiomyocyte RL-14 cell line expresses CYP isoenzymes constitutively like primary cells.

2- Mid-chain (5-, 8-, 12-, 15-HETEs) are directly involved in the development of cardiac hypertrophy.

3- The inhibition of mid-chain HETEs prevents the development of cardiac hypertrophy and DOX-induced HF.

1.7.3. Objectives

1- To investigate CYP gene expression in RL-14 cells as compared to the primary cells.

2- To determine the role of mid-chain HETEs in the development of cardiac hypertrophy in RL-14 cells.

3- To examine the effect of mid-chain HETEs on cardiac hypertrophy signaling pathways such as NF-κB and MAPK in RL-14 cells.

4- To determine whether inhibiting the formation of mid-chain HETEs confers cardioprotection against DOX-induced HF in vivo in rats and in vitro in RL-14 cells.

5- To explore the role of CYP1B1 and its associated mid-chain HETE metabolites in the development of cardiac hypertrophy induced by ISO in vivo in rats and in vitro in RL-14 cells.

6- To investigate the effect of 2ME on pressure overload-induced left ventricular hypertrophy in vivo in rats.

CHAPTER 2. MATERIALS

AND

METHODS

Portions of this chapter has been published in:

1-Maayah ZH, Abdelhamid G, El-Kadi AO (2015a). Development of cellular hypertrophy by 8-hydroxyeicosatetraenoic acid in the human ventricular cardiomyocyte, RL-14 cell line, is implicated by MAPK and NF-kappaB. *Cell biology and toxicology* **31**(4-5)**:** 241-259.

2-Maayah ZH, Althurwi HN, Abdelhamid G, Lesyk G, Jurasz P, El-Kadi AO (2016a). CYP1B1 inhibition attenuates doxorubicin-induced cardiotoxicity through a mid-chain HETEs-dependent mechanism. *Pharmacolgical Research* **105:** 28-43.

3-Maayah ZH, Althurwi HN, El-Sherbeni AA, Abdelhamid G, Siraki AG, El-Kadi AO (2017). The role of cytochrome P450 1B1 and its associated mid-chain hydroxyeicosatetraenoic acid metabolites in the development of cardiac hypertrophy induced by isoproterenol. *Molecular and Cellular Biochemistry* **429**(1-2)**:** 151-165.

4-Maayah ZH, El-Kadi AO (2016b). 5-, 12- and 15-Hydroxyeicosatetraenoic acids induce cellular hypertrophy in the human ventricular cardiomyocyte, RL-14 cell line, through MAPK- and NF-kappaB-dependent mechanism. *Archives of Toxicology* **90**(2)**:** 359-373.

5-Maayah ZH, El-Kadi AO (2016c). The role of mid-chain hydroxyeicosatetraenoic acids in the pathogenesis of hypertension and cardiac hypertrophy. *Archives of Toxicology* **90**(1)**:** 119-136.

6-Maayah ZH, Elshenawy OH, Althurwi HN, Abdelhamid G, El-Kadi AO (2015b). Human fetal ventricular cardiomyocyte, RL-14 cell line, is a promising model to study drug metabolizing enzymes and their associated arachidonic acid metabolites. *Journal of Pharmacological and Toxicological Methods* **71:** 33-41.

7-Maayah ZH, Levasseur J, Siva Piragasam R, Abdelhamid G, Dyck JRB, Fahlman RP*, et al.* (2018). 2-Methoxyestradiol protects against pressure overload-induced left ventricular hypertrophy. *Scientific Reports* **8**(1)**:** 2780.

2.1. Chemicals and Materials

Adriamycin was obtained from Pfizer Central Research, Sandwich, Kent, UK whereas, TMS, zileuton, PD146176, 4-[[trans-4-[[(tricyclo[3.3.1.13,7]dec-1-ylamino)carbonyl]amino]cyclohexyl]oxy]-benzoic acid (tAUCB), 2ME, 5-, 8-, 12- and 15-HETE as well as the deuterated metabolites (internal standards), were purchased from Cayman Chemical (Ann Arbor, MI). The cDNA of adult human primary cardiomyocytes (HMCa) and fetal human primary cardiomyocytes (HMC) were used and purchased from Science Cell Research Laboratories (Montreal, QC). HMCa and HMC have been extracted from a single donor. TCDD, >99% pure, was purchased from Cambridge Isotope Laboratories (Woburn, MA). Dulbecco's Modified Eagle's Medium/F-12 (DMEM/F-12), goat IgG peroxidase secondary antibody, Ammonium pyrrolidine dithiocarbamate (PDTC), U0126, nicotinamide adenine dinucleotide phosphate tetrasodium (NADPH), 4F11 mouse monoclonal primary antibody (C4868), 3-[4,5-dimethylthiazol-2-yl]-2,5-diphenyltetrazoliumbromide (MTT), pyrrolidinedithiocarbamate (PDTC), U0126, and fenofibrate were purchased from Sigma Chemical Co. (St. Louis, MO). 100X Antibiotic–antimycotic (10,000 units/ml of penicillin, 10,000 μg/ml of streptomycin, and 25 μg/ml of amphotericin B), fetal bovine serum (FBS) and TRIzol reagent was purchased from Invitrogen Co. (Grand Island, NY). Adult and fetal cDNA from human cardiac myocyte were purchased from Science Cell Research Laboratories (Montreal, QC). High Capacity cDNA Reverse Transcription kit and SYBR® Green PCR Master Mix were purchased from Applied Biosystems (Foster city, CA). Real-time PCR primers were synthesized by Integrated DNA Technologies Incorporation (San Diego, CA) according to previously published sequences. Nitrocellulose was purchased from Bio-Rad Laboratories (Hercules, CA). CYP1A1 rabbit polyclonal (sc-20772), CYP1B1 rabbit polyclonal (sc-32882), 5-lipoxygenase (5-LOX) mouse monoclonal (sc-136195), 12-LOX rabbit polyclonal (sc-32939), 15-LOX mouse monoclonal (sc-133085), cyclooxygenase-2 (COX-2) mouse monoclonal (sc-376861), glyceraldehyde-3-phosphate dehydrogenase (GAPDH) (sc 47724) mouse monoclonal and β-actin mouse monoclonal (sc-8432) primary antibodies, anti-rabbit IgG peroxidase secondary antibody, CRISPR-CYP1B1 (sc-437275) in addition to siRNA against CYP1B1 (sc-44546) were purchased from Santa Cruz Biotechnology,

Inc. (Santa Cruz, CA). The anti-mouse IgG peroxidase secondary antibody was purchased from R&D Systems (Minneapolis, MN, USA). CYP 2B6 rabbit polyclonal (ab140609), CYP2C8 rabbit polyclonal (ab88904), CYP2C19 rabbit polyclonal (ab137015), CYP4F2 rabbit polyclonal (ab125399), CYP2J2 mouse monoclonal (ab139160), EPHX2 mouse monoclonal (ab104299) primary antibodies in addition to phosphoTracer ERK1/2 (pT202/Y204) (ab176640), p38 MAPK (pT180/Y182) (ab176649), JNK1/2/3 (pT183/Y185) (ab176645) ELISA Kits were purchased from Abcam (Toronto, CA). NF-κB Family EZ-TFA Transcription Factor Assay Chemiluminescent Kit was purchased from Millipore (Millipore, Schwalbach/Ts., Germany, #70-660). ECLTM Chemiluminescence western blot detection kits were obtained from GE Healthcare Life Sciences (Piscataway, NJ). Reagents used for liquid chromatographic-electrospray ionization-mass spectrometry (LC-ESI-MS) were at HPLC-grade. Acetonitrile and water (HPLC grade) were purchased from EM Scientific (Gibbstawn, NJ). All other chemicals were purchased from Fisher Scientific Co. (Toronto, ON).

2.2. Cell culture

Human cardiomyocyte RL-14 cells (American Type Cell Culture Patent Deposit Designation No. PTA-1499, Manassas, VA) were maintained in DMEM/F-12, with phenol red supplemented with 12.5% fetal bovine serum, 20 µM L-glutamine, 100 IU/ml penicillin G and 100 µg/ml streptomycin. Cells were grown in 75 cm^2 tissue culture flasks at 37 °C under a 5% CO_2 humidified environment (Davidson, 2007). In all experiments, the cells were washed with phosphate-buffered saline (PBS) and then treated for the indicated time intervals in serum-free media with test compounds as indicated.

Rl-14 cells were authenticated by ATCC through the amplification of Seventeen short tandem repeat (STR) loci plus the gender determining locus, Amelogenin, using the commercially available PowerPlex® 18D Kit from Promega. The cell line sample was processed by the ABI Prism® 3500xl Genetic Analyzer. Data were analyzed via GeneMapper® ID-X v1.2 software (Applied Biosystems). STR profile showed that RL-14 cells are human and identical to a RL-14 cell line already in the ATCC database and

correspond to that of the same stock of cells held in the patent collection but not a match for any other profile in the ATCC STR database.

2.3. Chemical treatment

For the determination of AA metabolites, RL-14 cells were seeded at a petri dish in flat bottom with low evaporation lid petri dish. For RNA assay, cells were grown in 12-well cell culture plates in a DMEM culture media. For protein assay, cells were seeded at a cell density of $1.5*10^6$ cells/well in six-well cell culture plates, and plated at a cell density of $7.5*10^4$ cells/well in 96-well cell culture plates for CYP1B1 enzyme activity assay. Upon 70-80% confluence (2-3 days), the cells were treated in serum-free media with mid-chain HETEs, DOX and ISO in the presence and absence of CYP and LOX inhibitors or 2ME. For experiments using signaling pathway modulators, RL-14 cells were pretreated for indicated time intervals in serum-free media with various chemical inhibitors prior to the addition of hypertrophic agents as indicated, wherever applicable.

2.4. Measurement of cell viability

The effect of the tested chemical on cell viability was determined by measuring the capacity of reducing enzymes in viable cells to convert 3-[4,5-dimethylthiazol-2-yl]-2,5-diphenyltetrazolium bromide (MTT) to formazan crystals as described previously (Liu *et al.*, 1997; Maayah *et al.*, 2013) . Briefly, the tested chemical was incubated in RL-14 cells for 24 hours in a 96-well plate at 37°C under a 5% CO_2 humidified incubator. The medium was then removed and replaced with 100 μl of serum-free medium containing 1.2 mM of MTT dissolved in PBS, pH 7.2. The plate was then re-incubated at 37°C under a 5% CO_2 humidified incubator for 2 h. The medium was then decanted off by inverting the plate, and 100 μl of isopropyl alcohol was added to each well with shaking for 1 h to dissolve the formazan crystals. The color intensity in each well was measured at wavelength of 550 nm using a Synergy H1 hybrid multi-mode microplate reader (Biotek Instruments Inc., VT, USA).

The level of LDH release was estimated by a commercially available kit (CytoTox- One kit, Promega). LDH is measured with a 15-min coupled enzymatic assay that results in the

conversion of resazurin into florescent resurofin. The fluorescence produced was then recorded with an excitation wavelength of 560 nm and an emission wavelength of 590 nm according to manufacturer's instructions (Promega) using a Synergy H1 hybrid multi-mode microplate reader (Biotek Instruments Inc., VT, USA). The amount of produced fluorescence is proportionate to the amount of LDH which was calculated relative to the control.

2.5. Measurement of cell surface area and volume

Relative changes in cell surface area, as an indicator for hypertrophy in response to treatments, were measured using phase contrast imaging, which was taken with a Zeiss Axio Observer Z1 inverted microscope using the 20X objective lens as described previously (Zordoky *et al.*, 2010b; Tse *et al.*, 2013). Briefly, RL-14 cells were treated with test compounds for 24 h; thereafter, phase contrast images were taken with Zeiss Axio Observer Z1 inverted microscope using the 20X objective lens. Surface area was then quantified by imaging to the complete boundary of individual cells with Zeiss AxioVision Software (Carl Zeiss Imaging Solutions). Five different images have been taken and fifty cells were counted for each treatment group.

Relative changes in cell volume, as an indicator of hypertrophy, were measured using a flow cytometer as described by Oyama et al. with slight modification (Oyama *et al.*, 2009; Korashy *et al.*, 2014). Briefly, RL-14 cells were treated for the indicated time periods with test compounds; thereafter, the medium was removed, and cells were washed with cold PBS before trypsinization. The collected cells were centrifuged at 1500 g for 5 min and then resuspended with 0.7 ml 10% BSA in PBS. Approximately, 10^4 cells were analyzed using a Beckman Coulter Quanta SC Flow Cytometer (Beckman Coulter, Inc., CA), and the Coulter electronic volume (EV) and side scatter (SS) were measured for each cell to determine the volume and granularity, respectively. Within control cells a gate was established that encompassed the upper 10% of cells by volume. This gate was defined as enlarged cells and the percent of cells falling into this gate was determined for DOX and TMS-treated cells.

2.6. Transfecting RL-14 cells with CYP1B1 siRNA

RL-14 cells were plated onto 6-well cell culture plates. Each well of cells was transfected with CYP1B1 siRNA at the concentration of 25 nM using INTERFERin reagent according to manufacturer's instructions (Polyplus). siRNA against CYP1B1 (SC-44546) was purchased from Santa Cruz Biotechnology, Inc. (Santa Cruz, CA) The experimental medium was added to the cells after 48 hours of transfection, followed by ISO treatment (100 μM).

2.7. Transfecting RL-14 cells with CYP1B1 CRISPR Activation Plasmid

Cells were transiently transfected with CRISPR-CYP1B1 (sc-437275, Santa Cruz, CA) according to the manufacturer's protocol. Briefly, as the density of the cultured cells reached ~50%–70%, a complex of UltraCruz® Transfection Reagent and CYP1B1 CRISPR Activation Plasmid was prepared immediately prior to transfection and added to Plasmid Transfection Medium. The serum-free medium was added to the cells 48 hours after transfection.

2.8. Determination of superoxide radical

RL-14 cells grown to 90% confluence in 96-well cell culture plates were treated with test compounds for 24 h. Thereafter, cells were washed with PBS before incubation for 30 min in fresh media containing 10 μM dihydroethidium (DHE). Fluorescence measurements at excitation/emission (545/575 nm) of the wells were recorded using the Bio-Tek Synergy H1Hybrid Multi-Mode Microplate Readers (Bio-Tek Instruments, Winooski, VT, USA).

2.9. Determination of MAPK signaling pathway

RL-14 cells grown to 90% confluence in 6-well cell culture plates were treated with test compounds for the indicated time. Thereafter, the PhosphoTracer ERK1/2 (pT202/Y204), p38 MAPK (pT180/Y182), JNK1/2/3 (pT183/Y185) ELISA Kits (Abcam, Cambridge, UK) were used to determine MAPK protein phosphorylation in cytoplasmic protein extracts. The kits detect ERK1 and 2, p38 and JNK1, 2 and 3 when phosphorylated at the indicated conserved threonine or tyrosine sites of each protein and was used according to manufacturer's instructions. Fluorescence measurements at excitation/emission (545 /575

nm) of the wells were recorded using the Bio-Tek Synergy H1Hybrid Multi-Mode Microplate Readers (Bio-Tek Instruments, Winooski, VT, USA). Fluorescent data was normalized against total protein concentration from the same sample.

2.10. Preparation of nuclear extract

Nuclear extracts from RL-14 cells were prepared according to a previously described procedure with minor modifications to determine NF-κB binding activity (Andrews *et al.*, 1991). Briefly, RL-14 cells were grown on 100-mm Petri dishes and treated with test compounds for indicated time. Thereafter, cells were washed twice with cold PBS, pelleted and suspended in cold buffer A [10 mM Hepes-KOH, 1.5 mm MgCl2, 10 mM KC1, 0.5 mM dithiothreitol and 0.5 mM phenylmethylsulphonyl fluoride (PMSF)] pH 7.9, at 4 °C. After 15 min on ice, the cells were spun at 6500g and the pellets were dissolved again in high salt concentration cold buffer C (20 mM Hepes-KOH, pH 7.9, 25% glycerol, 420 mM NaCl, 1.5 mM MgCl$_2$, 0.2 mM EDTA, 0.5 mM dithiothreitol and 0.5 mM PMSF) to extract nuclear proteins. The cells were then incubated on ice with vigorous agitation for 60 min followed by centrifugation for 10 min at 12,000g at 4°C. The nuclear extracts (supernatant) were stored at -80 °C till further use.

2.11. Determination of NF-κB binding activity

The NF-κB Family EZ-TFA Transcription Factor Assay Chemiluminescent Kit (Millipore, Schwalbach/Ts., Germany, #70-660) was used according to the manufacturer's protocol (Bhattacharya *et al.*, 2010). Briefly, the NFκB capture probe, a double-stranded biotinylated oligonucleotide containing the flanked DNA binding consensus sequence for NFκB (5'-GGGACTTTCC-3'), was incubated with nuclear extract in the assay buffer. When incubated together, the active NFκB binds to its consensus sequence. The extract/probe/buffer mixture was then directly transferred to the streptavidin-coated plate. The active NFκB protein was immobilized on the biotinylated double-stranded oligonucleotide capture probe bound to the streptavidin plate well, and any inactive, unbound material was washed away. The bound NFκB transcription factor subunits, P50 and P65, were detected with specific primary antibodies directed against them. A horseradish peroxidase (HRP)-conjugated secondary antibody was then used for

chemiluminescent detection using the Bio-Tek Synergy H1Hybrid Multi-Mode Microplate Readers (Bio-Tek Instruments, Winooski, VT, USA).

2.12. AA incubation

RL-14 cells were treated with tested compounds, and then the cells were incubated with 50 μM AA for 3 h. AA metabolites were extracted with 1 ml ethyl acetate and dried using speed vacuum (Savant, Farmingdale, NY). Extracted AA metabolites were analyzed using liquid chromatography–electrospray ionization mass spectrometry (LC–ESI–MS) (Micromass ZQ 4000 spectrometer; Waters, Milford, MA) method as described previously (Nithipatikom *et al.*, 2001).

2.13. sEH catalytic activity

To determine sEH activity in RL-14 cells, cells were plated in 100 mm Petri dishes and treated with test compounds for 24 h then the cells were incubated with 5 μM 14,15-EET for 30 min. 14, 15-EET and 14, 15-DHET metabolites were extracted from the media by ethyl acetate and dried using speed vacuum (Savant, Farmingdale, NY). Extracted 14, 15-EET and 14, 15-DHET metabolites were analyzed using LC–ESI–MS method as described previously (Nithipatikom *et al.*, 2001).

2.14. Animals

The study follows the Guide for the Care and Use of Laboratory Animals published by the US National Institutes of Health (Publication No. 85-23, eighth edition; revised 2011). The protocol of this study was approved by the University of Alberta Health Sciences Animal Policy and Welfare Committee. Male Sprague-Dawley rats, weighing 200–250 g, were purchased from Charles River Canada (St. Constant, QC, Canada). All animals were housed in cages under controlled environmental condition, a 12-hour light/dark cycle, and had free acess to food and water available ad libitum.

2.15. Experimental design and treatment protocol

To determine whether inhibiting the formation of mid-chain HETEs confers cardioprotection against DOX-induced HF, the rats were randomly segregated into four

groups. The first group (n= 6) consisted of control rats that received saline (i.p.). The second group (n= 6) consisted of TMS-treated rats that received TMS (0.3 mg kg-1 every 3rd day i.p.). The third group (n= 6) consisted of DOX-treated rats that received multiple intraperitoneal injections of DOX for a cumulative dose of 15 mg/kg DOX divided into five injections within 2 weeks. The fourth group (n= 6) consisted of rats that were treated with both DOX and TMS as described in the aforementioned groups. On day 15, rats were dissected and hearts were quickly excised, washed with saline, blotted with filter paper and then the left ventricle was divided into two segments. One segment was homogenized to evaluate the tissue level of mid-chain HETEs, using a Branson homogenizer (VWR Scientific, Danbury, Conn., USA), whereas the other segment was fixed in 10% formalin for histopathology evaluation.

To determine the capacity of ISO to increase the level of cardiac mid-chain HETEs in vivo, male Sprague-Dawley rats were randomly segregated into three groups. The first group (n= 6) consisted of control rats that received an intraperitoneal injection (i.p.) injection of saline. The second group (n= 6) consisted of ISO-treated rats that received i.p. injection of ISO (5 mg kg^{-1} for 12 h). The third group (n= 6) consisted of ISO-treated rats that received three i.p. injections of ISO (5 mg kg^{-1} day^{-1} for three days). Thereafter, rats were dissected and hearts were quickly excised, washed with saline, blotted with filter paper and then immediately frozen in liquid nitrogen, then stored at -80 ^{0}C until analysis.

To investigate the effect of 2ME on pressure overload-induced left ventricular hypertrophy, male Sprague-Dawley rats of 12 weeks old, weighing 180-200 g were randomly assigned into four groups and were subjected to sham (n=12) or AAC surgery (n=12) to induce cardiac hypertrophy. The first group (n= 6) consisted of sham control rats that received polyethylene glycol (PEG 400) in mini osmotic pumps. The second group (n= 6) consisted of AAC rats that received polyethylene glycol in mini osmotic pumps. The third group (n= 6) consisted of sham 2ME-treated rats that received 2ME (5 mg/kg/day) in mini-osmotic pumps (Alzet Model 2ML4, 2.5 µl/h for 4 weeks). The fourth group (n= 6) consisted of AAC rats that were treated with 2ME as described in the aforementioned group.

All rats were anesthetized by isoflurane anesthesia (3% induction and 1–1.5% maintenance), disinfected with chlorohexidine soap and swabbed with betadine solution on the abdomen. Then a small incision was made through the skin beginning at the xyphoid sternum approximately 3-4 cm. The abdominal aorta was surgically dissected from the inferior vena cava at a site slightly above the renal arteries. A double-blunt needle was then placed along the side of the isolated aorta segment. The abdominal aorta was ligated with a syringe needle sized 21G together by the silk suture sized 0. The needle was then removed, thus producing severe aortic constriction above the renal arteries. Visera were replaced carefully, the abdominal wall was sutured and abdominal skin was closed with wound clips. The Sham procedure was performed as above with no ligation. One week after surgery, the osmotic mini-pumps were implanted sc under isoflurane anesthesia (3% induction and 1–1.5% maintenance).

Five weeks post-surgery, rats were echoed then euthanized under isoflurane anesthesia (3% induction and 1–1.5% maintenance) and hearts were quickly excised, washed with saline, blotted with filter paper and then the left ventricle was divided into two segments. One segment was further fragmented and homogenized to evaluate the mRNA, protein and metabolite levels using a Branson homogenizer (VWR Scientific, Danbury, Conn., USA), whereas the other segment was fixed in 10% formalin for histopathology evaluation.

2.16. In vivo evaluation of heart function

Animals from each group were anesthetized with isoflurane and transthoracic M-mode echocardiography (30–40 MHz; Vevo 3100, Visual Sonics, Toronto, Canada) was performed using a small animal imaging ultrasound system to measure cardiac function and wall thickness. Images were retained and analyzed using VisualSonics software version: 3.0.0. Left ventricular dimensions (LVD: left ventricular diameter; LVPW: left ventricular posterior wall thickness; and IVS: inter ventricular septum), left ventricular mass (LV mass), diastolic function and tissue droppler parameters in addition to ejection fraction (%EF) and fractional shortening (%FS) were determined using M-mode measurements taken from parasternal long and short axis views at the mid-papillary level. Left ventricular dimensions were recorded in systole and diastole. Measurements were

averaged from 3 to 6 cardiac cycles in line with the American Society of Echocardiography (Barbieri *et al.*, 2012; Byrd *et al.*, 2015), and digitally transferred online to a computer, and subsequently analyzed by an analyst blinded to the treatment groups.

2.17. Histopathology

Heart tissues from all studied groups of rats were analyzed histologically. Three micron thick sections were cut from formalin-fixed, paraffin embedded tissue of the heart and the sections were stained with hematoxylin and eosin stains (H&E) in addition to Trichrome's stain. The sections were studied under the optic microscope by a histopathologist. The adequacy of the sample in each case was checked on the semi-thin sections. The thin sections were stained with uranyl acetate and lead citrate then all the sections were examined and photographed by the histopathologist.

2.18. RNA extraction and cDNA synthesis

Total RNA from frozen tissues or treated cells was isolated using TRIzol reagent (Invitrogen®) according to the manufacturer's instructions. Briefly, approximately 0.6 to 1 ml of TRIzol reagent was added to each twelve-well cell culture plate to lyse cells or 0.2 g tissue. Cell lysates or tissue homogenates were then collected into 1.5 ml tubes and mixed with 0.2 ml of chloroform followed by shaking for 15 seconds and then centrifugation at 12,000 x g for 15 min at 4 °C. The aqueous phase which contains RNA was then transferred to new eppindorf tube and 0.3 ml isopropyl alcohol was then added to each tube to precipitate the RNA by freezing the samples at – 20 °C for 2 h. Following centrifugation at 12,000 x g for 10 min at 2 °C, the RNA pellet was washed once with 75% ethanol in diethylpyrocarbonate (DEPC)-treated water and followed by centrifugation at 12,000 x g for 5 min at 4 °C then the supernatant was removed and the pellet was allowed to dry for 10 min. Pellets were then dissolved in DEPC-treated water and incubated at 55 – 60 °C for 10 minute to ensure total re-suspension. Total RNA was quantified by measuring the absorbance at 260 nm and the purity of RNA was determined by measuring 260/280 ratio (~2).

Thereafter, first, strand cDNA synthesis was performed using the High-Capacity cDNA reverse transcription kit (Applied Biosystems), according to the manufacturer's instructions. Briefly, 1.5 μg of total RNA from each sample was mixed with high capacity cDNA reverse transcription reagents as following: 2.0 μl of 10x reverse transcriptase buffer, 0.8 μl of 25x dNTP mix (100 mM), 2.0 μl of 10x reverse transcriptase random primers, 1.0 μl of MultiScribe reverse transcriptase, and 4.2 μl of nuclease-free water (DEPC-treated water). The total volume in each microcentrifuge tube was 20 μl. The final reaction mix was kept at 25 °C for 10 min, heated to 37 °C for 120 min, heated for 85 °C for 5 s, and finally cooled to 4 °C.

2.19. Quantification of mRNA expression by quantitative real-time polymerase chain reaction (real time-PCR)

Quantitative analysis of specific mRNA expression was performed by real time-PCR by subjecting the resulting 1.5 μg cDNA to PCR amplification using 96-well optical reaction plates in the ABI Prism 7500 System (Applied Biosystems) (Livak *et al.*, 2001). The 25 μl reaction mixture contained 0.1 μl of 10 μM forward primer and 0.1 μl of 10 μM reverse primers (40 nM final concentration of each primer), 12.5 μl of SYBR Green Universal Master mix, 11.05 μl of nuclease-free water (DEPC-treated water), and 1.25 μl of cDNA sample. Human and rat primer sequences and probes for CYP1A1, 1A2, 1B1, 2B6, 2C8, 2C9, 2C19, 2J2, 4A11, 4F2, 4F3, 4F11, 5-LOX, 12/15-LOX, procollagen III (pro III) and transforming growth factor beta 1 (TGF-β1), α-myocin heavy chain (α-MHC), β-myocin heavy chain (β-MHC), atrial natriuretic peptide (ANP), brain natriuretic peptide (BNP), Tumor necrosis factor-α (TNF-α), rat GAPDH and human β-actin are listed in Table 1. These primers were purchased from Integrated DNA technologies (IDT, Coralville, IA). The ratio of β-MHC to α-MHC expression was quantitated by assessing relative cDNA levels of the genes compared with β-actin expression from the same sample. The real time-PCR data was analyzed using the relative gene expression (i.e.,ΔΔ CT) method, as described and explained previously (Livak *et al.*, 2001). Briefly, the data are presented as the fold change in gene expression normalized to the endogenous reference gene β-actin and relative to a calibrator. The fold change in the level of target genes between treated and untreated cells, corrected by the level of β-ACTIN, was determined using the following

equation: fold change $= 2^{-\Delta(\Delta Ct)}$, where $\Delta Ct = Ct_{(target)} - Ct_{(\beta\text{-actin})}$ and $\Delta(\Delta Ct) = \Delta Ct_{(treated)} - \Delta Ct_{(untreated)}$. The Ct slope method was used to measure the efficiency of the real time-PCR reactions. This method involves generating a dilution series of the target template and determining the Ct value for each dilution. A plot of Ct versus log cDNA concentration range (with four concentrations points at 0.06, 0.6, 6 and 60 ng/μL) was made. Exponential amplification was calculated using the equation: A = 10(-1/slope). Efficiency was calculated using the equation: Ex = 10(-1/slope) -1 (Table 2.2).

Table 2.1. Primer sequences used for real time- PCR reactions.

Gene	Species	Forward primer	Reverse primer
α-MHC	Human	GCCCTTTGACATTCGCACTG	GGTTTCAGCAATGACCTTGCC
β-MHC	Human	TCACCAACAACCCCTACGATT	CTCCTCAGCGTCATCAATGGA
NPPA	Human	CAACGCAGACCTGATGGATTT	AGCCCCCGCTTCTTCATT
NPPB	Human	AGAAGCTGCTGGAGCTGATAAG	TGTAGGGCCTTGGTCCTTTG
CYP1A1	Human	CCAAACGAGTTCCGGCCT	TGCCCAAACCAAAGAGAATGA
CYP1A2	Human	GAATGGCTTCTAGTCCCA	TCATCTTCTCACTAAGGGCT
CYP1B1	Human	CAGAAGCTGCTGGAGCTGATAAG	TGTAGGGCCTTGGTCCTTTG
CYP2B6	Human	CCGGGGATATGGTGTGATCTT	CCGAAGTCCCTCATAGTGGTC
CYP2C8	Human	CATTACTGACTTCCGTGCTACAT	CTCCTGCACAAATTCGTTTTCC
CYP2C9	Human	GCCTGAAACCCATAGTGGTG	GGGGCTGCTCAAAATCTTGATG
CYP2C19	Human	GGAAAACGGATTTGTGTGGGA	GGTCCTTTGGGTCAATCAGAGA
CYP2J2	Human	GAGCTTAGAGGAACGCATTCAG	GAAATGAGGGTCAAAAGGCTGT
CYP4A11	Human	CCATCCCCATTGCACGACTT	CAGGTAGACAAGCAGGTAGGG
CYP4F2	Human	GAGGGTAGTGCCTGTTTGGAT	CAGGAGGATCTCATGGTGTCTT
CYP4F3	Human	CCCCGAAACGGAATTGGTTCT	TGTGTGTATAGGAGACCTTCCTC
CYP4F11	Human	CATCTCCCGATGTTGCACG	TCTCTTGGTCGAAACGGAAGG
EPHX2	Human	GTGCCACTACCCGGCTTATG	GGCAGACTTTAGCGGTCTCG
IL-6	Human	CTGGCACCCAGCACAATG	GCCGATCCACACGGAGTACT
TNF-α	Human	GCTTTACTGTGCAAGGGAGACA	GGAAGGAGGATTCAAGTCAGGA
β-actin	Human	ACCAGTTCCTGAATGGCTGC	GGC TGCACTCCACCATTTCT
CYP1B1	Rat	CCTGGTTCTGCAACCTCATCA	CTCAACATGACAAGAGGGGCA
5-LOX	Rat	ACAGAGTGCTTCGTGCCTGAT	CGAATTTCGGAGGGTTCTGC
12/15LOX	Rat	CGCTCAGTCATGGCGGAT	GCCCCAAATGCAGCCAT
α-MHC	Rat	CAGCTGGCCTTCCTCAGACT	TGCTGTTTTTGCAGTGGTATGTAA
β-MHC	Rat	ACCTGCAAGACCATCGACATG	CGAGCCTTAGTTTGGACAGGAT
Pro III	Rat	CCCACCAGCTCTGAACAGTTC	GTGTCTCCCCAGCCATCCT
TGF-β1	Rat	ATGCTCTTCTTTTTGCGGAAA	CAGCTTTGAGGTTCGTGTTTGT
BAX	Rat	GGTACATCCTCGACGGCATCT	GTGCCTCTTTGCTGCTTTCAC
P53	Rat	GAGGCCAAGCCCTGGTATG	CGGGCCGATTGATCTCAGC
GAPDH	Rat	CAAGGTCATCCATGACAACTTTG	GGGCCATCCACAGTCTTCTG

Table 2.2 Efficiency used for real time-PCR reactions.

Gene	Species	Slope	Amplification	Efficiency
a-MHC	Human	-2.999	2.15	1.15
β-MHC	Human	-3.009	2.14	1.14
NNPA	Human	-3.21	2.04	1.04
NNPB	Human	-3.33	1.99	0.995
CYP1A1	Human	-3.19	2.05	1.05
CYP1A2	Human	-3.11	2.09	1.09
CYP1B1	Human	-3.35	1.98	0.985
CYP2B6	Human	-3.343	1.99	0.99
CYP2C8	Human	-3.21	2.005	1.005
CYP2C9	Human	-3.15	2.077	1.077
CYP2C19	Human	-3.08	2.11	1.11
CYP2J2	Human	-3.3	1.99	0.99
CYP4A11	Human	-3.36	1.98	0.98
CYP4F2	Human	-3.17	2.06	1.06
CYP4F3	Human	N.D.	N.D	N.D.
EPHX2	Human	-3.28	2.01	1.01
CYP4F11	Human	-3.11	2.09	1.09
IL-6	Human	-3.22	2.04	1.04
TNF-α	Human	-3.18	2.06	1.06
β-actin	Human	-3.00	2.15	1.15
CYP1B1	Rat	-3.12	2.09	1.09
5-LOX	Rat	-3.33	1.99	0.99
12/15-LOX	Rat	-3.345	1.99	0.99
a-MHC	Rat	-3.09	2.1	1.1
β-MHC	Rat	-3.31	2.0	1.0
Pro III	Rat	-3.3	2.009	1.009
TGF-β1	Rat	-3.4	1.96	0.96
BAX	Rat	-3.35	1.98	0.98
P53	Rat	-3.29	2.01	1.01
GAPDH	Rat	-3.29	2.01	1.01

Table 2.3 Ct values for human primers at basal level.

Gene	Ct values (means)	SEM
a-MHC	28.55	1.38
β-MHC	28.72	0.90
NNPA	29.55	0.67
NNPB	28.85	1.07
CYP1A1	28.4	0.57
CYP1A2	30.35	1.93
CYP1B1	36.2	0.22
CYP2B6	28.4	1.49
CYP2C8	33.49	0.49
CYP2C9	36.99	0.28
CYP2C19	35	0.27
CYP2J2	31.69	0.75
CYP4A11	27.58	1.45
CYP4F2	31.54	0.13
CYP4F3	ND	ND
CYP4F11	35.08	0.63
EPHX2	27	0.76
IL-6	22.3	0.59
TNF-α	27.22	0.66
β-actin	28.1	1.24

Table 2.4 Ct values for rat primers at basal level.

Gene	Ct values (means)	SEM
Rat CYP1B1	27.55	0.54
Rat 5-LOX	30.66	0.16
Rat 12/15-LOX	38.2	0.7
Rat a-MHC	22.1	0.37
Rat β-MHC	25.3	0.57
Rat Pro III	23.5	0.68
Rat TGF-β1	24.2	0.26
Rat BAX	25.7	0.4
Rat P53	24.7	0.138
Rat GAPDH	20.7	0.24

2.20. Preparation of microsomal proteins

Heart microsomal proteins were prepared by differential centrifugation of homogenized tissues. Briefly, individual heart tissues were rapidly removed, washed in ice-cold potassium chloride [1.15% (w/v)] and cut in pieces. Thereafter, cold sucrose solution (1 g of tissue in 5 ml of 0.25 M sucrose) was used to homogenize heart tissue pieces. The homogenate was spun at 10,000g for 20 minutes, and the resulting supernatant was spun once again at 100,000g for 60 minutes to obtain the microsomal pellet. The final pellets were dissolved in cold sucrose and stored at -80 ºC. Thereafter, the Lowry method with bovine serum albumin as a standard was used to determine microsomal protein concentrations.

2.21. Measurement of mid-chain HETEs in heart tissue

Measurement of heart tissue mid-chain HETEs was performed using a previously described method (Chun *et al.*, 2001). Briefly, 250 mg heart tissue was dissected and homogenized on ice with 1 mL of methanol containing the deuterated metabolites (internal standards), acetic acid, butylated hydroxytoluene and ethylenediaminetetraacetic acid. Thereafter, the homogenates were centrifuged at 10,000 g for 15 min at 0 °C. AA metabolites were extracted from the resulted supernatant by the solid-phase cartridge (Oasis®HLB). Conditioning and equilibration of the solid-phase cartridge were performed with 1 mL of each of methanol, ethyl acetate, 0.2% formic acid (v/v), and 10% methanol in 0.2% formic acid (v/v), in sequence. After sample application, cartridges were washed with 1 mL of each of 0.2% formic acid (v/v), and 10% methanol in 0.2% formic acid (v/v), in sequence. Finally, AA metabolites were eluted by 1 mL of each of 1% formic acid in acetonitrile (v/v) and ethyl acetate, in sequence. Sample eluents were dried using speed vacuum (Savant, Farmingdale, NY), reconstituted in 60 µL of 0.01% formic acid in acetonitrile to be analyzed by mass spectrometry.

2.22. Separation of AA Metabolites by LC–ESI–MS

Extracted AA and metabolites were analyzed using LC–ESI–MS (Micromass ZQ 4000 spectrometer; Waters, Milford, MA) method as described previously (Nithipatikom *et al.*, 2001). Briefly, a gradient separation was performed on a reverse-phase C18 column

(Alltima HP, 150 × 2.1 mm; GRACE Davison, Lokeren, Belgium) at 35°C. Mobile phase A consisted of water with 0.01% formic acid and 0.005% triethylamine (v/v), whereas mobile phase B consisted of 8% methanol, 8% isopropanol, and 84% acetonitrile with 0.01% formic acid and 0.005% triethylamine (v/v). Injection volume of 40 µL was used, and the mass spectrometer was run under negative ionization mode with single ion monitoring of AA at m/z= 303, HETEs and EETs at m/z=319, DHETs at m/z=337 and internal standards at m/z=311, m/z=327, m/z=348.2 and m/z=360 for AA-d8, 15-HETE-d8, 14,15-DHET-d11 and PGE2-d9, respectively.

Calibration samples of AA metabolites were prepared in acetonitrile containing 0.001, 0.01, 0.1 and 1.0 µg/ml of each of the AA metabolites. Calibration curves performed on three separate days were analyzed to evaluate the linearity. Accuracy and precision were determined using quality-control samples at four levels in the range of expected concentrations in incubates, 0.001, 0.01, 0.1 and 1.0 µg/ml for AA metabolites. Each quality-control sample (10 µl) was injected in triplicate on three different days to permit an assessment of intraday and interday accuracy and precision. Accuracy was determined by the calculating the concentration of each quality-control sample based on the calibration curve equations. Bias was assessed by calculating percentage of error [%error = (Ccalculated − Cnominal)/Cnominal × 100] for all injections at each level analyzed. Precision was assessed by calculating the coefficient of variation (%CV = S.D./mean × 100) for all injections at each level analyzed. Figure 2.1 and Figure 2.2 show a representative example of calibration curve for 15-HETE metabolite and a trace of AA metabolites with their retention time, respectively.
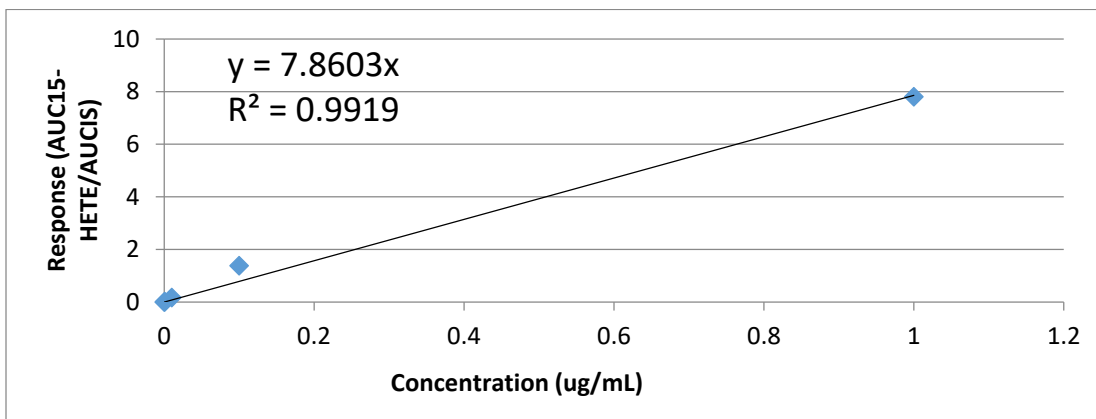
Figure 2.1. Representative example of calibration curve for 15-HETE metabolite.
Response was calculated by dividing area under the curve (AUC) of each single
concentration over AUC of the internal standard (IS) for each single concentration.
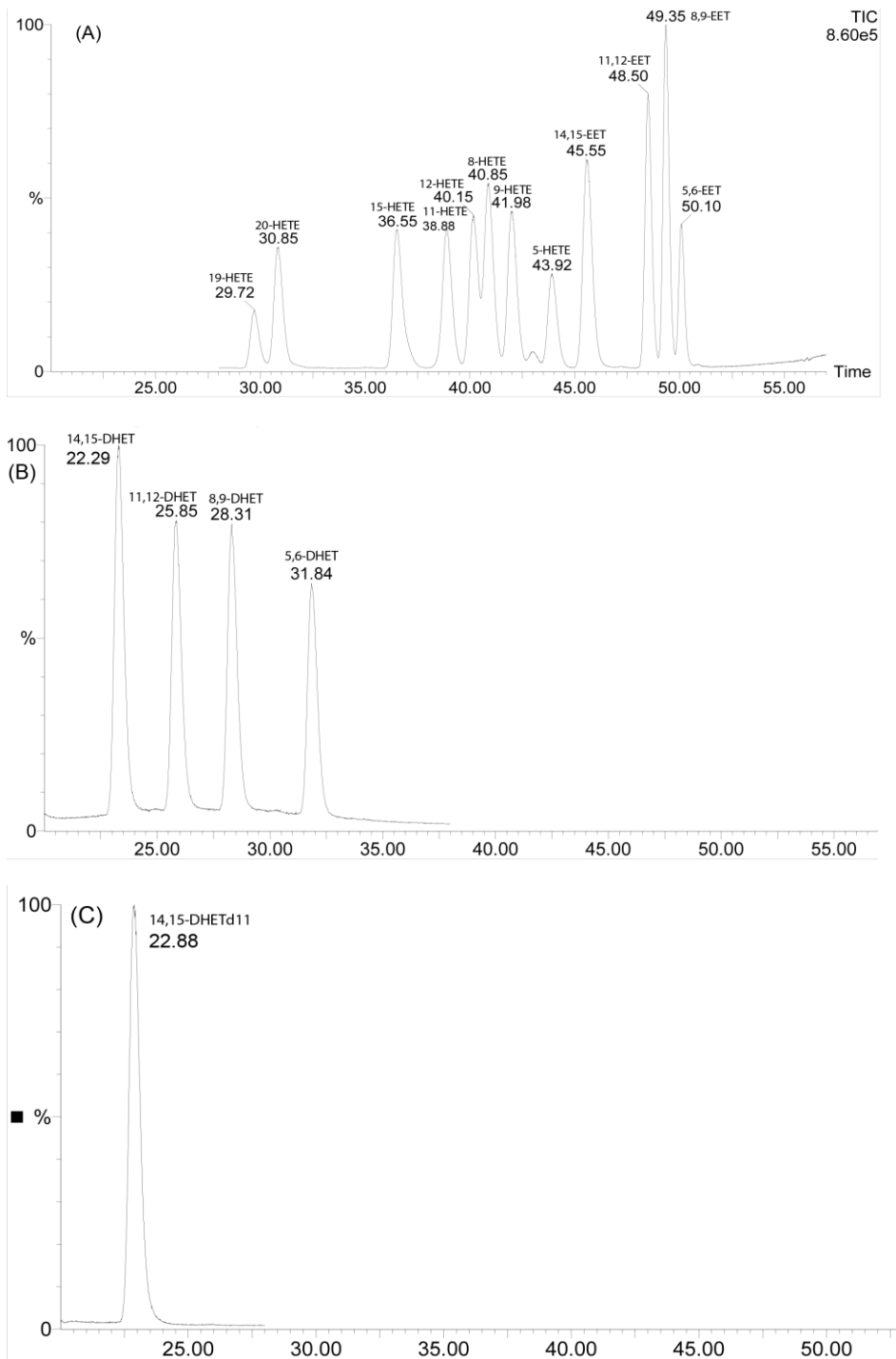
Figure 2.2. Separation of AA metabolites by LC-ESI-MS
(A) Peaks and retention time for 20-, 19-, 15-, 12-, 11-, 9-, 8- and 5-HETE in addition to 14,15-, 11,12-, 8,9- and 5,6-EET standards (min). (B) Peaks and retention time for 14,15-, 11,12-, 8,9- and 5,6-DHET standards (min). (C) The peak and retention time for 14,15-DHETd11 internal standard (min).

74

2.23. Protein extraction from RL-14 cells

Twenty-four hours after incubation with the 10 μM DOX in the presence and absence of 0.5 μM TMS, approximately 1.5 x 10^6 cells per six-well culture plate were collected in 100 μl lysis buffer (50 mM HEPES, 0.5 M sodium chloride, 1.5 mM magnesium chloride, 1 mM EDTA, 10% glycerol (v/v), 1% Triton X-100, and 5μl/ml of protease inhibitor cocktail). Total cellular proteins were obtained by incubating the cell lysates on ice for 1 h, with intermittent vortex mixing every 10 min, followed by centrifugation at 12,000x g for 10 min at 4°C.

2.24. Western blot analysis

Western blot analysis under denaturing and reducing conditions was performed using a previously described method (Liu *et al.*, 1997; Sambrook *et al.*, 1989). Briefly, proteins from each treated group were diluted with same amount (1:1) of 2X loading buffer (0.1 M tris(hydroxymethyl)aminomethane (Tris)-HCl, pH 6.8, 4% sodium dodecyl sulfate (SDS), 1.5% bromophenol blue, 20% glycerol, 5% β-mercaptoethanol), boiled and loaded onto a 10% SDS-polyacrylamide gel. Samples were electrophoresed at 120 V for 2 h and separated proteins were transferred to Trans-Blot nitrocellulose membrane (0.45 μm) in a buffer containing 25 mM Tris–HCl, 192 mM glycine, and 20% (v/v) methanol. The membranes were blocked overnight at 4°C in a solution containing 5% skim milk powder, 2% BSA and 0.5% Tween-20 in Tris-buffered saline (TBS) solution (0.15 M NaCl, 3 mM KCl, 25 mM Tris-base). After blocking, the blots were washed 6 times for 1 h with TBS-Tween-20 before being incubated with a primary antibody (0.2 μg/ml) for 2 h at room temperature in TBS solution containing 0.05% (v/v) Tween-20 and 0.02% sodium azide. Incubation with a peroxidase conjugated anti-rabbit or anti-mouse IgG secondary antibody was carried out in blocking solution for 1 h at room temperature. The bands were visualized using the enhanced chemiluminescence method according to the manufacturer's instructions (GE Healthcare, Mississauga, ON). The intensity of protein band was semi-quantified relative to the signals obtained for GAPDH protein, using ImageJ® image processing program (National Institutes of Health, Bethesda, MD, http://rsb.info.nih.gov/ij).

2.25. In-gel digestion and LC–MS/MS analysis

Samples were prepared and electrophoresed as described in the aforementioned western blot method. After electrophoresis, Coomassie Brilliant Blue was used to stain the SDS gel then the gel was destained overnight using de-staining solution (H_2O: Methanol: Acetic acid, 50:40:10). The gel was then visualized using an LI-COR Odyssey gel scanner to quantify the intensity of protein content in each lane. Each lane on the gel was excised into 12 equal pieces after being de-stained using 100 mM NH_4HCO_3/acetonitrile (50:50). Each gel piece was subjected to in-gel tryptic digestion as previously described (Khan *et al.*, 2015). The final extracted peptides from the gel were suspended in 5% acetonitrile and 1% formic acid then analyzed on an LTQ Oribitrap XL, with the resulting data being searched against the *Rattus norvegicus* protein database using Proteome Discoverer 1.3 as previously described (Alsaikhan *et al.*, 2015). At least two high confidence peptides were used as a cut off for protein identification. With this criterion, more than 500 proteins were identified. The protein's extracted ion chromatogram (EIC) was used to compare the abundance between samples.

2.26. Determination of CYP1B1 enzymatic activity

CYP1B1-dependent methoxyresorufin O-deethylase (MROD) activity was performed on intact living RL-14 cells (Kennedy *et al.*, 1993; Lo *et al.*, 2013). After incubation of the cells with test compounds, 100 µl of 2 µM methoxyresorufin in assay buffer (0.05 M Tris, 0.1 M NaCl, pH 7.8), were then added to each well. In vivo, microsomes from heart of various treatments (1 mg protein/ml) were incubated in the incubation buffer (5 mM magnesium chloride hexahydrate dissolved in 0.1 M potassium phosphate buffer, pH 7.4) with 2 µM of methoxyresorufin in a shaking water bath at 37 °C and then the reaction started after the addition of 1 mM NADPH. After incubation at 37 °C (10 min), the reaction was stopped by adding 0.5 mL of cold methanol. Immediately, an initial fluorescence measurement (t=0) at excitation/emission (545 /575 nm) followed by an additional set of fluorescence measurements of the samples were recorded every 5 min for a 40 min interval using the Bio-Tek Synergy H1Hybrid Multi-Mode Microplate Readers (Bio-Tek Instruments, Winooski, VT, USA). The amount of resorufin formed in each sample was

determined by comparison with a standard curve of known concentrations and normalized to protein levels determined using a modified fluorescent assay (Lorenzen *et al.*, 1993).

2.27. Statistical analysis

The comparative analysis of the results from various experimental groups with their corresponding controls was performed using SigmaPlot® for Windows (Systat Software, Inc, CA). All means are reported with SEM. One-way analysis of variance (ANOVA) followed by Tukey-Kramer multiple comparison test or unpaired two sided student *t* test were carried out to assess which treatment group(s) showed a significant difference from the control group. A result was considered statistically significant when $p < 0.05$.

CHAPTER 3. RESULTS

Portions of this chapter has been published in:

1-Maayah ZH, Abdelhamid G, El-Kadi AO (2015a). Development of cellular hypertrophy by 8-hydroxyeicosatetraenoic acid in the human ventricular cardiomyocyte, RL-14 cell line, is implicated by MAPK and NF-kappaB. *Cell biology and toxicology* **31**(4-5)**:** 241-259.

2-Maayah ZH, Althurwi HN, Abdelhamid G, Lesyk G, Jurasz P, El-Kadi AO (2016a). CYP1B1 inhibition attenuates doxorubicin-induced cardiotoxicity through a mid-chain HETEs-dependent mechanism. *Pharmacolgical Research* **105:** 28-43.

3-Maayah ZH, Althurwi HN, El-Sherbeni AA, Abdelhamid G, Siraki AG, El-Kadi AO (2017). The role of cytochrome P450 1B1 and its associated mid-chain hydroxyeicosatetraenoic acid metabolites in the development of cardiac hypertrophy induced by isoproterenol. *Molecular and Cellular Biochemistry* **429**(1-2)**:** 151-165.

4-Maayah ZH, El-Kadi AO (2016b). 5-, 12- and 15-Hydroxyeicosatetraenoic acids induce cellular hypertrophy in the human ventricular cardiomyocyte, RL-14 cell line, through MAPK- and NF-kappaB-dependent mechanism. *Archives of Toxicology* **90**(2)**:** 359-373.

5-Maayah ZH, El-Kadi AO (2016c). The role of mid-chain hydroxyeicosatetraenoic acids in the pathogenesis of hypertension and cardiac hypertrophy. *Archives of Toxicology* **90**(1)**:** 119-136.

6-Maayah ZH, Elshenawy OH, Althurwi HN, Abdelhamid G, El-Kadi AO (2015b). Human fetal ventricular cardiomyocyte, RL-14 cell line, is a promising model to study drug metabolizing enzymes and their associated arachidonic acid metabolites. *Journal of Pharmacological and Toxicological Methods* **71:** 33-41.

7-Maayah ZH, Levasseur J, Siva Piragasam R, Abdelhamid G, Dyck JRB, Fahlman RP*, et al.* (2018). 2-Methoxyestradiol protects against pressure overload-induced left ventricular hypertrophy. *Scientific Reports* **8**(1)**:** 2780.

3.1. Human fetal ventricular cardiomyocyte RL-14 cell line is a promising model to study drug metabolizing enzymes and cellular hypertrophy

3.1.1. Constitutive expression of CYP ω-hydroxylases and epoxygenases mRNA and protein in RL14 cells

The constitutive expression of various CYP isoenzymes in fetal human ventricular cardiomyocytes RL-14 cell line was determined by real-time PCR. CYP2C9 was the lowest expressed gene in RL-14 cells and thus it was considered as a calibrator (as a relative control).

Analysis of mRNA expression in RL-14 cells revealed that the order of expression in CYP1 family ω-hydroxylases was from highest to lowest as follows: CYP1A1> CYP1A2 > CYP1B1. With respect to the CYP4 family ω-hydroxylases, the order of expression was: CYP4A11 > CYP4F2 > CYP4F11. CYP4F3 was not detected in RL-14 cells. Regarding the CYP epoxygenases family the order of expression was: CYP2B6 > CYP2J2 > CYP2C8 > CYP2C19 > CYP2C9. Of interest, EPHX2 mRNA was highly expressed in RL-14 cells (Fig. 3.1A).

To further examine whether the expression of CYP mRNA in RL-14 cells is translated into functional protein, the constitutive expression of various CYPs in RL-14 cells was determined by Western blot analysis. Figure 3.1B shows that the pattern of CYP ω-hydroxylases and epoxygenases is similar to what was observed with mRNA level except for CYP1B1 and CYP2J2. The order of expression in CYP ω-hydroxylases was from highest to lowest as follows: CYP1B1> CYP1A > CYP4F2 > CYP4F11. Regarding the CYP epoxygenases family the order of expression in RL-14 cells was: CYP2J2 > CYP2B6 > CYP2C8 > CYP2C19 (Fig. 3.1B). Similar to mRNA, EPHX2 is also expressed at the protein level in RL-14 cells.
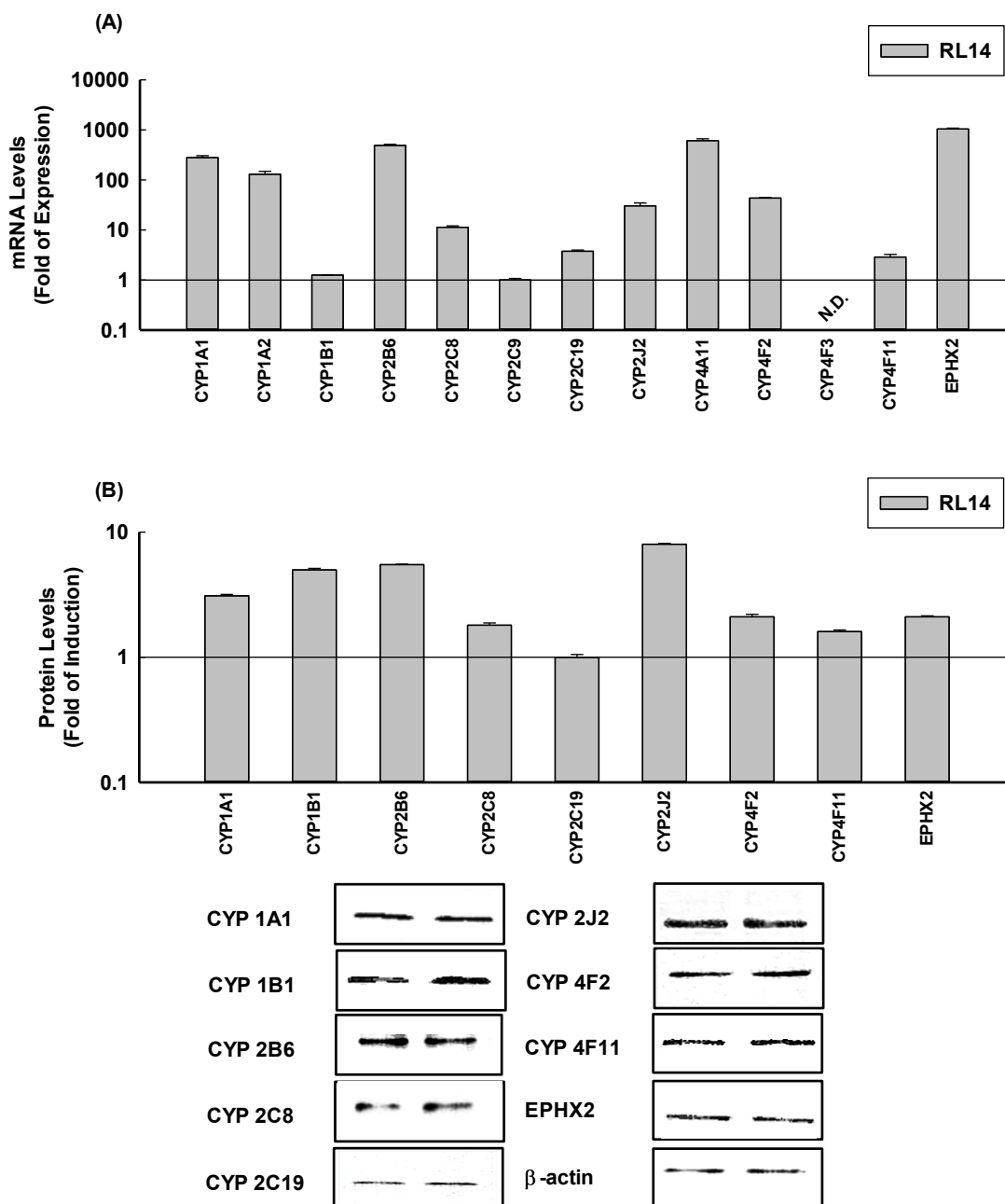
Figure. 3.1. **Constitutive expression of different CYP families at mRNA and protein levels in RL-14**

      (A) The mRNA level was quantified using real time-PCR. CYP2C9 was the lowest expressed gene in RL-14 cells and thus it was considered as a calibrator. (B) CYP proteins were determined by Western blot analysis. The intensity of CYP proteins band was normalized to the signals obtained for β-actin protein and relative to CYP2C19 being the lowest expressed CYP. Two of the six representative experiments are shown. The values represent mean ± SEM (n = 6).

3.1.2. Fold expression of CYP ω-hydroxylases and epoxygenases in RL14 and fetal human primary cardiomyocyte cells relative to adult human primary cardiomyocytes

Our results showed that CYP1A1 and CYP1A2 were constitutively expressed in adult human primary cardiomyocytes (HMCa), fetal human primary cardiomyocytes (HMC), and RL-14 cells (Figure 3.2), whereas CYP1B1 was expressed only in the RL-14 cells but not in HMCa and HMC cells. Of importance, CYP1A1 and CYP1A2 mRNAs were detected in RL-14 and HMC cells at higher level than HMCa cells (Figure 3.2A). On the other hand, CYP4A11, CYP4F2, and CYP4F11 were highly expressed in RL-14 and HMCa cells but very little if any in HMC cells (Figure 3.2B). Interestingly, CYP4A11, 4F2, and 4F11 mRNAs were detected in RL-14 cells at higher amounts than that in HMCa cells.

The expression of CYP epoxygenases, CYP2B6, 2C8, 2C19 and 2J2, in RL-14 cells compared with those expressed in HMCa and HMC cells are shown in Figure 3.2C. Our results showed that all CYP2 mRNA are highly expressed in the RL-14 cells, while they are expressed to varying degrees in HMCa and HMC cells. CYP2B6 and CYP2C19 were found to be highly expressed in RL-14 cells and their expression level is slightly comparable to that of the HMC cells but significantly higher than that of the HMCa cells. On the other hand, CYP2C8 was detected at lower levels in RL-14 cells in comparison to the HMC and HMCa cells (Figure 3.2C). Interestingly, CYP2J2 was detected at almost equal amounts in HMC cells and HMCa cells but lower than in RL-14 cells (Figure 3.2C).
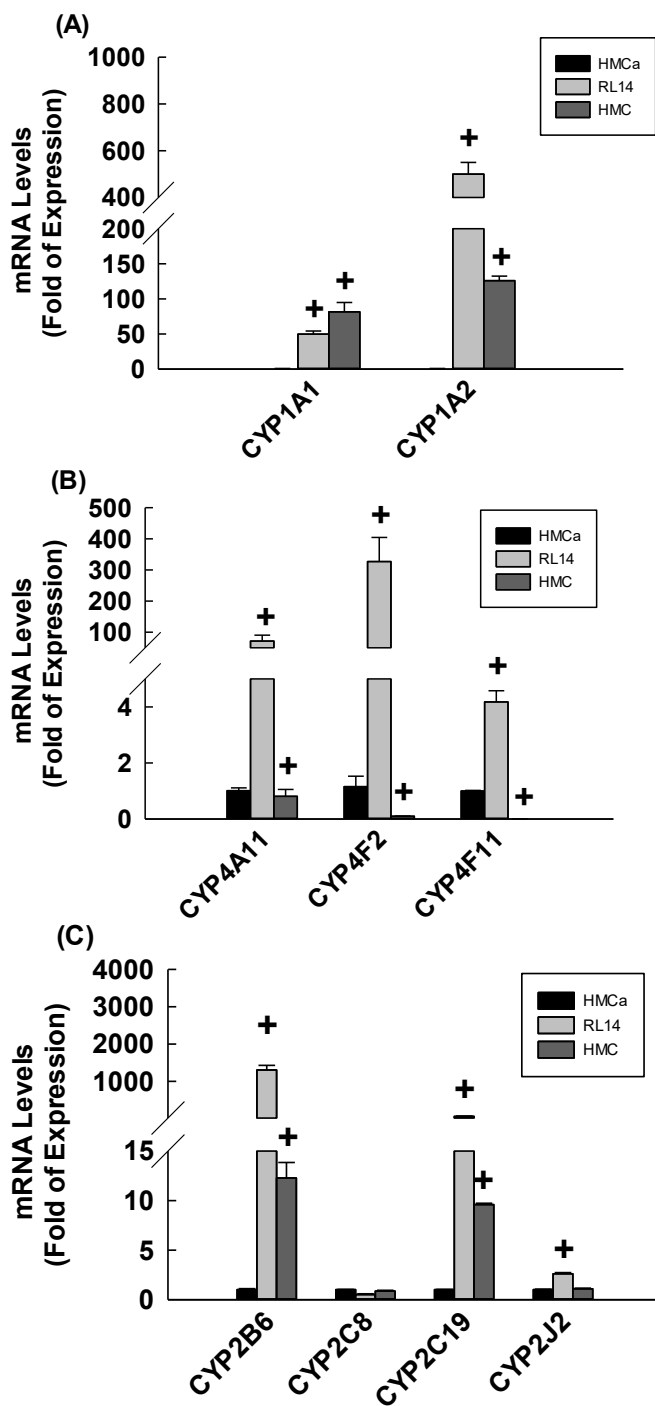
Fig. 3.2. Fold expression of CYP ω-hydroxylases and epoxygenases in RL14 and HMC cells relative to HMCa cells

Fold expression of CYP ω-hydroxylases (A and B) and epoxygenases (C) in RL14 and HMC cells relative to HMCa cells. The mRNA level was quantified using real time-PCR. The values represent mean ± SEM (n = 6). $^{+}p<0.05$ compared to HMCa.

3.1.3. Effect of CYP inducers of ω-hydroxylases and epoxygenases in RL-14 cells

3.1.3.1. Induction of CYP1A1 gene expression by TCDD in RL-14 cells

To examine the effect of a CYP1 inducer, TCDD, on the expression of CYP1A genes, RL-14 cells were treated with TCDD for 6 h. Thereafter, CYP1A genes were measured using real time-PCR. Figure 3.3A shows that TCDD caused a significant induction of CYP1A1 and CYP1A2 mRNA by approximately 10 and 40-fold, respectively.

To further examine whether the induction of CYP1A1 mRNA in RL-14 cells in response to TCDD treatment is translated into functional protein, RL-14 cells were treated for 24 h with TCDD; thereafter, CYP1A1 protein expression was determined by Western blot analysis. Figure 3.3B shows that, in a pattern similar to what was observed with mRNA, TCDD-induced CYP1A1 protein in RL-14 cells by approximately 7-fold.

3.1.3.2. Induction of CYP2 and CYP4 genes expression by fenofibrate in RL-14 cells

To investigate the effect of CYP2 and CYP4 inducer, fenofibrate, on the expression of CYP2 and CYP4 genes, RL-14 cells were treated with fenofibrate for 6 h. Thereafter, the mRNA expression of CYP2B6 and CYP4F2 genes was measured using real time-PCR. Figure 3.4A shows that fenofibrate caused a significant induction of CYP2B6 and CYP4F2 mRNA by approximately 70 and 5-fold, respectively.

To further test whether the induction of CYP2B6 and CYP4F2 mRNA in RL-14 cells in response to fenofibrate treatment is translated into functional protein, RL-14 cells were treated for 24 h with fenofibrate, thereafter, CYP2B6 and CYP4F2 protein expressions were determined by Western blot analysis. Figure 3.4B shows that fenofibrate significantly induced CYP2B6 and CYP4F2 protein expression in RL-14 cells by approximately 7- and 2-fold, respectively.
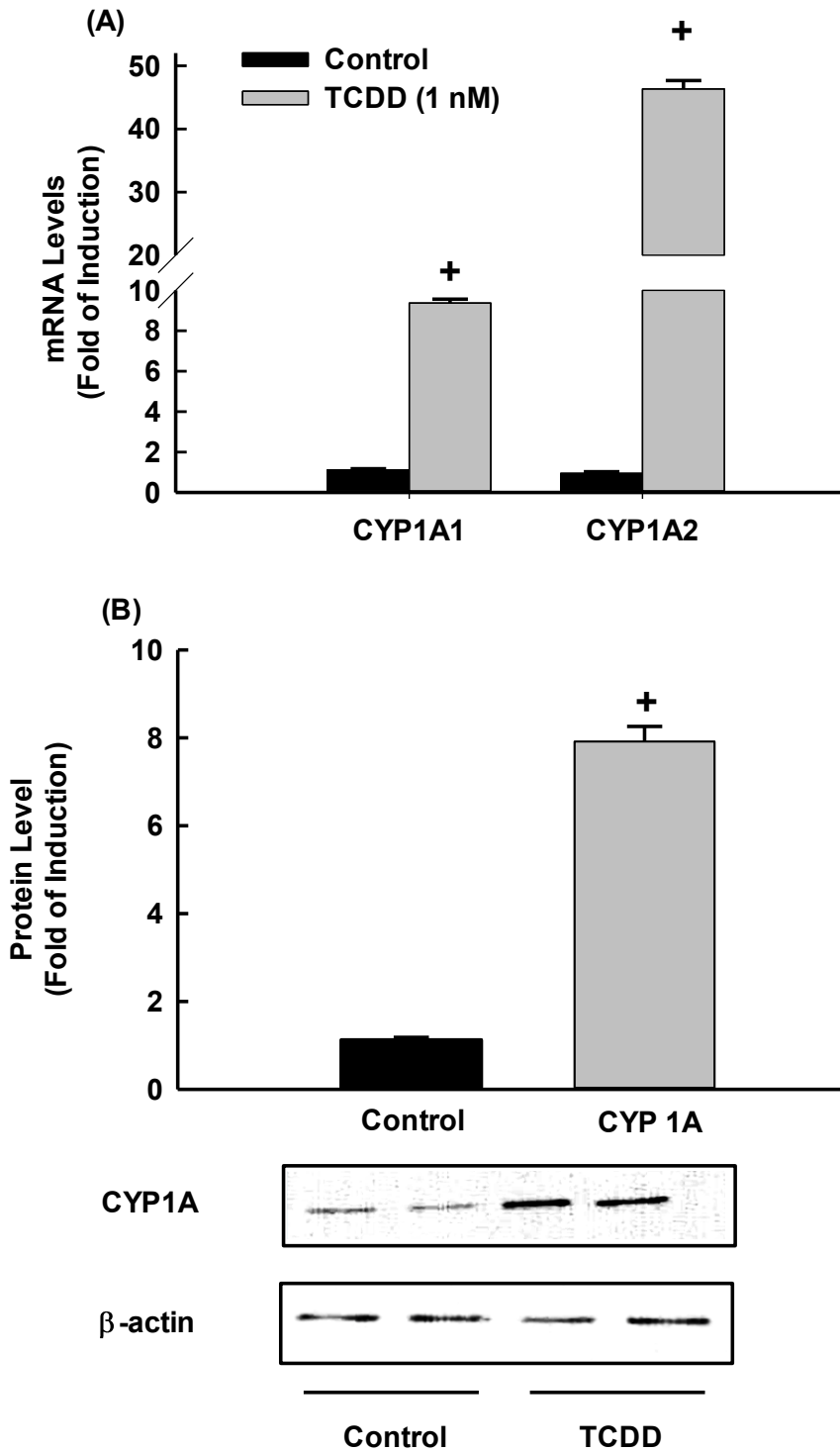
Figure. 3.3. Effects of TCDD on CYP 1A1 mRNA and protein levels in RL-14 cells
(A) RL-14 cells were treated for 6 h with TCDD. The CYP1A1 and 1A2 mRNAs were quantified by real time-PCR. (B) RL-14 cells were treated for 24 h with TCDD; thereafter, CYP1A1 protein levels were determined by Western blot analysis. The values represent mean $\pm$ SEM (n = 6). $^{+}p<0.05$ compared to control.
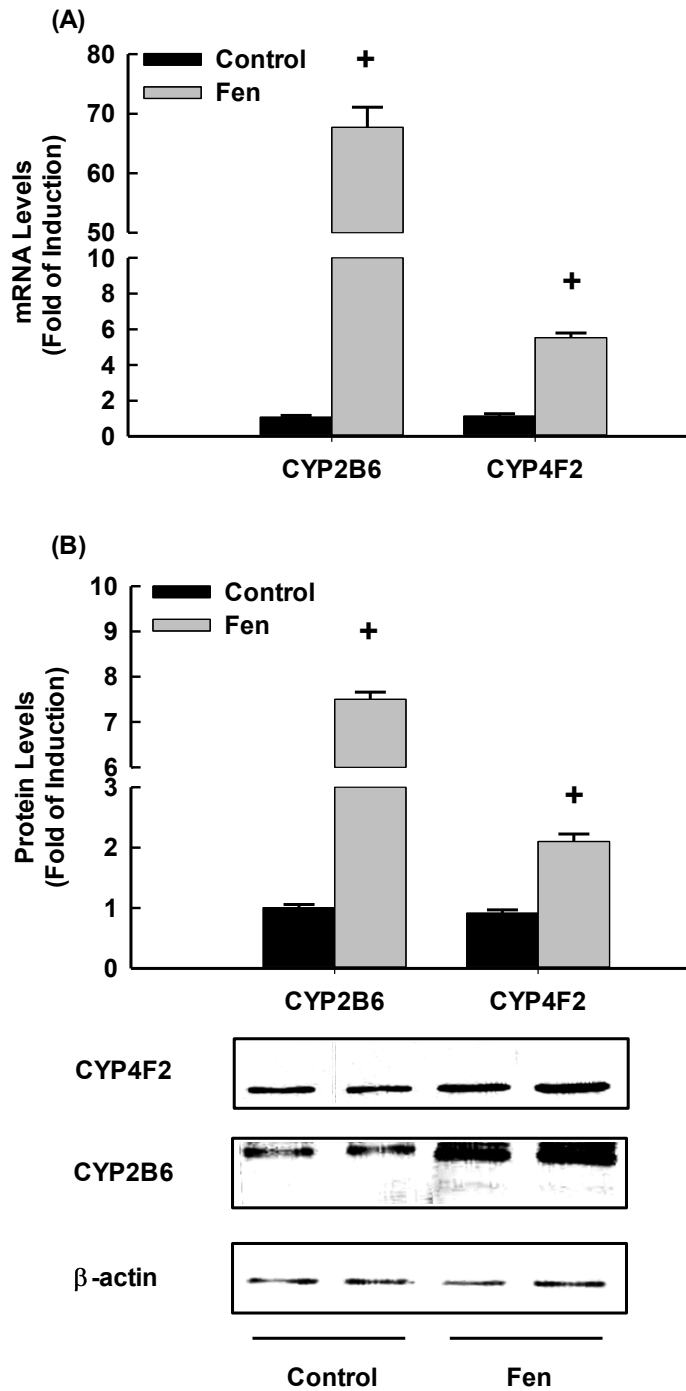
Figure 3.4. Effect of fenofibrate on CYP2B6 and CYP4F2 mRNA and protein levels in RL-14 cells

    (A) RL-14 cells were treated for 6 h with fenofibrate. The CYP2B6 and CYP4F2 mRNAs were quantified by real time-PCR. (B) RL-14 cells were treated for 24 h with fenofibrate; thereafter, CYP2B6 and CYP4F2 protein levels were determined by Western blot analysis. The values represent mean ± SEM (n = 6). $^{+}p<0.05$ compared to control.

3.1.4. Fold expression of cardiac hypertrophic markers in RL-14 and fetal human primary cardiomyocyte cells relative to adult human primary cardiomyocyte

The expression of cardiac hypertrophic markers, α-MHC, β-MHC, ANP and BNP, in RL-14 cells compared with those expressed in HMCa and HMC cells are shown in Figure 3.5. Our results showed that all cardiac hypertrophy markers are highly expressed in the RL-14 and HMC cells, while they are expressed to varying degrees in HMCa cells. α-MHC was found to be highly expressed in RL-14 cells and the expression level is slightly comparable to that of the HMC cells but significantly higher than that of the HMCa cells. Also, β-MHC was highly expressed in RL-14 and HMC cells but very little if any in HMCa cells. On the other hand, ANP and BNP mRNAs were detected in HMC cells at higher amounts than that of RL-14 cells (Figure 3.5A and B).

To further examine whether the pattern of MHC proteins in RL-14 cells are similar to what was observed with mRNA, the constitutive expression of α-MHC and β-MHC in RL-14 cells was determined by Western blot analysis. Consistent with mRNA, our results showed that α-MHC and β-MHC proteins are constitutively expressed in the RL-14 cells. On the other hand, Figure 3.5C shows that α-MHC is expressed abundantly in RL-14 cells compared with β-MHC at the protein level.
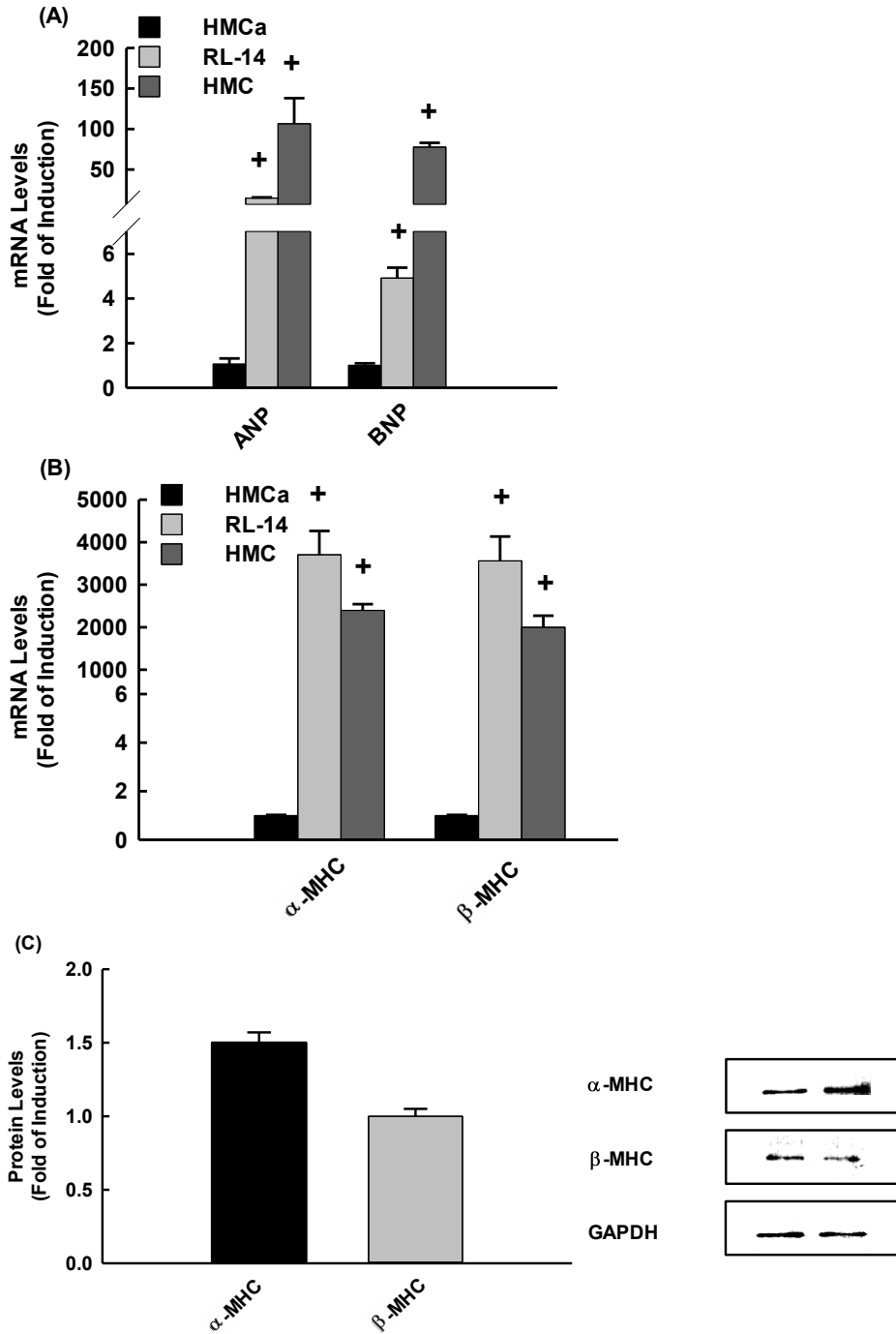
Figure 3.5. Fold expression of cardiac hypertrophy markers in RL14 and HMC cells relative to HMCa cells

       Fold expression of cardiac hypertrophy markers, (A) ANP and BNP and (B) α-MHC and β-MHC in RL14 and HMC cells relative to HMCa cells. The amount of mRNA was quantified using real time-PCR. (C) The level of MHC proteins was determined by Western blot analysis. The values represent mean ± SEM (n = 6). $^{+}p<0.05$ compared to HMCa.

87

3.2. Mid-chain hydroxyeicosatetraenoic acids induce cellular hypertrophy in the human ventricular cardiomyocyte RL-14 cell line through MAPK- and NF-κB-dependent mechanism

3.2.1. Effect of mid-chain HETEs on RL-14 cells viability

To determine the maximum non-toxic concentrations of mid-chain HETEs to be utilized in the current study, RL-14 cells were exposed for 24 h to wide range concentrations of 5-, 8-, 12- and 15-HETE (0, 0.5, 1, 2.5, 5, 10, 20 and 40 μM). Thereafter, the cell viability was determined using the MTT assay. Our results showed that 5-, 12- and 15-HETE concentrations ranging from 0.5 to 20 μM in addition to 8-HETE concentrations ranging from 0.5 to 10 μM did not significantly affect cell viability (Figure 3.6). However, 40 μM 5-, 12- and 15-HETE and 20 μM 8-HETE significantly decreased the cell viability by approximately 40% and 60%, respectively, in comparison to control. Based on these findings, 5-, 12- and 15-HETE concentrations of 2.5, 5, 10 and 20 μM in addition to 2.5, 5 and 10 μM 8-HETE were selected to be utilized in all subsequent in vitro experiments in RL-14 cells (Figure 3.6).

3.2.2. Concentration- and time-dependent effects of mid-chain HETEs on α-MHC, β-MHC, ANP and BNP mRNA levels

To investigate the capacity of mid-chain HETEs to induce cellular hypertrophy, RL-14 cells were treated for 6 h with increasing concentrations of 5-, 12- and 15-HETE (0, 1, 2.5, 5, 10 and 20 μM) in addition to 8-HETE (0, 2.5, 5, and 10 μM). Thereafter, the mRNA expression of the hypertrophic marker, α-MHC, β-MHC, ANP and BNP was determined using real time-PCR. Figures 3.7 and 3.8 show that mid-chain HETEs increased the mRNA expression levels of α-MHC, β-MHC and BNP in a concentration-dependent manner. The maximum induction of α-MHC was observed at the highest concentration tested, 20 μM, by approximately 3.5-, 1.5-and 3-fold for 5, 12, and 15 HETE, respectively (Figure 3.7A). 5-, 12- and 15-HETE significantly induced β-MHC by approximately 6.5-, 2.5-, and 4.5-fold at 20 μM (Figure 3.7B). In contrast to 5-HETE, 12- and 15-HETE significantly induced ANP by about 2.5-and 1.5-fold, respectively (Figure 3.7C). 5-, 12- and 15-HETE caused a maximum induction of BNP by approximately 2-, 2.5- and 4-fold at 20 μM concentration, respectively (Figure 3.7D). 8-HETE increased the mRNA expression of α-

MHC, β-MHC, ANP and BNP in a concentration-dependent manner (Figure 3.8). The maximum induction was observed at the highest concentration tested, 10 μM, by approximately 2-, 3-, 2- and 3-fold with α-MHC, β-MHC, ANP and BNP, respectively (Figure 3.8).

To better understand the kinetics of the induction of cardiac hypertrophic markers in response to mid-chain HETEs, β-MHC/ α-MHC mRNA were measured at various time points (0, 2, 6, 12, 18 and 24 h) following the incubation of RL-14 cells with a single concentration of 5-, 12-, and 15-HETE (20 μM) in addition to 8-HETE (10 μM). The concentration of mid-chain HETEs was chosen based on their ability to cause maximal induction of the hypertrophic markers. Thereafter, the mRNA expressions of hypertrophic markers were determined by real time-PCR. The onset of β-MHC/α-MHC induction was detectable as early as 6 h and reached the maximum induction at least 24 h after treatment (Figure 3.9).

(A)

(B)
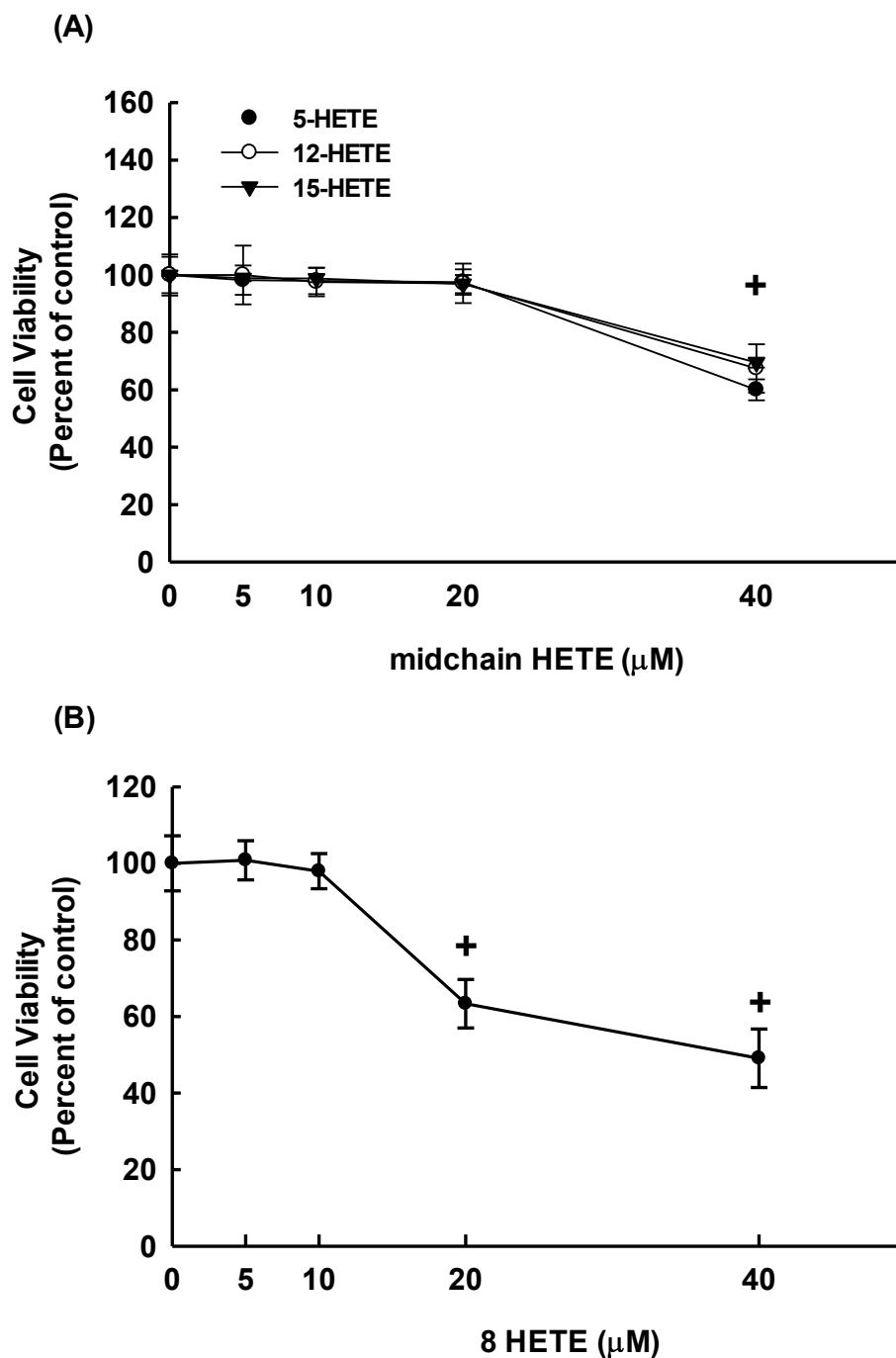
Figure 3.6. Effect of mid-chain HETEs on cells viability

RL-14 cells were treated for 24 h with various concentrations of 5-, 8-, 12- and 15-HETE (0, 0.5, 1, 2.5, 5, 10, 20 and 40 μM) and then cell viability was measured using the MTT assay. The values represent mean of expression levels ± SEM (n = 6).
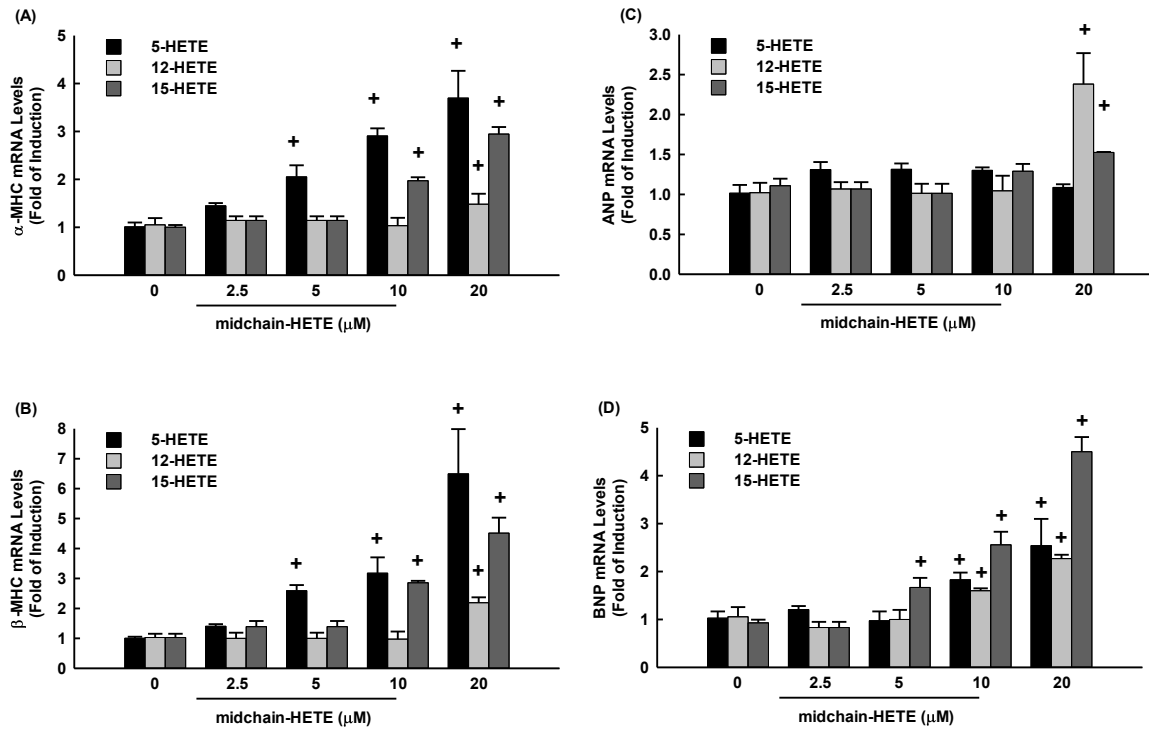
Figure 3.7. Concentration-dependent effects of mid-chain HETEs on ANP, BNP, α-MHC, and β-MHC mRNA levels

RL-14 cells were treated for 6 h with various concentrations of 5-, 12- and 15-HETEs (0, 2.5, 5, 10 and 20 μM). Thereafter, the mRNA levels of, (A) α-MHC, (B) β-MHC, (C) ANP and (D) BNP were quantified using real time-PCR. The values represent mean of fold change ± SEM (n = 6). $^{+}p<0.05$ compared to control (concentration = 0 μM).
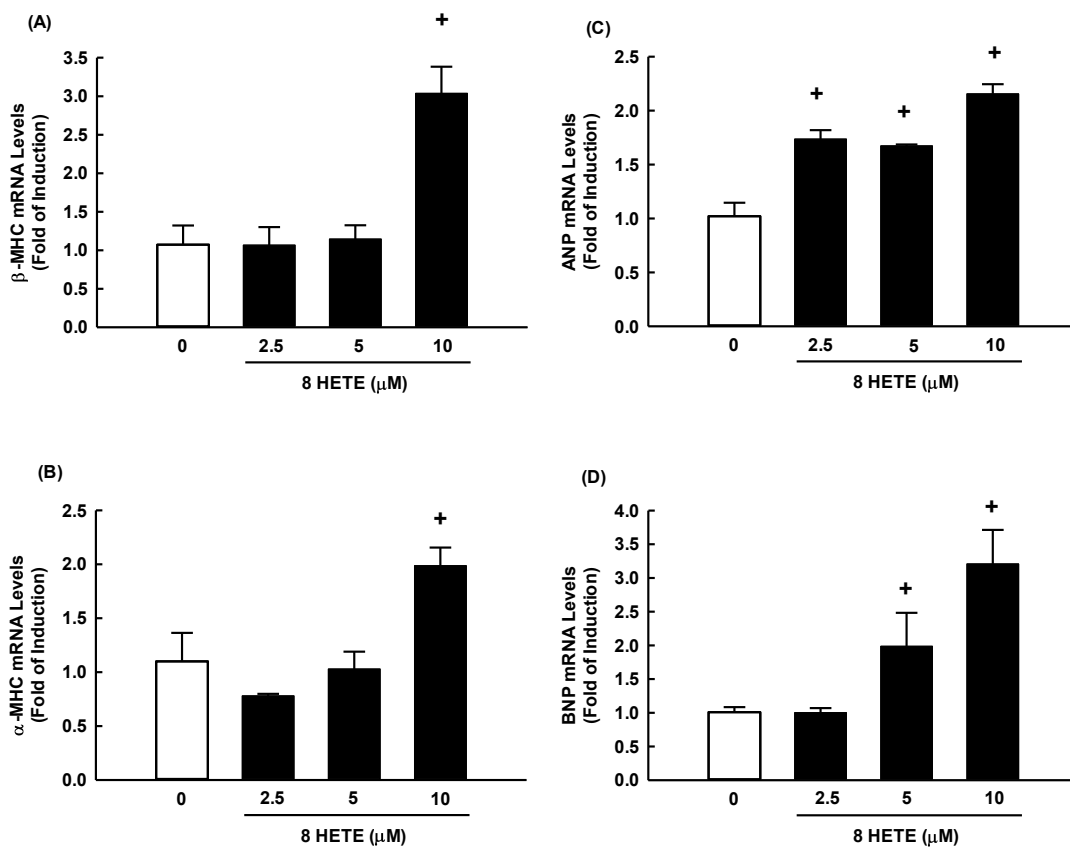
Figure 3.8. Concentration-dependent effects of 8-HETE on ANP, BNP, α-MHC, and β-MHC mRNA levels

RL-14 cells were treated for 6 h with various concentrations of 8-HETE (0, 1, 2.5, 5 and 10 μM). Thereafter, the mRNA levels of, (A) α-MHC, (B) β-MHC, (C) ANP and (D) BNP were quantified using real time-PCR. The values represent mean of fold change ± SEM (n = 6). $^+p<0.05$ compared to control (concentration = 0 μM).

(A)

(B)
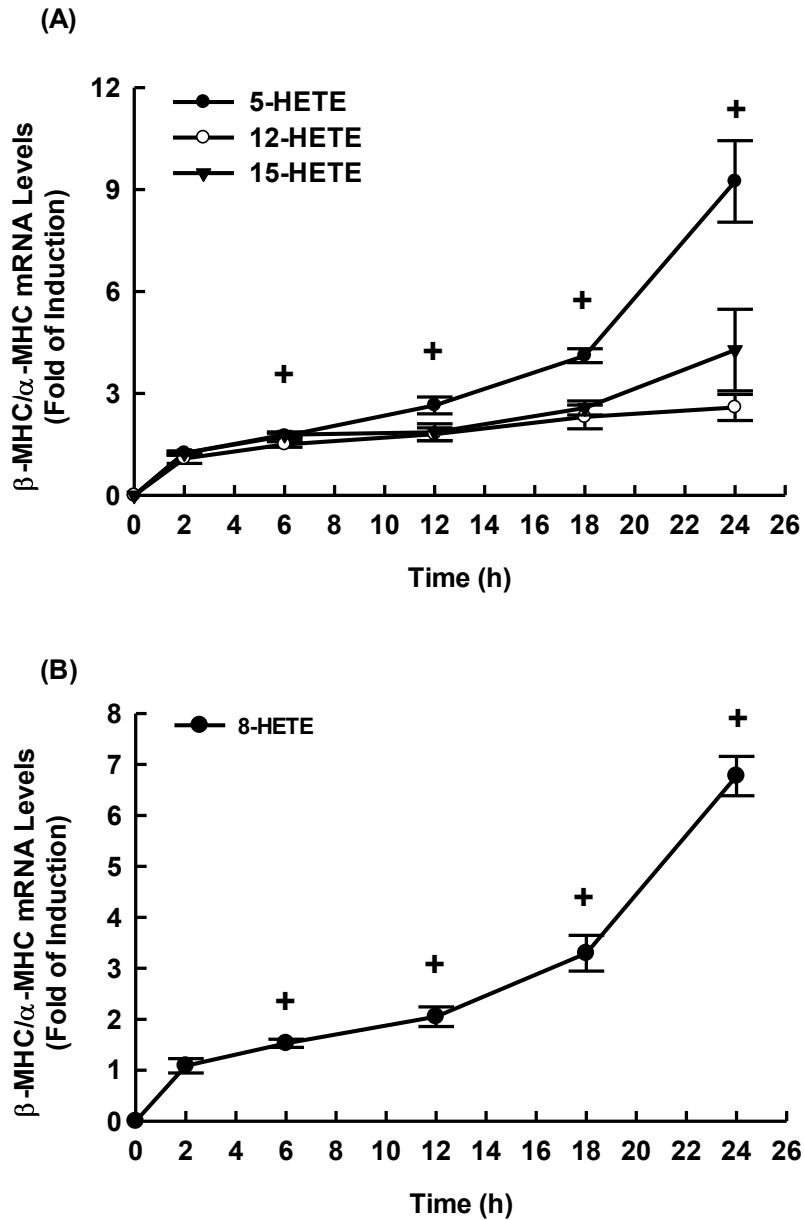
Fig. 3.9. Time-dependent effects of mid-chain HETEs on β-MHC/α-MHC mRNA level
RL-14 cells were treated with (A) 20 µM 5-, 12- and 15-HETE in addition to (B) 10 µM 8-HETE for different time intervals (0, 2, 6, 12, 18 and 24 h). Thereafter, the mRNA level of β-MHC/α-MHC was quantified using real time-PCR and normalized to β-actin housekeeping gene. The values represent mean of fold change ± SEM (n = 6). $^+p<0.05$ compared to control (concentration = 0 µM) or (time = 0 h).

3.2.3. Hypertrophy and increase in RL-14 cell surface area by mid-chain HETEs

To determine whether the mid-chain HETEs-induced hypertrophic markers at the mRNA (Fig. 2 and 3) were associated with cellular hypertrophy and increased the cell surface area, RL-14 cells were treated for 24 h with 5-, 12-, and 15-HETE (20 µM) in addition to 8-HETE (10 µM); thereafter, cell surface area was determined by phase contrast imaging taken with a Zeiss Axio Observer Z1 inverted microscope using a 20 objective lens. Figure 3.10 shows that treatment of RL-14 cells for 24 h with mid-chain HETEs significantly increased the percentage of cell surface area by about 50% as compared with control.

3.2.4. Effect of mid-chain HETEs on MAPK signaling pathway

To assess the role of MAPK signaling pathway on the mid-chain HETEs-induced cellular hypertrophy, RL-14 cells were treated with 5-, 12-, and 15-HETE (20 µM) in addition to 8-HETE (10 µM). Thereafter, phosphorylated MAPK levels were determined using a commercially available kit. Figure 3.11A shows that incubation of the cells with 5-, 8-, 12- and 15-HETE significantly induced the phosphorylated ERK1/2 by 220%, 230%, 250% and 200% , respectively, in comparison to control whereas no significant changes were observed on phosphorylated P38 or JNK (Figure 3.11A).

To examine whether the induction of the cellular hypertrophy and cardiac hypertrophic markers in RL-14 cells by mid-chain HETEs is an ERK1/2-dependent mechanism, we tested the effect of a selective ERK1/2inhibitor, U0126, on mid-chain HETEs-induced β-MHC/α-MHC mRNA. For this purpose, RL-14 cells were treated for 2 h with U0126 (10 µM) before the addition of mid-chain-HETEs for 6 h. Thereafter, the mRNA expression of the hypertrophic markers, β-MHC/α-MHC, were measured by Real Time-PCR. Figure 3.11B shows that mid-chain HETEs alone caused a significant induction of β-MHC/α-MHC genes. Importantly, pretreatment with U0126 significantly blocked the induction of β-MHC/α-MHC mRNA in response to mid-chain HETEs, suggesting that ERK1/2 is essential for mid-chain HETEs-mediated induction of cellular hypertrophy.
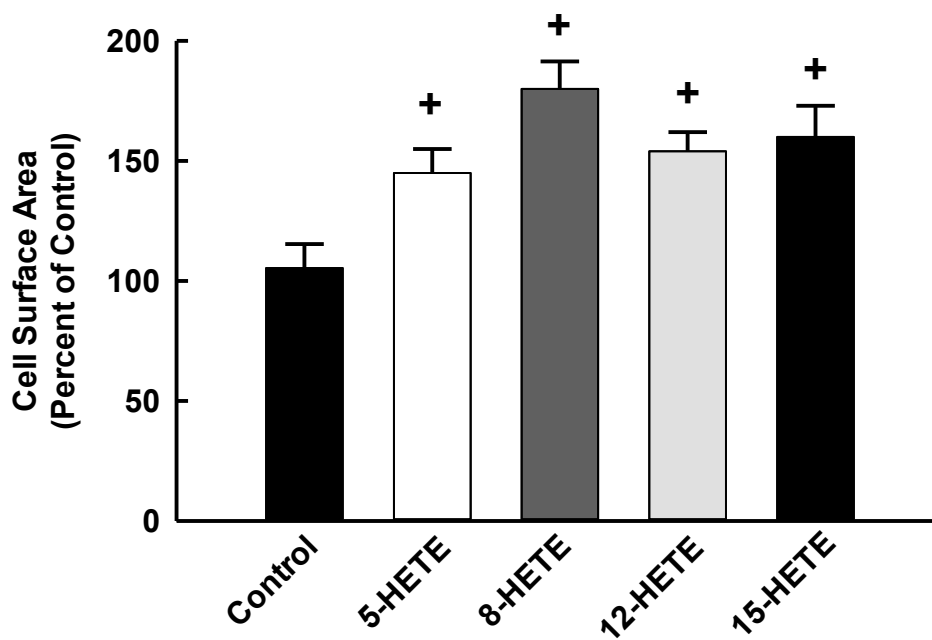
Figure 3.10. Effect of mid-chain HETEs on cell surface area
RL-14 cells were treated with 20 µM 5-, 12- and 15-HETE in addition to 10 µM 8-HETE for 24 h. Thereafter, cell surface area was determined by phase contrast images which were taken with Zeiss Axio Observer Z1 inverted microscope using 20 objective lens. The values represent mean of fold change ± SEM (n = 6). $^+p<0.05$ compared to control (concentration = 0 µM).
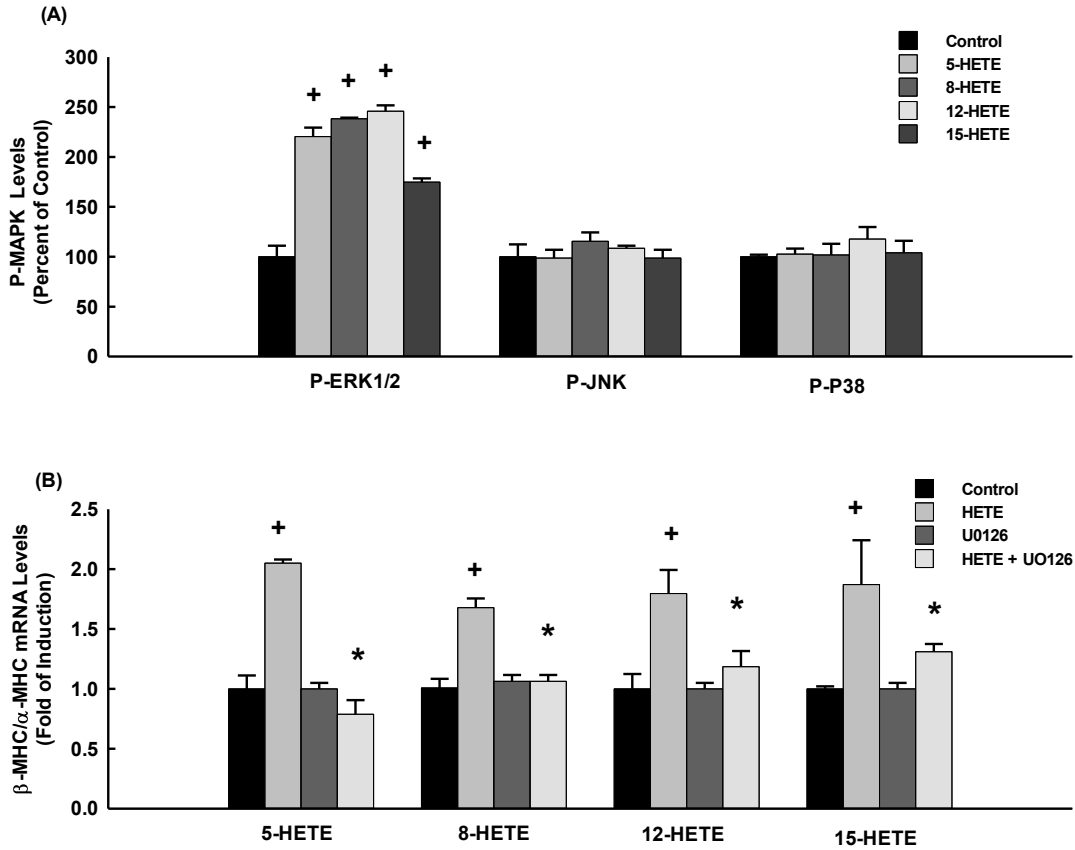
Figure 3.11. Effect of mid-chain HETEs on MAPK signaling pathway
(A) RL-14 cells were treated with 20 µM 5-, 12- and 15-HETE in addition to 10 µM 8-HETE for 2 h. Thereafter, MAPK protein phosphorylation was determined using the PhosphoTracer Elisa Kit (Abcam, Cambridge, UK). (B) RL-14 cells were treated with 10 µM U0126 for 2 h before the addition of mid-chain-HETEs for 6 h. Thereafter, the mRNA level of β-MHC/α-MHC was quantified using real time-PCR. The values represent mean of fold change ± SEM (n = 6). [+]$p<0.05$ compared to control. [*]$p<0.05$ compared to mid-chain HETEs.

3.2.5. Effect of mid-chain HETEs on the NF-κB signaling pathway

To investigate whether mid-chain HETEs trigger NF-κB activation, we tested the capacity of 5-, 8-, 12- and 15-HETE to increase NF-κB binding activity using a commercially available kit. Our results showed that the positive control, lipopolysaccharide (LPS), significantly increased DNA binding activity by 600%-and 250% for P50 and P65, respectively, in comparison to control (Figure 3.12A). Furthermore, all mid-chain HETEs were able to induce the binding activity of NF-κB to its responsive element in a HETE-dependent manner. Figure 2.12A shows that 12-HETE was the most potent inducer of P50 NF-κB binding activity by approximately 1300%, whereas 15-HETE caused the highest induction of P65 NF-κB binding activity by about 750% in comparison to control. 5-HETE significantly induced P50 NF-κB and P65 NF-κB by approximately 300% and 600%, respectively, in comparison to control. 8-HETE was able to induce the binding activity of NF-κB to its responsive element by approximately 500% and 200% for P50 and P65, respectively, in comparison to control.

To further confirm the NF-κB-dependent induction of the cellular hypertrophy and cardiac hypertrophic markers in RL-14 cells by mid-chain HETEs, we tested the effect of a selective NF-κB inhibitor, PDTC, on mid-chain HETEs-induced β-MHC/α-MHC mRNA. For this purpose, RL-14 cells were treated for 2 h with PDTC (10 μ M) before the addition of mid-chain-HETEs for 6 h. Thereafter, the mRNA expression of the hypertrophic markers, β-MHC/α-MHC, were measured by real time-PCR. Figure 3.12B shows that mid-chain HETEs alone caused a significant induction of β-MHC/α-MHC genes. Importantly, pretreatment with PDTC significantly blocked the induction of β-MHC/α-MHC mRNA in response to mid-chain HETEs.

(A)

(B)
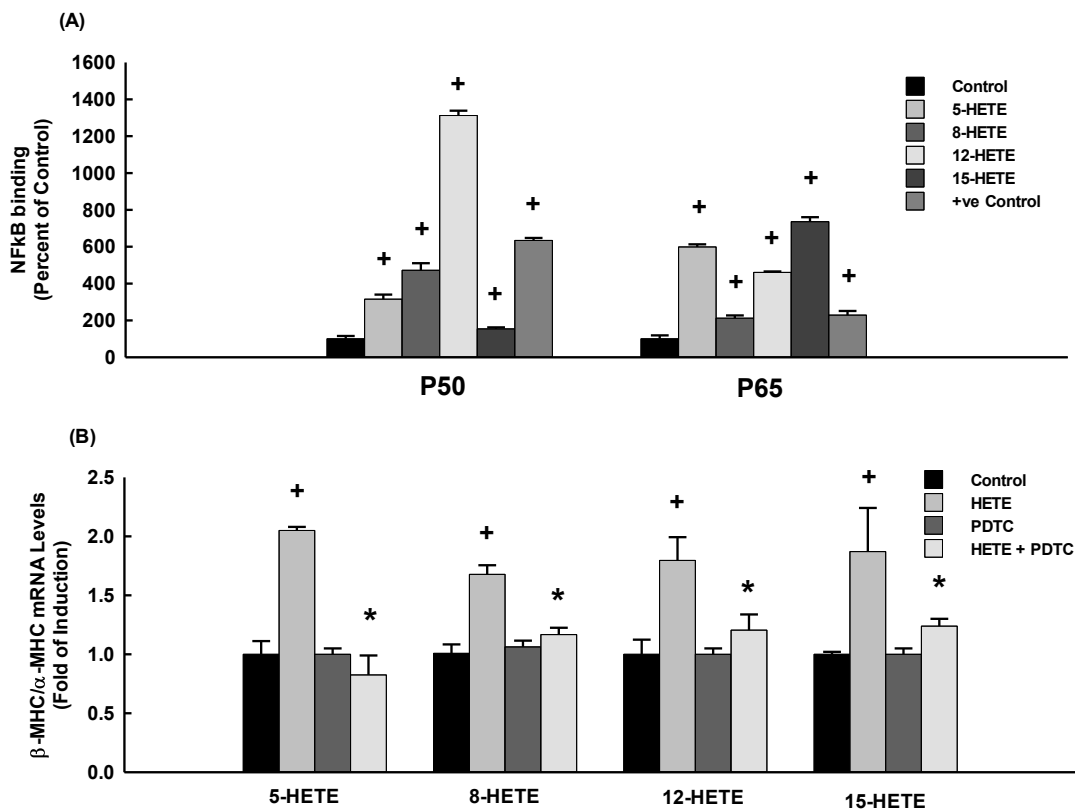
Figure 3.12. Effect of mid-chain HETEs on NF-κB signaling pathway

(A) RL-14 cells were treated with 20 μM 5-, 12- and 15-HETEs in addition to 10 μM 8-HETE for 2 h. Thereafter, NF-κB binding activity was determined using a commercially available kit. (B) RL-14 cells were treated with 10 μM PDTC for 2 h before the addition of mid-chain-HETEs for 6 h. Thereafter, the mRNA level of β-MHC/α-MHC was quantified using real time-PCR. The values represent mean fold change $\pm$ SEM (n = 6). $^{+}p<0.05$ compared to control. $^{*}p<0.05$ compared to mid-chain HETEs.

3.2.5. Effect of mid-chain HETEs on the expression of CYP epoxygenases and ω-hydroxylases mRNA and protein levels in RL-14 Cells

To examine the effect of mid-chain HETEs on the expression of CYP epoxygenases, CYP2B6, CYP2C8, and CYP2J2 and CYP ω-hydroxylases, CYP4F2 and CYP4F11, RL-14 cells were treated with 5-, 12- and 15-HETE (20 µM) in addition to 8-HETE (10 µM) for 6 h. Thereafter, CYP epoxygenases and ω-hydroxylases genes were measured using real time-PCR. Figure 3.13A and 3.14A show that all mid-chain HETEs did not significantly alter the expression of CYP epoxygenases and ω-hydroxylases mRNA levels.

To further examine whether CYP epoxygenases and ω-hydroxylases would be induced in response to mid-chain HETEs at the translational level, RL-14 cells were treated for 24 h with 5-, 12- and 15-HETE (20 µM) in addition to 8-HETE (10 µM); thereafter, CYP protein expression levels were determined by western blot analysis. Figure 3.13B and 3.14B show that, in a pattern similar to what was observed with mRNA, all mid-chain HETEs did not significantly alter the protein levels of CYP epoxygenases and ω-hydroxylases.
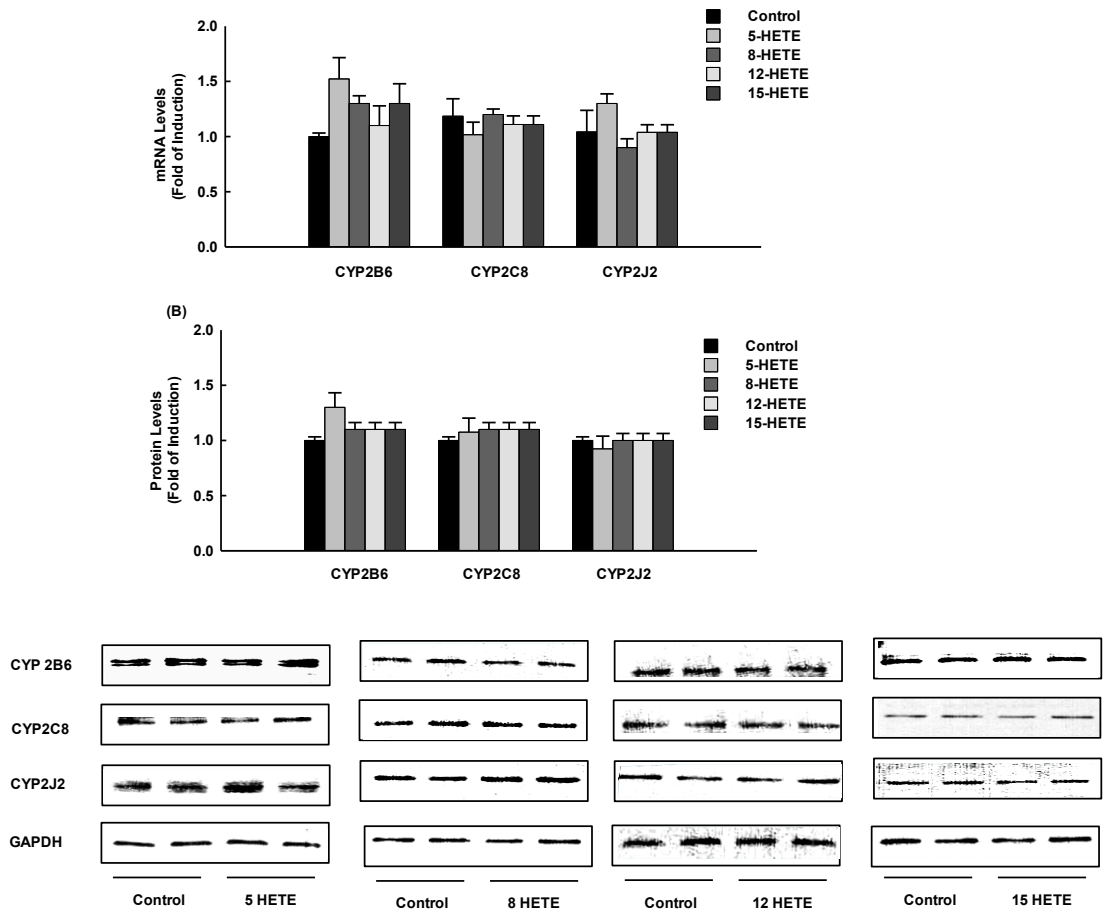
Figure 3.13. Effect of mid-chain HETEs on CYP epoxygenases in RL-14 cells

(A) RL-14 cells were treated with 20 µM 5-, 12- and 15-HETEs in addition to 10 µM 8-HETE for 6 h. Thereafter, the mRNA levels of CYP epoxygenases were quantified using real time-PCR. (B) RL-14 cells were treated for 24 h with 20 µM 5-, 12- and 15-HETE in addition to 10 µM 8-HETE; thereafter, CYP epoxygenase protein levels were determined by Western blot analysis. The values represent mean of fold change ± SEM (n = 6). +$p<0.05$ compared to control (concentration = 0 µM).
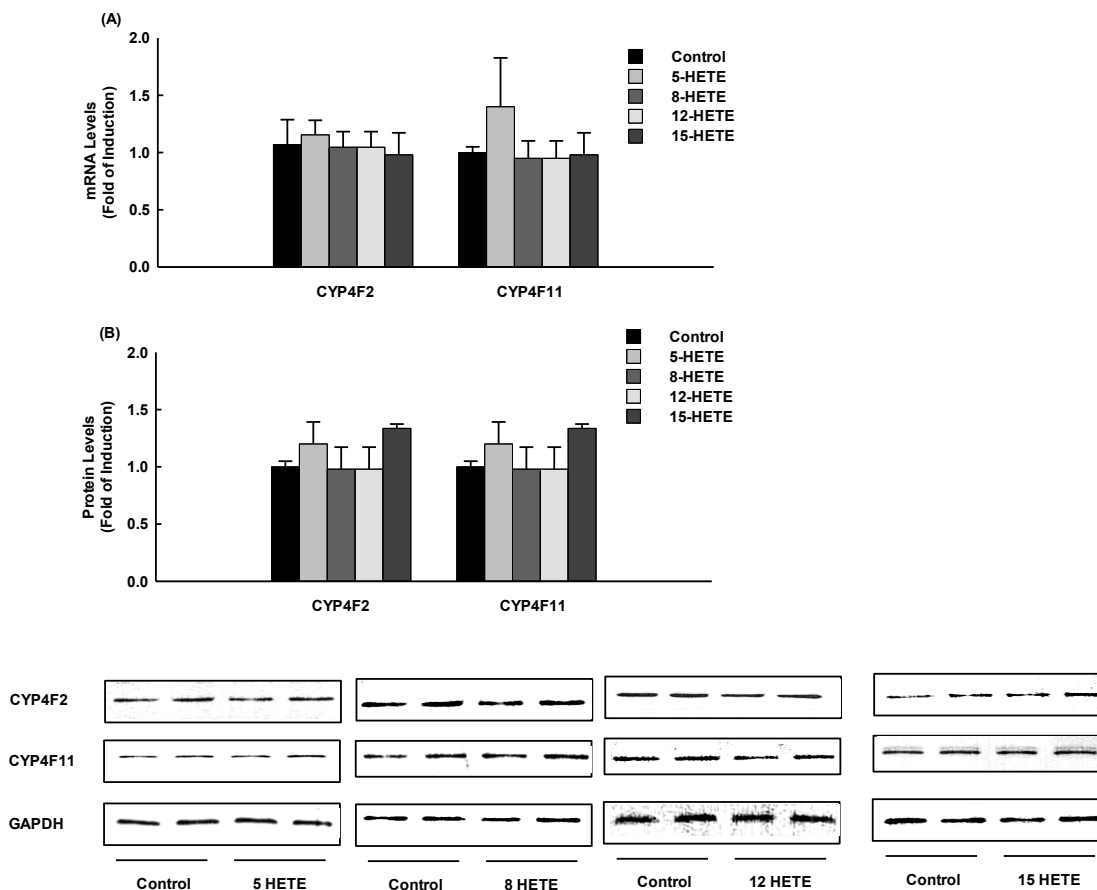
Figure 3.14. Effect of mid-chain HETEs on CYP ω-hydroxylases in RL-14 cells
(A) RL-14 cells were treated with 20 µM 5-, 12- and 15-HETEs in addition to 10 µM 8-HETE for 6 h. Thereafter, the mRNA levels of CYP ω-hydroxylases were quantified using real time-PCR. (B) RL-14 cells were treated for 24 h with 20 µM 5-, 12- and 15-HETE in addition to 10 µM 8-HETE; thereafter, CYP ω-hydroxylase protein levels were determined by Western blot analysis. The values represent mean of fold change ± SEM (n = 6). [+]$p<0.05$ compared to control.

3.2.6. Effect of mid-chain HETEs on CYP-mediated AA metabolism

To examine the effect of mid-chain HETEs on CYP-mediated AA metabolism, RL-14 cells were treated with 5-, 12- and 15-HETE (20 µM) in addition to 8-HETE (10 µM) for 24 h. Thereafter, AA metabolites were measured using LC–ESI–MS. Figure 3.15A shows that 8-HETE and 12-HETE were able to significantly inhibit the formation of 14,15-EET and 11,12-EET by approximately 60 % and 40 %, respectively, in comparison to control levels. On the other hand, 5-, 8-, 12- and 15-HETE significantly induced the formation of 14,15-DHET by 1.8-,2-, 1.79- and 1.6-fold of induction, respectively, whereas 5-, 8- and 12-HETE caused a significant induction of 11,12- DHET by approximately 1.8-, 1.8- and 2-fold, respectively (Figure 3.15B).

To determine the effect of 5-, 8-, 12- and 15-HETE on CYP ω-hydroxylases activity, we measured the level of 20 HETE formation. Our results showed that with RL-14 all mid-chain HETEs did not significantly change the formation of 20 HETE in comparison to control levels (Figure 3.15C).
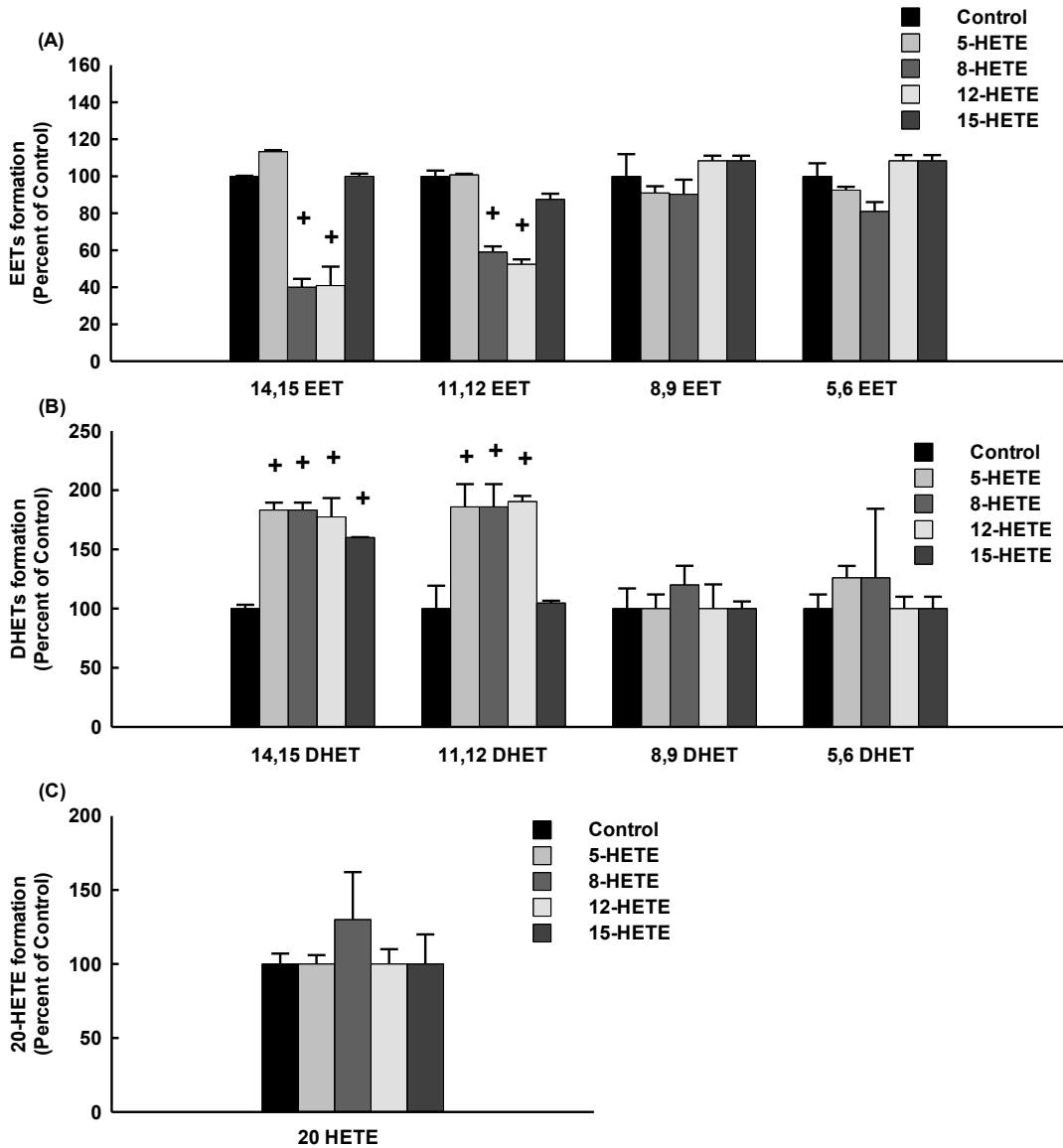
Figure 3.15. Effect of mid-chain HETEs on CYP-mediated AA metabolism
RL-14 cells were treated with 20 µM 5-, 12- and 15-HETE in addition to 10 µM 8-HETE for 24 h. Thereafter, (A) EETs, (B) DHETs, (C) 20-HETE were quantified using LC–ESI–MS. The values represent mean ± SEM (n = 6). $^+p<0.05$ compared to control.

3.2.7. Role of sEH in mid-chain HETEs mediated effect

To investigate the mechanism responsible for high levels of DHETs in RL-14 cells in response to mid-chain HETEs, the activity level of sEH was determined. Our results showed that incubation of the RL-14 cells with 5-, 8-, 12- and 15-HETE caused a significant induction of sEH catalytic activity in RL-14 cells by 270%, 470%, 430%, and 400%, respectively, in comparison to control (Figure 3.16).

In an attempt to explore whether sEH is directly involved in the induction of cellular hypertrophic and the cardiac hypertrophy markers, RL-14 cells were treated for 2 h with a sEH inhibitor, tAUCB, before the addition of mid-chain HETEs for 6 h. Thereafter, the mRNA expression of the hypertrophic markers, β-MHC/α-MHC, were measured by real time-PCR. Figure 3.16B shows that mid-chain HETEs alone caused a significant induction of β-MHC/α-MHC genes. Importantly, pretreatment with tAUCB significantly blocked the induction of β-MHC/α-MHC mRNA in response to mid-chain HETEs, suggesting that sEH is essential for mid-chain HETEs-mediated induction of cellular hypertrophy.
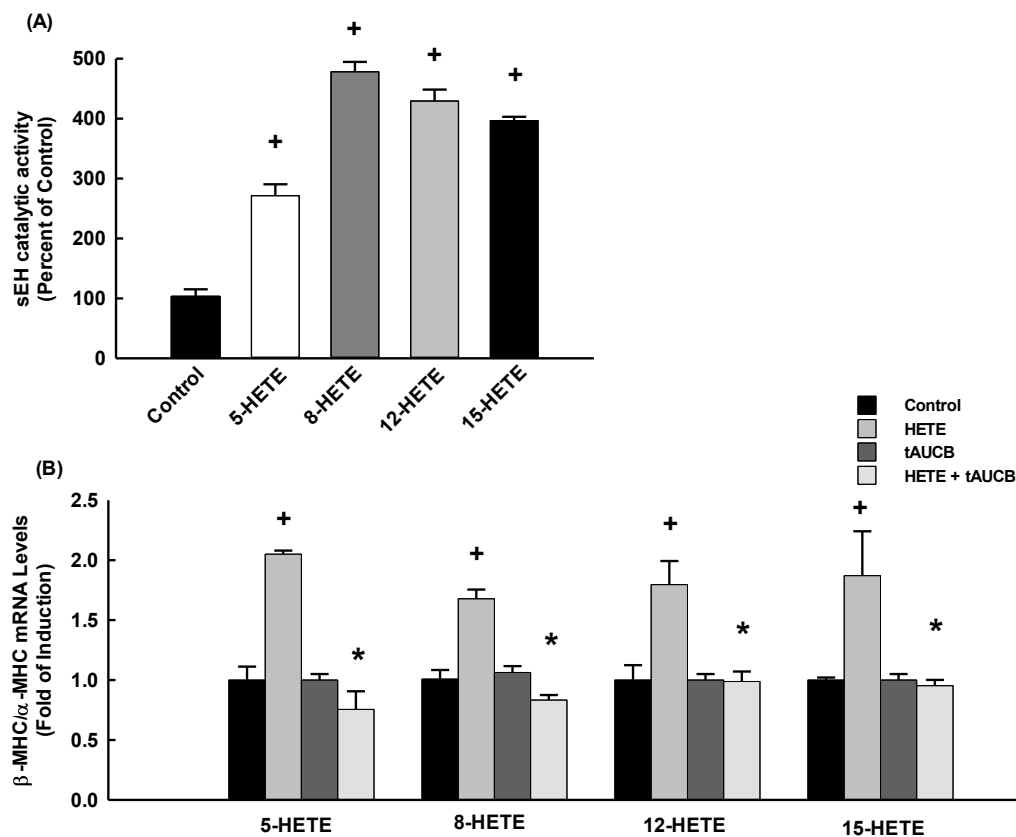
Figure 3.16. Role of sEH in mid-chain HETEs-mediated effect
    (A) RL-14 cells were treated with 20 µM 5-, 12- and 15-HETE in addition to 10 µM 8-HETE for 24 h and then the cells were incubated with 5 µM EETs for 30 min. Thereafter, EETs and DHETs were quantified using LC–ESI–MS. sEH activity was calculated as the ratio of total DHETs/total EETs. (B) RL-14 cells were treated for 2 h with tAUCB before the addition of mid-chain-HETEs for 6 h. Thereafter, the mRNA level of β-MHC/α-MHC was quantified using real time-PCR. The values represent mean ± SEM (n = 6). $^{+}p<0.05$ compared to control. $^{*}p<0.05$ compared to mid-chain HETEs.

3.3. CYP1B1 inhibition attenuates doxorubicin-induced cardiotoxicity through a mid-chain HETEs-dependent mechanism

3.3.1. Effect of TMS on DOX-induced cardiotoxicity in rats

To investigate whether TMS confers cardioprotection against DOX-induced cardiotoxicity in rats, cardiotoxicity parameters were assessed via echocardiography and by measuring heart weight-to-tibial length ratio (HW/TL). Echocardiogrphy assessment of DOX treated rats showed thinning of the LVPWd, LVIDd, IVSD, IVSs and LVPWs in addition to a significant decrease in CO and SV (Table 3.1). Importantly, TMS treatment significantly restored the DOX-mediated inhibition of CO, SV and left ventricular morphology. Additionally, DOX significantly decreased the HW/TL to 0.021 ± 0.001 from control level of 0.034 ± 0.0005 ($P < 0.05$), whereas treatment with TMS significantly blocked the DOX-mediated decrease in the HW/TL ratio to 0.030 ± 0.002 ($P < 0.05$). Furthermore, no significant differences were observed between the control and the TMS treatment alone (Table 3.1).

3.3.2. Effect of TMS on DOX-induced histopathological changes in rat cardiac tissues

The cardiotoxicity induced by DOX was further assessed via histology. Representative transverse views of whole heart sections from the similar layers of each group are shown in Figure 3.17. Using the H&E stain, the heart from control group showed regular cell distribution and normal myocardium morphology (Figure 3.17A). In the DOX-treated group, several lesions were observed which concerned the majority of the myocardium. These lesions consisted of a modification of the normal architecture with myofiber disarray (elongated cells) and muscular fiber dissociation (arrow). This was a typical finding in DOX-induced cardiomyopathy. Fortunately, TMS treatment reduced myocardial lesions induced by DOX (Figure 3.17A). In addition to H&E stain, cardiac sections were stained with Trichrome's stain for the detection of fibrillar collagen and hence fibrosis (Figure 3.17B). Microscopic view of the myocardial tissue, showed the presence of fibrosis in the hearts of rats treated with DOX. Importantly, these changes were prevented by TMS treatment (Figure 3.17B).

Table 3.1. Hemodynamic parameters and LV morphology in rats

	Control	TMS	DOX	DOX+TMS
HW/TL	0.034$\pm$.0005	0.034$\pm$.002	0.021$\pm$.001[+]	0.030$\pm$.002[*]
CO (ml)	108.8$\pm$5.6	102.4$\pm$8.1	52.6$\pm$9.6[+]	89.9$\pm$13.8[*]
SV (ml)	276.8$\pm$10.8	266.3$\pm$19.8	144.8$\pm$17.4[+]	233.2$\pm$36.8[*]
LV mass	1003.3$\pm$11.9	1004.6$\pm$44.9	624.3$\pm$39.8[+]	930.9$\pm$158[*]
IVSD (mm)	2.04$\pm$.04	2.01$\pm$.03	1.7$\pm$.02[+]	2.04$\pm$.09[*]
LVIDd (mm)	7.96$\pm$.17	7.8$\pm$.22	6.4$\pm$.25[+]	7.6$\pm$.51[*]
LVPWd (mm)	2.08$\pm$.03	2.02$\pm$.02	1.69$\pm$.03[+]	2.01$\pm$.11[*]
IVSs (mm)	3.19$\pm$.11	3.03$\pm$.08	2.61$\pm$.12[+]	3.15$\pm$.1[*]
LVPWs (mm)	3.49$\pm$.11	3.22$\pm$.07	2.51$\pm$.16[+]	3.08$\pm$.07[*]
LVIDs (mm)	4.45$\pm$.18	4.14$\pm$.15	3.86$\pm$.26	4.05$\pm$.31
Sd (mm)	4.52$\pm$.19	4.53$\pm$.2	3.34$\pm$.42[+]	4.4$\pm$.24[*]
Dd (mm)	8.21$\pm$.17	8.15$\pm$.25	6.6$\pm$.4[+]	7.94$\pm$.49[*]
% EF	75.8$\pm$1.6	72.7$\pm$1.5	67.2$\pm$5.6	74.3$\pm$2.38
% FS	46.3$\pm$1.5	43.3$\pm$1.2	38.8$\pm$4.4	44.8$\pm$2.3
TEI	.8$\pm$.03	.82$\pm$.06	.95$\pm$.03[+]	.79$\pm$.01[*]
E (mm/sec)	1063$\pm$55	1051$\pm$91	653$\pm$85[+]	1021$\pm$152[*]
A (mm/sec)	821$\pm$35	719$\pm$91	448$\pm$84[+]	827$\pm$136[*]
E`	62.3$\pm$3.9	63.03$\pm$5.8	35.4$\pm$1.7[+]	40.5$\pm$1.8
A`	60.3$\pm$5.1	62.6$\pm$5.9	34.6$\pm$3.7[+]	40.13$\pm$1.1
S	48.1$\pm$2.1	46.4$\pm$3.1	37.1$\pm$2.6[+]	42.7$\pm$2.9

The values represent mean $\pm$ SEM (n = 6). +p<0.05 compared to control. *p<0.05 compared to DOX. HW/TL, Heart weight/tibial length; CO, cardiac output; SV, stroke volume; LV mass, left ventricular mass; IVSD, intraventricular septum, diastole; LVIDd, left ventricular internal diameter, diastole; LVPWd, left ventricular posterior wall, diastole; IVSs, intraventricular septum, systole; LVIDs, left ventricular internal diameter, systole; Sd, diameter in systole from trace; Dd, diameter in diastole from trace; EF, ejection fraction; FS, fractional shortening; TEI, Tei index = (isovolumic relaxation time+ isovolumic contraction time)/ ejection time; E, A , wave velocity; E`, A`, tissue doppler wave; S, sytolic tissue movement.
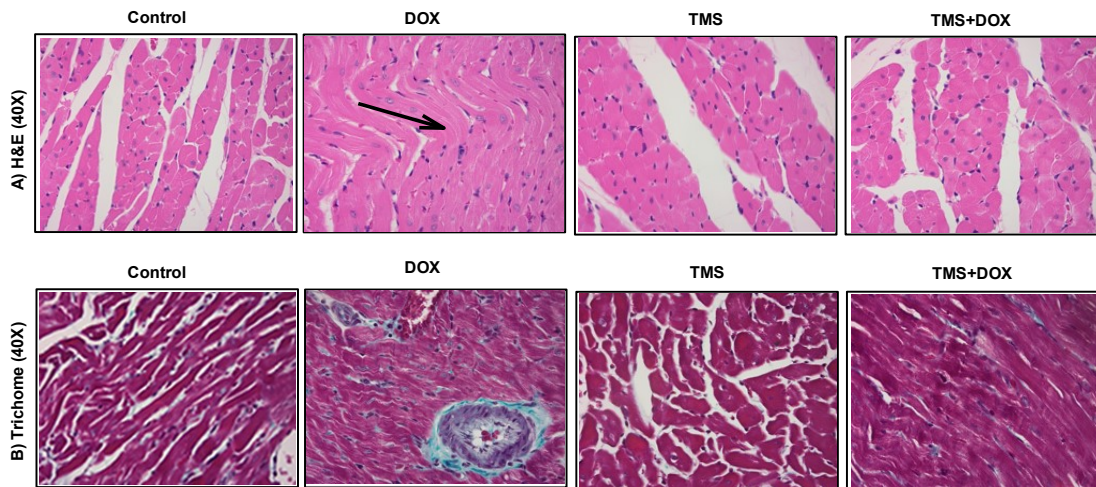
Figure 3.17. Effect of TMS on DOX-induced histopathological changes in cardiac tissues

Rats were injected with either DOX or vehicle in the presence and absence of TMS. Thereafter, histopathological changes were determined using H&E and Trichrome's stains. (A) H&E staining revealed myofiber disarray and muscular fiber dissociation in addition to the presence of fibrosis in response to DOX, which appeared to be reduced by TMS treatment. (B) Trichrome staining revealed increased fibrosis (intense blue staining) in the cardiac tissues from DOX-treated rats but was reduced in animals also treated with TMS.

3.3.3. Effect of TMS on DOX-mediated effect on α-MHC, β-MHC and β-MHC/α-MHC mRNA expression

To further confirm the protective effect of TMS against DOX-induced cardiotoxicity, we tested the effect of the TMS on DOX-mediated effects on β-MHC/α-MHC mRNA expression. For this purpose, total RNA was extracted from the heart of treated rats and the mRNA levels of β-MHC/α-MHC were determined by real time-PCR. Figure 3.18A and 3.18B show that DOX alone caused a significant inhibition of α-MHC to 60% ± 12 in addition to a significant induction of β-MHC and β-MHC/α-MHC expression to 850% ± 114 and 1400% ± 182, respectively. Importantly, treatment with TMS significantly modulated the effect of DOX on α-MHC, β-MHC in addition to β-MHC/α-MHC (Figure 3.18).

3.3.4. Effect of TMS on DOX-mediated formation of mid-chain HETEs in heart tissues

To determine the capacity of TMS to inhibit the formation of mid-chain HETEs altered by DOX, AA metabolites were extracted from heart tissues using Oasis®HLB SPE cartridges. Thereafter, mid-chain HETE metabolites were measured using LC–ESI–MS. Table 3.2 shows that DOX was able to significantly increase the formation of cardiac mid-chain HETEs/AA to 177 % ± 5.8 in comparison to control. Importantly, treatment with TMS significantly reduced the increase in mid-chain HETEs/AA formation to 99.14% ± 4.45 in comparison to control (Table 3.2).
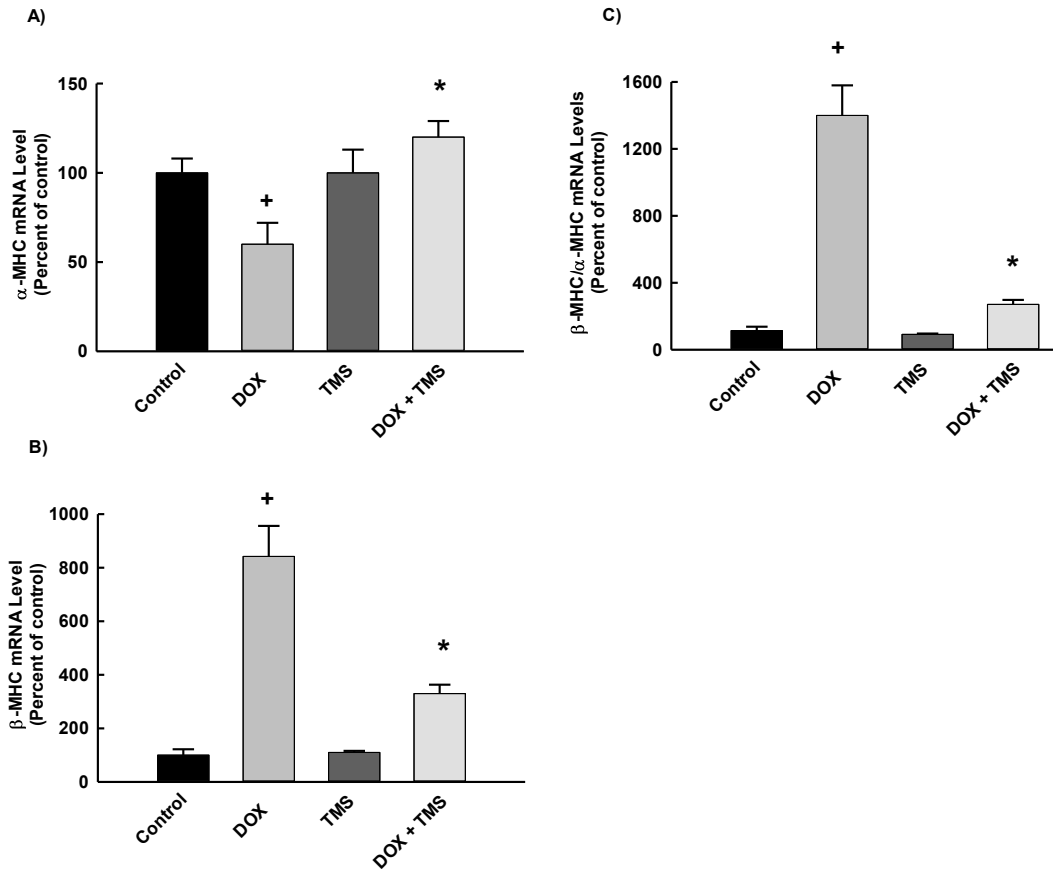
Figure 3.18. Effect of TMS on DOX-mediated induction of β-MHC/α-MHC mRNA expression
Rats were injected with either DOX or vehicle in the presence and absence of TMS. Thereafter, the mRNA level of β-MHC/α-MHC was quantified using real time-PCR. The values represent mean ± SEM (n = 6). $^+p<0.05$ compared to control. $^*p<0.05$ compared to DOX.

3.3.4. Effect of TMS on DOX-mediated formation of mid-chain HETEs in heart tissues

To determine the capacity of TMS to inhibit the formation of mid-chain HETEs altered by DOX, AA metabolites were extracted from heart tissues using Oasis®HLB SPE cartridges. Thereafter, mid-chain HETE metabolites were measured using LC–ESI–MS. Table 3.2 shows that DOX was able to significantly increase the formation of cardiac mid-chain HETEs/AA to 177 % ± 5.8 in comparison to control. Importantly, treatment with TMS significantly reduced the increase in mid-chain HETEs/AA formation to 99.14% ± 4.45 in comparison to control (Table 3.2).

Table 3.2. Effect of TMS on DOX-induced mid chain HETEs formation

Group	HETEs	AA	HETEs/AA
Control	100 ± 2.3	100 ± 7.9	100 ± 8.6
DOX	$262 \pm 2.2^{+}$	$153.3 + 4.5^{+}$	$176.9 + 5.8^{+}$
TMS	$96.3 + 3.7$	108 ± 24	88.7 ± 7.95
DOX+TMS	$192 + 2.4^{*}$	$193 \pm 14.7^{+}$	$99.14 \pm 4.45^{*}$

Rats were injected with either DOX or vehicle in the presence and absence of TMS and then AA metabolites were extracted from the heart tissues using Oasis®HLB SPE cartridges. Thereafter, mid-chain HETE metabolites were measured using LC–ESI–MS. The values are expressed as a % of control and represent mean ± SEM (n = 6). $^{+}p<0.05$ compared to control. $^{*}p<0.05$ compared to DOX.

3.3.5. Effect of TMS on DOX-induced expression of CYP1B1 mRNA and catalytic activity in rats

To determine the capacity of TMS to alter the induction of CYP1B1 gene expression by DOX, total RNA was extracted from the heart of treated rats and the CYP1B1 mRNA level was determined by real time-PCR. Figure 3.19A shows that DOX significantly induced CYP1B1 mRNA expression level by approximately $350\% \pm 14.1$ in comparison to control level. Although TMS alone did not significantly alter CYP1B1 gene expression level, treatment of rats with TMS significantly inhibited the DOX-mediated induction of CYP1B1 gene expression to $120\% \pm 34$ (Figure 3.19A).

To further examine whether the effect obtained at mRNA in response to DOX and TMS treatment is translated into functional catalytic activity, microsomes were extracted from the heart of treated rats and CYP1B1 catalytic activity was determined by MROD assay. Figure 3.19B shows that DOX significantly increased the formation of resorufin to 33.3 ± 3.1 pmol/min/mg protein from control level of 16 ± 0.8 pmol/min/mg protein. On the other hand, TMS significantly inhibited the DOX-induced CYP1B1 catalytic activity using MROD assay to approximately 20 ± 1.9 pmol/min/mg protein (Fig. 3.19B).
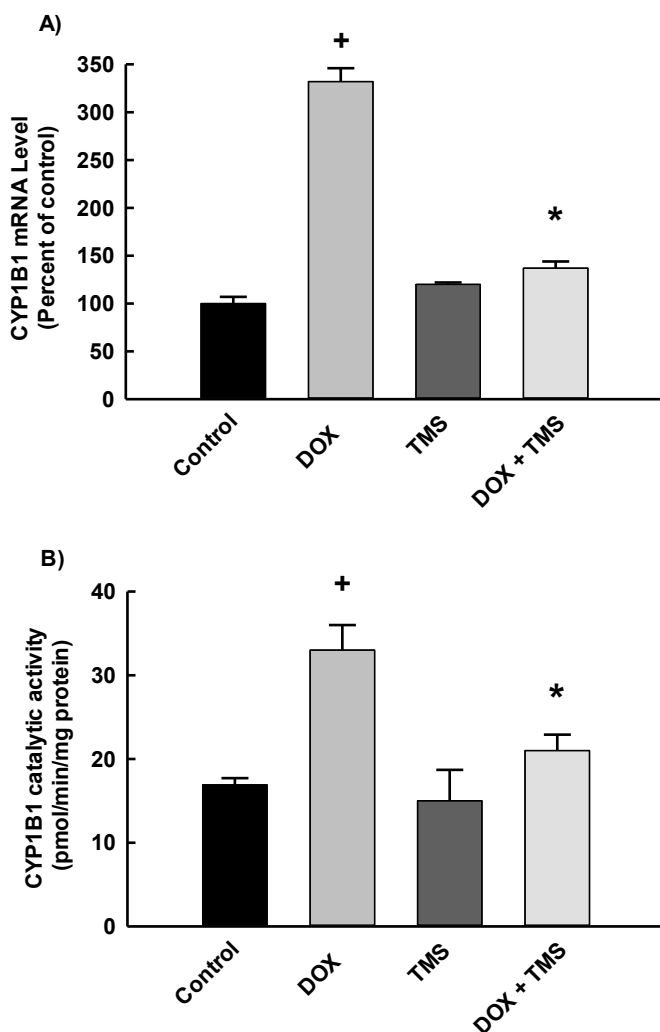
Figure 3.19. Effect of TMS on the expression of CYP1B1 altered by DOX
(A) Rats were injected with either DOX or vehicle in the presence and absence of TMS. Thereafter, total RNA was extracted from the heart of treated rats and the mRNA level of CYP1B1 was quantified using real time-PCR. (B) Rats were injected with either DOX or vehicle in the presence and absence of TMS. Thereafter, microsomes were extracted from the hearts of treated rats and CYP1B1 catalytic activity level was determined by the MROD assay. The values represent mean $\pm$ SEM (n = 6). $^{+}p<0.05$ compared to control. $^{*}p<0.05$ compared to DOX.

3.3.6. Effect of TMS and DOX on the expression of LOXs mRNA and protein levels in rats

Mid-chain HETEs are known to be formed by LOXs enzymes in addition to CYP1B1. Therefore, we investigated whether the increase in mid-chain HETEs and cardiotoxicity by DOX could also be attributed to the activation of LOX enzymes. For this purpose, total RNA was extracted from the heart of treated rats and the mRNA level of LOX was determined by real time-PCR. Our results showed that treatment of rats with DOX in the presence and absence of TMS did not significantly alter the expression of 5-LOX and 12/15-LOX mRNA levels (Figure 3.20A).

To further examine whether LOXs would be altered in response to DOX and TMS at translational level, 5-LOX and 12/15-LOX protein expression levels were determined by Western blot analysis. Figure 3.20B shows that, in a pattern similar to what was observed with the mRNA, treatment of rats with DOX in the presence and absence of TMS did not significantly alter the expression of 5-LOX and 12/15-LOX protein levels, confirming the role of CYP1B1 in the formation of mid-chain HETE and cardiotoxicity mediated by DOX.
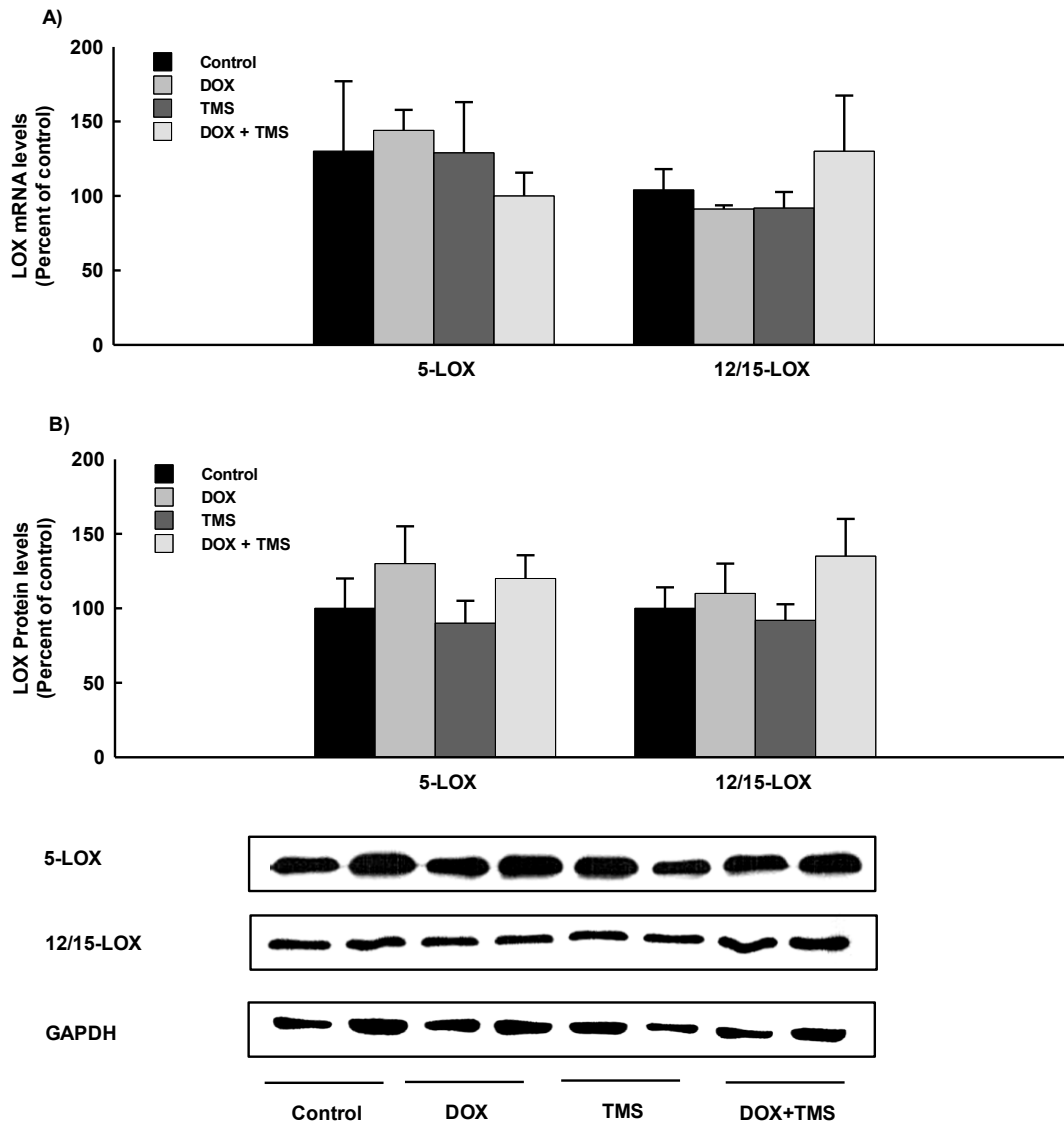
Figure 3.20. Effect of DOX and TMS on the expression of LOXs mRNA and protein levels in rats

(A) Rats were injected with either DOX or vehicle in the presence and absence of TMS. Thereafter, the mRNA levels of 5-LOX and 12/15-LOX were quantified using real time-PCR. (B) 5-LOX and 12/15-LOX protein expression levels were determined by Western blot analysis. The values represent mean $\pm$ SEM (n = 6).

3.3.7. Effect of DOX on RL-14 cells viability and cellular hypertrophy

To determine the cytotoxic effect of DOX, RL-14 cells, human ventricular cardiomyocytes, were exposed to 10 µM DOX for different time intervals (0, 2, 6, 12 and 24 h). Thereafter, the cell viability was determined using MTT assay. Our results showed that a 10 µM DOX did not significantly affect cell viability at 2 and 6 h (Figure 3.21A). However, 10 µM DOX significantly decreased the cell viability to 77% ± 2.2 and 55% ± 7.6 at 12 and 24 h, respectively, from control levels of 100% (Figure 3.21A).

To further examine the effect of DOX to induce cellular hypertrophy, RL-14 cells were treated with a single concentration of DOX (10 µM) at various time points (0, 2, 6, 12 and 24 h). Thereafter, the mRNA expressions of hypertrophic markers were determined by real time-PCR. Figure 3.21B shows that DOX significantly induced β-MHC/α-MHC expression in a time-dependent manner. The onset of β-MHC/α-MHC induction was detectable as early as 6 h and reached the maximum expression at 12 h after treatment and remained elevated for at least 24 h. (Figure 3.21B).

To determine whether the increase in β-MHC/α-MHC mRNA induced by DOX (Figure 3.21B) was associated with cellular hypertrophy, RL-14 cells were treated with 10 µM DOX for various periods of time (0, 2, 6, 12 and 24 h). Thereafter, cell volume was determined by flow cytometry. Figure 3.21C shows that treatment of RL-14 cells for 6, 12 and 24 h with 10 µM DOX significantly increased the number of enlarged cells to 16% ± 0.73, 23.3% ± 0.5 and 22.1% ± 0.33 from control levels of 10%, respectively. Since a 12 h exposure to 10 µM DOX exhibited a maximum hypertrophic effect, it was selected to be utilized in all subsequent in vitro experiments in RL-14 cells.
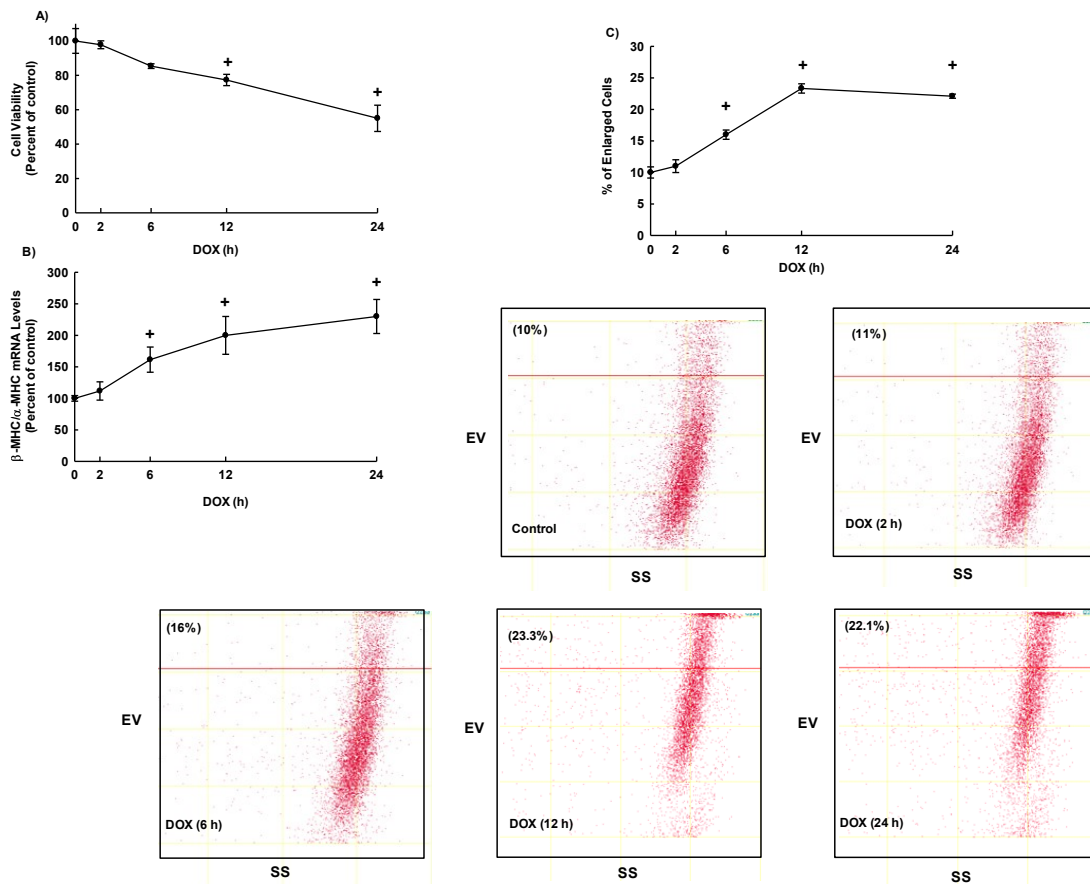
Figure 3.21. Time-dependent effects of DOX on RL-14 cell viability, hypertrophic markers, and cell volume

RL-14 cells were treated with 10 µM DOX for different time intervals (0, 2, 6, 12 and 24 h). Thereafter, (A) cell viability was determined using MTT assay. (B) The mRNA level of β-MHC/α-MHC was quantified using real time-PCR. (C) Cell volume was determined by flow cytometry. The values represent mean ± SEM (n = 6). $^+p<0.05$ compared to control.

To investigate the potential involvement of CYP1B1/mid-chain HETEs in DOX-mediated cardiotoxicity. Aseries of independent experiments was conducted using the selective CYP1B1 inhibitor, TMS, in RL-14 cells.

3.3.8. Effect of TMS on DOX-mediated cytotoxicity and cellular hypertrophy

To examine whether the cytotoxicity in RL-14 cells induced by DOX is due to a mid-chain HETE-dependent mechanism, we used a selective CYP1B1 inhibitor, TMS, which is known to inhibit mid-chain HETE formation. For this purpose, RL-14 cells were treated for 12 h with 10 µM DOX in the presence and absence of 0.5 µM TMS. Thereafter, RL-14 cell viability was determined using MTT assay. Our results showed that DOX significantly decreased RL-14 cell viability to 75% ± 3.24 from control levels of 100% (Figure 3.22A). Although TMS alone did not significantly alter RL-14 cell viability, treatment of RL-14 cells with TMS significantly prevented the DOX-mediated cytotoxicity (96% ± 2.4 viable vs. 100% control) (Figure 3.22A).

To further confirm the protective effect of TMS against DOX-induced cytotoxicity, we tested the effect of TMS on DOX-mediated action on cellular hypertrophy markers. For this purpose, RL-14 cells were treated for 12 h with 10 µM DOX in the presence and absence of 0.5 µM TMS. Thereafter, the mRNA levels of β-MHC/α-MHC were determined by real time-PCR. Figure 3.22B shows that DOX alone caused a significant induction of β-MHC/α-MHC expression to 200% ± 30 from control levels of 100% ± 6.1. Importantly, treatment with TMS significantly reduced the induction of β-MHC/α-MHC in response to DOX to 110% ± 9.2 from control levels of 100% ± 6.1 (Figure 3.22B).

3.3.9. Effect of TMS on DOX-mediated increase of cell volume

To determine the effect of TMS on DOX-induced cellular hypertrophy, cell volume was analyzed once again by flow cytometry. Our results showed that DOX caused a significant increase in cell volume as enlarged cells accounted for 22.1% ± 0.5 of cells (Figure 3.22C). Although TMS alone did not significantly alter RL-14 cell volume, treatment of RL-14 cells with TMS significantly inhibited the DOX-mediated increase in the number of enlarged cells to 14% ± 0.54 from control levels of 10% ± 2.1 (Figure 3.22C).

118

3.3.10. Effect of TMS on DOX-induced the expression of CYP1B1 mRNA, protein and catalytic activity in RL-14 cells

To determine the capacity of TMS to alter the induction of CYP1B1 gene expression by DOX, RL-14 cells were treated for 12 h with 10 µM DOX in the presence and absence of 0.5 µM TMS; thereafter, CYP1B1 mRNA and protein levels were determined using real time-PCR and western blot analysis, respectively. Figure 3.23 shows that DOX significantly induced CYP1B1 mRNA and protein expression levels to 800% ± 9.1 and 280% ± 20, respectively, in comparison to control level (Figure 3.23A and B). Furthermore, we examined the ability of TMS to inhibit DOX-induced CYP1B1 catalytic activity. For this purpose, RL-14 cells were treated for 12 h with 10 µM DOX in the presence and absence of 0.5 µM TMS. Thereafter, CYP1B1 catalytic activity level was determined by MROD assay. Figure 3.23C shows that DOX significantly increased the formation of resorufin to 0.15 ± 5.8841e-3 pmol/min/mg protein from control levels of 0.01 ± 1.6833e-3 pmol/min/mg protein. On the other hand, TMS significantly inhibited the DOX-induced CYP1B1 catalytic activity using MROD assay to 0.07 ± 1.4882e-3 pmol/min/mg protein (Figure 3.23C).

3.3.11. Effect of TMS on DOX-mediated increase of mid-chain HETEs formation

To determine the capacity of TMS to inhibit the formation of mid-chain HETEs by DOX, RL-14 cells were treated for 12 h with 10 µM DOX in the presence and absence of 0.5 µM TMS. Subsequently, the cells were incubated with 50 µM AA for 3 h, and AA metabolites were measured using LC–ESI–MS. Figure 3.24A shows that DOX was able to significantly increase the formation of 15-HETE, 12&8-HETE and 5-HETE to 260% ± 20.1, 300% ± 15.6 and 680% ± 50.35, respectively, from control levels of 100%. Importantly, treatment of RL-14 cells with 0.5 µM TMS significantly inhibited the formation of 15-HETE, 12&8-HETE and 5-HETE to 160.5% ± 4.2, 150.32% ± 5.2 and 200.45% ± 14.3, respectively, from control levels of 100% (Figure 3.24A).

To investigate whether 5-HETE alone or in combination with other mid-chain HETEs is sufficient to abolish the protective effect of TMS against DOX-induced cardiotoxicity, RL-14 cells were treated for 12 h with DOX in the presence and absence of TMS and 5-HETE

or mid-chain HETEs. Thereafter, RL-14 cell viability was determined using MTT assay. Our results showed that DOX significantly decreased RL-14 cell viability to 74.9% ± 2.03 (Figure 3.24B). Although TMS significantly inhibited the DOX-mediated cytotoxicity, treatment of RL-14 cells with 5-HETE significantly abolished the protective effect mediated by TMS (Figure 3.24B). Further, treatment of RL-14 cells with mid-chain HETEs in the presence of DOX and TMS significantly decreased RL-14 cell viability to 30% (Figure 3.24B).

To further confirm the ability of 5-HETE to inhibit the protective effect of TMS against DOX-induced cardiotoxicity, RL-14 cells were treated for 12 h with DOX in the presence and absence of TMS and 5-HETE. Thereafter, the mRNA levels of β-MHC/α-MHC were determined by real time-PCR. Figure 3.24C shows that DOX alone caused a significant induction of β-MHC/α-MHC expression to 185% ± 10.8. Although TMS significantly reduced the increase of β-MHC/α-MHC in response to DOX to 95.2% ± 10.4, treatment of RL-14 cells with 5-HETE significantly abolished TMS-mediated inhibition of β-MHC/α-MHC expression to 175% ± 30 (Figure 3.24C) suggesting an important role of 5-HETE in DOX-induced cardiotoxicity.
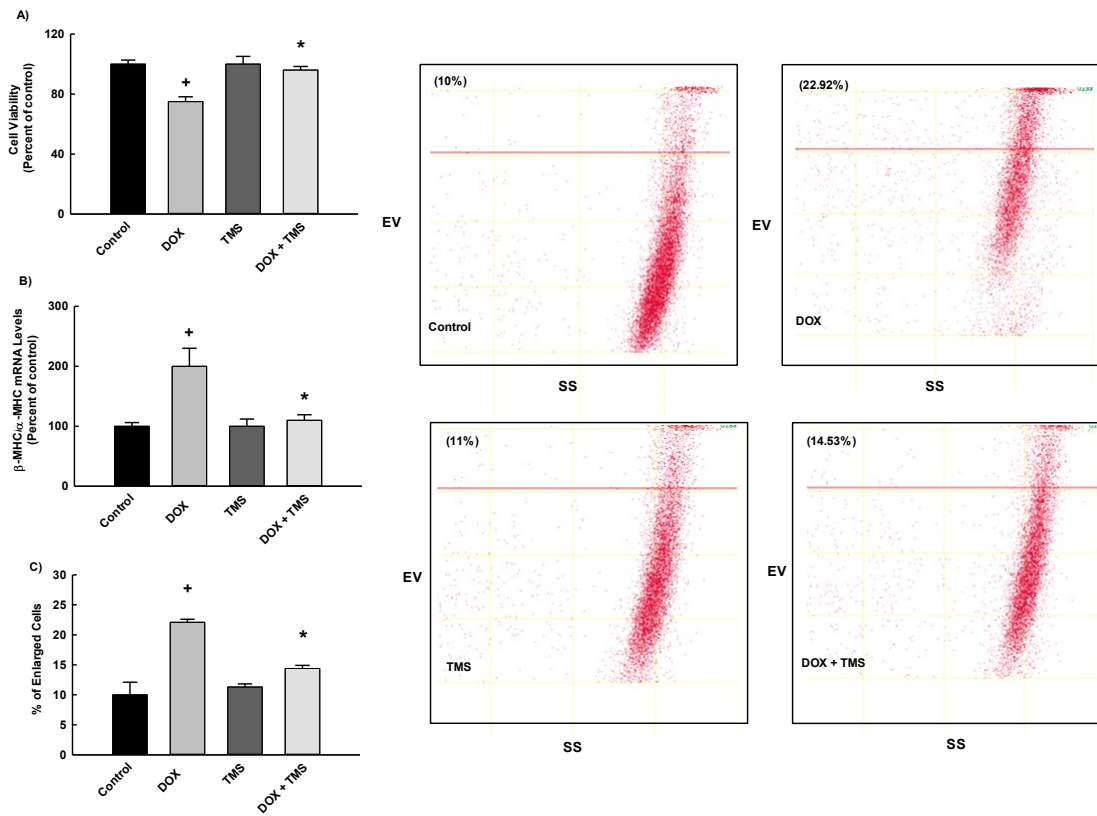
Figure 3.22. Effects of TMS on DOX-mediated cardiotoxicity in RL-14 cells

RL-14 cells were treated for 12 h with 10 μM DOX in the presence and absence of 0.5 μM TMS. (A) Thereafter, cell viability was determined using MTT assay. (B) The mRNA levels of β-MHC/α-MHC were quantified using real time-PCR. (C) Cell volume was determined by flow cytometry. The values represent mean ± SEM (n = 6). $^+p<0.05$ compared to control. $^*p<0.05$ compared to DOX.
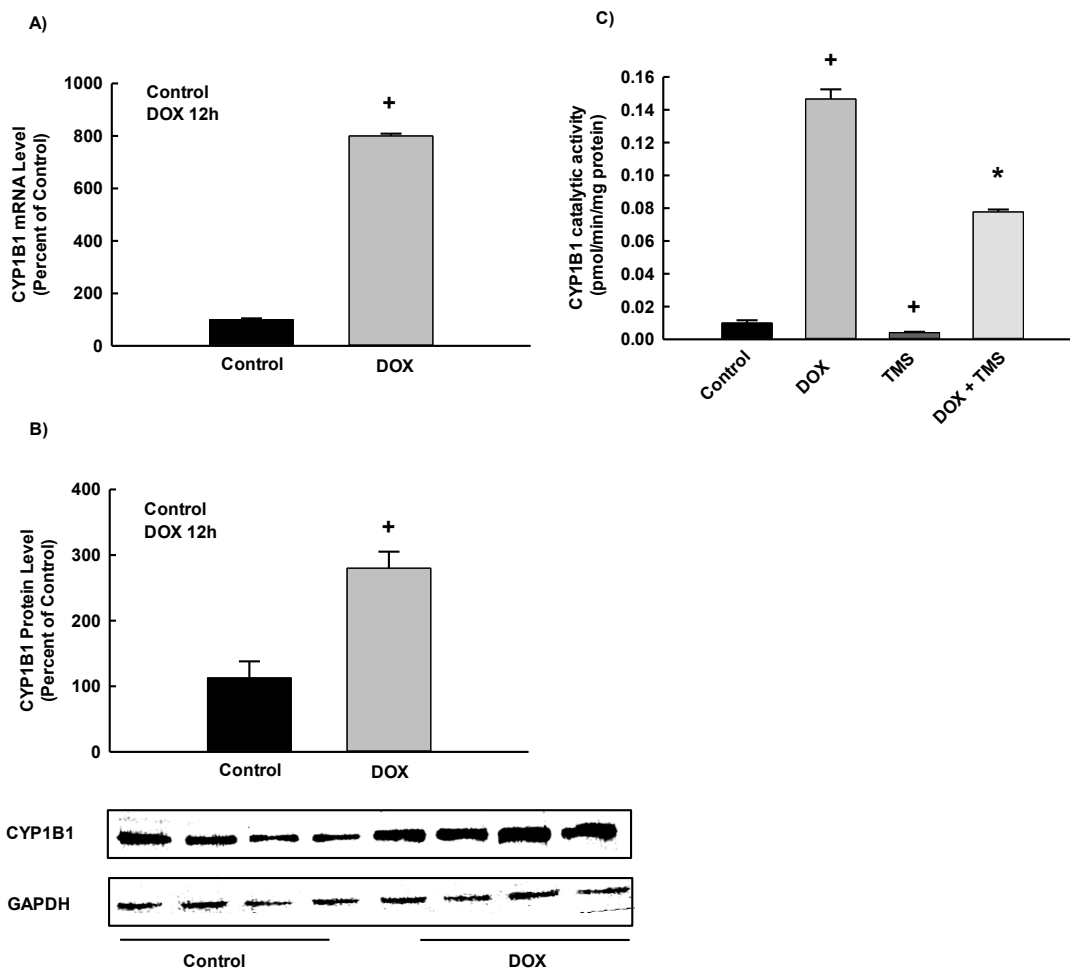
Figure 3.23. Effect of TMS on the expression of CYP1B1 altered by DOX

(A) RL-14 cells were treated with 10 μM DOX for 12 h. Thereafter, the mRNA level of CYP1B1 was quantified using real time-PCR. (B) RL-14 cells were treated for 12 h with 10 μM DOX; thereafter, CYP1B1 protein levels were determined by Western blot analysis. (C) RL-14 cells were treated for 12 h with 10 μM DOX in the presence and absence of 0.5 μM TMS. Thereafter, CYP1B1 catalytic activity level was determined by the MROD assay. The values represent mean ± SEM (n = 6). $^+p<0.05$ compared to control. $^*p<0.05$ compared to DOX.
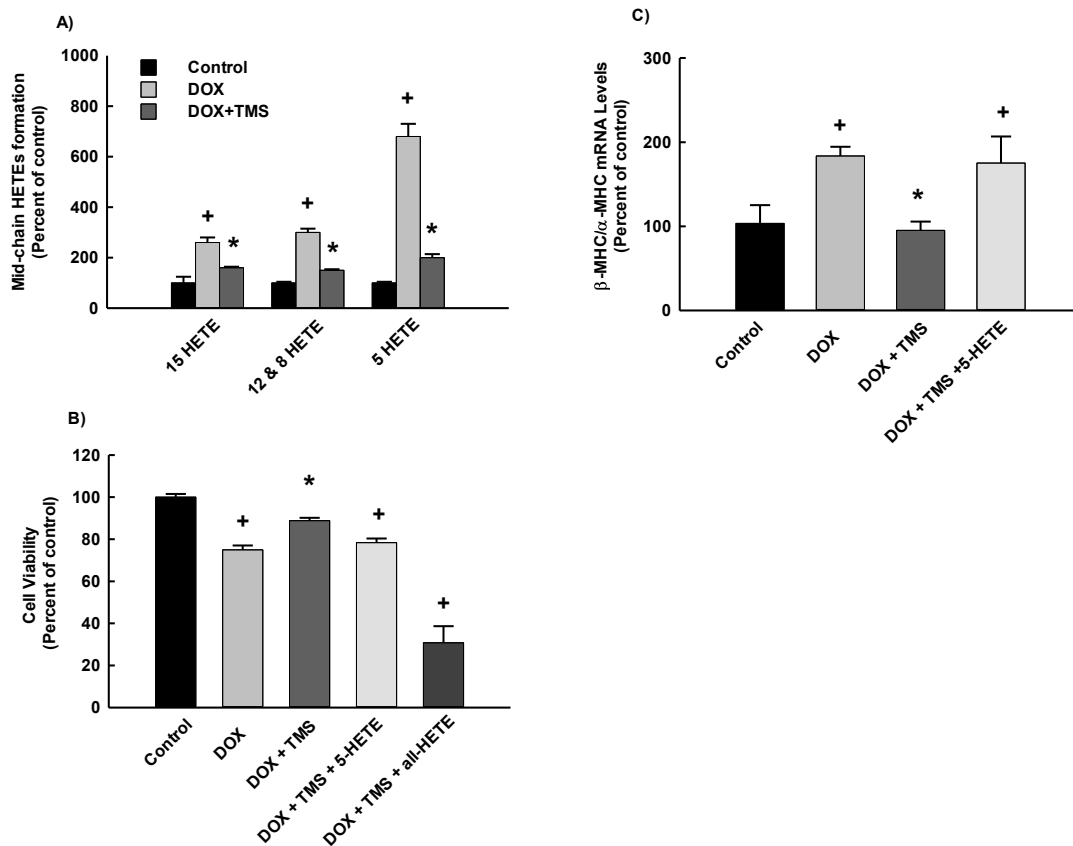
Figure 3.24. Effects of TMS on DOX-induced mid-chain HETEs formation
(A) RL-14 cells were treated for 12 h with 10 μM DOX in the presence and absence
of 0.5 μM TMS. Thereafter, 15-HETE, 12&8-HETE and 5-HETE were quantified
using LC–ESI–MS. (B) RL-14 cells were treated for 12 h with DOX in the presence
and absence of TMS and 5-HETE or mid-chain HETEs. Thereafter, RL-14 cell
viability was determined using MTT assay. (C) RL-14 cells were treated for 12 h
with DOX in the presence and absence of TMS and 5-HETE. Thereafter, the mRNA
levels of β-MHC/α-MHC were determined by real time-PCR. The values represent
mean ± SEM (n = 6). $^{+}p<0.05$ compared to control. $^{*}p<0.05$ compared to DOX.

3.3.12. Effect of LOX inhibitors on DOX-mediated increase of cell volume and mid-chain HETEs formation

Mid-chain HETEs are known to be formed by LOX enzymes in addition to CYP1B1. Therefore, we investigated whether the induction of mid-chain HETEs and cardiotoxicity by DOX is also attributed to the activation of LOX enzymes. Initially, we have determined the maximum non-toxic concentrations of LOX inhibitors to be utilized in the current study. For this purpose, RL-14 cells were treated for 24 h with 10 µM DOX in the presence and absence of different concentrations of zileuton (0, 0.05, 0.1, 0.25, 0.5 and 1 µM) and PD146176 (0, 0.05, 0.1, 0.25 and 0.5 µM). Thereafter, RL-14 cell viability was determined using MTT assay. Our results showed that DOX significantly decreased RL-14 cell viability to 70% ± 2.5 from control levels of 100% (Figure 3.25A). Treatment of RL-14 cells with concentrations ranging from 0.05 to 0.5 µM of zileuton and 0.05 to 0.25 µM of PD146176 did not significantly affect the DOX-mediated cytotoxicity. However, zileuton 1 µM and PD146176 0.5 µM significantly potentiated the DOX-mediated cytotoxicity to 60% ± 1.5 and 63% ± 2.43, respectively. Based on these findings, zileuton 0.5 µM and PD146176 0.25 µM were utilized in all subsequent experiments in RL-14 cells (Figure 3.25A).

To examine the effect of LOX inhibitors on DOX induced cellular hypertrophy, RL-14 cells were treated for 12 h with 10 µM DOX in the presence and absence of LOX inhibitors, 0.5 µM zileuton and 0.25 µM PD146176. Thereafter, cell volume was analyzed by flow cytometry. Our results showed that DOX significantly increased the cell volume belonging to the region of hypertrophy to about 24.46% ± 1.08 of control. Importantly, treatment of RL-14 cells with LOX inhibitors did not significantly alter cellular hypertrophy induced by DOX, confirming the role of CYP1B1 in DOX-induced cardiotoxicity (Figure 3.25B).

To determine the role of LOX inhibitors in mid-chain HETE formation mediated by DOX, RL-14 cells were treated for 12 h with 10 µM DOX in the presence and absence of 0.5 µM zileuton and 0.25 µM PD146176, and then, the cells were incubated with 50 µM AA for 3 h. Thereafter, AA metabolites were measured using LC–ESI–MS. Figure 3.25C shows that DOX was able to significantly increase the formation of mid-chain HETE to 320.6% ±

19.2 from control levels of 100% ± 12.51. Importantly, treatment of RL-14 cells with LOX inhibitors did not significantly inhibit the formation of mid-chain HETE in response to DOX, confirming the role of CYP1B1 in the formation of mid-chain HETEs-mediated by DOX. Importantly, concentrations greater than 0.5 µM and 0.25 µM for zileuton and PD, respectively, potentiate the cytotoxicity induced by DOX (Figure 3.25A).
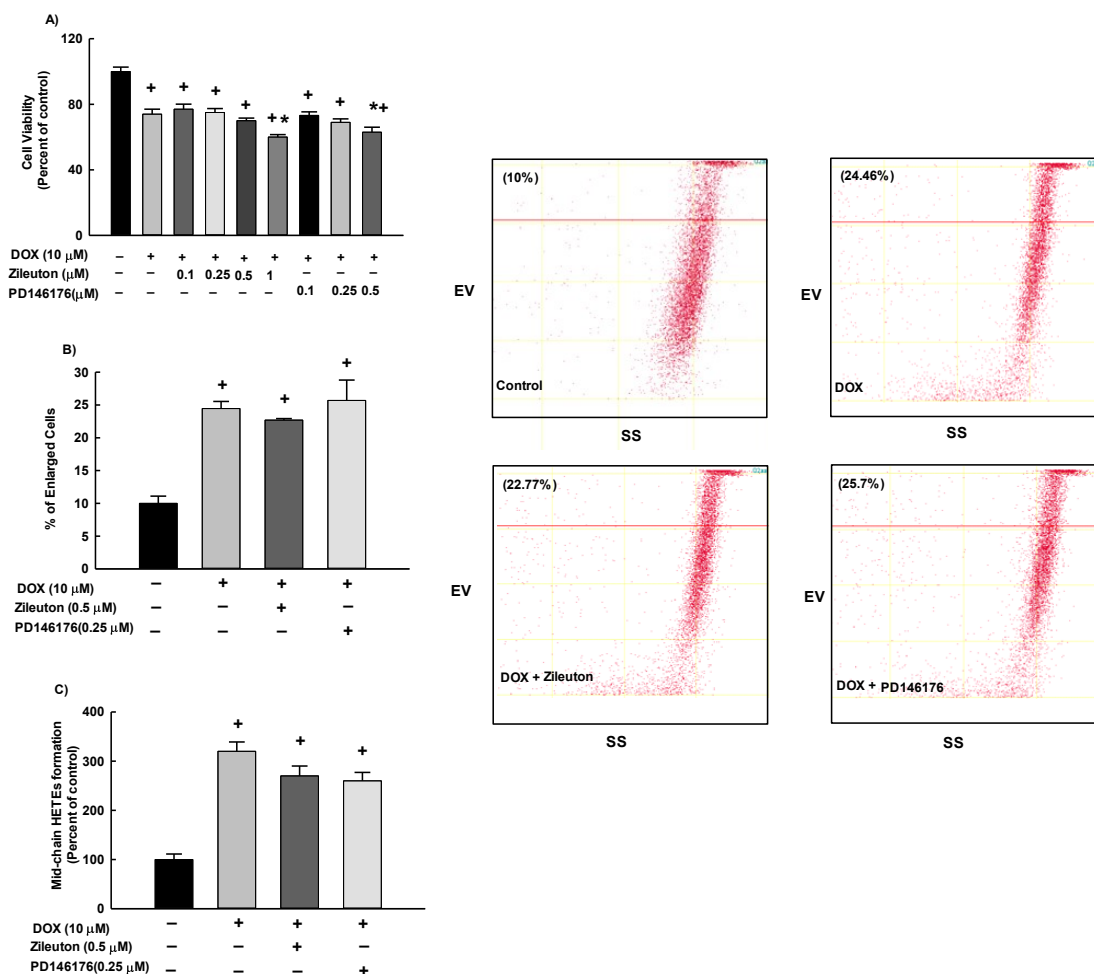
Figure 3.25. Effects of LOX inhibitors on DOX-mediated cardiotoxicity and mid-chain HETEs formation

RL-14 cells were treated for 12 h with 10 μM DOX in the presence and absence of different concentrations of zileuton (0, 0.05, 0.1, 0.25, 0.5 and 1 μM) and PD146176 (0, 0.05, 0.1, 0.25 and 0.5 μM). Thereafter, (A) RL-14 cell viability was determined using MTT assay. RL-14 cells were treated for 12 h with 10 μM DOX in the presence and absence of 0.5 μM zileuton and 0.25 μM PD146176. Thereafter, (B) cell volume was determined by flow cytometry. (C) RL-14 cells were treated for 12 h with 10 μM DOX in the presence and absence of 0.5 μM zileuton and 0.25 μM PD146176. Thereafter, mid-chain HETEs were quantified using LC–ESI–MS for metabolite determination. The values represent mean ± SEM (n = 6). [+]$p<0.05$ compared to control. [*]$p<0.05$ compared to DOX.

3.3.13. Effect of TMS on DOX-mediated induction of MAPK and NF-κB signaling pathways

To assess the role of the MAPK signaling pathway on the TMS-induced cardioprotection, RL-14 cells were treated for 2 h with 10 μM DOX in the presence and absence of 0.5 μM TMS. Thereafter, phosphorylated MAPK levels were determined using a commercially available kit. Figure 3.26A shows that incubation of the cells with 10 μM of DOX significantly induced phosphorylation of p38, JNK and ERK1/2 to 325.8% ± 1.98, 183% ± 7.8 and 149.8% ± 17, respectively, from control levels of 100%. Importantly, treatment with TMS significantly reduced the induction of phosphorylated p38, JNK and ERK1/2 in response to DOX to 136% ± 6.6, 64%± 40 and 100.3% ± 3.31, respectively, from control levels of 100%, suggesting an important role of MAPK on TMS-mediated protection against DOX induced-cardiotoxicity.

To investigate whether TMS reversal of DOX-induced cardiotoxicity is also mediated through the inhibition of NF-κB, RL-14 cells were treated for 2 h with 10 μM DOX in the presence and absence of 0.5 μM TMS. Thereafter, NF-κB binding activity was determined using a commercially available kit. Figure 3.25B shows that DOX alone was able to induce the binding activity of NF-κB to its responsive element to 175.05% ± 6.2 and 167.57% ± 1.6 for P50 and P65, respectively, from control levels of 100%. Importantly, treatment with TMS significantly reduced the induction of P50 and P65 binding activity in response to DOX to 90.32% ± 9.6 and 136.1% ± 4.1, respectively, suggesting that NF-κB is essential for TMS-mediated protection against DOX-induced cardiotoxicity.
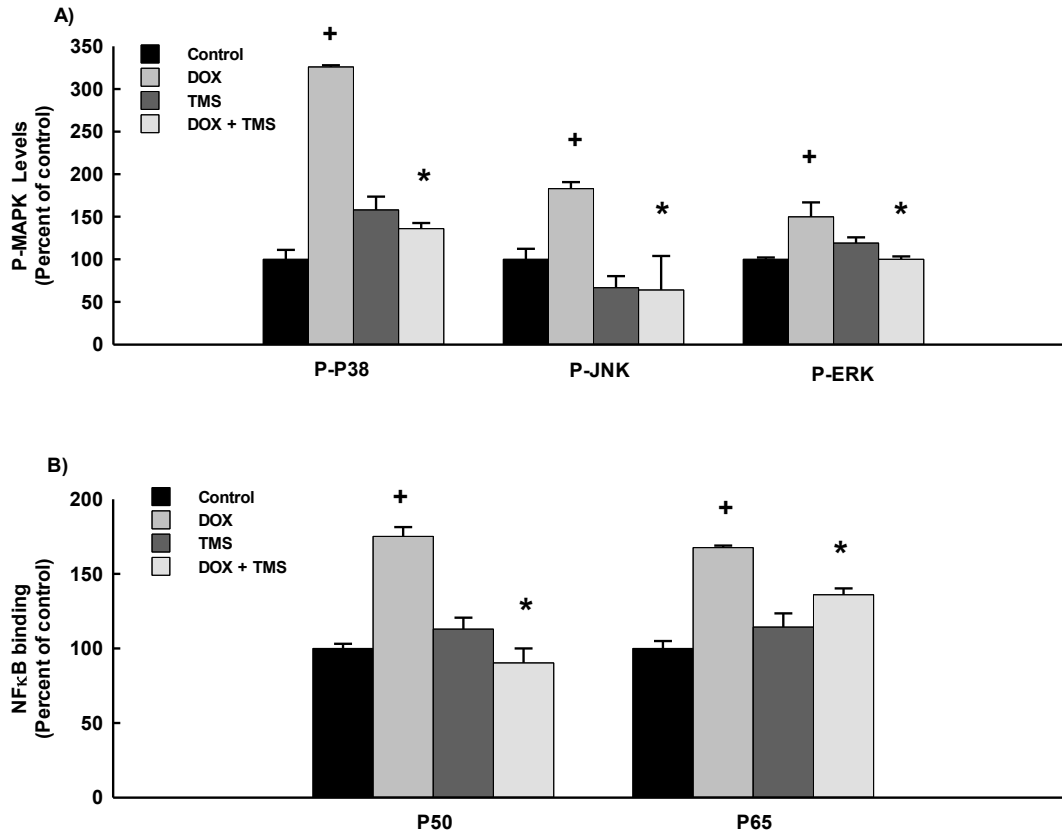
Figure 3.26. Effect of TMS on DOX-induced MAPK and NF-κB signaling pathways
RL-14 cells were treated for 2 h with 10 μM DOX in the presence and absence of 0.5 μM TMS. Thereafter, (A) MAPK protein phosphorylation was determined in cytoplasmic protein extracts using the MAPK Elisa Kit (Abcam, Cambridge, UK). (B) NF-κB binding activity was determined using a commercially available kit. The values represent mean ± SEM (n = 6). $^+p<0.05$ compared to control. $^+p<0.05$ compared to control. $^*p<0.05$ compared to DOX.

3.4. The role of cytochrome P450 1B1 and its associated mid-chain hydroxyeicosatetraenoic acid metabolites in the development of cardiac hypertrophy induced by ISO

3.4.1. Effect of ISO on the expression of CYP1B1, LOXs and COX protein and mid-chain HETEs levels in rats

Recently, we have demonstrated that ISO-induced cardiac hypertrophy in vivo in rats in a time-dependent phenomenon (Althurwi *et al.*, 2015). Hypertrophy initiation induced by ISO was assessed and confirmed by heart weight/body weight ratio (HW/BW) and echocardiography (Althurwi *et al.*, 2015). Echocardiographic examination of ISO-treated rats showed structural changes in left ventricular morphology such as intraventricular septum and left ventricular posterior wall thickness after 3 days of ISO treatment. The early onset of cardiac hypertrophy was further confirmed by a significant increase in HW/BW in comparison to control (Althurwi *et al.*, 2015). Currently, our aim is to determine the capacity of ISO to increase the level of cardiac mid-chain HETEs in vivo in rats at the pre-hypertrophic stage, 12 h, and at the hypertrophic stage, 72 h. For this purpose, mid-chain HETE metabolites were determined using LC–ESI–MS. Figure 3.27A shows that ISO significantly increases the level of cardiac mid-chain HETEs by about 500% and 200% at 12 and 72 h, respectively, in comparison to control.

Mid-chain HETEs are known to be formed by LOXs in addition to CYP1B1 and degraded by cyclooxygenase-2 (COX-2) enzyme. Therefore, we investigated whether the induction of mid-chain HETEs by ISO is attributed to the activation of LOXs and CYP1B1 or the inhibition of the COX-2 enzyme. For this purpose, CYP1B1, LOXs, and COX-2 protein expression levels were determined by Western blot analysis. Figure 1B shows that treatment of rats with ISO significantly induced CYP1B1 and COX-2 at 12 and 72 h by approximately 200% in comparison to control. On the other hand, ISO significantly inhibited the expression of 5-LOX, 12-LOX and 15-LOX at 72 h by approximately 70% in comparison to control (Figure 3.27B).
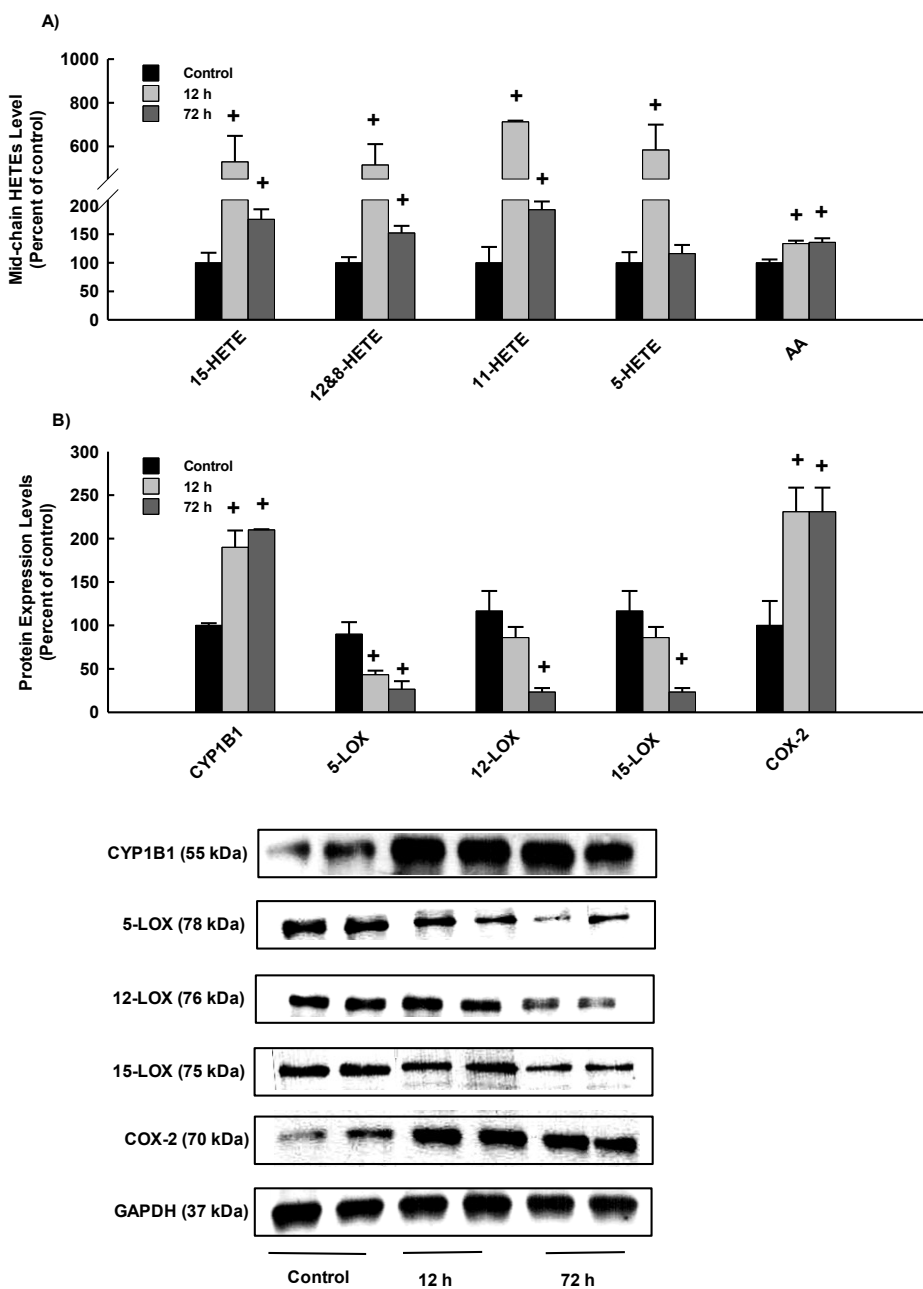
3.27. Effect of ISO on the expression of CYP1B1, LOXs and COX-2 protein levels in rats

Rats were injected with vehicle or ISO (5mg/kg i.p.) for 12 and 72 h and (A) then, mid-chain HETE metabolites were measured using LC–ESI–MS. (B) CYP1B1, 5-LOX, 12-LOX, 15-LOX and COX-2 protein expression levels were determined by Western blot analysis. The values represent mean ± SEM (n = 6). $^{+}p<0.05$ compared to control.

3.4.2. Effect of ISO, TMS and CYP1B1-siRNA on RL-14 cells viability

To determine the effect of ISO in the presence and absence of TMS or CYP1B1-siRNA on RL-14 cell viability, MTT and LDH assays were used. Our results showed that treatment of RL-14 cells with 100 μM ISO in the presence and absence of 0.5 μM TMS or 25 nM CYP1B1-siRNA at 24 and 48 h, respectively, did not significantly affect RL-14 cell viability using MTT and LDH assays (Figure 3.28A and B). Therefore, the obtained changes were not due to the decreased cell viability or toxicity.

3.4.3. Effect of ISO on hypertrophic markers and RL-14 cell surface area

The effect of ISO on hypertrophic markers was determined by real time-PCR. Figure 3.29A shows that treatment of RL-14 cells for 24 h with 100 μM ISO significantly induced β-MHC by about 150% and inhibited α-MHC by approximately 70% in comparison to control. However, treatment of RL-14 cells with ISO for 24 h did not significantly alter the expression of ANP and BNP mRNA levels (Figure 3.29A).

To determine whether the ISO-induced hypertrophy markers at the mRNA (Figure 3.29A) were associated with cellular hypertrophy and increase the cell surface area, RL-14 cells were treated for 24 h with ISO 100 μM; thereafter, cell surface area was determined. Figure 3.29B shows that ISO significantly increased the percentage of cell surface area by about 100% as compared with control. Based on the above finding, α-MHC hypertrophic marker and cell surface area were selected to be utilized in all subsequent experiment.

A)

B)
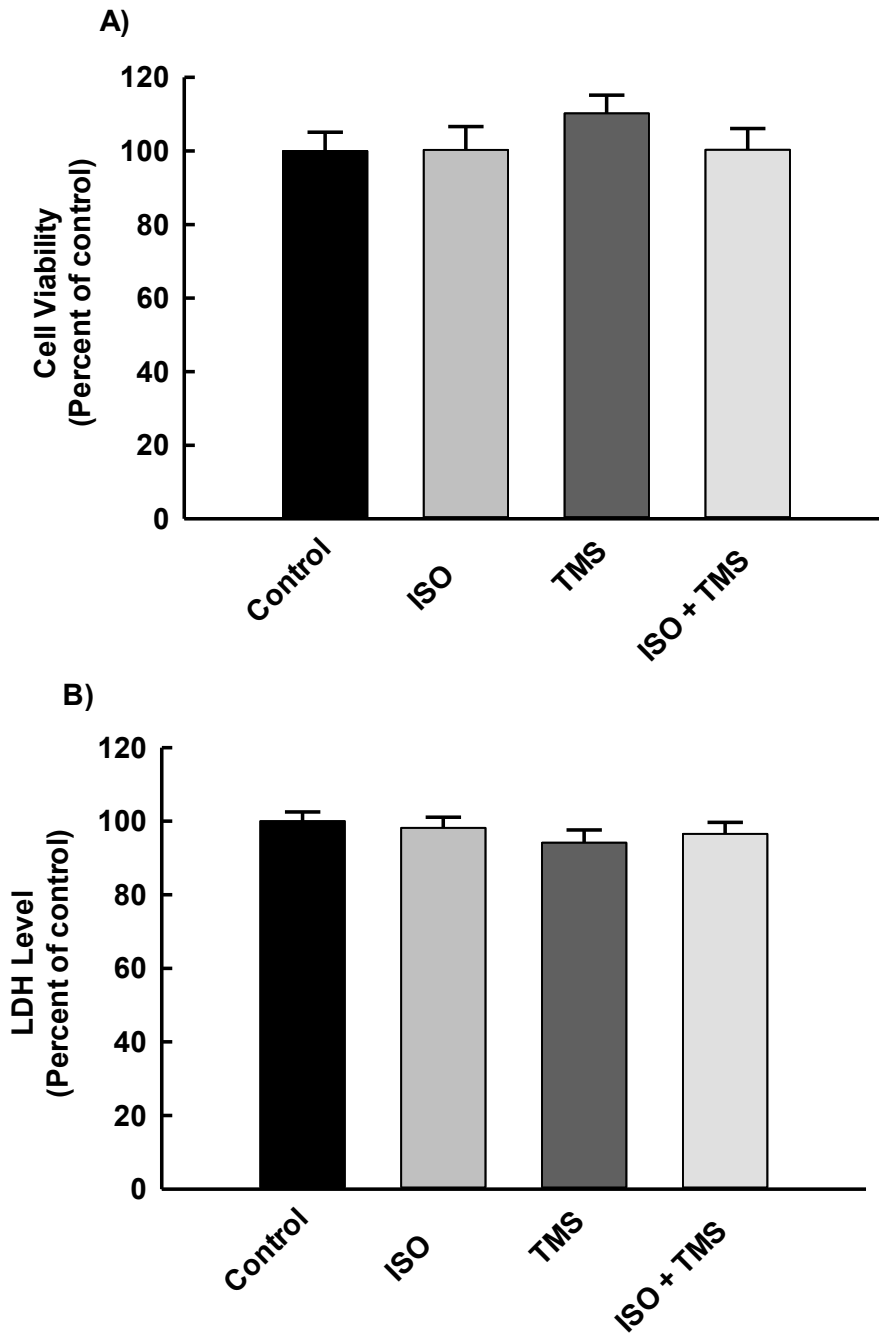
Figure 3.28. Effect of ISO, TMS and CYP1B1-siRNA on RL-14 cells viability

RL-14 cells were exposed to 100 μM ISO in the presence and absence of 0.5 μM TMS or 25 nM CYP1B1siRNA at 24 and 48 h, respectively. Thereafter, RL-14 cell viability was determined using MTT and LDH assays. The values represent mean $\pm$ SEM (n = 6). $^+p<0.05$ compared to control. $^*p<0.05$ compared to ISO.
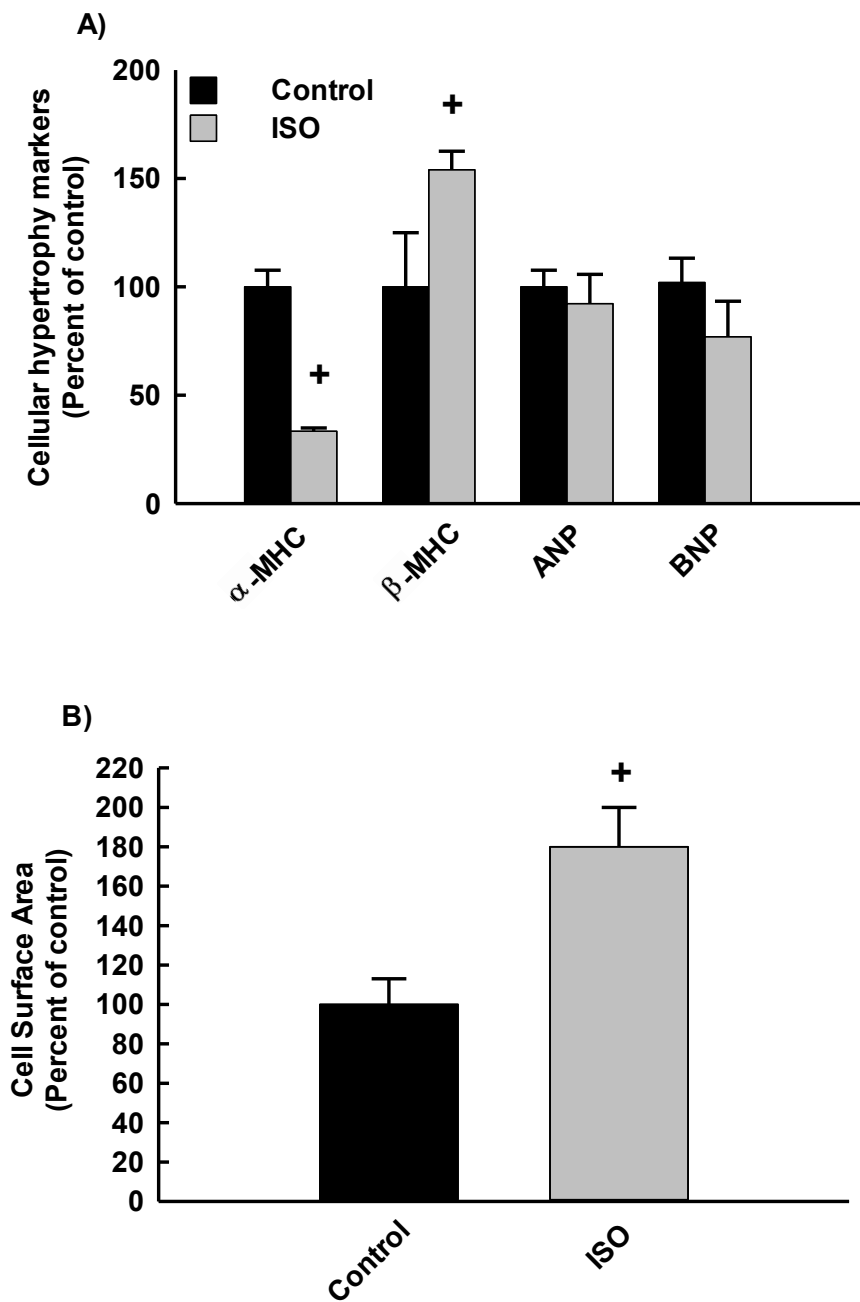
Figure 3.29. Effect of ISO on hypertrophic markers and RL-14 cell surface area
(A) RL-14 cells were treated for 24 h with 100 μM ISO. Thereafter, the mRNA level of ANP, BNP, α-MHC, β-MHC were quantified using real time-PCR. (B) RL-14 cells were treated with 100 μM ISO for 24. Thereafter, cell surface area was analyzed by phase contrast imaging. The values represent mean ± SEM (n = 6). [+]$p<0.05$ compared to control.

3.4.4. Effect of CYP1B1 inhibitor, TMS, and CYP1B1-siRNA on ISO-mediated cellular hypertrophy

To examine whether the induction of the cellular hypertrophy in RL-14 cells by ISO is a CYP1B1-dependent mechanism, CYP1B1-siRNA or TMS were used. Figure 3.30B shows that ISO alone caused a significant inhibition of α-MHC gene expression by approximately 70% in comparison to control. Importantly, treatment of the cells with TMS or CYP1B1-siRNA significantly restored the ISO-mediated inhibition of α-MHC gene expression, suggesting a possible role for CYP1B1 in the ISO-induced cellular hypertrophy (Figure 3.30B and C).

The effect of TMS on ISO-induced cellular hypertrophy was further confirmed by the measurement of cell surface area. Our results showed that ISO increased the percentage of cell surface area by about 100% in comparison to control. Although TMS alone did not significantly alter RL-14 cell surface area, treatment of RL-14 cells with TMS significantly inhibited the ISO-mediated hypertrophy by approximately 70% in comparison to ISO (Figure 3.30C).
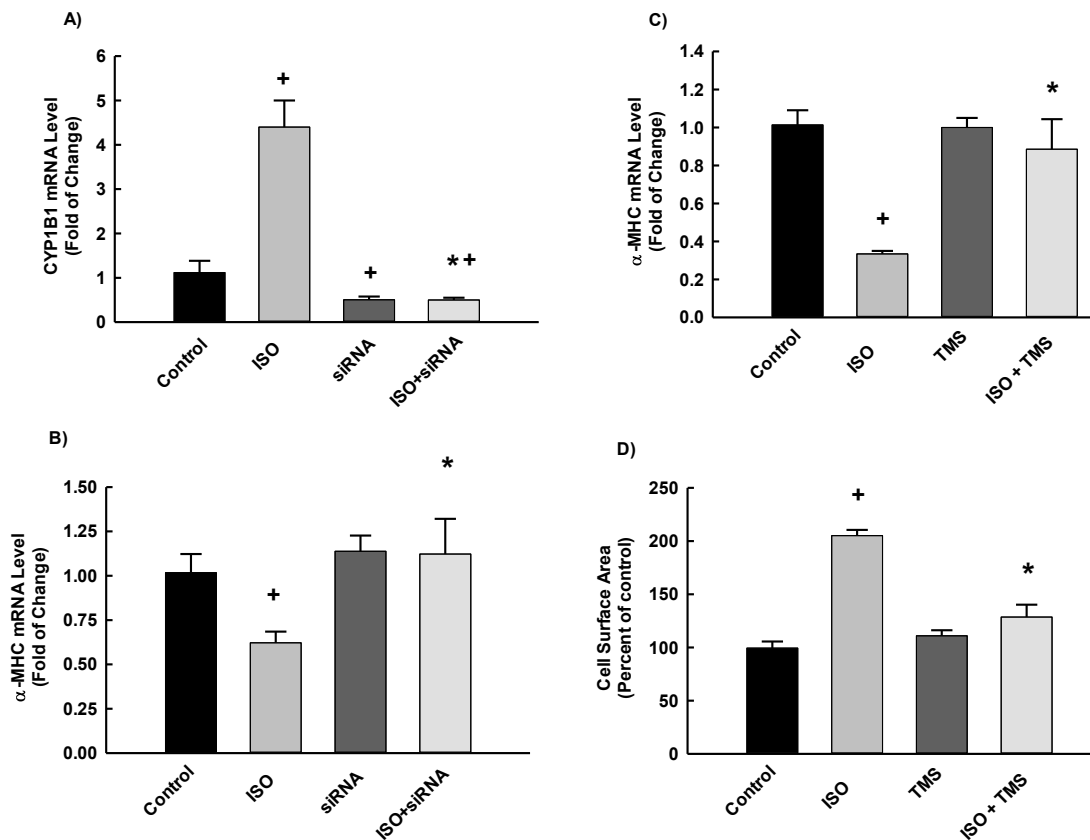
Figure 3.30. Effect of CYP1B1 inhibitor, TMS, and CYP1B1-siRNA on ISO-mediated cellular hypertrophy

      (A), (B) and (C) RL-14 cells were treated with 100 μM ISO in the presence and absence of 0.5 μM TMS or 25 nM CYP1B1siRNA at 24 and 48 h, respectively. Thereafter, the mRNA level of α-MHC was quantified using real time-PCR. (D) RL-14 cells were treated with 100 μM ISO in the presence and absence of 0.5 μM TMS for 24. Thereafter, cell surface area was analyzed by phase contrast imaging. The values represent mean ± SEM (n = 6). $^+p<0.05$ compared to control. $^*p<0.05$ compared to ISO.

3.4.5. Effect of CYP1B1 overexpression on the development of cellular hypertrophy

To further confirm the role of CYP1B1 in the development of cellular hypertrophy, RL-14 cells were transiently transfected with CRISPR-CYP1B1. Thereafter, the mRNA expression of CYP1B1 and hypertrophic markers, α-MHC and β-MHC, was determined by real time-PCR. Figure 3.31A shows that CRISPR-CYP1B1 delivery led to the induction CYP1B1 gene expression by about 400% in comparison to mock-transfected cells. Importantly, this was accompanied by a significant decrease of α-MHC by approximately 60% and a significant increase of β-MHC/ α-MHC by about 150% in comparison to mock-transfected cells confirming the role of CYP1B1 in the development of cellular hypertrophy (Figure 3.31A).

3.4.6. The role of CYP1B1 in the formation of mid-chain HETE metabolites

CYP1B1 overexpression and CYP1B1siRNA were used to explore the role of CYP1B1 in the formation of mid-chain HETE metabolites. Figure 3.31B shows that CRISPR-CYP1B1 delivery led to a significant increase in the formation of the formation of 15-, 12- and 8-, 11- and 5-HETE by approximately 280%, 220%, 300%, and 290%, respectively, in comparison to control. On the other hand, treatment of cells with CYP1B1-siRNA significantly inhibited the formation of 15-, 12- and 8-, 11- and 5-HETE by about 40% in comparison to control (Figure 3.31C), confirming the role of CYP1B1 in the formation of mid-chain HETE metabolites. The effect of CYP1B1-siRNA on mid-chain HETEs is consistent with its effect on CYP1B1 mRNA levels (Figure 3.30A).
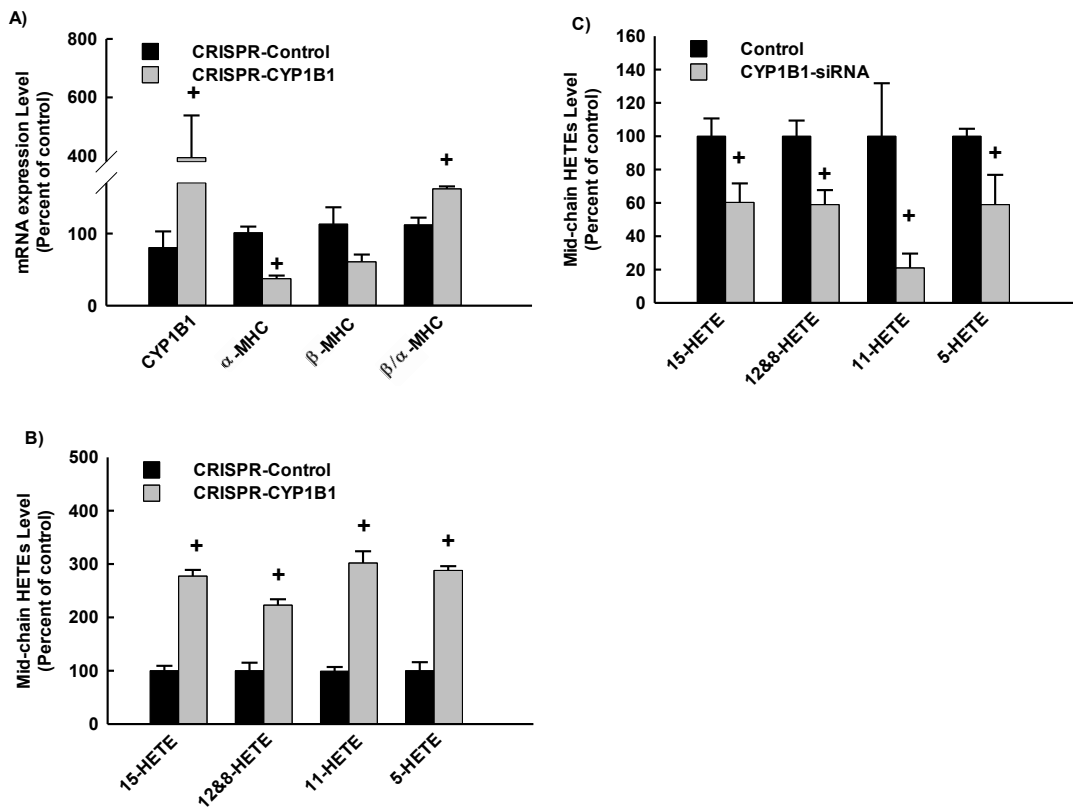
Figure 3.31. The role of CYP1B1 overexpression in the development of cellular hypertrophy and the formation of mid-chain HETEs

RL-14 cells were transiently transfected with CRISPR-CYP1B1. Thereafter, (A) the mRNA expression of CYP1B1 and α-MHC was determined by real time-PCR. (B) and (C) RL-14 cells were transiently transfected with CRISPR-CYP1B1 or CYP1B1-siRNA for 48 h and then the cells were incubated with 50 μM AA for 3 h. Thereafter, AA metabolites were measured using LC–ESI–MS. The values represent mean ± SEM (n = 6). $^+p<0.05$ compared to control. $^*p<0.05$ compared to ISO.

3.4.7. Effect of TMS on ISO-mediated effect on superoxide radical, MAPK and NF-κB signaling pathways

The level of superoxide radical and MAPK signaling pathway were determined to explore the mechanism by which TMS mediates its protective effect against ISO-induced cellular hypertrophy. Figure 3.32A shows that incubation of the cells with 100 μM of ISO significantly increased superoxide radical formation by approximately 180% and inhibited the phosphorylated ERK1/2 by about 70% in comparison to control. Importantly, treatment with TMS significantly reduced the increased formation of superoxide radical and restored the inhibition of phosphorylated ERK1/2 in response to ISO by approximately 80%, suggesting an important role of superoxide radical and phosphorylated ERK1/2 in TMS-mediated protection against ISO-induced cardiac hypertrophy (Figure 3.32B). Treatment of cells with TMS did not significantly alter the phosphorylated levels of p38 and JNK.

To investigate whether the effect of TMS on ISO-induced cellular hypertrophy is mediated through the inhibition of NF-κB, P50, and P65 binding activity was determined. Figure 3.32C shows that ISO alone was able to induce the binding activity of NF-κB to its responsive element to 148% for P50 in comparison to control. Importantly, treatment with TMS significantly reduced the P50 binding activity in response to ISO to 103% in comparison to control, suggesting that inhibition of NF-κB is essential for TMS-mediated protection against ISO-induced cellular hypertrophy.
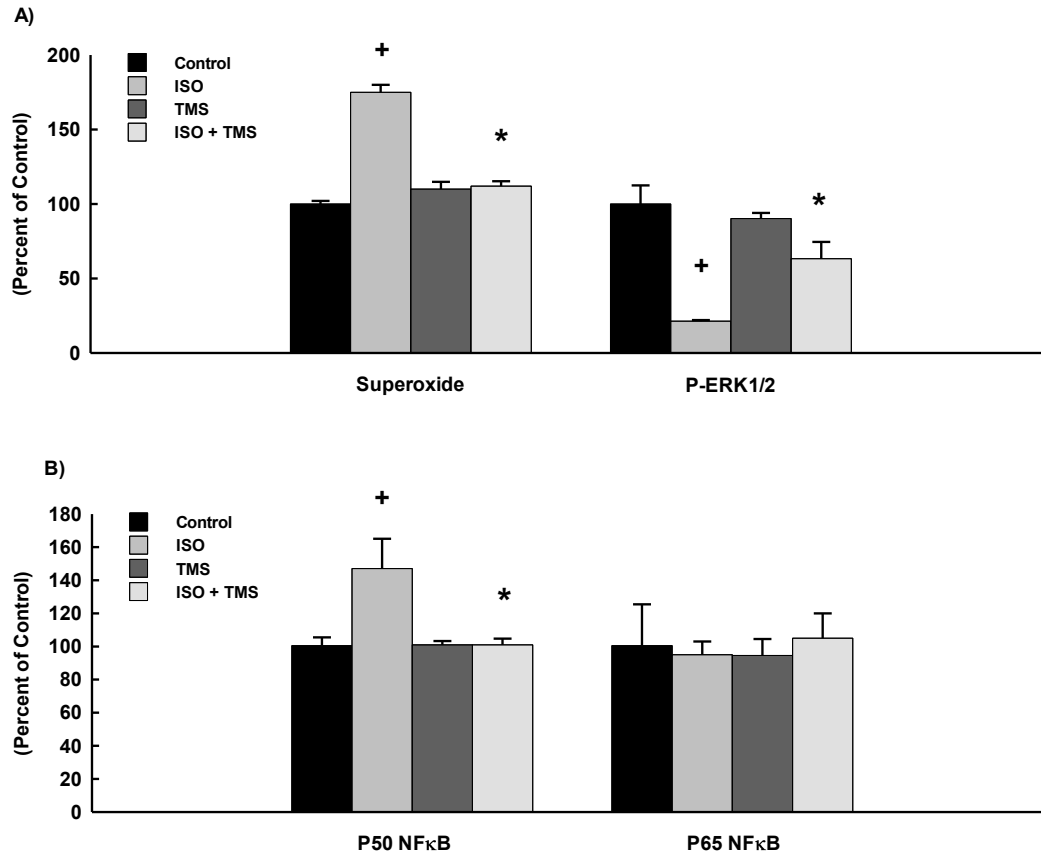
Figure 3.32. Effect of TMS on ISO-mediated effect on superoxide radical, MAPK and NF-κB signaling pathway

RL-14 cells were treated for 24 h with 100 μM ISO in the presence and absence of 0.5 μM TMS. Thereafter, (A) superoxide anion was determined using the DHE assay. MAPK protein phosphorylation was determined in cytoplasmic protein extracts using a PhosphoTracer Elisa Kit (Abcam, Cambridge, UK). (B) NF-κB binding activity was determined using a commercially available kit. The values represent mean ± SEM (n = 6). $^{+}p<0.05$ compared to control. $^{*}p<0.05$ compared to ISO.

3.5. 2-Methoxyestradiol protects against pressure overload-induced left ventricular hypertrophy

3.5.1. Effect of 2ME on AAC-induced cardiac hypertrophy in rats

To investigate whether 2ME confers cardioprotection against AAC-induced cardiac hypertrophy in rats, overall morphology was assessed in vivo via echocardiography and ex vivo by measuring heart weight-to-tibial length ratio (HW/TL). Echocardiography assessment of AAC rats showed thickening of the left ventricular wall as evidenced by an increase in LVPWs, LVPWd, IVSD, and IVSs in addition to a significant increase in LV mass (Table 3.3). Importantly, 2ME treatment resulted in a substantial reduction in the AAC-mediated thickening of left ventricular morphology. Additionally, AAC significantly increased the HW/TL to 0.39 from the control level of 0.26, whereas treatment with 2ME significantly inhibited the AAC-mediated increase in the HW/TL ratio to 0.257 (Figure 3.33). Although the echocardiographic assessment revealed that 2ME did not significantly influence heart rate or parameters of systolic function such as EF% and %FS in the AAC rats, 2ME was able to significantly decrease the level of pressure gradient-increased by AAC (Table 3.3).

Table 3.3. Hemodynamic parameters in rats

	Control	AAC	2ME	AAC+2ME
BW (baseline)	200 ± 8	195 ± 6	$190 + 10$	189 ± 17
BW(after 5 weeks)	504 ± 19	508 ± 10	$310 + 32^+$	$358 \pm 7^{+*}$
LV-Mass (mg)	1172 ± 52	$1820 \pm 160^+$	$1137 + 235$	$1073 \pm 55^*$
LVPWd (mm)	2.6 ± 0.1	$3.73 \pm 0.22^+$	2.6 ± 0.21	$2.8 \pm 0.1^*$
LVPWs (mm)	1.8 ± 0.06	$2.6 \pm 0.12^+$	1.8 ± 0.22	$1.9 \pm 0.17^*$
IVSd (mm)	1.8 ± 0.02	$2.57 \pm 0.12^+$	1.89 ± 0.18	$1.9 \pm 0.06^*$
IVSs (mm)	2.5 ± 0.1	$3.44 \pm 0.19^+$	2.64 ± 0.22	$2.7 \pm 0.1^*$
Heart Rate (bpm)	336 ± 17	371 ± 23	321 ± 31	316 ± 24
% EF	73 ± 2.9	77.4 ± 4.3	75.7 ± 2.8	78 ± 2.5
% FS	46.3 ± 1.5	43.3 ± 1.2	38.8 ± 4.4	44.8 ± 2.3
TEI	0.6 ± 0.04	0.75 ± 0.02	0.66 ± 0.08	0.72 ± 0.03
ME/A (ratio)	1.26 ± 0.15	1.23 ± 0.11	1.1 ± 0.08	1.3 ± 0.07
E/ E` (mm/sec)	25.4 ± 1.4	21 ± 3.1	25.7 ± 8.5	20.6 ± 1.9
A`/E` (mm/sec)	1.2 ± 0.07	1.08 ± 0.12	1.16 ± 0.24	1.1 ± 0.15
E`/A` (mm/sec)	0.8 ± 0.06	0.98 ± 0.11	0.9 ± 0.21	0.96 ± 0.11
S (mm/s)	45.5 ± 2.5	$53 \pm 1.9^+$	43 ± 1.7	$44 \pm 3.2^*$
PG (mmHG)	3.4 ± 0.3	$5.8 \pm 0.4^+$	4.4 ± 0.3	$2.9 \pm 0.3^*$

The values represent mean $\pm$ SEM (n = 6). $^+p<0.05$ compared to control. $^*p<0.05$ compared to AAC. BW, body weight, LV mass, left ventricular mass; LVPWs, left ventricular posterior wall, systole; LVPWd, left ventricular posterior wall, diastole; IVSs, intraventricular septum, systole; IVSd, intraventricular septum, diastole; Heart rate; EF, ejection fraction; FS, fractional shortening; TEI, Tei index = (isovolumic relaxation time+ isovolumic contraction time)/ ejection time; E, A , wave velocity; E`, A`, tissue doppler wave; S, sytolic tissue movement PG, Pressure Gradient.
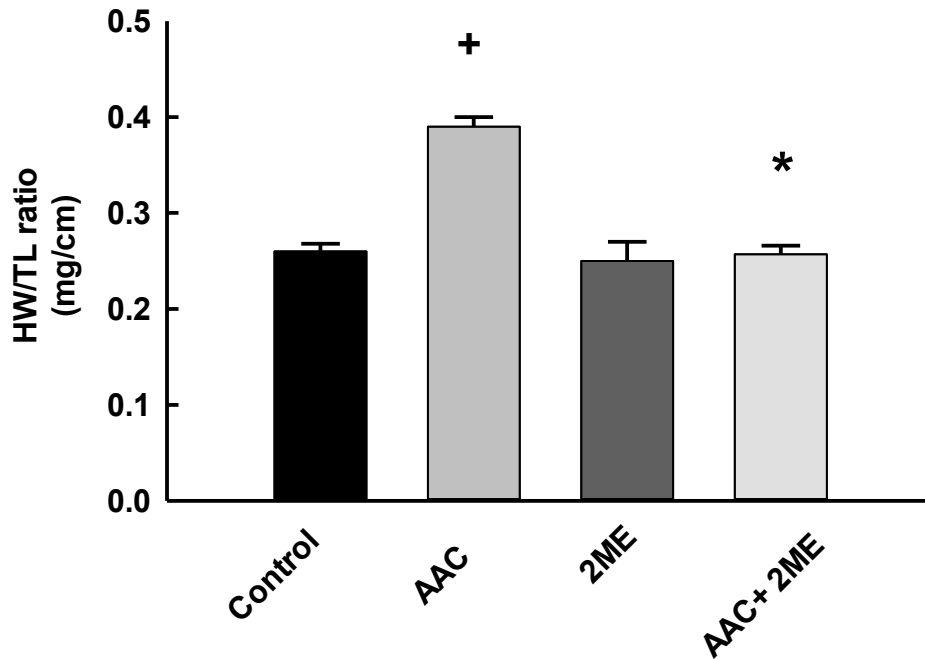
Figure 3.33. Effect of 2ME on AAC-induced HW/TL ratio
  Sham and AAC rats were treated with 2ME (5 mg/kg/day) in a mini osmotic pump.
  Thereafter, HW/TL ratio (in mg per cm) was determined for each animal. The
  values represent mean ± SEM (n = 6). $^{+}p<0.05$ compared to control. $^{*}p<0.05$
  compared to AAC.

3.5.2. Effect of 2ME on AAC-induced fibrosis in rat cardiac tissues

Chronic pressure overload is usually associated with excessive cardiac fibrosis and apoptosis which further burdens left ventricular remodeling and affects myocardial compliance. Because of this, we investigated whether the protective effect of 2ME against left ventricular remodeling is attributed to an inhibition of cardiac fibrosis and apoptosis induced by AAC. For this purpose, we measured the cardiac gene expression of the fibrotic and apoptotic markers, pro III, TGFβ-1, P53 and BAX relative to AAC rats using real-time PCR. Our results showed that AAC caused a significant induction of the fibrotic and apoptotic markers, pro-III, TGFβ-1, P53 and BAX by 400%, 250%, 200% and 170%, respectively in comparison to control (Figure 3.34A). On the other hand, 2ME treatment significantly inhibited the AAC-mediated induction of pro-III, TGFβ-1, P53 and BAX (Figure 3.34A). Furthermore, no significant differences were observed between the control and the 2ME treatment alone.

To further confirm the protective effect of 2ME against AAC-induced fibrosis, cardiac sections were stained with Trichrome's stain for the detection of fibrillar collagen and hence fibrosis (Figure 3.34B). A microscopic view of the myocardial tissue showed a significant increase in the fibrotic area in the hearts of AAC rats by approximately 120% in comparison to control. Importantly, this parameter was significantly reduced by 2ME treatment (Figure 3.34B), demonstrating that 2ME reduces the degree of fibrosis in rats with established cardiac hypertrophy.
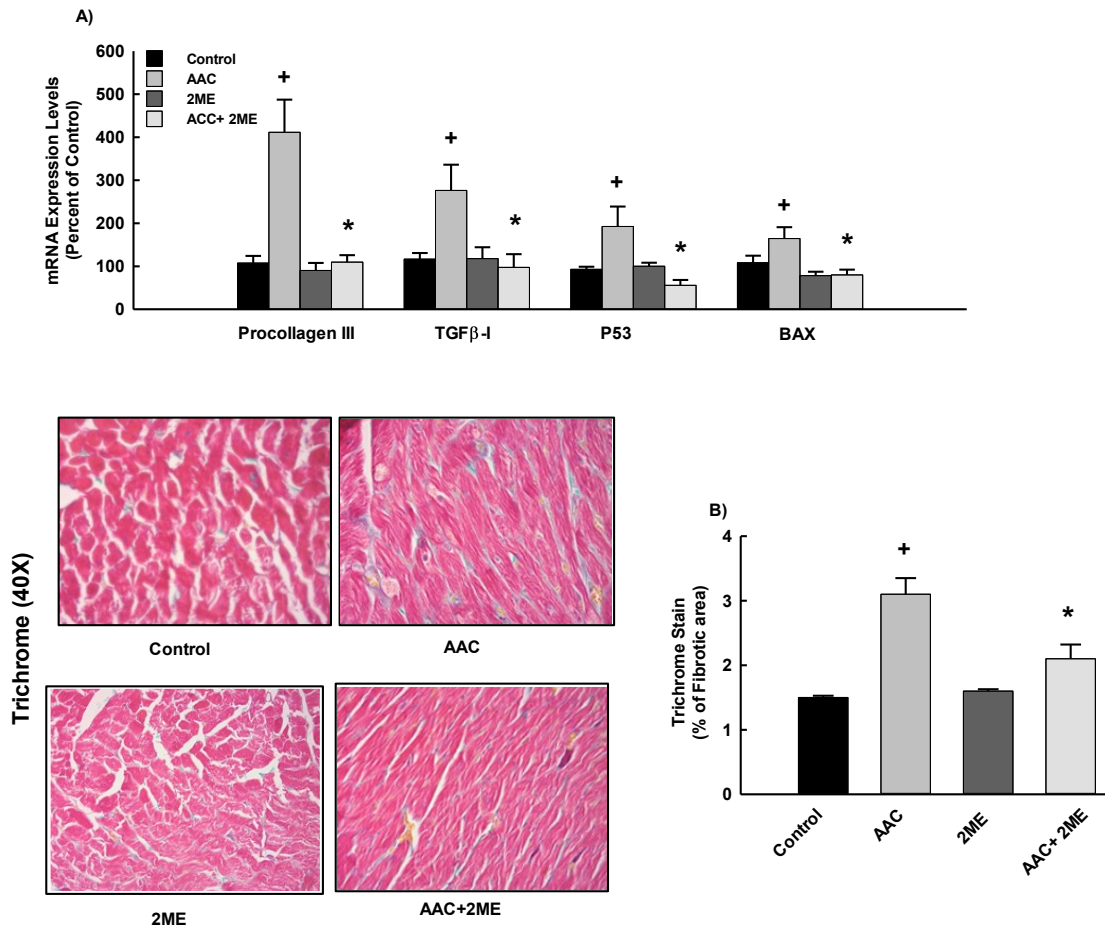
Figure 3.34. Effect of 2ME on AAC-mediated induction of fibrotic and apoptotic markers

Sham and AAC rats were treated with 2ME (5 mg/kg/day) in the mini osmotic pump. Thereafter, (A) the mRNA level of pro III, TGFβ-I, p53 and BAX were quantified using real time-PCR. (B) Fibrotic areas were determined using Trichrome stain (intense blue staining), quantified and expressed as % area. The values represent mean ± SEM (n = 6). $^+p<0.05$ compared to control. $^*p<0.05$ compared to AAC.

3.5.3. Effect of AAC and 2ME on mid-chain HETEs level and the expression of CYP1B1, LOXs and COX-2 proteins in rats

To determine the capacity of 2ME to inhibit the formation of mid-chain HETEs altered by AAC, mid-chain HETE metabolites were determined using LC–ESI–MS. The level of 5-, 11-, 12-, and 15-HETE formation were significantly increased to 150%, 140%, 150% and 160%, respectively, in hypertrophied heart microsomes in comparison to control (Figure 3.35A). On the other hand, treatment with 2ME significantly reduced the increase in mid-chain HETEs formation to 90%, 85%, 60%, and 110% in comparison to hypertrophied heart (Figure 3.35A).

Since mid-chain HETEs were shown to be formed by CYP1B1 as well as LOX and degraded by cyclooxygenase-2 (COX-2) enzyme, we examined whether the decrease in the formation of mid-chain HETEs by 2ME is due to the inhibition of LOXs and CYP and/or the activation of the COX-2 enzyme. For this purpose, CYP1B1, LOXs, and COX-2 protein expression levels were determined by Western blot analysis. Our results showed that AAC rats have demonstrated a significant increase in the expression of CYP1B1 and 12-LOX to 200% and 190%, respectively, in comparison to control. However, no significant changes were observed in the expression of COX-2, 5-LOX and 15-LOX between the control and the AAC group. Importantly, 2ME significantly inhibited the expression of CYP1B1 and 12-LOX-induced by AAC to 110% and 95%, respectively in comparison to AAC group (Figure 3.35B). On the other hand, treatment with 2ME significantly increased the expression of in COX-2 to 190% in comparison to the AAC group (Figure 3.35B).
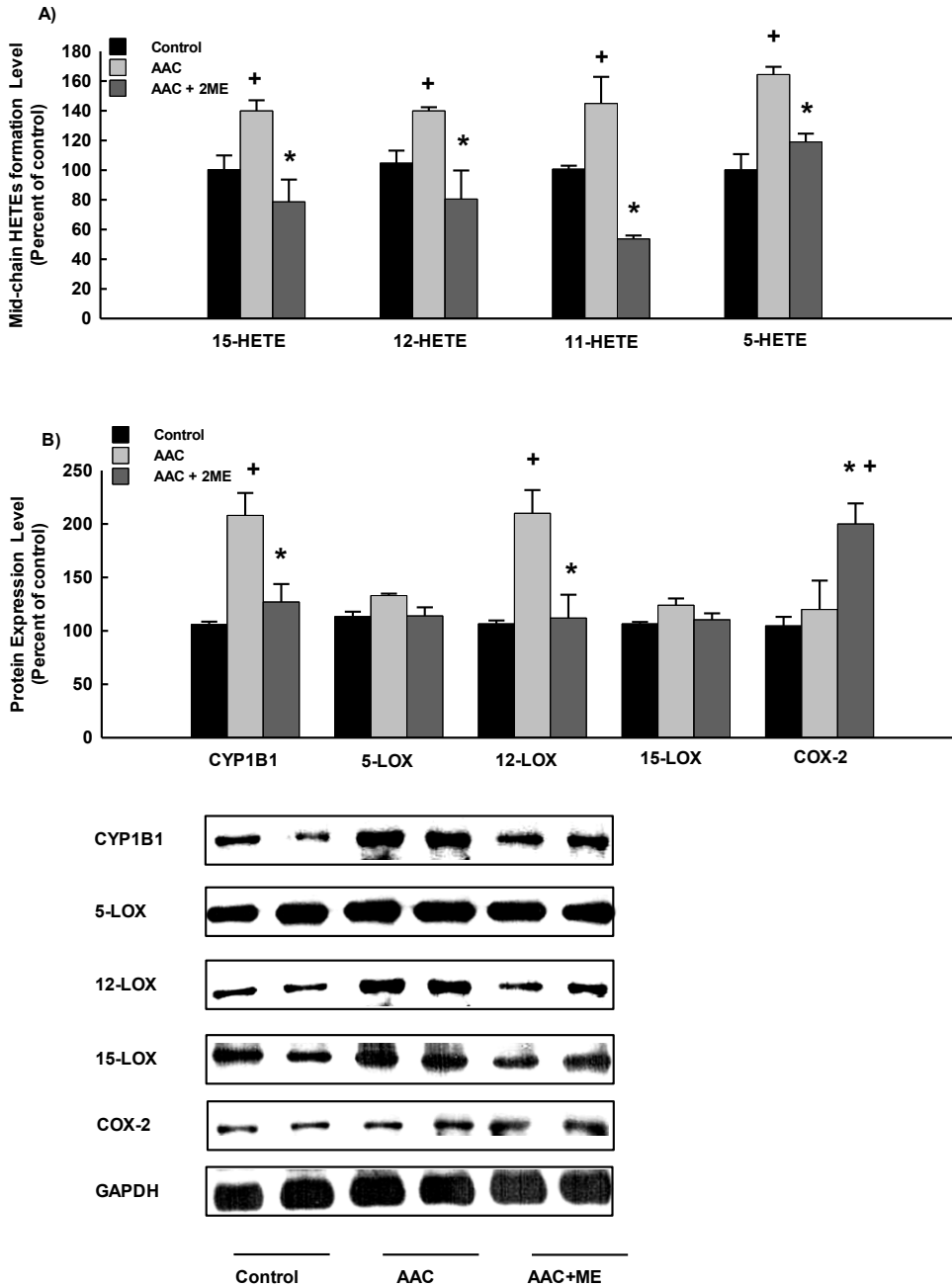
Figure 3.35. Effect of AAC and 2ME on mid-chain HETE levels and the expression of CYP1B1, LOXs and COX protein
Sham and AAC rats were treated with 2ME (5 mg/kg/day) in mini osmotic pumps and then, (A) mid-chain HETE metabolites were measured using LC–ESI–MS. (B) CYP1B1, 5-LOX, 12-LOX, 15-LOX and COX-2 protein expression levels were determined by Western blot analysis. The values represent mean ± SEM (n = 6). $^+p<0.05$ compared to control. $^*p<0.05$ compared to AAC.

3.5.4. Differential protein expression profile in the AAC group and 2ME treated rats

The proteins altered during cardiac hypertrophy in comparison to control and in the AAC rats treated with 2ME in comparison to AAC group were determined using LC–MS/MS and have been listed in Table 3.4 along with their mean fold change ratios.

The cardiac remodeling induced by AAC was associated with a significant increase in the expression of the hypertrophic protein, ADP-ribosylhydrolase-like 1 by 1.44 fold of change in comparison to control. Consistent with echocardiography, the protective effect of 2ME against AAC-induced cardiac hypertrophy was associated with a substantial increase in the expression of cardioprotective proteins, protein FAM65B and vinculin, and a significant decrease in the creatine kinase B-type protein, a biomarker of heart disease, by 3.9, 1.33 and 0.44 fold of change, respectively, in comparison to the AAC group (Table 3.4). Muscle contraction protein system, sarcoplasmic/endoplasmic reticulum calcium ATPase 2, was significantly decreased in the AAC group by 0.55 fold of change in comparison to control. However, 2ME-treated rats showed an exclusive increase in the protein expression of myosin light polypeptide 6 and myosin light chain 3 by 4.2 and 1.9 fold of change in comparison to the AAC group (Table 3.4).

The profile of inflammatory and fibrotic proteins altered in response to cardiac hypertrophy induced by AAC showed a significant increase in the expression of the fibrotic protein, galectin-1, by 2.5 fold of change in comparison to control. On the other hand, anti-inflammatory and anti-fibrotic proteins, Ig gamma-2A chain C region and Ig kappa chain C region, were significantly decreased in AAC rats treated with 2ME by 2.1 and 1.9 fold of change, respectively, in comparison to the AAC group (Table 3.4). Contrary to fibrotic proteins, proteins related to the apoptotic pathway, dynamin-1-like protein, P38 MAPK and mitochondrial phosphate carrier protein, were significantly reduced in the AAC group by 0.4, 0.3 and 0.6 fold of change, respectively, in comparison to control. Moreover, treatment of rats with 2ME further decreased the AAC-mediated inhibition of P38 MAPK (Table 3.4).

Our data showed that proteins under the category of cardiac metabolism were the most affected in the AAC rats and AAC rats treated with 2ME. Proteins involved in fatty acid and branched-chain amino acid oxidation, enoyl-CoA delta isomerase 1, acyl-CoA dehydrogenase, enoyl-CoA hydratase, electron transfer flavoprotein-ubiquinone oxidoreductase and 2-oxoisovalerate dehydrogenase, were significantly decreased in the AAC rats by 0.48, 0.59, 0.6, 0.55 and 0.63 folds of change, respectively, in comparison to control. Although 2ME did not significantly affect proteins involved in fatty acid and branched-chain amino acid oxidation altered by AAC, 2ME significantly decreased those responsible for the suppression of glucose oxidation, pyruvate dehydrogenase kinase, and pyruvate carboxylase, by 0.4 and 0.6 fold of change, respectively, in comparison to AAC group (Table 3.4). The indirect increase in proteins involved in glucose oxidation was associated with the ability of 2ME to prevent the increase in body weight in sham and AAC rats treated by approximately 38% and 30% in comparison to control (Table 3.4); however, treatment with 2-ME was not associated with any toxic adverse effects.

Protein expression of antioxidants, NADH-ubiquinone oxidoreductase, and prohibitin-1 were significantly decreased in the AAC group by 0.5 and 0.4 fold, respectively, in comparison to the control. On the other hand, 2ME significantly increased the expression of antioxidant proteins such as glutathione S-transferase P, glutathione S-transferase Mu, ferritin heavy chain and prohibitin-2, by a 1.9, 1.8, 2.8 and 1.8 fold of change, respectively, in comparison to the AAC group (Table 3.4).

3.5.5. Effect of AAC and 2ME on the MAPK signaling pathway

AAC rats demonstrated a significant decrease in the expression of phosphorylated p38 and ERK1/2 by approximately 50% and 40%, respectively, in comparison to the control (Figure 3.36). However, no significant changes were observed in the expression of phosphorylated JNK between the control and the AAC group. Although treatment of rats with 2ME further decreased the AAC-mediated inhibition of phosphorylated p38, 2ME significantly normalized the AAC-mediated effect on the phosphorylated ERK1/2, indicating a crucial role of the MAPK signaling pathway in the protective effect of 2ME against AAC-induced left ventricular hypertrophy (Figure 3.36). No significant differences were observed between the control and the 2ME treatment alone.

Table 3.4. Proteins altered during AAC and AAC+2ME.

Accession No.	Protein name	Mean fold change ratio-AAC vs C (*p* value)	Mean fold change ratio-2ME+AAC vs AAC (*p* value)
Q64119	Myosin light polypeptide 6	0.44 (0.13)	4.24 (0.01)
P11507	Sarcoplasmic/endoplasmic reticulum calcium ATPase 2	0.55 (0.033)	1.44 (0.36)
P07335	Creatine kinase B-type	1.25 (0.33)	0.44 (0.035)
P85972	Vinculin	0.92 (0.063)	1.33 (0.044)
Q7TP54	Protein FAM65B	1.06 (0.75)	3.93 (0.005)
Q5XIB3	ADP-ribosylhydrolase-like 1	1.44 (0.008)	0.68 (0.23)
P20760	Ig gamma-2A chain C region	0.90 (0.84)	2.16 (0.0005)
P01835	Ig kappa chain C region, B allele	0.79 (0.56)	1.93 (0.009)
P11762	Galectin-1	2.58 (0.005)	1.01 (0.97)
O35303	Dynamin-1-like protein	0.46 (0.01)	5.77 (0.44)
Q9WTY9	P38 MAPK	0.34 (0.02)	-
P16036	Phosphate carrier protein, mitochondrial	0.67 (0.027)	1.15 (0.41)
Q64536	Pyruvate dehydrogenase kinase	0.88 (0.72)	0.46 (0.008)
P52873	Pyruvate carboxylase	0.8 (0.382)	0.69 (0.035)
P23965	Enoyl-CoA delta isomerase 1	0.48 (0.025)	0.97 (0.921)
P45953	Acyl-CoA dehydrogenase	0.59 (0.025)	1.44 (0.15)
P14604	Enoyl-CoA hydratase	0.60 (0.039)	1.01 (0.97)
Q64591	2,4-Dienoyl-CoA reductase	0.39 (0.145)	2.76 (0.038)
Q5XIT9	Methylcrotonoyl-CoA carboxylase beta chain	0.85 (0.086)	1.63 (0.041)
P35738	2-Oxoisovalerate dehydrogenase	0.63 (0.028)	2.61 (0.14)
Q920L2	Succinate dehydrogenase	0.56 (0.022)	1.55 (0.013)
P80254	D-dopachrome decarboxylase	2.65 (0.039)	0.63 (0.21)
P29419	ATP synthase subunit e	1.74 (0.12)	0.54 (.037)
P35434	ATP synthase subunit delta	1.44 (0.008)	1.27 (0.63)
Q6UPE1	Electron transfer flavoprotein-ubiquinone oxidoreductase	0.55 (0.033)	1.26 (0.46)
P04906	Glutathione S-transferase P	0.80 (0.68)	1.95 (0.009)
P08010	Glutathione S-transferase Mu	0.81 (0.29)	1.85 (0.047)
Q66HF1	NADH-ubiquinone oxidoreductase	0.52 (0.029)	0.86 (0.59)
P19132	Ferritin heavy chain	0.66 (0.24)	2.84 (0.02)
P67779	Prohibitin-1	0.408 (.006)	1.45 (0.44)
Q5XIH7	Prohibitin-2	0.40 (0.105)	1.87 (0.04)

Sham and AAC rats were treated with 2ME (5 mg/kg/day) in mini osmotic pump and then, proteomic as determined using LC-MS/MS. The values represent mean ± SEM (n = 4).
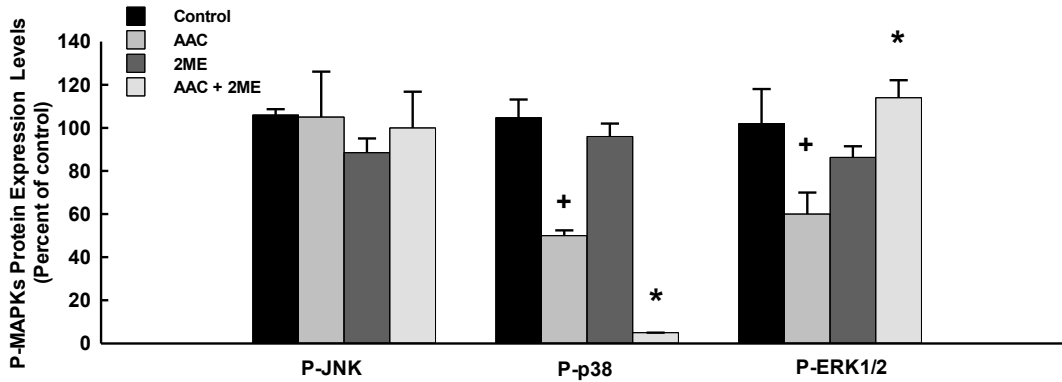
Figure 3.36. Effect of 2ME and AAC on the MAPK signaling pathway
Sham and AAC rats were treated with 2ME (5 mg/kg/day) in mini osmotic pumps. Then, the MAPK protein phosphorylation, P-JNK, P-p38 and P-ERK1/2 was determined. The values represent mean ± SEM (n = 6). $^+p<0.05$ compared to control. $^*p<0.05$ compared to AAC.

3.5.6. Effect of 2ME on ISO-mediated cellular hypertrophy

In order to investigate whether 2ME has a direct antihypertrophic effect in the cardiac cells in a manner similar to in vivo, we examined the ability of 2ME to inhibit cellular hypertrophy induced by ISO as cardiac hypertrophy induced by AAC is not possible in cells. Initially, we have demonstrated that treatment of RL-14 cells with 100 μM ISO with or without 0.25 μM 2ME for 24 h did not significantly affect RL-14 cell viability using MTT and LDH assays (Figure 3.37A). Figure 3.37B and C show that ISO alone caused a significant inhibition of α-MHC gene expression by about 50% and a significant induction of β-MHC, TNF-α and IL-6 gene expression by approximately 150%, 180% and 200%, respectively in comparison to the control. Although treatment of the cells with 2ME did not significantly alter the ISO-mediated inhibition of α-MHC gene expression, 2ME significantly inhibited ISO-induced β-MHC, β-MHC/α-MHC ratio, TNF-α and IL-6 genes expression by about 70%, 50%, 45% and 30%, respectively in comparison to the ISO treatment (Figure 3.37B and C). No significant changes were observed with the expression level of BNP (Figure 3.37B). The effect of 2ME on ISO-induced cellular hypertrophy was further confirmed by the ability of 2ME to completely restore the ISO-mediated increase in cell surface area (Figure 3.37D).
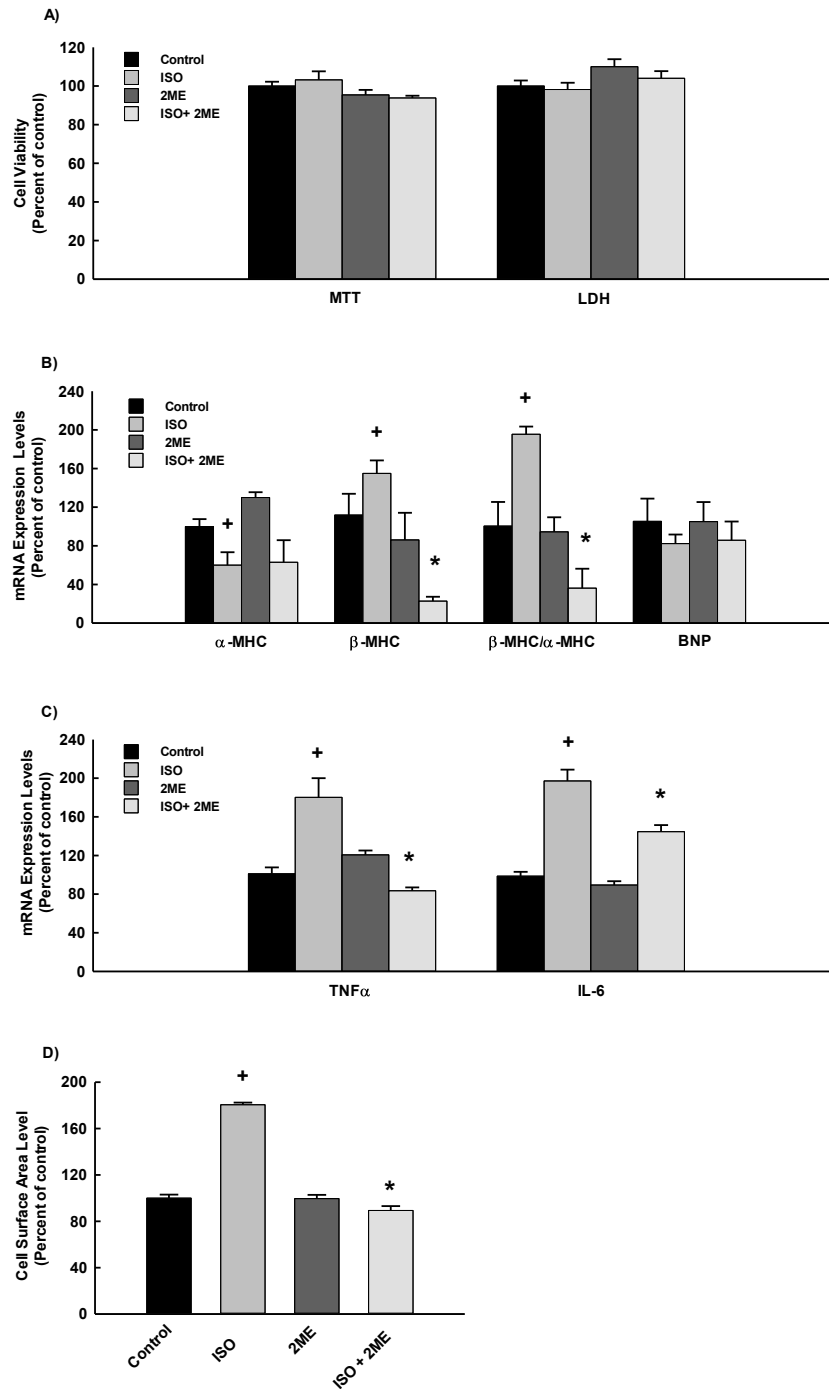
Figure 3.37. Effect of ISO and 2ME on RL-14 cell viability and hypertrophic markers
RL-14 cells were exposed to 100 μM ISO in the presence and absence of 0.25 μM 2ME for 24 h. Thereafter, (A) RL-14 cell viability was determined using MTT and LDH assays. (B) & (C) The mRNA level of α-MHC, β-MHC, BNP, TNF-α and IL-6 was quantified using real time-PCR. (D) Cell surface area was analyzed by phase contrast imaging.The values represent mean ± SEM (n = 6). $^{+}p<0.05$ compared to control. $^{*}p<0.05$ compared to ISO.

3.5.7. Effect of 2ME on ISO-mediated effect on superoxide radical, MAPK and NF-κB signaling pathways

Figure 3.38 shows that incubation of the cells with 100 µM of ISO significantly increased superoxide radical formation, phosphorylation of p38 and JNK in addition to the binding activity level of NF-κB P50 by approximately 180%, 160%, 150%, and 145%, respectively, whereas it inhibited the phosphorylation of ERK1/2 by approximately 50% in comparison to the control. No significant changes were observed with the activity level of NF-κB P65 (Figure 3.38C). Importantly, treatment with 2ME significantly normalized the ISO-mediated effect on the superoxide radical, MAPK and NF-κB signaling pathways (Figure 6), suggesting a crucial role of the aforementioned pathways in the protective effect of 2ME against ISO induced RL-14 cellular hypertrophy.
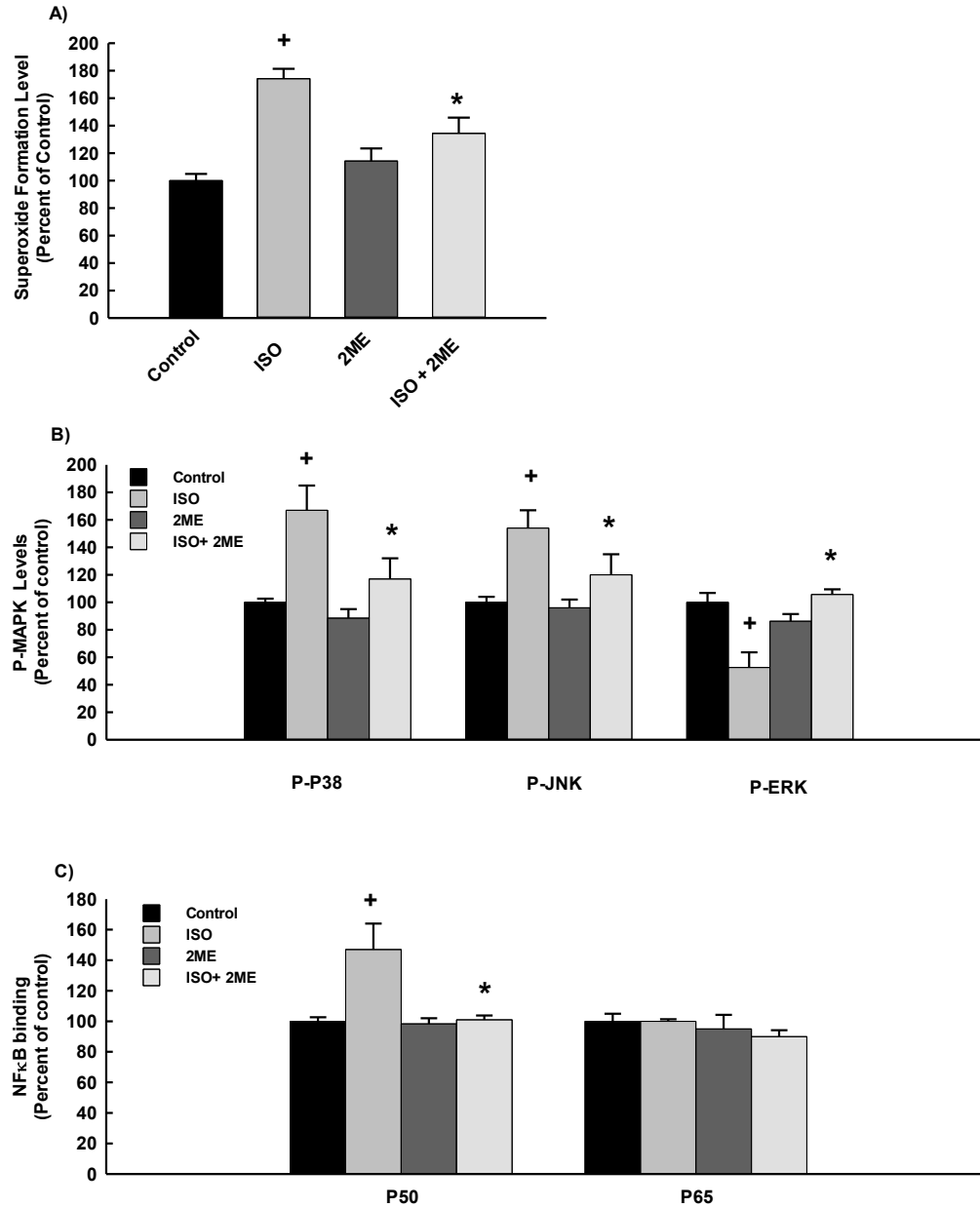
Figure 3.38. Effect of 2ME on ISO-mediated effect on superoxide radical, MAPK and NF-κB signaling pathways

RL-14 cells were treated for 24 h with 100 μM ISO in the presence and absence of 0.25 μM 2ME. Thereafter, (A) Superoxide anion was determined using the DHE assay. (B) MAPK protein phosphorylation was determined in cytoplasmic protein extracts using the PhosphoTracer Elisa Kit (Abcam, Cambridge, UK). (C) NF-κB binding activity was determined using a commercially available kit. The values represent mean ± SEM (n = 6). $^{+}p<0.05$ compared to control. $^{*}p<0.05$ compared to ISO.

CHAPTER 4. DISCUSSION

Portions of this chapter has been published in:

1-Maayah ZH, Abdelhamid G, El-Kadi AO (2015a). Development of cellular hypertrophy by 8-hydroxyeicosatetraenoic acid in the human ventricular cardiomyocyte, RL-14 cell line, is implicated by MAPK and NF-kappaB. *Cell biology and toxicology* **31**(4-5)**:** 241-259.

2-Maayah ZH, Althurwi HN, Abdelhamid G, Lesyk G, Jurasz P, El-Kadi AO (2016a). CYP1B1 inhibition attenuates doxorubicin-induced cardiotoxicity through a mid-chain HETEs-dependent mechanism. *Pharmacolgical Research* **105:** 28-43.

3-Maayah ZH, Althurwi HN, El-Sherbeni AA, Abdelhamid G, Siraki AG, El-Kadi AO (2017). The role of cytochrome P450 1B1 and its associated mid-chain hydroxyeicosatetraenoic acid metabolites in the development of cardiac hypertrophy induced by isoproterenol. *Molecular and Cellular Biochemistry* **429**(1-2)**:** 151-165.

4-Maayah ZH, El-Kadi AO (2016b). 5-, 12- and 15-Hydroxyeicosatetraenoic acids induce cellular hypertrophy in the human ventricular cardiomyocyte, RL-14 cell line, through MAPK- and NF-kappaB-dependent mechanism. *Archives of Toxicology* **90**(2)**:** 359-373.

5-Maayah ZH, El-Kadi AO (2016c). The role of mid-chain hydroxyeicosatetraenoic acids in the pathogenesis of hypertension and cardiac hypertrophy. *Archives of Toxicology* **90**(1)**:** 119-136.

6-Maayah ZH, Elshenawy OH, Althurwi HN, Abdelhamid G, El-Kadi AO (2015b). Human fetal ventricular cardiomyocyte, RL-14 cell line, is a promising model to study drug metabolizing enzymes and their associated arachidonic acid metabolites. *Journal of Pharmacological and Toxicological Methods* **71:** 33-41.

7-Maayah ZH, Levasseur J, Siva Piragasam R, Abdelhamid G, Dyck JRB, Fahlman RP*, et al.* (2018). 2-Methoxyestradiol protects against pressure overload-induced left ventricular hypertrophy. *Scientific Reports* **8**(1)**:** 2780.

4.1. Human fetal ventricular cardiomyocyte RL-14 cell line is a promising model to study drug metabolizing enzymes and cellular hypertrophy

CYP enzymes have been detected in the cardiovascular tissue and their specific isoforms have been detected in rat heart (Imaoka *et al.*, 2005) and in different regions of human heart (Roman, 2002; Delozier *et al.*, 2007). Several lines of evidence support the role of CYP metabolites in the maintenance of cardiovascular health, including the regulation of vascular tone, extracellular fluid volume, and heart contractility (Roman, 2002). Previous studies used different models to examine the expression of CYP enzymes in the heart (Thum *et al.*, 2000a; Thum *et al.*, 2002); however, each model has its difficulties and limitations. For instance, in vivo experiments may not be readily suited to detailed investigations at a cellular and molecular level. Isolation of primary cardiomyocytes is a complicated technique as heart muscle cells are firmly connected to each other and it is hard to cleave these connections without injuring the cells (Schluter *et al.*, 2005). Moreover, it is difficult to quantify CYP metabolites using primary cardiomyocytes because of their low yield and limited viability. Rat cardiomyoblast cells, H9c2 cells, and a mouse atrial cardiomyocyte cell line, HL-1 cells, are useful tools for cardiovascular research as they can be passaged serially, differentiate, and maintain the characteristics of rat and mouse cardiomyocytes (Kimes *et al.*, 1976; Claycomb *et al.*, 1998). However, mouse and rat cell lines cannot definitely answer questions that are specific to the human system.

Therefore, there is an urgent need for a reliable human in vitro cell line model to study the role of drug metabolizing enzymes in the heart. Currently, the human fetal ventricular cardiomyocytes, RL-14 cells, are a commercially available cell line (American Type Cell Culture Patent Deposit Designation No. PTA-1499, Manassas, VA) that has been established from non-proliferating primary cultures derived from human fetal heart tissues using a mitochondrial function-based method to indirectly introduce the SV-40 gene into cells (Davidson, 2007). In contrast to mouse and rat models, the RL-14 cell line offers a unique model since it can evaluate the complex molecular and genetic mechanisms underlying heart disease that are specific to the human. Although it lacks contractility and obvious voltage-activated conductances in whole-cell voltage-clamp recordings, it

expresses β-myosin heavy chain and the gap junction protein, connexin-43 (Davidson, 2007). The presence of gap junctions and the major cardiac-specific gap junction protein, connexin-43, may allow the cells to form a syncytium and to integrate functionally with normal or myopathic cardiac tissue (Davidson, 2007; Zhang *et al.*, 2009b). However, the expression of different CYP isoenzymes in RL-14 cells has not been fully elucidated yet. Accordingly, we investigated the expression of different CYP isoenzymes in RL-14 cells as a new proposed model. Also, we correlated this expression to primary cardiomyocytes.

Initially, we demonstrated here that RL-14 cells constitutively expresse CYP ω-hydroxylases, CYP1A, CYP1B1, CYP4A and CYP4F in addition to CYP epoxygenases, CYP2B, CY2C and CY2J at mRNA and protein levels. Our findings are consistent with previous reports suggesting that these CYP isoforms are constitutively expressed in the normal human heart (Bieche *et al.*, 2007; Delozier *et al.*, 2007). However, our results showed low levels of CYP1B1 and 2J2 mRNA compared with their protein levels. The discrepancy between mRNA and protein could be attributed to the differences in stability of the proteins or the rate of translation of each protein.

Although numerous researchers investigating the molecular processes that regulate cardiac function use primary cardiomyocytes as the standard experimental in vitro system, our study proposed the use of RL-14 cell line as it expresses CYP genes at comparable level to those expressed in the primary cardiomyocytes. This conclusion is supported by several pieces of evidence. First, CYP1A1 and 1A2 mRNAs were detected in RL-14 and HMC cells at higher levels than that in HMCa cells. Similar to our observations, it has been previously reported that CYP1 family was more highly expressed in fetal cardiomyocytes than in adult cardiomyocytes (Aragon *et al.*, 2008). Second, CYP4A11, CYP4F2, and CYP4F11 were expressed abundantly in RL-14 and HMCa cells but very little if any in HMC cells, suggesting that RL-14 cells are similar to adult cardiomyocytes in the expression of CYP4 family. Consistent with our results, it has been demonstrated that CYP4 was mainly expressed in freshly isolated cardiomyocytes of control animals and adult human cardiomyocytes (Simpson, 1997; Thum *et al.*, 2000a; Chaudhary *et al.*, 2009). Third, CYP2B6, 2C and 2J2 were highly expressed in RL-14 cells compared with HMCa

and HMC. Our results not only suggest the capability of RL-14 cells to express CYP ω-hydroxylases and epoxygenases at the same or higher levels compared with adult and fetal human primary cardiomyocytes but also validate the importance of RL-14 cells as a model for in vitro studies of drug metabolizing enzymes.

In the present study, we have demonstrated the inducibility of CYP ω-hydroxylases and epoxygenases gene expression in RL-14 cells using TCDD and fenofibrate. The genes in the CYP1 family are known to be inducible by AhR ligands such as TCDD, whereas CYP2 and CYP4 genes are known to be induced by fenofibrate (Denison *et al.*, 1986; Sehgal *et al.*, 2012; Althurwi *et al.*, 2014). We found that CYP1A1 and CY1A2 were induced by TCDD whereas CYP2B6 and CYP4F2 were induced by fenofibrate at mRNA and protein levels. Interestingly, the induction pattern of CYP1A1 at mRNA and protein levels by TCDD was similar to those obtained with H9c2 and Hepa 1c1c7 cells (Korashy *et al.*, 2005; Aboutabl *et al.*, 2007), whereas the induction of CYP2B6 by fenofibrate appeared to be consistent with its induction in vivo in heart tissue (Althurwi *et al.*, 2014).

Lastly, our study proposed the use of RL-14 cell line as a unique in vitro model to study cellular hypertrophy. This conclusion is supported by the finding that cardiac hypertrophic marker α-MHC, β-MHC, ANP and BNP were constitutively expressed in RL-14 cells at mRNA and protein levels like adult and fetal human primary cardiomyocytes.

In conclusion, the current study provides the first evidence for the ability of the human ventricular cardiomyocytes RL-14 cell line to express CYP and hypertrophic markers like primary cardiomyocytes and thus validates RL-14 cells as a promising model for studying drug metabolizing enzymes and cellular hypertrophy in the heart.

4.2. Mid-chain hydroxyeicosatetraenoic acids induce cellular hypertrophy in the human ventricular cardiomyocyte RL-14 cell line through MAPK-and NF-κB - dependent mechanisms

Mid-chain HETEs are biologically active eicosanoids resulting from the metabolism of AA by both LOX and a CYP-catalyzed bis-allylic oxidation reaction (LOX-like reaction). Recent studies have established the role of mid-chain HETEs in the development of cardiovascular disease (Jenkins *et al.*, 2009). For example, 5-HETE has been reported to have vasoconstrictive and pro-inflammatory action (Burhop *et al.*, 1988). 8-HETE has been shown to be detected in cardiac tissue and was reported to have a proliferator and pro-inflammatory action as it directly stimulates human neutrophil chemotaxis in vitro (Hunter *et al.*, 1985; El-Sherbeni *et al.*, 2014b). In addition, 12-HETE has been reported to act as a vasoconstrictor in small renal arteries and induce cellular hypertrophy and fibrosis, whereas 15-HETE has been proposed to be implicated in heart failure by induction of cardiac fibrosis. However, most of these previous studies were conducted on vascular smooth muscle, and none of them have utilized in vitro human cardiomyocytes to study the cardiac hypertrophic effect of mid-chain HETEs. In addition, the involvement of NF-κB and MAPK pathways has never been investigated before in human cardiomyocytes. Therefore, the current study was conducted to determine the potential cellular hypertrophic effect of mid-chain HETEs in the human ventricular cardiomyocytes RL-14 cells and to explore the involvement of MAPK and NF-κB signaling pathways.

Prior to commencing our research, the in vitro concentrations of mid-chain HETEs used in the current study were chosen after determining the ability of a wide range of concentrations to modulate the expression of hypertrophic markers and increase cell surface area without significantly affecting RL-14 cell viability. Although the concentrations of mid-chain HETE metabolites have not been determined in patients with cardiac hypertrophy yet, a recent study has demonstrated a physiologic concentration of mid-chain HETEs ranging from 50 to 250 nM (Yasumoto *et al.*, 2017). In addition, a previous report has demonstrated the effect of 8-HETE on the differentiation of primary

keratinocytes utilizing concentrations ranging from 5-10 µM (Muga *et al.*, 2000). Taken together, and beside the fact that mid-chain HETEs are unstable, the excessive concentrations of glucose combined with the presence of growth factor in culture media each collectively provide a high degree of in vivo relevance to the results arising from the concentrations of mid-chain HETEs (2.5-20 µM) used in the presently described in vitro experiments.

One of the hallmarks of cardiac hypertrophy and heart failure in patients is the increase in β-MHC/α-MHC, ANP and BNP expression levels (Barry *et al.*, 2008). Thus, their expressions have been considered as a good predictor of ventricular dysfunction and decompensated heart failure. The ability of mid-chain HETEs to induce cellular hypertrophy in the current study was evidenced first by the induction of the cardiac hypertrophic markers β-MHC/α-MHC, ANP and BNP in time- and concentration-dependent manners. Our results are supported by the previous observations that ischemic and dilated cardiomyopathies are associated with the increased level of the β-MHC/ α-MHC ratio (Reiser *et al.*, 2001). Furthermore, increased ANP and BNP expression levels have been shown to be associated with heart failure and ventricular hypertrophy induced by ISO (Zordoky *et al.*, 2008). The second piece of evidence for the induction of cellular hypertrophy is the increase in cell surface area. The increase in cell surface area was also reported with hypertrophic agonists' treatment, including endothelin and Ang II (Gu *et al.*, 2014; Vanezis *et al.*, 2014).

MAPK are intracellular signal transduction factors that are critically involved in the regulation of signaling pathways, ultimately leading to cardiac hypertrophy and heart failure (Zhang *et al.*, 2003). The three best-characterized MAPK include p38, JNK and ERK1/2. Recent reports have demonstrated that persistent activation of p38 and JNK can promote apoptosis, resulting in cardiac dilation and dysfunction (Pearson *et al.*, 2001). ERK1/2 has been proposed to regulate smooth muscle contraction and to promote cellular hypertrophy (Pearson *et al.*, 2001). Importantly, the exact role of MAPK in mid-chain HETEs-induced cardiac hypertrophy is still unclear. Thus, the second objective of the current study was to explore the role of MAPK in mid-chain HETEs-induced cardiac

hypertrophy. Our results showed that mid-chain HETEs significantly induced phosphorylated ERK1/2, whereas no significant changes were observed on phosphorylated p38 or JNK. The direct involvement of ERK1/2 was assessed by determining the effects of the ERK1/2 inhibitor, U0126. Our results clearly demonstrated that the activation of the ERK1/2 signaling pathway positively regulates the induction of the cardiac hypertrophic markers in response to mid-chain HETEs. The premise of this observation emerges from the fact that the activation of phosphorylated ERK1/2 is crucial for cellular hypertrophy. This is supported by the finding that Ang II induced cellular hypertrophy in H9c2 cells through ERK1/2 but not p38 or JNK (Zong *et al.*, 2013). Of particular interest in this study, baicalin, a CYP/LOX inhibitor, blocked the cellular hypertrophic effect of Ang II through the inhibition of ERK1/2 signaling pathway (Zong *et al.*, 2013).

Previous studies have indicated that NF-κB has a wide range of pathophysiological functions in cardiac hypertrophy (Hirotani *et al.*, 2002). NF-κB has been shown to be activated in the failing human heart (Grabellus *et al.*, 2002). Furthermore, it has been demonstrated that blockade of NF-κB ameliorates myocardial hypertrophy in response to aortic banding and chronic infusion of Ang-II, suggesting an important role of NF-κB as a signaling pathway in the regulation of cardiac hypertrophy (Kawano *et al.*, 2005). In this regard, we demonstrated that mid-chain HETEs were able to induce the binding activity of NF-κB to their responsive elements in a HETE-dependent manner. The direct evidence for the involvement of NF-κB in the mid-chain HETEs-mediated induction of cellular hypertrophy was supported by the observation that blocking of NF-κB using PDTC significantly resulted in restoration of the mRNA expression of the hypertrophic markers to their normal levels, implying that the activation of NF-κB is required for the induction of cardiac hypertrophy. Consistent with our results, it has been shown that activation of NF-κB is required for hypertrophic growth of cardiomyocytes in response to hypertrophic agonists, including phenylephrine, endothelin-1 and Ang II (Hirotani *et al.*, 2002). In addition, cardioprotective metabolites, EETs, are reported to have cardioprotective effects through several mechanisms, most notably by inhibiting the activation of NF-κB, whereas DOX has been shown to induce myocardial apoptosis through activation of NF-κB (Xu *et al.*, 2006; Li *et al.*, 2008).

CYP enzymes have been detected in cardiovascular tissue and their specific isoforms have been detected in rat heart (Imaoka *et al.*, 2005) and in different regions of human heart (Roman, 2002; Delozier *et al.*, 2007). Several lines of evidence support the role of CYP metabolites in the maintenance of cardiovascular health, including the regulation of vascular tone, extracellular fluid volume, heart contractility and cardiac hypertrophy (Roman, 2002). Therefore, we investigated the effect of mid-chain HETEs on the expression of different CYP genes involved in cardiac hypertrophy. Our results demonstrated that all mid-chain HETEs did not significantly alter the expression of CYP ω-hydroxylases and epoxygenases at mRNA and protein levels. However, we found a significant decrease in 14, 15- and 11, 12-EET formation in RL-14 cells treated with 8- and 12-HETE. This decrease in EET formation was accompanied by a significant increase in the formation of their corresponding DHETs. Therefore, it was necessary to investigate the effect of mid-chain HETEs on the activity of sEH which promotes the conversion of EETs to their corresponding inactive diols form, DHETs (Yu *et al.*, 2000; Imig *et al.*, 2002). Interestingly, our results clearly demonstrated that mid-chain HETEs caused a significant induction of sEH catalytic activity in RL-14 cells which explains the high level of DHETs. Importantly, the mid-chain HETEs-induced cellular hypertrophy was significantly attenuated by pretreatment of RL-14 cells with a selective sEH inhibitor, tAUCB, suggesting that sEH is essential for mid-chain HETEs-mediated induction of cellular hypertrophy. The induction of sEH and DHETs has been reported to increase in animal models of Ang II- and ISO-induced cardiac hypertrophy (Zordoky *et al.*, 2008; Ai *et al.*, 2009). Moreover, sEH inhibitors have been shown to prevent and/or reverse the development of cardiac hypertrophy in several models (Xu *et al.*, 2006).

In conclusion, our study provides the first evidence that mid-chain HETEs induce cellular hypertrophy in the human ventricular cardiomyocytes RL-14 cells through MAPK- and NF-κB-dependent mechanisms and could be used as novel targets in the treatment of cardiac hypertrophy and heart failure.

4.3. CYP1B1 inhibition attenuates doxorubicin-induced cardiotoxicity through a mid-chain HETEs-dependent mechanism

DOX is a broad-spectrum anthracycline antibiotic widely used to treat various types of human neoplastic disease, including lymphoblastic, hematopoietic and a wide range of solid tumors, such as lung, breast and thyroid cancer (Minotti *et al.*, 2004). Unfortunately, clinical usefulness of DOX is badly compromised by its cumulative cardiotoxicity leading to irreversible cardiomyopathy and congestive heart failure. Despite several studies the have demonstrated a role for oxidative stress, inhibition of topoisomerase II and apoptosis in DOX-induced cardiomyocyte toxicity (Minotti *et al.*, 2004; Takemura *et al.*, 2007), the specific mechanisms regulating cardiotoxic effect of DOX are still unclear. Intriguingly, it has been shown that DOX increases the formation of mid-chain HETEs in cancer cells (Catalano *et al.*, 2004). Furthermore, several studies have established the role of mid-chain HETEs in the development of cardiac toxicity (Nozawa *et al.*, 1990; Cyrus *et al.*, 1999; Jenkins *et al.*, 2009). Taken together, the exact mechanism of DOX-induced cardiotoxicity and its progression to heart failure has not been fully elucidated yet and the role of mid-chain HETEs in DOX-induced cardiotoxicity has never been reported before and could not be ruled out. Therefore, the current study was conducted to examine the capacity of DOX to increase mid-chain HETEs in cardiomyocytes in vitro and in vivo and to explore whether inhibiting the formation of mid-chain HETEs confers cardioprotection against DOX-induced cardiotoxicity.

Prior to commencing the current experiments, the cumulative dose of DOX (15 mg/kg) used in the current study was selected based on previous studies and comparable with doses given to cancer patients, which causes bradycardia and reduces cardiac contractility in many cancer patients (van Acker *et al.*, 1996; Taniyama *et al.*, 2002). For example DOX 2 mg/kg is equivalent to a dose of 6.5 mg/m^2 in patients (Ottewell *et al.*, 2009). Furthermore, the chronic cardiotoxicity induced by DOX occurs in patients given cumulative dose of ≥500 mg/m^2 (Petit, 2004; Mitra *et al.*, 2007). Taken together, the chronic human exposure to DOX, its long half-life, and the high possibility of accumulation in cardiac tissue make the dose used in the present study highly relevant to the corresponding clinical situation. With regard to the TMS, the dose was selected based on its pharmacokinetic properties, its

long half-life and the high TMS tissue distribution (Lin *et al.*, 2010). Previous studies showed that TMS 300 µg/kg every 3rd day was able to decrease CYP1B1 catalytic activity, as well as prevent the toxicity observed following Ang II and deoxycorticosterone infusion (Jennings *et al.*, 2010; Malik *et al.*, 2012).

In vivo, we have demonstrated for the first time that TMS, a selective CYP1B1 inhibitor, attenuates DOX-induced cardiotoxicity in rats as TMS significantly prevented the DOX mediated inhibition of cardiac output, stroke volume, HW/TL ratio and thinning of the LVPWd, LVIDd, IVSD, IVSs and LVPWs. This is in agreement with the observation that resveratrol, a TMS analogue, prevents systolic dysfunction in hearts of DOX-treated mice by improving CO, SV and left ventricular morphology (Dolinsky *et al.*, 2013). Second, histopathological examination of cardiac tissues revealed myofiber disarray and muscular fiber dissociation in addition to the presence of fibrosis in response to DOX, which appeared to be reduced by TMS treatment. The antifibrotic effect of TMS has been reported to prevent Ang II-induced collagen deposition in the interstitial space of the kidney (Jennings *et al.*, 2012a).

The induction of cardiotoxicity was associated with a proportional increase in the formation of mid-chain HETE metabolites. Interestingly, the inhibition of cardiotoxicity by TMS was associated with a dramatic decrease in the formation of mid-chain HETEs in heart tissues, suggesting a mid-chain HETE-dependent mechanism. The role of mid-chain HETEs in the pathogenesis of CVDs including heart failure and cardiomyopathy has been reported before (Nozawa *et al.*, 1990; Cyrus *et al.*, 1999; Jenkins *et al.*, 2009). In this regard, it has been demonstrated that up-regulation of 12- and 15-HETE metabolites induces systolic dysfunction and cardiac fibrosis in rats (Wallukat *et al.*, 1994; Kayama *et al.*, 2009). Furthermore, treatment of mice with streptozotocin has been shown to induce cardiomyopathy and fibrosis through a 12- and 15-HETE-dependent mechanism (Kumar *et al.*, 2013; Suzuki *et al.*, 2015).

The RL-14 cell line was utilized in the current study to validate the in vitro model and explore the mechanistic role of CYP1B1 and its associated mid-chain HETEs metabolite

in DOX-induced cardiotoxicity. Initially, the concentration of DOX used in the current study was maintained within the therapeutic range of plasma concentration reported in human. For example, human subjects given a dose of 60~75 mg/m^2 DOX for the treatment of metastatic breast cancer had mean plasma concentrations ranging from 5 to 15 μM and an average half-life of ~25 h (Robert *et al.*, 1985; Mross *et al.*, 1988). In addition, several in vitro studies on cardiomyocytes to explore the cardiotoxicity of DOX used concentrations ranging from 1 to 10 μM (Doroshow *et al.*, 1990; McHowat *et al.*, 2001). With regards to TMS, the concentration used in the current study was selected based on a previous study showing that concentrations ranging from 0.1 to 1 μM exhibited the maximum inhibitory activity against CYP1B1 (Chun *et al.*, 2001) and did not affect RL-14 cells viability alone or in combination with DOX.

At the in vitro level, treatment of RL-14 cells with DOX caused cardiotoxicity which is evidenced first by the induction of β-MHC/α-MHC in a time-dependent manner. The relative ratio of β-MHC to α-MHC has been considered as a good predictor of ventricular dysfunction and was reported to be altered during heart failure and in DOX treated heart (Alpert *et al.*, 1982; Holubarsch *et al.*, 1985; Harris *et al.*, 1994; de Beer *et al.*, 2000; Hydock *et al.*, 2008). MHC isoform switching from α-MHC to β-MHC decreases the myosin ATPase enzyme velocity and depletes the intracellular energy level, thereby disrupting myocardial twitch kinetics. This detrimentally affects the systolic function and decreases contractile performances of the cardiomyocytes that significantly contributes to the progression of heart failure (Fatkin *et al.*, 2000; Kiriazis *et al.*, 2000; Locher *et al.*, 2011). The second piece of evidence for the induction of cardiotoxicty is the increase in cell volume. The increase in cell volume was also reported with DOX treatment of H9c2 cells (Karagiannis *et al.*, 2010). Furthermore, the increase in cell volume in response to DOX is consistent with fiber disarray occurring at in vivo level (Zhu *et al.*, 2008). Interestingly, the induction of β-MHC/α-MHC was associated with a proportional increase in CYP1B1 mRNA, protein, and catalytic activity levels and its associated mid-chain HETE metabolites in RL-14 cells. Taken together, these results suggest an important role of CYP1B1 enzyme and mid-chain HETEs in DOX-induced cardiotoxicity.

Direct evidence for the involvement of CYP1B1 in the DOX-induced cardiotoxicity was provided by the observation that blocking of CYP1B1 catalytic enzyme activity using TMS, a selective CYP1B1 inhibitor, significantly reduced the cytotoxicity, mRNA expression of hypertrophic markers and cell volume in response to DOX to their normal levels. This was associated with a proportional decrease in the formation of mid-chain HETEs suggesting a CYP1B1/mid-chain HETE-dependent mechanism. In contrast to TMS, inhibition of LOXs using zileuton and PD146176 did not affect the formation of mid-chain HETEs and failed to protect against DOX induced-cardiotoxicity, confirming the role of CYP1B1 in the formation of mid-chain HETEs. In agreement with our results, it has been shown that disruption of the cyp1b1 gene through the deletion exons 2 and 3 inhibits the formation of mid-chain HETEs and provides a significant protective effect against Ang II-induced renal toxicity (Jennings *et al.*, 2012b). The premise of this observation emerges from the finding that the levels of LOXs, Cyp4a, and Cyp4f protein were not changed in the cyp1b1-/- mice, suggesting a CYP1B1-selective production of mid-chain HETEs. Furthermore, it has been demonstrated that non-selective CYP inhibitors such as SKF-525A inhibit cellular hypertrophy whereas LOX inhibitors such as zileuton failed to produce such an effect (Nieves *et al.*, 2006). The inhibition of cellular growth in response to SKF-525A was associated with the impairment of mid-chain HETE synthesis. Interestingly, exogenous addition of mid-chain HETEs reversed the effect of SKF-525A, confirming an important role of CYP in the regulation of mid-chain HETEs (Nieves *et al.*, 2006).

Mechanistically, we have demonstrated previously that mid-chain HETEs induce their toxic effect in the human ventricular cardiomyocytes RL-14 cells through MAPK- and NF-κB-dependent mechanisms. MAPK and NF-κB are intracellular signal transduction factors that are critically involved in the regulation of signaling pathways, ultimately leading to cardiotoxicity and heart failure (Zhang *et al.*, 2003). Several reports have demonstrated that persistent activation of NF-κB, p38 and JNK by DOX promotes apoptosis, resulting in cardiac dilation and dysfunction (Pearson *et al.*, 2001; Xu *et al.*, 2006; Li *et al.*, 2008). ERK1/2 has been proposed to regulate smooth muscle contraction and to promote cellular hypertrophy (Pearson *et al.*, 2001). Taken together, the possibility that the inhibition of

mid-chain HETE formation by TMS would inhibit the activation of MAPK and NF-κB by DOX has never been investigated before and could not be ruled out. Thus, the third objective of the current study was to explore the role of TMS on DOX-mediated activation of NF-κB and MAPK. Our results showed that DOX-treatment significantly increased phosphorylation of ERK1/2, p38 and JNK as well as the binding activity of NF-κB to its responsive elements. Importantly, the inhibition of CYP1B1 via TMS significantly blocked the activation of phosphorylated MAPK and NF-κB in response to DOX, suggesting that MAPK and NF-κB are essential for TMS-mediated protection against DOX-induced cardiotoxicity. In agreement with our results, resveratrol, a TMS analogue, has been reported to possess a significant cardioprotective effect against DOX-induced cardiotoxicity through the inhibition of MAPK and NF-κB (Cao *et al.*, 2004; Beedanagari *et al.*, 2009; Dolinsky *et al.*, 2009). In addition, cardioprotective metabolites such as EETs are reported to have cardioprotective effects through several mechanisms most notably by inhibiting the activation of NF-κB (Xu *et al.*, 2006; Li *et al.*, 2008).

Our study provides the first evidence that inhibition of CYP1B1 and hence mid-chain HETEs attenuates DOX-induced cardiotoxicity in vitro in RL-14 human ventricular cardiomyocytes and in vivo in rats.

4.4. The role of cytochrome P450 1B1 and its associated mid-chain hydroxyeicosatetraenoic acid metabolites in the development of cardiac hypertrophy induced by ISO

Several lines of evidence support the role of CYP1B1 and its associated mid-chain HETE metabolites in the development of cardiac hypertrophy (Korashy *et al.*, 2006; Malik *et al.*, 2012). For example, the expression of CYP1B1 protein and the formation of mid-chain HETE metabolites were shown to be increased during pressure overload-induced cardiac hypertrophy (El-Sherbeni *et al.*, 2014a). In addition, the induction of CYP1B1 has been demonstrated in the rat heart exposed to ISO and Ang-II and in the left ventricular tissue of spontaneously hypertensive rats (Thum *et al.*, 2002; Zordoky *et al.*, 2008; Jennings *et al.*, 2012b). Taken together, the possibility that the inhibition of CYP1B1 and its associated

mid-chain HETE metabolites would protect against cardiac hypertrophy induced by ISO has never been investigated before and could not be ruled out. Therefore, the current study was conducted to examine the capacity of ISO to induce CYP1B1 and its associated mid-chain HETE metabolites in cardiomyocyte at in vitro and in vivo levels and to explore whether inhibiting the expression of CYP1B1 and the formation of mid-chain HETEs confers cardioprotection against ISO-induced cardiac hypertrophy.

Initially, we demonstrated recently that ISO-induced cardiac hypertrophy in vivo in rats is evident by the increase in HW/BW ratio and thickening of left ventricular morphology (Althurwi et al., 2015). Interestingly, treatment of rats with ISO was associated with a proportional induction of cardiac CYP1B1 enzyme and its associated mid-chain HETE metabolites at pre-hypertrophic and hypertrophic stages. The induction of CYP1B1 enzyme and its associated metabolites seems to be detrimental and it may deteriorate cardiac function (Nozawa et al., 1990; Cyrus et al., 1999; Jenkins et al., 2009). This was supported by a recent study that demonstrated the ability of 5-, 8-, 12- and 15-HETE to induce cellular hypertrophy in vitro in human ventricular cardiomyocytes (Maayah et al., 2015b; Maayah et al., 2015c; Maayah et al., 2015d). In vivo, the up-regulation of 12- and 15-HETE metabolites was shown to induce systolic dysfunction and cardiac fibrosis in rats (Wallukat et al., 1994; Kayama et al., 2009). On the other hand, CYP1B1 inhibition has been reported to attenuate the adverse cardiac events associated with DOX treatment and in spontaneously hypertensive rats through a mid-chain HETEs-dependent mechanism suggesting an important role of CYP1B1 and its metabolites in the development of cardiac hypertrophy and heart failure (Jennings et al., 2014b; Maayah et al., 2016a).

The importance of CYP1B1 relies on the fact that the levels of CYP1B1 and mid-chain HETEs were induced at pre-hypertrophic and hypertrophic stages whereas LOX enzymes were just decreased from the basal level at hypertrophic stages, implying CYP1B1 as a promising target in the treatment of cardiac hypertrophy. This is supported by a previous finding that demonstrated that in contrast to TMS, a selective CYP1B1 inhibitor, inhibition of LOXs using zileuton and PD146176 did not affect the formation of mid-chain HETEs and failed to protect against DOX-induced cardiotoxicity confirming the role of CYP1B1

169

in the formation of mid-chain HETEs (Maayah *et al.*, 2016a). Furthermore, it was shown that CYP inhibitors such as SKF-525A persuade a cell cycle delay and inhibit cellular hypertrophy whereas, LOX inhibitors such as nordihydroguaiaretic acid have failed to produce such an effect (Nieves *et al.*, 2006). The inhibition of cellular growth in response to SKF-525A was associated with CYP inhibition and the subsequent impairment of synthesis of mid-chain HETEs. Interestingly, exogenous addition of mid-chain HETEs reversed the effects of SKF-525A confirming an important role of CYP in the regulation of mid-chain HETEs (Nieves *et al.*, 2006).

In vitro, treatment of RL-14 cells with ISO caused cellular hypertrophy which is evidenced first by the induction of β-MHC, inhibition of α-MHC and the increase in cell surface area. However, there was no significant change in the expression of ANP and BNP mRNA levels. The relative ratio of β-MHC to α-MHC has been considered as a good predictor of ventricular dysfunction and was reported to be altered during cardiac hypertrophy (Barry *et al.*, 2008). MHC isoform switching from α-MHC to β-MHC decreases the myosin ATPase enzyme velocity and depletes the intracellular energy level, thereby disrupting myocardial twitch kinetics. This detrimentally affects the systolic function and decreases contractile performances of the cardiomyocytes that significantly contributes to the progression of heart failure (Fatkin *et al.*, 2000; Kiriazis *et al.*, 2000; Locher *et al.*, 2011). On the other hand, natriuretic peptides, such as ANP and BNP are considered as potent endogenous inhibitors of hypertrophy and they are released from cardiomyocytes in response to increased ventricular wall stress (Maayah *et al.*, 2016b). BNP has been considered as a good predictor of heart failure (Maayah *et al.*, 2016c) whereas ANP may serve as a marker of cardiac stress but not essentially as a hypertrophic marker, especially at an organ level (Maayah *et al.*, 2015a).

Direct evidence for the involvement of CYP1B1 in the development of cardiac hypertrophy induced by ISO was provided by the following observations: (a) inhibition of CYP1B1 using TMS, a selective CYP1B1 inhibitor, or knockdown of CYP1B1 gene expression using CYP1B1-siRNA significantly restored the mRNA expression of hypertrophic marker and the increase in cell surface area in response to ISO to their normal level. In agreement

with our results, it has been shown that disruption of a cyp1b1 gene in addition to TMS, a selective CYP1B1 inhibitor, provides a significant protective effect against deoxycorticosterone salt-induced cardiac hypertrophy (Sahan-Firat *et al.*, 2010; Jennings *et al.*, 2012c). The premise of this observation emerges from the finding that the levels of LOXs, Cyp4a, and Cyp4f protein were not changed in the cyp1b1-/- mice suggesting a CYP1B1-dependent mechanism. (b) Overexpression of CYP1B1 using CRISPR-CYP1B1 plasmid significantly induced cellular hypertrophy as evident by the inhibition of α-MHC gene expression. Low expression level of α-MHC significantly accelerates myocardial twitch kinetics, thereby enhancing systolic function in the large mammalian myocardium (Locher *et al.*, 2011). Similar to our observation, it has been previously reported that induction of CYP1B1 by the AhR ligands BaP and 3-MC causes significant cardiac hypertrophy in vivo in rats (Aboutabl *et al.*, 2009). In addition, TCDD and β-naphthoflavone, CYP1 family inducers, cause hypertrophy in cardiac-derived H9c2 cells through the induction of CYP1B1 gene expression (Zordoky *et al.*, 2010b).

The above information suggests a role of CYP1B1 in cardiac hypertrophy and in the formation of mid-chain HETE metabolites induced by ISO. This raises the question of whether or not CYP1B1 is directly involved in the formation of mid-chain HETE metabolites. Therefore, we examined the ability CYP1B1 overexpression to increase the formation of mid-chain HETEs in RL-14 cells. Perhaps the finding of greatest interest in the current study was the observation that CRISPR-CYP1B1 delivery led to a significant increase in the formation of 15-, 12- and 8-, 11- and 5-HETE, implying that CYP1B1 is directly involved in the formation of these metabolites. Consistent with our findings, it has been demonstrated previously that the recombinant CYP1B1 enzyme catalyzes the formation of mid-chain HETEs (Choudhary *et al.*, 2004; El-Sherbeni *et al.*, 2014a). Importantly, the above finding was further confirmed by the ability of CYP1B1-siRNA to inhibit the formation of mid-chain HETEs suggesting an important role of CYP1B1 in the formation of theses metabolites.

Mechanistically, CYP1B1 has been reported to cause cardiac hypertrophy through the generation of superoxide radical (Morgan, 2001; Malik *et al.*, 2012). Superoxide anion was

shown to be implicated in the hypertrophy process through the increase of proto-oncogenes factors, such as c-my and c-fos, mediating the linkage of Na^+/K^+ ATPase to hypertrophy and modulation of the activity of MAPK (Xie *et al.*, 1999; Wassmann *et al.*, 2001). Treatment with antioxidants inhibited the hypertrophic response of cardiomyocytes (Nakamura *et al.*, 1998; Tanaka *et al.*, 2001). Currently, we have demonstrated that ISO treatment significantly increased the generation of superoxide anion. Of interest, the inhibition of CYP1B1 using TMS significantly inhibited the formation of superoxide anion in response to ISO. Our results are supported by a previous observation showing that the induction of CYP1B1 by TCDD caused cardiac hypertrophy, which was attributed to the generation of superoxide anion and elevation of blood pressure (Kopf *et al.*, 2008). Furthermore, TMS displayed an antihypertensive effect and inhibited its associated cardiovascular events in spontaneously hypertensive rats, primarily by inhibiting the generation of superoxide anion and the MAPK signaling pathway (Jennings *et al.*, 2014b).

MAPK and NF-κB are intracellular signal transduction factors that are critically involved in the regulation of signaling pathways, ultimately leading to cardiac hypertrophy and heart failure (Zhang *et al.*, 2003). Accumulating data provide convincing evidence that persistent activation of NF-κB, p38 and JNK promotes apoptosis, resulting in cardiac hypertrophy (Pearson *et al.*, 2001; Esposito *et al.*, 2002; Xu *et al.*, 2006; Li *et al.*, 2008). ERK1/2 has been proposed to regulate smooth muscle contraction and to promote cellular hypertrophy (Pearson *et al.*, 2001). Genetic inhibition of ERK1/2 has been reported to promote stress-induced apoptosis and heart failure (Purcell *et al.*, 2007). Taken together, the possibility that the inhibition of CYP1B1 and its associated mid-chain HETEs and superoxide anion by TMS would inhibit the modulation of MAPK and NF-κB by ISO has never been investigated before and could not be ruled out. Thus, the third objective of the current study was to explore the role of TMS on the ISO-mediated effect on NF-κB and MAPK signaling pathways.

Our results showed that ISO-treatment significantly inhibited the phosphorylated ERK1/2, whereas it increased the binding activity of P50 NF-κB to its responsive elements. This was similar to a previous observation demonstrating that ISO dephosphorylates and

inactivates phosphorylated ERK in human cells through the activation of protein phosphatases (Chen *et al.*, 2002). Importantly, the inhibition of CYP1B1 using TMS significantly abolished the effect of ISO on the phosphorylated MAPK and the binding activity of NF-κB, suggesting that MAPK and NF-κB are essential for TMS-mediated protection against ISO-induced cardiac hypertrophy. In agreement with our results, resveratrol, a TMS analog, has been reported to possess a significant cardioprotective effect against Ang-II-induced cardiac hypertrophy through the inhibition of MAPK (Cheng *et al.*, 2004). NF-κB inhibition was shown to ameliorate myocardial hypertrophy in response to aortic banding, ISO and chronic infusion of Ang-II (Kawano *et al.*, 2005; Hu *et al.*, 2015).

To reiterate, our findings may cast light on the role of CYP1B1 in the development of cardiac hypertrophy and indicate that CYP1B1 can serve as a novel target in the treatment of heart diseases. Such observations will raise the potential of having selective inhibitors of this enzyme to be used clinically in the treatment of cardiovascular diseases.

4.5. 2-Methoxyestradiol protects against pressure overload-induced left ventricular hypertrophy

2ME is a naturally occurring metabolite resulting from the hydroxylation of estradiol to catechol estradiol by CYP1B1, followed by the methylation of catechol estradiol by COMT. 2-ME has been shown to protect the heart and blood vessels from pathological processes, particularly those involving vascular smooth muscle cells and cardiac fibroblast migration and proliferation (Barchiesi *et al.*, 2002). However, the role of 2ME in the treatment of cardiac hypertrophy is yet unknown (Tevaarwerk *et al.*, 2009). Therefore, the major impetus for the present study was to determine the effects, if any, of 2ME on cardiac hypertrophy induced by the AAC model and explore the mechanism(s) involved.

Initially, AAC was used as a model of cardiac hypertrophy because it is more clinically relevant and similar to the human form of the disease since the hypertrophy is developed over a relatively longer period of time (Ni *et al.*, 2011). Although the induction of cardiac hypertrophy surgically using the AAC model was associated with an increase in the left ventricular wall thickness in addition to the presence of fibrosis, systolic and diastolic

functions were not significantly changed. This is not surprising since significant cardiac dysfunction occurs within 6-10 weeks in the AAC model (Ni *et al.*, 2011). Furthermore, the presence of fibrosis has been reported in the hypertrophic heart with normal cardiac function (Siddiq *et al.*, 1996; Matsui *et al.*, 2004; Qi *et al.*, 2011). The delivery of 2ME by osmotic pumps at 5 mg/kg/day used in the current study was selected based on previous studies and comparable with a dose of 25 mg/kg/day given daily gavage in the absence of toxicity (Brahn *et al.*, 2008; Plum *et al.*, 2009).

In the current study, the induction of cardiac hypertrophy surgically using the AAC model was evidenced by the following facts: first, the increase in the LV mass and HW/TL ratio; second, thickening of the ventricular wall parameters LVPWs, LVPWd, IVSD, and IVSs; third, the induction of fibrotic and apoptotic markers; and fourth: histopathological investigation into cardiac tissues revealed the presence of fibrosis in the hearts of AAC rats. These results are in agreement with the finding of other investigators who have reported that AAC induced thickening of the left ventricular morphology and fibrosis (Siddiq *et al.*, 1996; Doggrell *et al.*, 1998).

The first novel finding of the present study was that 2ME exerts protective effects against ventricular hypertrophy induced by AAC surgery as evident by the ability of 2ME to restore the changes of all cardiac hypertrophic and fibrotic parameters. Supporting this view was the finding that 2ME diminishes hypertension and associated coronary hypertrophy in ovariectomized spontaneously hypertensive rats and prevents DOCA-salt–induced hypertension in male rats (Bonacasa *et al.*, 2008; Yuan *et al.*, 2013). Furthermore, 2ME has been shown to inhibit cardiac fibroblast development and aortic smooth muscle cell growth (Dubey *et al.*, 1998). Although our result suggests a direct antihypertrophic effect of 2ME against AAC-induced cardiac hypertrophy, the effect of 2ME on blood pressure could potentially contribute to the changes in cardiac hypertrophy as AAC is known to induce cardiac hypertrophy through the increase in blood pressure. Also, 2ME was able to significantly decrease the level of pressure gradient-increased by AAC.

The interesting element revealed by this study was the unique inhibition of CYP1B1 and its associated cardiotoxic mid-chain HETE metabolites by 2ME in AAC cardiac tissues suggesting a CYP1B1/mid-chain HETE-dependent mechanism. The importance of this finding has been inspired by the fact that CYP1B1 cuts both ways as it does not only catalyze the formation of cardiotoxic metabolites but it also metabolizes substrates, like estradiol, into 2ME which could exert cardioprotective effects. Therefore, repurposing 2ME to modulate CYP1B1-mediated AA metabolism could prove to be a more selective and effective strategy, comparable to its conventional inhibitor, TMS. This is supported by the previous finding demonstrating that TMS enhances Ang II-induced rise in systolic blood pressure in Cyp1b1$_{(+/+)}$ female mice. Unlike TMS, 2ME protects against Ang II-induced hypertension and oxidative stress in Cyp1b1$_{(-/-)}$ female mice (Jennings *et al.*, 2014a). Being that 2ME has few or no feminizing effects, it could also be used to treat cardiovascular disease in males (Dantas *et al.*, 2006).

Another important finding of the present study that may have a significant clinical ramification is the ability of 2ME to inhibit the protein level of 12-LOX whereas it significantly increased the expression of the COX-2 enzyme. Activation of COX-2 or inhibition of 12-LOX has an important impact in the maintenance of cardiovascular health probably through the synthesis of cardioprotective prostaglandins or the decrease in the formation of cardiotoxic HETEs. Consistent with our finding, it has been reported that 2ME mediated vasoprotection and inhibited smooth muscle cell growth through the upregulation of COX-2 (Barchiesi *et al.*, 2006; Barchiesi *et al.*, 2010).

The mechanism(s) by which 2ME exerts its cardioprotective effects seems to be independent of the classical genomic estrogen receptor. However, the exact mechanism is yet unknown and unsuspected. Therefore, the second objective of the current study was to elucidate the mechanism(s) by which 2ME exerts its cardioprotective effects. For this purpose, the large-scale analysis of proteins, proteomics, was performed to provide a holistic understanding of the molecular and cellular mechanisms involved in the cardioprotective effect of 2ME. The importance of proteomics relies on the fact that that

the final product of a gene is fundamentally more multifaceted and closer to function than the gene itself (Pandey *et al.*, 2000).

The present study depicts for the first time a comprehensive list of the proteins involved in the protective effect of 2ME against cardiac hypertrophy induced by AAC. Initially, our proteomic data confirmed the cardiac hypertrophy induced in response to AAC. This is because AAC group has shown a significant increase in the expression of the hypertrophic protein, ADP-ribosylhydrolase-like 1, in addition to the fibrotic protein, Galectin-1. Recently, ADP-ribosylhydrolase-like 1 has been reported to be essential for heart chamber outgrowth (Smith *et al.*, 2016) whereas, Galectin-1 is an important marker of cardiac fibrosis and both were associated with an increased risk for incident heart failure (Song *et al.*, 2015a).

Consistent with echocardiography, the antihypertrophic effect of 2ME was accompanied with a substantial increase in the expression of the cardioprotective proteins FAM65B and Vinculin. Down-regulation of FAM65B protein expression was shown to induce muscle abnormalities and high mortality (Balasubramanian *et al.*, 2014), whereas a defect in vinculin protein expression has been reported in obstructive hypertrophic cardiomyopathy (Vasile *et al.*, 2006). Furthermore, the anti-fibrotic effect of 2ME against AAC induced cardiac fibrosis was associated with an exclusive increase in the expression of anti-inflammatory and anti-fibrotic proteins. This is not surprising since 2-ME has been shown to inhibit serum-induced proliferation and collagen synthesis in rat cardiac fibroblasts (Dubey *et al.*, 2004).

Hypertrophy and apoptosis both propel the heart towards severe dilation and heart failure. Hypertrophic stress signals impact cardiomyocyte apoptosis at different levels, the consequence of which is cell survival promotion (Hayakawa *et al.*, 2003). Consistent with this notion, our proteomic data showed that pro-apoptotic proteins, like dynamin-1-like protein and P38 MAPK were significantly reduced in the hypertrophic cardiac tissues. Of particular interest, 2ME seems to have a salutary effect by supporting cell survival through a massive inhibition of P38 MAPK and the increase in the expression of ERK1/2. This may

explain, at least in part, the protective effect of 2ME since heart failure results from disturbing the balance between cell survival and apoptotic signals (van Empel *et al.*, 2005). Furthermore, 2ME has been shown previously to increase the activity of ERK1/2 (Brown *et al.*, 2001) in vitro probably through a novel 7-transmembrane G-protein coupled receptor, GPR30 (Prossnitz *et al.*, 2007).

The heart is the most metabolically demanding organ in the body, acting as an omnivore using a variety of energy substrates to continually generate ATP (Lopaschuk *et al.*, 2010). Upon analysis of protein mapping, it is feasible to determine that the most predominantly affected proteins are those involved in various stages of the cardiac metabolic machinery. Hypertrophied cardiac tissues in the present study were associated with a substantial decrease in the protein expression of many enzymes involved in fatty acid oxidation. Our findings are typically consistent with the previous reports demonstrating an inhibition of fatty acid oxidation during cardiac hypertrophy (Desvergne *et al.*, 2006; Lopaschuk *et al.*, 2010). Of particular interest, the anti-hypertrophic effect of 2ME was associated with an inhibition of pyruvate dehydrogenase kinase which may increase the reliance of myocardium on glucose as a source of energy at the expense of fatty acid oxidation. This particular novel finding is of great importance since a plethora of studies have shown that increased ATP supplied from glucose oxidation constitutes a bona fide therapeutic device in the treatment of cardiac hypertrophy and heart failure (Piao *et al.*, 2010; Atherton *et al.*, 2011).

Overweight and obesity increase risks for cardiovascular disease and are associated with many cardiac implications such as hypertension, heart failure, and sudden death (Barchiesi *et al.*, 2006). In the current study, treatment with 2-ME significantly reduced the body weight in both sham and AAC rats. In agreement with our results, weight loss was observed previously, but this disappeared rapidly with cessation of 2ME (Dingli *et al.*, 2002). Furthermore, 2ME was shown to exert cardioprotective effects in part via the reduction of body weight (Barchiesi *et al.*, 2006). Since 2ME treatment was not associated with any sign of toxicity, we speculate that the weight reduction may be due to an indirect increase in proteins involved in glucose oxidation. In addition, 2ME has been reported to improve

glucose tolerance via increasing muscle consumption of glucose and reduction of fat and cholesterol levels which subsequently prevents weight gain (Sibonga *et al.*, 2003; Yorifuji *et al.*, 2011). 2-Hydroxyestradiol, precursor of 2ME, was shown to reduce weight gain in obese ZSF1 rats at least in part by suppressing appetite (Tofovic *et al.*, 2001). Also, the previous finding has prompted us to investigate the effect of 2ME on diabetes- and obesity-induced cardiomyopathy.

A wealth of information suggests the involvement of oxidative stress in the pathogenesis of cardiac hypertrophy which stresses the importance of unravelling the factors involved in providing protection against noxious ROS (Maulik *et al.*, 2012). In this context, we have demonstrated that AAC significantly inhibited the protein expression of many antioxidant enzymes such as NADH-ubiquinone oxidoreductase. On the other hand, the beneficial effect of 2ME in AAC-induced cardiac hypertrophy may be partly due to an increase in the protein expression of glutathione S-transferase and ferritin heavy chain. Our results are in agreement with the previous observation showing that 2ME is a potent antioxidant (Seeger *et al.*, 1997) and displayed antihypertensive effects in spontaneously hypertensive rats, primarily by inhibiting the generation of superoxide anion (Bonacasa *et al.*, 2008).

In light of the information described above, our results suggest a direct evidence for the protective effect of 2ME against pressure-overload-induced cardiac hypertrophy. This raises the question of whether or not 2ME has a direct antihypertrophic effect in the cardiac cells. For this purpose, we examined the ability of 2ME to inhibit cellular hypertrophy induced by ISO using the RL-14 cell line. Treatment of RL-14 cells with 2ME significantly reduced the ISO-mediated cellular hypertrophy as evidenced by a decrease in the expression of hypertrophic markers and cell surface area therefore suggesting a direct antihypertrophic effect of 2ME.

Mechanistically, we have shown in vivo that 2ME mediates its protective effect, at least in part, through the modulation of antioxidant, anti-inflammatory and MAPK proteins. In vitro, we have demonstrated the effect of 2ME on ISO-mediated effect on superoxide anion and MAPK in addition to NF-κB, a pivotal intracellular mediator of the inflammatory

response. Consistent with our in vivo findings, the protective effect of 2ME against ISO-induced cellular hypertrophy was mediated through the inhibition of superoxide anion, P38 and NF-κB binding activity. This agrees with previous observation showing that 2ME exerts protective effects through the inhibition of reactive oxygen species and inflammatory mediators (Kumar *et al.*, 2003; Bonacasa *et al.*, 2008; Chen *et al.*, 2014). In a manner similar to what was observed in vivo, 2ME normalizes the ISO-mediated inhibition of p-ERK1/2 protein in vitro. Similarly, 2ME has been shown previously to increase the activity of ERK1/2 (Brown *et al.*, 2001) in vitro, probably through a novel 7-transmembrane G-protein coupled receptor, GPR30 (Prossnitz *et al.*, 2007).

To reiterate, our results may shed light on the role of CYP1B1 and its associated mid-chain HETE metabolites in the development of cardiac hypertrophy and suggest that CYP1B1 could be used as a novel target in the treatment of pressure overload-induced cardiac hypertrophy. Such observation may provide the potential of repurposing 2ME as a selective CYP1B1 inhibitor for the treatment of heart failure and, therefore, introducing a new paradigm into the current pharmacopoeia using estrogenic metabolites as promising candidates to treat cardiovascular diseases.

4.6. Summary and general conclusions

HF patients still have a poor prognosis, despite early diagnosis and aggressive medical management (Roger, 2013). Most HF patients have a history of hypertension and left ventricular hypertrophy (Gradman *et al.*, 2006). Understanding the molecular basis of cardiac hypertrophy is an often ignored but significant facet for identifying the best treatment of the HF (Gradman *et al.*, 2006). Another important nonischemic idiopathic HF cause is drug-induced cardiomyopathy such as DOX-induced cardiotoxicity (Minotti *et al.*, 2004). CYP enzyme mediating the formation of mid-chain HETEs has been shown to play a role in the pathogenesis of cardiovascular diseases (Nozawa *et al.*, 1990; Cyrus *et al.*, 1999; Jenkins *et al.*, 2009). Therefore, this work has been focused on exploring the role of CYP and CYP-mediated formation of mid-chain HETE metabolites in cardiac hypertrophy and DOX-induced HF.

In the present work, we have demonstrated the ability of 5-, 8-, 12- and 15-HETE to induce cellular hypertrophy. Our results showed that 5-, 8-, 12- and 15-HETE significantly induced cellular hypertrophy in RL-14 cells as evidenced by the induction of cardiac hypertrophic markers α- and β-myocin heavy chain and atrial and brain natriuretic peptide in addition to the increase in cell surface area. Mechanistically, 5-, 8-, 12- and 15-HETE were able to induce the binding activity of NF-κB to its responsive element and they significantly induced the phosphorylation of ERK1/2. Mid-chain HETEs caused a proportional increase in the formation of dihydroxyeicosatrienoic acids parallel to the induction of soluble epoxide hydrolase enzyme activity. The induction of cellular hypertrophy in response to mid-chain HETEs may suggest a crucial role of these metabolites in the development and progression of cardiac hypertrophy and subsequently HF.

To assess the involvement of mid-chain HETE metabolites in DOX-induced HF, we investigated whether inhibition of mid-chain HETE metabolites formation using TMS protects against DOX-induced HF. Furthermore, we examined the effect of TMS treatment on enzymes involved in the formation of mid-chain HETE metabolites. We have demonstrated that DOX induced cardiotoxicity in vivo and in vitro as evidenced by

deleterious changes in echocardiography, histopathology, and hypertrophic markers. Importantly, the TMS significantly reversed these changes. Moreover, the DOX-induced cardiotoxicity was associated with a proportional increase in the formation of cardiac mid-chain HETEs both in vivo and in RL-14 cells. Interestingly, the inhibition of cardiotoxicity by TMS was associated with a dramatic decrease in the formation of cardiac mid-chain HETEs suggesting a mid-chain HETEs-dependent mechanism. Mechanistically, the protective effect of TMS against DOX-induced cardiotoxicity was mediated through the inhibition of MAPK and NF-κB. In light of the information described above, inhibition of formation mid-chain HETEs could be considered a potential therapeutic target in the progression of DOX-induced HF.

In an attempt to explore the involvement of mid-chain HETE metabolites in cardiac hypertrophy progression, we investigated the ability of ISO to induce cardiac hypertrophy through a mid-chain HETEs-dependent mechanism. Our results showed that ISO-induced CYP1B1 protein expression and the level of cardiac mid-chain HETEs in vivo at pre-hypertrophic, 12 h, and hypertrophic stage, 72 h. In vitro, inhibition of CYP1B1 using TMS or CYP1B1-siRNA significantly attenuates ISO-induced hypertrophy. Furthermore, overexpression of CYP1B1 significantly induced cellular hypertrophy and mid-chain HETE metabolites. Mechanistically, the protective effect of TMS against cardiac hypertrophy was mediated through the modulation of superoxide anion, MAPK and NF-κB. Our findings may cast light on the role of CYP1B1 in the development of cardiac hypertrophy and indicate that CYP1B1 can serve as a novel target in the treatment of heart diseases. Such observations will raise the potential of having selective inhibitors of this enzyme to be used clinically in the treatment of cardiovascular diseases.

In contrast to the negative effects of the cardiotoxic metabolites generated by CYP1B1, CYP1B1 also has an important role in the formation of cardioprotective metabolites such as 2ME. Therefore, we have investigated whether 2ME would prevent cardiac hypertrophy induced by ACC. Our results showed that 2ME significantly inhibited AAC-induced left ventricular hypertrophy. The antihypertrophic effect of 2ME was associated with a significant inhibition of CYP1B1 and mid-chain HETEs. Based on proteomics data, the

protective effect of 2ME is linked to the induction of antioxidant and anti-inflammatory proteins in addition to the modulation of proteins involved in myocardial energy metabolism. In vitro, 2ME has shown a direct antihypertrophic effect through the modulation of superoxide radical, MAPK and NF-κB. Our findings may provide the potential for repurposing 2ME as a selective CYP1B1 inhibitor for the treatment of heart failure.

4.7. Future Research Directions

The results of the present work have highlighted the cardiotoxic effect of mid-chain HETE metabolites and the role of CYP1B1 enzyme in the initiation and progression of cardiac hypertrophy and DOX-induced HF. However, further studies need to be conducted in order to translate this research into clinical practice.

1- To examine whether 5-, 8-, 12- and 15-HETE accelerate the progression from compensated to decompensated cardiac hypertrophy.

Rationale: Studies from our lab and others have reported the role of mid-chain HETE metabolites in the development of cardiac hypertrophy and HF (Jennings *et al.*, 2010; Jennings *et al.*, 2012b). Mid-chain HETEs were shown to induce cellular hypertrophy (Maayah *et al.*, 2015b; Maayah *et al.*, 2015c; Maayah *et al.*, 2015d). However, to investigate their role in HF, we need to test their ability to accelerate the progression of cardiac hypertrophy to HF.

Approach: We will examine whether mid-chain-HETEs accelerate the progression of cardiac hypertrophy to HF. Therefore, ISO-treated (5 mg/kg/day i.p.) and AAC rats will be randomized to receive vehicle or 5-, 8-, 12-, 15-HETE at an infusion rate of 1 mg/kg/day after one week of ISO treatment or 4 weeks for AAC model. After that, the animals are to be euthanized after one week of treatment with mid-chain HETEs for ISO model or 4 weeks of treatment with mid-chain HETEs for AAC model and the hearts will be excised. Assessment of cardiac hypertrophy and HF in addition to the level of AA metabolites will be performed using echocardiography and LC-ESI-MS, respectively.

Anticipated outcome: These studies will provide a novel role of mid-chain HETE metabolites in the progression of cardiac hypertrophy. The inability of mid-chain HETE metabolites to accelerate the progression of established cardiac hypertrophy to HF may

specify their role for the development of compensated but not decompensated cardiac hypertrophy.

2- To explore whether the inhibition of mid-chain HETEs formation could reverse or prevent the progression (to decompensated) of established cardiac hypertrophy.

Rationale: Several studies have demonstrated that inhibition of mid-chain HETEs formation using TMS, a selective CYP1B1 inhibitor, prevented both Ang-II- and deoxycorticosterone-induced hypertension and cardiac hypertrophy (Jennings *et al.*, 2010; Jennings *et al.*, 2012b). However, whether the inhibition of mid-chain HETEs formation using the TMS would reverse or prevent the progression of cardiac hypertrophy to HF still needs further investigation.

Approach: We will examine whether inhibiting the formation of mid-chain HETE metabolites using TMS (300 μg/kg, i.p.) can reverse or prevent the progression of established cardiac hypertrophy to HF. Therefore, ISO-treated (5 mg/kg/day i.p.) and AAC rats will be randomized to receive vehicle or TMS (300 μg/kg, i.p.) after one week of ISO treatment or 4 weeks for the AAC model. Thereafter, the animals are to be euthanized after one week of treatment with TMS (for ISO model) or 4 weeks of treatment with TMS (for AAC model) and the hearts will be excised. Assessment of cardiac hypertrophy and HF in addition to the level of AA metabolites will be performed using echocardiography and LC-ESI-MS, respectively.

Anticipated outcome: These studies will provide the first evidence that the inhibition of mid-chain HETEs forming enzymes confers cardioprotection against HF. The inability of the inhibition of mid-chain HETEs forming enzymes to prevent the progression of established cardiac hypertrophy to HF may specify their effectiveness for the prevention but not for the treatment of cardiac hypertrophy.

3- To determine which regiospecific mid-chain HETEs induce cardiac hypertrophy in vitro and in vivo and (4-) mediate the progression from compensated to decompensated cardiac hypertrophy.

Rationale: We have demonstrated previously that racemic mixture of mid-chain HETE metabolites induced cellular hypertrophy. However, mid-chain HETEs have a hydroxyl

moiety in the S- and R-configuration and may be formed in vivo as S and R isomers. Both S- and R-isomers of mid-chain HETE metabolites exhibit a distinct functional activity. For example, unlike 12(R)-HETE, 12(S)-HETE was shown to induce cellular hypertrophy in vascular smooth muscle cells (Reddy *et al.*, 2002). However, the role of regiospecific mid-chain HETEs on the development of cardiac hypertrophy has never been investigated before.

Approach: To examine whether S and/or R isomers of mid-HETEs is involved in the development of cardiac hypertrophy, the effect of S and R isomers of 5-, 8-, 12-, 15-HETE on the cellular hypertrophy will be determined. For this purpose, adult rat cardiomyocytes will be treated with increasing concentrations of S and R isomers of 5-, 8-, 12-, 15-HETE (1-10 µM) for 24, 48 and 72 h. Thereafter, only the isomer that induces hypertrophy in vitro will be tested in vivo by treating rats with the selected isomer (1 mg/kg/day, by the miniosmotic pump) for 7 days. Thereafter, the animals will be euthanized at 24 h after the last treatment, and the hearts will be excised. Also, we will examine whether the isomers of mid-chain-HETEs accelerate the progression of cardiac hypertrophy to HF. The isomers that induced hypertrophy in vitro and in vivo will be selected. Thereafter, isoproterenol-treated and AAC rats will be randomized to receive vehicle or selected isomers of mid-chain-HETEs at an infusion rate of (1 mg/kg, via mini-osmotic pump) after 1 week of ISO treatment (5 mg/kg/day i.p.) or 4 weeks for AAC model. Thereafter, the animals are to be euthanized after 1 week of treatment with mid-chain HETEs for ISO model or 4 weeks of treatment with mid-chain HETEs for AAC model and the hearts will be excised. Assessment of cardiac hypertrophy and HF in addition to the level of AA metabolites will be performed using echocardiography and LC-ESI-MS, respectively.

Anticipated outcome: These studies will determine a specific isomer of mid-chain HETE metabolites involved in the development of cardiac hypertrophy and could be used as a novel specific target for the treatment of cardiac hypertrophy. The inability of the tested isomers to initiate or accelerate cardiac hypertrophy may suggest that these metabolites may contribute to the pathogenesis of cardiac hypertrophy when they are in a racemic mixture but are not as stereoisomers.

5- To determine which regiospecific mid-chain HETEs are involved in DOX-induced cardiotoxicity.

Rationale: We have demonstrated previously that DOX-induced cardiotoxicity through a mid-chain HETEs-dependent mechanism (Maayah *et al.*, 2016b). However, the specific regioisomers of mid-chain HETEs involved in the DOX-induced cardiotoxicity have never been investigated before.

Approach: Rats will be treated with a cumulative dose of DOX (15 mg/kg) divided into five injections within 2 weeks. Thereafter, the animals are to be euthanized after 14 days of treatment with DOX. Assessment of DOX-induced cardiotoxicity in addition to the level of regiospecific mid-chain HETEs metabolite will be performed using echocardiography and LC-ESI-MS, respectively.

Anticipated outcome: These studies will provide a specific isomer of mid-chain HETEs metabolite involved in the development of DOX-induced cardiotoxicity and could be used as a novel specific target for the treatment of DOX-induced cardiotoxicity. The inability of DOX to increase the level of any specific isomer of mid-chain HETEs metabolite may suggest that these metabolites may contribute to the DOX-induced cardiotoxicity when they are in a racemic mixture but not as stereoisomers.

6- To explore the mechanisms by which cardiac hypertrophy causes alterations in CYP expression and mid-chain HETE metabolites formation.

Rationale: We have shown that ISO- and AAC-induced cardiac hypertrophy were associated with a significant increase in the expression and the activity of CYP enzymes. However, the exact mechanism by which cardiac hypertrophy alters the expression and the activity of CYP enzymes are still unknown. Approach: Rats will be treated with ISO (5 mg/kg/day i.p.) or subjected to ACC. Thereafter, the animals are to be euthanized after 1 week of treatment with ISO model or 4 weeks for AAC model, and the hearts will be excised. Assessment of cardiac hypertrophy and HF in addition to the level of AA metabolites will be performed using echocardiography and LC-ESI-MS, respectively. Also, proteomics will be performed using in-gel digestion and LC-MS/MS analysis to determine the effect of cardiac hypertrophy on proteins involved in the regulation of CYPs' enzyme and the obtained results will be confirmed using western blot analysis.

Anticipated outcome: These studies will provide a specific mechanism by which cardiac hypertrophy modulate the expression of CYPs' enzyme.

7- To examine the ability of 2ME to prevent the progression of cardiac hypertrophy to HF in vivo in rats.

Rationale: 2-ME has been shown to protect the heart and blood vessels from pathological processes, particularly those involving vascular smooth muscle cells and cardiac fibroblasts migration and proliferation (Barchiesi *et al.*, 2002). Furthermore, we have shown that 2ME protected against AAC-induced left ventricular hypertrophy (Maayah *et al.*, 2018). However, 2ME would be able to prevent the progression of cardiac hypertrophy to HF has never been investigated before.

Approach: We will also examine whether 2ME metabolite (5 mg/kg, via mini-osmotic pump) can reverse or prevent the progression of established cardiac hypertrophy to HF. Therefore, ISO-treated and AAC rats will be randomized to receive vehicle or 2ME (5 mg/kg, via mini-osmotic pump) after 1 week of ISO treatment (5 mg/kg/day i.p.) or 4 weeks for AAC model. Thereafter, the animals are to be euthanized after 1 week of treatment with 2ME for ISO model or 4 weeks of treatment with 2ME for AAC model and the hearts will be excised. Assessment of cardiac hypertrophy and HF in addition to the level of AA metabolites will be performed using echocardiography and LC-ESI-MS, respectively.

Anticipated outcome: These studies will provide the first evidence that 2ME metabolite confers cardioprotection against HF. The inability of 2ME to prevent the progression of established cardiac hypertrophy to HF may specify its effectiveness for the prevention but not for the treatment of cardiac hypertrophy.

8- To investigate the effect of 2ME on DOX-induced cardiotoxicity.

Rationale: We have demonstrated previously that DOX-induced cardiotoxicity through mid-chain HETEs dependent mechanism (Maayah *et al.*, 2016b). Also, 2ME was able to protect against cardiac hypertrophy, at least in part, through the inhibition of mid-chain HETEs metabolite. Taken together, the possibility that 2ME would protect against DOX-induced cardiotoxicity has never been investigated before and could not be ruled out.

Approach: We will examine whether 2ME metabolite (5 mg/kg, via mini-osmotic pump) can prevent the DOX-induced cardiotoxicity. Therefore, rats will be treated with a cumulative dose of DOX (15 mg/kg) divided into five injections within 2 weeks in the presence and absence of vehicle or 2ME (5 mg/kg, via mini-osmotic pump). On day 15, the animals are to be euthanized, and the hearts will be excised. Assessment of cardiotoxicity in addition to the level of AA metabolites will be performed using echocardiography and LC-ESI-MS, respectively.

Anticipated outcome: These studies will provide the first evidence that 2ME metabolite confers cardioprotection against DOX-induced cardiotoxicity.

9- To investigate whether the effect of 2ME on body weight is involved in its cardioprotective effect using the model of diabetes- and obesity-induced cardiomyopathy. **Rationale:** we have shown that 2-ME significantly reduced the body weight in both sham and AAC rats (Maayah *et al.*, 2018). This finding was associated with the ability of 2ME to increase the expression of proteins involved in glucose oxidation. Furthermore, 2ME has been reported to improve glucose tolerance via increasing muscle consumption of glucose and reduction of fat and cholesterol levels which subsequently prevents weight gain (Sibonga *et al.*, 2003; Yorifuji *et al.*, 2011). However, to investigate whether the effect of 2ME on body weight is beneficial, we need to test its ability to protect against diabetes- and obesity-induced cardiomyopathy. **Approach:** Rats (n= 18) will be fed ad libitum for 12 weeks with a high-fat diet (HFD) (45% kcal fat, 35% kcal carbohydrate, 0.05% w/w cholesterol). After 12 weeks of HFD feeding, rats will be fasted for 5 h and injected with a single dose of streptozotocin (90 mg/kg i.p., freshly prepared solution in 0.1 mmol/L sodium citrate, pH 5.5). One week later, rats will be stratified by glucose and body weight and will be randomized to three groups that will be maintained on the HFD. Two groups will be injected once daily with vehicle or 2ME metabolite (5 mg/kg, via mini-osmotic pump). Rats will be fasted for 4 h prior to euthanizing. Assessment of cardiomyopathy and the level of AA metabolites will be performed using echocardiography and LC-ESI-MS, respectively. Body composition and fat mass will be assessed using an EchoMRI quantitative nuclear magnetic resonance system (Echo Medical Systems, Houston, TX). Oral glucose tolerance tests will be performed after an overnight fast

Anticipated outcome: These studies will provide the first evidence that 2ME metabolite confers cardioprotection against diabetes- and obesity-induced cardiomyopathy. The inability of 2ME to treat diabetes- and obesity-induced cardiomyopathy may suggest that its effect on the body weight does not contribute to cardioprotection and might be considered as an adverse effect due to anorexia.

REFERENCES

Abad MJ, de las Heras B, Silvan AM, Pascual R, Bermejo P, Rodriquez B*, et al.* (2001). Effects of furocoumarins from Cachrys trifida on some macrophage functions. *The Journal of pharmacy and pharmacology* **53**(8)**:** 1163-1168.

Aboutabl ME, El-Kadi AO (2007). Constitutive expression and inducibility of CYP1A1 in the H9c2 rat cardiomyoblast cells. *Toxicology in vitro : an international journal published in association with BIBRA* **21**(8)**:** 1686-1691.

Aboutabl ME, Zordoky BN, El-Kadi AO (2009). 3-methylcholanthrene and benzo(a)pyrene modulate cardiac cytochrome P450 gene expression and arachidonic acid metabolism in male Sprague Dawley rats. *British journal of pharmacology* **158**(7)**:** 1808-1819.

Aguiar M, Masse R, Gibbs BF (2005). Regulation of cytochrome P450 by posttranslational modification. *Drug Metab Rev* **37**(2)**:** 379-404.

Ai D, Pang W, Li N, Xu M, Jones PD, Yang J*, et al.* (2009). Soluble epoxide hydrolase plays an essential role in angiotensin II-induced cardiac hypertrophy. *Proceedings of the National Academy of Sciences of the United States of America* **106**(2)**:** 564-569.

Akazawa H, Komuro I (2003). Roles of cardiac transcription factors in cardiac hypertrophy. *Circulation research* **92**(10)**:** 1079-1088.

Alhurani RE, Chahal CA, Ahmed AT, Mohamed EA, Miller VM (2016). Sex hormone therapy and progression of cardiovascular disease in menopausal women. *Clinical science* **130**(13)**:** 1065-1074.

Alonso-Galicia M, Falck JR, Reddy KM, Roman RJ (1999). 20-HETE agonists and antagonists in the renal circulation. *The American journal of physiology* **277**(5 Pt 2)**:** F790-796.

Alonso-Galicia M, Maier KG, Greene AS, Cowley AW, Jr., Roman RJ (2002). Role of 20-hydroxyeicosatetraenoic acid in the renal and vasoconstrictor actions of angiotensin II. *American journal of physiology. Regulatory, integrative and comparative physiology* **283**(1)**:** R60-68.

Alpert NR, Mulieri LA (1982). Heat, mechanics, and myosin ATPase in normal and hypertrophied heart muscle. *Federation proceedings* **41**(2)**:** 192-198.

Alsaad AM, Zordoky BN, El-Sherbeni AA, El-Kadi AO (2012). Chronic doxorubicin cardiotoxicity modulates cardiac cytochrome P450-mediated arachidonic acid metabolism in rats. *Drug metabolism and disposition: the biological fate of chemicals* **40**(11)**:** 2126-2135.

Alsaikhan B, Fahlman R, Ding J, Tredget E, Metcalfe PD (2015). Proteomic profile of an acute partial bladder outlet obstruction. *Canadian Urological Association journal = Journal de l'Association des urologues du Canada* **9**(3-4)**:** E114-121.

Althurwi HN, Elshenawy OH, El-Kadi AO (2014). Fenofibrate modulates cytochrome P450 and arachidonic acid metabolism in the heart and protects against isoproterenol-induced cardiac hypertrophy. *Journal of cardiovascular pharmacology* **63**(2)**:** 167-177.

Althurwi HN, Maayah ZH, Elshenawy OH, El-Kadi AO (2015). Early Changes in Cytochrome P450s and Their Associated Arachidonic Acid Metabolites Play a Crucial Role in the Initiation of Cardiac Hypertrophy Induced by Isoproterenol. *Drug metabolism and disposition: the biological fate of chemicals* **43**(8)**:** 1254-1266.

Althurwi HN, Tse MM, Abdelhamid G, Zordoky BN, Hammock BD, El-Kadi AO (2013). Soluble epoxide hydrolase inhibitor, TUPS, protects against isoprenaline-induced cardiac hypertrophy. *British journal of pharmacology* **168**(8)**:** 1794-1807.

Ambros V (2003). MicroRNA pathways in flies and worms: growth, death, fat, stress, and timing. *Cell* **113**(6)**:** 673-676.

Andrews NC, Faller DV (1991). A rapid micropreparation technique for extraction of DNA-binding proteins from limiting numbers of mammalian cells. *Nucleic acids research* **19**(9)**:** 2499.

Anker SD, Chua TP, Ponikowski P, Harrington D, Swan JW, Kox WJ*, et al.* (1997). Hormonal changes and catabolic/anabolic imbalance in chronic heart failure and their importance for cardiac cachexia. *Circulation* **96**(2)**:** 526-534.

Anwar-Mohamed A, El-Sherbeni A, Kim SH, Elshenawy OH, Althurwi HN, Zordoky BN*, et al.* (2013). Acute arsenic treatment alters cytochrome P450 expression and arachidonic acid metabolism in lung, liver and kidney of C57Bl/6 mice. *Xenobiotica; the fate of foreign compounds in biological systems* **43**(8)**:** 719-729.

Anzenbacher P, Anzenbacherova E (2001). Cytochromes P450 and metabolism of xenobiotics. *Cellular and molecular life sciences : CMLS* **58**(5-6)**:** 737-747.

Aragon AC, Kopf PG, Campen MJ, Huwe JK, Walker MK (2008). In utero and lactational 2,3,7,8-tetrachlorodibenzo-p-dioxin exposure: effects on fetal and adult cardiac gene expression and adult cardiac and renal morphology. *Toxicological sciences : an official journal of the Society of Toxicology* **101**(2)**:** 321-330.

Arai M, Imai H, Metori A, Nakagawa Y (1997). Preferential esterification of endogenously formed 5-hydroxyeicosatetraenoic acid to phospholipids in activated polymorphonuclear leukocytes. *European journal of biochemistry / FEBS* **244**(2)**:** 513-519.

Asakawa M, Takano H, Nagai T, Uozumi H, Hasegawa H, Kubota N*, et al.* (2002). Peroxisome proliferator-activated receptor gamma plays a critical role in inhibition of cardiac hypertrophy in vitro and in vivo. *Circulation* **105**(10)**:** 1240-1246.

Atherton HJ, Dodd MS, Heather LC, Schroeder MA, Griffin JL, Radda GK*, et al.* (2011). Role of pyruvate dehydrogenase inhibition in the development of hypertrophy in the hyperthyroid rat heart: a combined magnetic resonance imaging and hyperpolarized magnetic resonance spectroscopy study. *Circulation* **123**(22)**:** 2552-2561.

Awasthi S, Vivekananda J, Awasthi V, Smith D, King RJ (2001). CTP:phosphocholine cytidylyltransferase inhibition by ceramide via PKC-alpha, p38 MAPK, cPLA2, and 5-lipoxygenase. *American journal of physiology. Lung cellular and molecular physiology* **281**(1)**:** L108-118.

Bailey JM, Makheja AN, Lee R, Simon TH (1995). Systemic activation of 15-lipoxygenase in heart, lung, and vascular tissues by hypercholesterolemia: relationship to lipoprotein oxidation and atherogenesis. *Atherosclerosis* **113**(2)**:** 247-258.

Balasubramanian A, Kawahara G, Gupta VA, Rozkalne A, Beauvais A, Kunkel LM*, et al.* (2014). Fam65b is important for formation of the HDAC6-dysferlin protein complex during myogenic cell differentiation. *FASEB journal : official publication of the Federation of American Societies for Experimental Biology* **28**(7)**:** 2955-2969.

Bandiera S, Weidlich S, Harth V, Broede P, Ko Y, Friedberg T (2005). Proteasomal degradation of human CYP1B1: effect of the Asn453Ser polymorphism on the post-translational regulation of CYP1B1 expression. *Mol Pharmacol* **67**(2)**:** 435-443.

Barbieri A, Bursi F, Mantovani F, Valenti C, Quaglia M, Berti E*, et al.* (2012). Left ventricular hypertrophy reclassification and death: application of the Recommendation of the American Society of Echocardiography/European Association of Echocardiography. *European heart journal cardiovascular Imaging* **13**(1)**:** 109-117.

Barchiesi F, Jackson EK, Fingerle J, Gillespie DG, Odermatt B, Dubey RK (2006). 2-Methoxyestradiol, an estradiol metabolite, inhibits neointima formation and smooth muscle cell growth via double blockade of the cell cycle. *Circulation research* **99**(3)**:** 266-274.

Barchiesi F, Jackson EK, Gillespie DG, Zacharia LC, Fingerle J, Dubey RK (2002). Methoxyestradiols mediate estradiol-induced antimitogenesis in human aortic SMCs. *Hypertension* **39**(4)**:** 874-879.

Barchiesi F, Lucchinetti E, Zaugg M, Ogunshola OO, Wright M, Meyer M*, et al.* (2010). Candidate genes and mechanisms for 2-methoxyestradiol-mediated vasoprotection. *Hypertension* **56**(5)**:** 964-972.

Barouki R, Morel Y (2001). Repression of cytochrome P450 1A1 gene expression by oxidative stress: mechanisms and biological implications. *Biochem Pharmacol* **61**(5)**:** 511-516.

Barry SP, Davidson SM, Townsend PA (2008). Molecular regulation of cardiac hypertrophy. *The international journal of biochemistry & cell biology* **40**(10)**:** 2023-2039.

Baruffa G (1966). Clinical trials in Plasmodium falciparum malaria with a long-acting sulphonamide. *Transactions of the Royal Society of Tropical Medicine and Hygiene* **60**(2)**:** 222-224.

Basu NK, Kubota S, Meselhy MR, Ciotti M, Chowdhury B, Hartori M*, et al.* (2004). Gastrointestinally distributed UDP-glucuronosyltransferase 1A10, which metabolizes estrogens and nonsteroidal anti-inflammatory drugs, depends upon phosphorylation. *The Journal of biological chemistry* **279**(27)**:** 28320-28329.

Beedanagari SR, Bebenek I, Bui P, Hankinson O (2009). Resveratrol inhibits dioxin-induced expression of human CYP1A1 and CYP1B1 by inhibiting recruitment of the aryl hydrocarbon receptor complex and RNA polymerase II to the regulatory regions of the corresponding genes. *Toxicol Sci* **110**(1)**:** 61-67.

Beigneux AP, Moser AH, Shigenaga JK, Grunfeld C, Feingold KR (2002). Reduction in cytochrome P-450 enzyme expression is associated with repression of CAR (constitutive androstane receptor) and PXR (pregnane X receptor) in mouse liver during the acute phase response. *Biochemical and biophysical research communications* **293**(1)**:** 145-149.

Berenji K, Drazner MH, Rothermel BA, Hill JA (2005). Does load-induced ventricular hypertrophy progress to systolic heart failure? *American journal of physiology. Heart and circulatory physiology* **289**(1)**:** H8-H16.

Bergholte JM, Soberman RJ, Hayes R, Murphy RC, Okita RT (1987). Oxidation of 15-hydroxyeicosatetraenoic acid and other hydroxy fatty acids by lung prostaglandin dehydrogenase. *Archives of biochemistry and biophysics* **257**(2)**:** 444-450.

Bertilsson G, Heidrich J, Svensson K, Asman M, Jendeberg L, Sydow-Backman M*, et al.* (1998). Identification of a human nuclear receptor defines a new signaling pathway for CYP3A induction. *Proceedings of the National Academy of Sciences of the United States of America* **95**(21)**:** 12208-12213.

Bhattacharya N, Sarno A, Idler IS, Fuhrer M, Zenz T, Dohner H*, et al.* (2010). High-throughput detection of nuclear factor-kappaB activity using a sensitive oligo-based chemiluminescent enzyme-linked immunosorbent assay. *International journal of cancer. Journal international du cancer* **127**(2)**:** 404-411.

Bieche I, Narjoz C, Asselah T, Vacher S, Marcellin P, Lidereau R*, et al.* (2007). Reverse transcriptase-PCR quantification of mRNA levels from cytochrome (CYP)1, CYP2 and CYP3 families in 22 different human tissues. *Pharmacogenetics and genomics* **17**(9)**:** 731-742.

Bisognano JD, Weinberger HD, Bohlmeyer TJ, Pende A, Raynolds MV, Sastravaha A*, et al.* (2000). Myocardial-directed overexpression of the human beta(1)-adrenergic receptor in transgenic mice. *Journal of molecular and cellular cardiology* **32**(5)**:** 817-830.

Bolick DT, Orr AW, Whetzel A, Srinivasan S, Hatley ME, Schwartz MA*, et al.* (2005). 12/15-lipoxygenase regulates intercellular adhesion molecule-1 expression and monocyte adhesion to endothelium through activation of RhoA and nuclear factor-kappaB. *Arteriosclerosis, thrombosis, and vascular biology* **25**(11)**:** 2301-2307.

Bonacasa B, Sanchez ML, Rodriguez F, Lopez B, Quesada T, Fenoy FJ*, et al.* (2008). 2-Methoxyestradiol attenuates hypertension and coronary vascular remodeling in spontaneously hypertensive rats. *Maturitas* **61**(4)**:** 310-316.

Borgeat P, Picard S, Vallerand P, Sirois P (1981). Transformation of arachidonic acid in leukocytes. Isolation and structural analysis of a novel dihydroxy derivative. *Prostaglandins and medicine* **6**(6)**:** 557-570.

Brahn E, Banquerigo ML, Lee JK, Park EJ, Fogler WE, Plum SM (2008). An angiogenesis inhibitor, 2-methoxyestradiol, involutes rat collagen-induced arthritis and suppresses gene expression of synovial vascular endothelial growth factor and basic fibroblast growth factor. *The Journal of rheumatology* **35**(11)**:** 2119-2128.

Brash AR, Boeglin WE, Chang MS (1997). Discovery of a second 15S-lipoxygenase in humans. *Proceedings of the National Academy of Sciences of the United States of America* **94**(12)**:** 6148-6152.

Braz JC, Gregory K, Pathak A, Zhao W, Sahin B, Klevitsky R*, et al.* (2004). PKC-alpha regulates cardiac contractility and propensity toward heart failure. *Nature medicine* **10**(3)**:** 248-254.

Brezinski ME, Serhan CN (1990). Selective incorporation of (15S)-hydroxyeicosatetraenoic acid in phosphatidilinositol of human neutrophils: agonist-induced deacylation and transformation of stored hydroxyeicosanoids. *Proceedings of the National Academy of Sciences of the United States of America* **87**(16)**:** 6248-6252.

Brinckmann R, Schnurr K, Heydeck D, Rosenbach T, Kolde G, Kuhn H (1998). Membrane translocation of 15-lipoxygenase in hematopoietic cells is calcium-dependent and activates the oxygenase activity of the enzyme. *Blood* **91**(1)**:** 64-74.

Broselid S, Berg KA, Chavera TA, Kahn R, Clarke WP, Olde B*, et al.* (2014). G protein-coupled receptor 30 (GPR30) forms a plasma membrane complex with membrane-associated guanylate kinases (MAGUKs) and protein kinase A-anchoring protein 5 (AKAP5) that constitutively inhibits cAMP production. *The Journal of biological chemistry* **289**(32)**:** 22117-22127.

Brown JW, Kesler CT, Neary T, Fishman LM (2001). Effects of androgens and estrogens and catechol and methoxy-estrogen derivatives on mitogen-activated protein kinase (ERK(1,2)) activity in SW-13 human adrenal carcinoma cells. *Hormone and metabolic research = Hormon- und Stoffwechselforschung = Hormones et metabolisme* **33**(3)**:** 127-130.

Bueno OF, Wilkins BJ, Tymitz KM, Glascock BJ, Kimball TF, Lorenz JN*, et al.* (2002). Impaired cardiac hypertrophic response in Calcineurin Abeta -deficient mice. *Proceedings of the National Academy of Sciences of the United States of America* **99**(7)**:** 4586-4591.

Burhop KE, Selig WM, Malik AB (1988). Monohydroxyeicosatetraenoic acids (5-HETE and 15-HETE) induce pulmonary vasoconstriction and edema. *Circulation research* **62**(4)**:** 687-698.

Byrd BF, 3rd, Abraham TP, Buxton DB, Coletta AV, Cooper JH, Douglas PS, *et al.* (2015). A Summary of the American Society of Echocardiography Foundation Value-Based Healthcare: Summit 2014: The Role of Cardiovascular Ultrasound in the New Paradigm. *Journal of the American Society of Echocardiography : official publication of the American Society of Echocardiography* **28**(7)**:** 755-769.

Cabral M, Martin-Venegas R, Moreno JJ (2013). Role of arachidonic acid metabolites on the control of non-differentiated intestinal epithelial cell growth. *The international journal of biochemistry & cell biology* **45**(8)**:** 1620-1628.

Cantley LC (2002). The phosphoinositide 3-kinase pathway. *Science* **296**(5573)**:** 1655-1657.

Cao Z, Li Y (2004). Potent induction of cellular antioxidants and phase 2 enzymes by resveratrol in cardiomyocytes: protection against oxidative and electrophilic injury. *Eur J Pharmacol* **489**(1-2)**:** 39-48.

Capdevila J, Chacos N, Werringloer J, Prough RA, Estabrook RW (1981). Liver microsomal cytochrome P-450 and the oxidative metabolism of arachidonic acid. *Proceedings of the National Academy of Sciences of the United States of America* **78**(9)**:** 5362-5366.

Capdevila J, Yadagiri P, Manna S, Falck JR (1986). Absolute configuration of the hydroxyeicosatetraenoic acids (HETEs) formed during catalytic oxygenation of arachidonic acid by microsomal cytochrome P-450. *Biochemical and biophysical research communications* **141**(3)**:** 1007-1011.

Care A, Catalucci D, Felicetti F, Bonci D, Addario A, Gallo P, *et al.* (2007). MicroRNA-133 controls cardiac hypertrophy. *Nature medicine* **13**(5)**:** 613-618.

Carter GW, Young PR, Albert DH, Bouska J, Dyer R, Bell RL, *et al.* (1991). 5-lipoxygenase inhibitory activity of zileuton. *The Journal of pharmacology and experimental therapeutics* **256**(3)**:** 929-937.

Catalano A, Caprari P, Soddu S, Procopio A, Romano M (2004). 5-lipoxygenase antagonizes genotoxic stress-induced apoptosis by altering p53 nuclear trafficking. *FASEB journal : official publication of the Federation of American Societies for Experimental Biology* **18**(14)**:** 1740-1742.

Chabova VC, Kramer HJ, Vaneckova I, Vernerova Z, Eis V, Tesar V, *et al.* (2007). Effects of chronic cytochrome P-450 inhibition on the course of hypertension and end-organ damage in Ren-2 transgenic rats. *Vascular pharmacology* **47**(2-3)**:** 145-159.

Chan HY, Chen ZY, Tsang DS, Leung LK (2002). Baicalein inhibits DMBA-DNA adduct formation by modulating CYP1A1 and CYP1B1 activities. *Biomedicine & pharmacotherapy = Biomedecine & pharmacotherapie* **56**(6)**:** 269-275.

Chang I, Mitsui Y, Fukuhara S, Gill A, Wong DK, Yamamura S, *et al.* (2015). Loss of miR-200c up-regulates CYP1B1 and confers docetaxel resistance in renal cell carcinoma. *Oncotarget* **6**(10)**:** 7774-7787.

Chatterjee K, Zhang J, Honbo N, Karliner JS (2010). Doxorubicin cardiomyopathy. *Cardiology* **115**(2)**:** 155-162.

Chaturvedi S (2004). The Seventh Report of the Joint National Committee on Prevention, Detection, Evaluation, and Treatment of High Blood Pressure (JNC 7): is it really practical? *The National medical journal of India* **17**(4)**:** 227.

Chaudhary KR, Batchu SN, Seubert JM (2009). Cytochrome P450 enzymes and the heart. *IUBMB life* **61**(10)**:** 954-960.

Chen J, Hoffman BB, Isseroff RR (2002). Beta-adrenergic receptor activation inhibits keratinocyte migration via a cyclic adenosine monophosphate-independent mechanism. *The Journal of investigative dermatology* **119**(6)**:** 1261-1268.

Chen W, Cui Y, Zheng S, Huang J, Li P, Simoncini T, *et al.* (2015). 2-methoxyestradiol induces vasodilation by stimulating NO release via PPARgamma/PI3K/Akt pathway. *PloS one* **10**(3)**:** e0118902.

Chen XS, Kurre U, Jenkins NA, Copeland NG, Funk CD (1994). cDNA cloning, expression, mutagenesis of C-terminal isoleucine, genomic structure, and chromosomal localizations of murine 12-lipoxygenases. *The Journal of biological chemistry* **269**(19)**:** 13979-13987.

Chen YY, Yeh CH, So EC, Sun DP, Wang LY, Hsing CH (2014). Anticancer drug 2-methoxyestradiol protects against renal ischemia/reperfusion injury by reducing inflammatory cytokines expression. *BioMed research international* **2014:** 431524.

Cheng TH, Liu JC, Lin H, Shih NL, Chen YL, Huang MT*, et al.* (2004). Inhibitory effect of resveratrol on angiotensin II-induced cardiomyocyte hypertrophy. *Naunyn-Schmiedeberg's archives of pharmacology* **369**(2)**:** 239-244.

Choudhary D, Jansson I, Schenkman JB, Sarfarazi M, Stoilov I (2003). Comparative expression profiling of 40 mouse cytochrome P450 genes in embryonic and adult tissues. *Archives of biochemistry and biophysics* **414**(1)**:** 91-100.

Choudhary D, Jansson I, Stoilov I, Sarfarazi M, Schenkman JB (2004). Metabolism of retinoids and arachidonic acid by human and mouse cytochrome P450 1b1. *Drug metabolism and disposition: the biological fate of chemicals* **32**(8)**:** 840-847.

Choudhary D, Jansson I, Stoilov I, Sarfarazi M, Schenkman JB (2005). Expression patterns of mouse and human CYP orthologs (families 1-4) during development and in different adult tissues. *Archives of biochemistry and biophysics* **436**(1)**:** 50-61.

Chun YJ, Kim S, Kim D, Lee SK, Guengerich FP (2001). A new selective and potent inhibitor of human cytochrome P450 1B1 and its application to antimutagenesis. *Cancer research* **61**(22)**:** 8164-8170.

Chuturgoon AA, Phulukdaree A, Moodley D (2014). Fumonisin B(1) modulates expression of human cytochrome P450 1b1 in human hepatoma (Hepg2) cells by repressing Mir-27b. *Toxicology letters* **227**(1)**:** 50-55.

Claycomb WC, Lanson NA, Jr., Stallworth BS, Egeland DB, Delcarpio JB, Bahinski A*, et al.* (1998). HL-1 cells: a cardiac muscle cell line that contracts and retains phenotypic characteristics of the adult cardiomyocyte. *Proceedings of the National Academy of Sciences of the United States of America* **95**(6)**:** 2979-2984.

Conrad DJ, Kuhn H, Mulkins M, Highland E, Sigal E (1992). Specific inflammatory cytokines regulate the expression of human monocyte 15-lipoxygenase. *Proceedings of the National Academy of Sciences of the United States of America* **89**(1)**:** 217-221.

Conway DE, Sakurai Y, Weiss D, Vega JD, Taylor WR, Jo H*, et al.* (2009). Expression of CYP1A1 and CYP1B1 in human endothelial cells: regulation by fluid shear stress. *Cardiovascular research* **81**(4)**:** 669-677.

Cyrus T, Witztum JL, Rader DJ, Tangirala R, Fazio S, Linton MF*, et al.* (1999). Disruption of the 12/15-lipoxygenase gene diminishes atherosclerosis in apo E-deficient mice. *The Journal of clinical investigation* **103**(11)**:** 1597-1604.

Dahut WL, Lakhani NJ, Gulley JL, Arlen PM, Kohn EC, Kotz H*, et al.* (2006). Phase I clinical trial of oral 2-methoxyestradiol, an antiangiogenic and apoptotic agent, in patients with solid tumors. *Cancer biology & therapy* **5**(1)**:** 22-27.

Danielson PB (2002). The cytochrome P450 superfamily: biochemistry, evolution and drug metabolism in humans. *Current drug metabolism* **3**(6)**:** 561-597.

Dantas AP, Sandberg K (2006). Does 2-methoxyestradiol represent the new and improved hormone replacement therapy for atherosclerosis? *Circulation research* **99**(3)**:** 234-237.

Davidson MM (2007). Immortalization of human post-mitotic cells: Google Patents.

Dawling S, Roodi N, Parl FF (2003). Methoxyestrogens exert feedback inhibition on cytochrome P450 1A1 and 1B1. *Cancer research* **63**(12)**:** 3127-3132.

de Beer EL, Bottone AE, van Der Velden J, Voest EE (2000). Doxorubicin impairs crossbridge turnover kinetics in skinned cardiac trabeculae after acute and chronic treatment. *Molecular pharmacology* **57**(6)**:** 1152-1157.

DeForrest JM, Knappenberger RC, Antonaccio MJ, Ferrone RA, Creekmore JS (1982). Angiotensin II is a necessary component for the development of hypertension in the two kidney, one clip rat. *The American journal of cardiology* **49**(6)**:** 1515-1517.

Delozier TC, Kissling GE, Coulter SJ, Dai D, Foley JF, Bradbury JA*, et al.* (2007). Detection of human CYP2C8, CYP2C9, and CYP2J2 in cardiovascular tissues. *Drug metabolism and disposition: the biological fate of chemicals* **35**(4)**:** 682-688.

Deng S, Yan T, Jendrny C, Nemecek A, Vincetic M, Godtel-Armbrust U*, et al.* (2014). Dexrazoxane may prevent doxorubicin-induced DNA damage via depleting both topoisomerase II isoforms. *BMC cancer* **14:** 842.

Denison MS, Vella LM, Okey AB (1986). Structure and function of the Ah receptor for 2,3,7,8-tetrachlorodibenzo-p-dioxin. Species difference in molecular properties of the receptors from mouse and rat hepatic cytosols. *J Biol Chem* **261**(9)**:** 3987-3995.

Deschamps JD, Kenyon VA, Holman TR (2006). Baicalein is a potent in vitro inhibitor against both reticulocyte 15-human and platelet 12-human lipoxygenases. *Bioorganic & medicinal chemistry* **14**(12)**:** 4295-4301.

Desvergne B, Michalik L, Wahli W (2006). Transcriptional regulation of metabolism. *Physiological reviews* **86**(2)**:** 465-514.

Dewundara SS, Wiggs JL, Sullivan DA, Pasquale LR (2016). Is Estrogen a Therapeutic Target for Glaucoma? *Seminars in ophthalmology* **31**(1-2)**:** 140-146.

Dhanya BL, Swathy RP, Indira M (2014). Selenium downregulates oxidative stress-induced activation of leukotriene pathway in experimental rats with diabetic cardiac hypertrophy. *Biological trace element research* **161**(1)**:** 107-115.

Di Marco A, Gaetani M, Scarpinato B (1969). Adriamycin (NSC-123,127): a new antibiotic with antitumor activity. *Cancer chemotherapy reports* **53**(1)**:** 33-37.

Dingli D, Timm M, Russell SJ, Witzig TE, Rajkumar SV (2002). Promising preclinical activity of 2-methoxyestradiol in multiple myeloma. *Clinical cancer research : an official journal of the American Association for Cancer Research* **8**(12)**:** 3948-3954.

DiNicolantonio JJ, Fares H, Niazi AK, Chatterjee S, D'Ascenzo F, Cerrato E*, et al.* (2015). beta-Blockers in hypertension, diabetes, heart failure and acute myocardial infarction: a review of the literature. *Open heart* **2**(1)**:** e000230.

Doggrell SA, Brown L (1998). Rat models of hypertension, cardiac hypertrophy and failure. *Cardiovascular research* **39**(1)**:** 89-105.

Dolegowska B, Blogowski W, Kedzierska K, Safranow K, Jakubowska K, Olszewska M*, et al.* (2009). Platelets arachidonic acid metabolism in patients with essential hypertension. *Platelets* **20**(4)**:** 242-249.

Dolinsky VW, Chan AY, Robillard Frayne I, Light PE, Des Rosiers C, Dyck JR (2009). Resveratrol prevents the prohypertrophic effects of oxidative stress on LKB1. *Circulation* **119**(12)**:** 1643-1652.

Dolinsky VW, Rogan KJ, Sung MM, Zordoky BN, Haykowsky MJ, Young ME*, et al.* (2013). Both aerobic exercise and resveratrol supplementation attenuate doxorubicin-induced cardiac injury in mice. *American journal of physiology. Endocrinology and metabolism* **305**(2)**:** E243-253.

Doroshow JH, Akman S, Chu FF, Esworthy S (1990). Role of the glutathione-glutathione peroxidase cycle in the cytotoxicity of the anticancer quinones. *Pharmacology & therapeutics* **47**(3)**:** 359-370.

Dreyer C, Krey G, Keller H, Givel F, Helftenbein G, Wahli W (1992). Control of the peroxisomal beta-oxidation pathway by a novel family of nuclear hormone receptors. *Cell* **68**(5)**:** 879-887.

Dube P, Weber KT (2011). Congestive heart failure: pathophysiologic consequences of neurohormonal activation and the potential for recovery: part I. *The American journal of the medical sciences* **342**(5)**:** 348-351.

Dubey RK, Gillespie DG, Jackson EK, Keller PJ (1998). 17Beta-estradiol, its metabolites, and progesterone inhibit cardiac fibroblast growth. *Hypertension* **31**(1 Pt 2)**:** 522-528.

Dubey RK, Gillespie DG, Zacharia LC, Barchiesi F, Imthurn B, Jackson EK (2003). CYP450- and COMT-derived estradiol metabolites inhibit activity of human coronary artery SMCs. *Hypertension* **41**(3 Pt 2)**:** 807-813.

Dubey RK, Imthurn B, Jackson EK (2007). 2-Methoxyestradiol: a potential treatment for multiple proliferative disorders. *Endocrinology* **148**(9)**:** 4125-4127.

Dubey RK, Jackson EK (2009). Potential vascular actions of 2-methoxyestradiol. *Trends in endocrinology and metabolism: TEM* **20**(8)**:** 374-379.

Dubey RK, Jackson EK, Gillespie DG, Rosselli M, Barchiesi F, Krust A*, et al.* (2005). Cytochromes 1A1/1B1- and catechol-O-methyltransferase-derived metabolites mediate estradiol-induced antimitogenesis in human cardiac fibroblast. *The Journal of clinical endocrinology and metabolism* **90**(1)**:** 247-255.

Dubey RK, Tofovic SP, Jackson EK (2004). Cardiovascular pharmacology of estradiol metabolites. *The Journal of pharmacology and experimental therapeutics* **308**(2)**:** 403-409.

Dunn KM, Renic M, Flasch AK, Harder DR, Falck J, Roman RJ (2008). Elevated production of 20-HETE in the cerebral vasculature contributes to severity of ischemic stroke and oxidative stress in spontaneously hypertensive rats. *American journal of physiology. Heart and circulatory physiology* **295**(6)**:** H2455-2465.

Dwarakanath RS, Sahar S, Lanting L, Wang N, Stemerman MB, Natarajan R*, et al.* (2008). Viral vector-mediated 12/15-lipoxygenase overexpression in vascular smooth muscle cells

enhances inflammatory gene expression and migration. *Journal of vascular research* **45**(2)**:** 132-142.

Dyck JR, Lopaschuk GD (2006). AMPK alterations in cardiac physiology and pathology: enemy or ally? *The Journal of physiology* **574**(Pt 1)**:** 95-112.

Dzitoyeva S, Imbesi M, Ng LW, Manev H (2009). 5-Lipoxygenase DNA methylation and mRNA content in the brain and heart of young and old mice. *Neural plasticity* **2009:** 209596.

El-Sherbeni AA, El-Kadi AO (2014a). Alterations in cytochrome P450-derived arachidonic acid metabolism during pressure overload-induced cardiac hypertrophy. *Biochemical pharmacology* **87**(3)**:** 456-466.

El-Sherbeni AA, El-Kadi AO (2014b). Characterization of arachidonic acid metabolism by rat cytochrome P450 enzymes: the involvement of CYP1As. *Drug metabolism and disposition: the biological fate of chemicals* **42**(9)**:** 1498-1507.

El-Sherbeni AA, El-Kadi AO (2014c). The role of epoxide hydrolases in health and disease. *Archives of toxicology* **88**(11)**:** 2013-2032.

Elbekai RH, El-Kadi AO (2006). Cytochrome P450 enzymes: central players in cardiovascular health and disease. *Pharmacology & therapeutics* **112**(2)**:** 564-587.

Elshenawy OH, Anwar-Mohamed A, El-Kadi AO (2013). 20-Hydroxyeicosatetraenoic acid is a potential therapeutic target in cardiovascular diseases. *Current drug metabolism* **14**(6)**:** 706-719.

Eltom SE, Zhang L, Jefcoate CR (1999). Regulation of cytochrome P-450 (CYP) 1B1 in mouse Hepa-1 variant cell lines: A possible role for aryl hydrocarbon receptor nuclear translocator (ARNT) as a suppressor of CYP1B1 gene expression. *Mol Pharmacol* **55**(3)**:** 594-604.

Engelhardt S, Hein L, Keller U, Klambt K, Lohse MJ (2002). Inhibition of Na(+)-H(+) exchange prevents hypertrophy, fibrosis, and heart failure in beta(1)-adrenergic receptor transgenic mice. *Circulation research* **90**(7)**:** 814-819.

Engelhardt S, Hein L, Wiesmann F, Lohse MJ (1999). Progressive hypertrophy and heart failure in beta1-adrenergic receptor transgenic mice. *Proceedings of the National Academy of Sciences of the United States of America* **96**(12)**:** 7059-7064.

Esposito G, Rapacciuolo A, Naga Prasad SV, Takaoka H, Thomas SA, Koch WJ*, et al.* (2002). Genetic alterations that inhibit in vivo pressure-overload hypertrophy prevent cardiac dysfunction despite increased wall stress. *Circulation* **105**(1)**:** 85-92.

Fagard RH (1997). Impact of different sports and training on cardiac structure and function. *Cardiology clinics* **15**(3)**:** 397-412.

Fard A, Wang CY, Takuma S, Skopicki HA, Pinsky DJ, Di Tullio MR*, et al.* (2000). Noninvasive assessment and necropsy validation of changes in left ventricular mass in ascending aortic banded mice. *J Am Soc Echocardiogr* **13**(6)**:** 582-587.

Farh KK, Grimson A, Jan C, Lewis BP, Johnston WK, Lim LP*, et al.* (2005). The widespread impact of mammalian MicroRNAs on mRNA repression and evolution. *Science* **310**(5755)**:** 1817-1821.

Fatkin D, McConnell BK, Mudd JO, Semsarian C, Moskowitz IG, Schoen FJ*, et al.* (2000). An abnormal Ca(2+) response in mutant sarcomere protein-mediated familial hypertrophic cardiomyopathy. *The Journal of clinical investigation* **106**(11)**:** 1351-1359.

Fava C, Ricci M, Melander O, Minuz P (2012). Hypertension, cardiovascular risk and polymorphisms in genes controlling the cytochrome P450 pathway of arachidonic acid: A sex-specific relation? *Prostaglandins & other lipid mediators* **98**(3-4)**:** 75-85.

Felker GM, Thompson RE, Hare JM, Hruban RH, Clemetson DE, Howard DL*, et al.* (2000). Underlying causes and long-term survival in patients with initially unexplained cardiomyopathy. *The New England journal of medicine* **342**(15)**:** 1077-1084.

Ferguson AD, McKeever BM, Xu S, Wisniewski D, Miller DK, Yamin TT*, et al.* (2007). Crystal structure of inhibitor-bound human 5-lipoxygenase-activating protein. *Science* **317**(5837)**:** 510-512.

Finck BN, Lehman JJ, Leone TC, Welch MJ, Bennett MJ, Kovacs A*, et al.* (2002). The cardiac phenotype induced by PPARalpha overexpression mimics that caused by diabetes mellitus. *The Journal of clinical investigation* **109**(1)**:** 121-130.

Fitzpatrick FA, Ennis MD, Baze ME, Wynalda MA, McGee JE, Liggett WF (1986). Inhibition of cyclooxygenase activity and platelet aggregation by epoxyeicosatrienoic acids. Influence of stereochemistry. *The Journal of biological chemistry* **261**(32)**:** 15334-15338.

Florez H, Reaven PD, Bahn G, Moritz T, Warren S, Marks J, *et al.* (2015). Rosiglitazone treatment and cardiovascular disease in the Veterans Affairs Diabetes Trial. *Diabetes, obesity & metabolism* **17**(10)**:** 949-955.

Fox KF, Cowie MR, Wood DA, Coats AJ, Gibbs JS, Underwood SR, *et al.* (2001). Coronary artery disease as the cause of incident heart failure in the population. *European heart journal* **22**(3)**:** 228-236.

Frantz S, Stoerk S, Ok S, Wagner H, Angermann CE, Ertl G, *et al.* (2004). Effect of chronic heart failure on nuclear factor kappa B in peripheral leukocytes. *The American journal of cardiology* **94**(5)**:** 671-673.

Freeman RH, Davis JO, Watkins BE, Lohmeier TE (1977). Mechanisms involved in two-kidney renal hypertension induced by constriction of one renal artery. *Circulation research* **40**(5 Suppl 1)**:** I29-35.

Frey N, Katus HA, Olson EN, Hill JA (2004). Hypertrophy of the heart: a new therapeutic target? *Circulation* **109**(13)**:** 1580-1589.

Frey N, Olson EN (2003). Cardiac hypertrophy: the good, the bad, and the ugly. *Annual review of physiology* **65:** 45-79.

Furstenberger G, Hagedorn H, Jacobi T, Besemfelder E, Stephan M, Lehmann WD, *et al.* (1991). Characterization of an 8-lipoxygenase activity induced by the phorbol ester tumor promoter 12-O-tetradecanoylphorbol-13-acetate in mouse skin in vivo. *The Journal of biological chemistry* **266**(24)**:** 15738-15745.

Gall WE, Zawada G, Mojarrabi B, Tephly TR, Green MD, Coffman BL, *et al.* (1999). Differential glucuronidation of bile acids, androgens and estrogens by human UGT1A3 and 2B7. *The Journal of steroid biochemistry and molecular biology* **70**(1-3)**:** 101-108.

Garcia-Verdugo I, BenMohamed F, Tattermusch S, Leduc D, Charpigny G, Chignard M, *et al.* (2012). A role for 12R-lipoxygenase in MUC5AC expression by respiratory epithelial cells. *The European respiratory journal* **40**(3)**:** 714-723.

Gebremedhin D, Lange AR, Lowry TF, Taheri MR, Birks EK, Hudetz AG, *et al.* (2000). Production of 20-HETE and its role in autoregulation of cerebral blood flow. *Circulation research* **87**(1)**:** 60-65.

Gellner K, Eiselt R, Hustert E, Arnold H, Koch I, Haberl M*, et al.* (2001). Genomic organization of the human CYP3A locus: identification of a new, inducible CYP3A gene. *Pharmacogenetics* **11**(2)**:** 111-121.

Gilde AJ, Van Bilsen M (2003). Peroxisome proliferator-activated receptors (PPARS): regulators of gene expression in heart and skeletal muscle. *Acta physiologica Scandinavica* **178**(4)**:** 425-434.

Goetzl EJ, Sun FF (1979). Generation of unique mono-hydroxy-eicosatetraenoic acids from arachidonic acid by human neutrophils. *The Journal of experimental medicine* **150**(2)**:** 406-411.

Goldstein JA, de Morais SM (1994). Biochemistry and molecular biology of the human CYP2C subfamily. *Pharmacogenetics* **4**(6)**:** 285-299.

Gonzalez-Nunez D, Claria J, Rivera F, Poch E (2001). Increased levels of 12(S)-HETE in patients with essential hypertension. *Hypertension* **37**(2)**:** 334-338.

Grabellus F, Levkau B, Sokoll A, Welp H, Schmid C, Deng MC*, et al.* (2002). Reversible activation of nuclear factor-kappaB in human end-stage heart failure after left ventricular mechanical support. *Cardiovascular research* **53**(1)**:** 124-130.

Gradman AH, Alfayoumi F (2006). From left ventricular hypertrophy to congestive heart failure: management of hypertensive heart disease. *Progress in cardiovascular diseases* **48**(5)**:** 326-341.

Granberg AL, Brunstrom B, Brandt I (2000). Cytochrome P450-dependent binding of 7,12-dimethylbenz[a]anthracene (DMBA) and benzo[a]pyrene (B[a]P) in murine heart, lung, and liver endothelial cells. *Archives of toxicology* **74**(10)**:** 593-601.

Granvil CP, Yu AM, Elizondo G, Akiyama TE, Cheung C, Feigenbaum L*, et al.* (2003). Expression of the human CYP3A4 gene in the small intestine of transgenic mice: in vitro metabolism and pharmacokinetics of midazolam. *Drug metabolism and disposition: the biological fate of chemicals* **31**(5)**:** 548-558.

Gregorio CC, Antin PB (2000). To the heart of myofibril assembly. *Trends in cell biology* **10**(9)**:** 355-362.

Gribben JG, Ryan DP, Boyajian R, Urban RG, Hedley ML, Beach K*, et al.* (2005). Unexpected association between induction of immunity to the universal tumor antigen

CYP1B1 and response to next therapy. *Clinical cancer research : an official journal of the American Association for Cancer Research* **11**(12)**:** 4430-4436.

Gross GJ, Falck JR, Gross ER, Isbell M, Moore J, Nithipatikom K (2005). Cytochrome P450 and arachidonic acid metabolites: role in myocardial ischemia/reperfusion injury revisited. *Cardiovascular research* **68**(1)**:** 18-25.

Grossman W, Jones D, McLaurin LP (1975). Wall stress and patterns of hypertrophy in the human left ventricle. *The Journal of clinical investigation* **56**(1)**:** 56-64.

Gu JL, Natarajan R, Ben-Ezra J, Valente G, Scott S, Yoshimoto T*, et al.* (1994). Evidence that a leukocyte type of 12-lipoxygenase is expressed and regulated by angiotensin II in human adrenal glomerulosa cells. *Endocrinology* **134**(1)**:** 70-77.

Gu S, Zhang W, Chen J, Ma R, Xiao X, Ma X*, et al.* (2014). EPC-derived microvesicles protect cardiomyocytes from Ang II-induced hypertrophy and apoptosis. *PloS one* **9**(1)**:** e85396.

Guido DM, McKenna R, Mathews WR (1993). Quantitation of hydroperoxy-eicosatetraenoic acids and hydroxy-eicosatetraenoic acids as indicators of lipid peroxidation using gas chromatography-mass spectrometry. *Analytical biochemistry* **209**(1)**:** 123-129.

Guo AM, Liu X, Al-Wahab Z, Maddippati KR, Ali-Fehmi R, Scicli AG*, et al.* (2011a). Role of 12-lipoxygenase in regulation of ovarian cancer cell proliferation and survival. *Cancer chemotherapy and pharmacology* **68**(5)**:** 1273-1283.

Guo L, Tang X, Chu X, Sun L, Zhang L, Qiu Z*, et al.* (2009). Role of protein kinase C in 15-HETE-induced hypoxic pulmonary vasoconstriction. *Prostaglandins, leukotrienes, and essential fatty acids* **80**(2-3)**:** 115-123.

Guo W, Sun J, Jiang L, Duan L, Huo M, Chen N*, et al.* (2012). Imperatorin attenuates LPS-induced inflammation by suppressing NF-kappaB and MAPKs activation in RAW 264.7 macrophages. *Inflammation* **35**(6)**:** 1764-1772.

Guo Y, Zhang W, Giroux C, Cai Y, Ekambaram P, Dilly AK*, et al.* (2011b). Identification of the orphan G protein-coupled receptor GPR31 as a receptor for 12-(S)-hydroxyeicosatetraenoic acid. *The Journal of biological chemistry* **286**(39)**:** 33832-33840.

Hada T, Hagiya H, Suzuki H, Arakawa T, Nakamura M, Matsuda S, *et al.* (1994). Arachidonate 12-lipoxygenase of rat pineal glands: catalytic properties and primary structure deduced from its cDNA. *Biochimica et biophysica acta* **1211**(2)**:** 221-228.

Hahn HS, Marreez Y, Odley A, Sterbling A, Yussman MG, Hilty KC*, et al.* (2003). Protein kinase Calpha negatively regulates systolic and diastolic function in pathological hypertrophy. *Circulation research* **93**(11)**:** 1111-1119.

Hammond VJ, Morgan AH, Lauder S, Thomas CP, Brown S, Freeman BA*, et al.* (2012). Novel keto-phospholipids are generated by monocytes and macrophages, detected in cystic fibrosis, and activate peroxisome proliferator-activated receptor-gamma. *The Journal of biological chemistry* **287**(50)**:** 41651-41666.

Han X, Liehr JG (1994). DNA single-strand breaks in kidneys of Syrian hamsters treated with steroidal estrogens: hormone-induced free radical damage preceding renal malignancy. *Carcinogenesis* **15**(5)**:** 997-1000.

Harding VB, Jones LR, Lefkowitz RJ, Koch WJ, Rockman HA (2001). Cardiac beta ARK1 inhibition prolongs survival and augments beta blocker therapy in a mouse model of severe heart failure. *Proceedings of the National Academy of Sciences of the United States of America* **98**(10)**:** 5809-5814.

Harris DE, Work SS, Wright RK, Alpert NR, Warshaw DM (1994). Smooth, cardiac and skeletal muscle myosin force and motion generation assessed by cross-bridge mechanical interactions in vitro. *Journal of muscle research and cell motility* **15**(1)**:** 11-19.

Hayakawa Y, Chandra M, Miao W, Shirani J, Brown JH, Dorn GW, 2nd*, et al.* (2003). Inhibition of cardiac myocyte apoptosis improves cardiac function and abolishes mortality in the peripartum cardiomyopathy of Galpha(q) transgenic mice. *Circulation* **108**(24)**:** 3036-3041.

Hayes CL, Spink DC, Spink BC, Cao JQ, Walker NJ, Sutter TR (1996). 17 beta-estradiol hydroxylation catalyzed by human cytochrome P450 1B1. *Proceedings of the National Academy of Sciences of the United States of America* **93**(18)**:** 9776-9781.

Hill JA, Rothermel B, Yoo KD, Cabuay B, Demetroulis E, Weiss RM*, et al.* (2002). Targeted inhibition of calcineurin in pressure-overload cardiac hypertrophy. Preservation of systolic function. *The Journal of biological chemistry* **277**(12)**:** 10251-10255.

Hirotani S, Otsu K, Nishida K, Higuchi Y, Morita T, Nakayama H*, et al.* (2002). Involvement of nuclear factor-kappaB and apoptosis signal-regulating kinase 1 in G-

protein-coupled receptor agonist-induced cardiomyocyte hypertrophy. *Circulation* **105**(4)**:** 509-515.

Holubarsch C, Goulette RP, Litten RZ, Martin BJ, Mulieri LA, Alpert NR (1985). The economy of isometric force development, myosin isoenzyme pattern and myofibrillar ATPase activity in normal and hypothyroid rat myocardium. *Circulation research* **56**(1)**:** 78-86.

Honda HM, Leitinger N, Frankel M, Goldhaber JI, Natarajan R, Nadler JL*, et al.* (1999). Induction of monocyte binding to endothelial cells by MM-LDL: role of lipoxygenase metabolites. *Arteriosclerosis, thrombosis, and vascular biology* **19**(3)**:** 680-686.

Honkakoski P, Moore R, Washburn KA, Negishi M (1998). Activation by diverse xenochemicals of the 51-base pair phenobarbital-responsive enhancer module in the CYP2B10 gene. *Molecular pharmacology* **53**(4)**:** 597-601.

Honn KV, Nelson KK, Renaud C, Bazaz R, Diglio CA, Timar J (1992). Fatty acid modulation of tumor cell adhesion to microvessel endothelium and experimental metastasis. *Prostaglandins* **44**(5)**:** 413-429.

Hood KY, Montezano AC, Harvey AP, Nilsen M, MacLean MR, Touyz RM (2016). Nicotinamide Adenine Dinucleotide Phosphate Oxidase-Mediated Redox Signaling and Vascular Remodeling by 16alpha-Hydroxyestrone in Human Pulmonary Artery Cells: Implications in Pulmonary Arterial Hypertension. *Hypertension* **68**(3)**:** 796-808.

Hoopes SL, Garcia V, Edin ML, Schwartzman ML, Zeldin DC (2015). Vascular actions of 20-HETE. *Prostaglandins & other lipid mediators* **120:** 9-16.

Horenstein MS, Vander Heide RS, L'Ecuyer TJ (2000). Molecular basis of anthracycline-induced cardiotoxicity and its prevention. *Molecular genetics and metabolism* **71**(1-2)**:** 436-444.

Hu W, Sorrentino C, Denison MS, Kolaja K, Fielden MR (2007). Induction of cyp1a1 is a nonspecific biomarker of aryl hydrocarbon receptor activation: results of large scale screening of pharmaceuticals and toxicants in vivo and in vitro. *Molecular pharmacology* **71**(6)**:** 1475-1486.

Hu X, Wang H, Lv X, Chu L, Liu Z, Wei X*, et al.* (2015). Cardioprotective Effects of Tannic Acid on Isoproterenol-Induced Myocardial Injury in Rats: Further Insight into 'French Paradox'. *Phytotherapy research : PTR*.

Hunt SA, Abraham WT, Chin MH, Feldman AM, Francis GS, Ganiats TG*, et al.* (2005). ACC/AHA 2005 Guideline Update for the Diagnosis and Management of Chronic Heart Failure in the Adult: a report of the American College of Cardiology/American Heart Association Task Force on Practice Guidelines (Writing Committee to Update the 2001 Guidelines for the Evaluation and Management of Heart Failure): developed in collaboration with the American College of Chest Physicians and the International Society for Heart and Lung Transplantation: endorsed by the Heart Rhythm Society. *Circulation* **112**(12)**:** e154-235.

Hunter JA, Finkbeiner WE, Nadel JA, Goetzl EJ, Holtzman MJ (1985). Predominant generation of 15-lipoxygenase metabolites of arachidonic acid by epithelial cells from human trachea. *Proceedings of the National Academy of Sciences of the United States of America* **82**(14)**:** 4633-4637.

Hydock DS, Lien CY, Schneider CM, Hayward R (2008). Exercise preconditioning protects against doxorubicin-induced cardiac dysfunction. *Medicine and science in sports and exercise* **40**(5)**:** 808-817.

Iemitsu M, Miyauchi T, Maeda S, Sakai S, Kobayashi T, Fujii N*, et al.* (2001). Physiological and pathological cardiac hypertrophy induce different molecular phenotypes in the rat. *American journal of physiology. Regulatory, integrative and comparative physiology* **281**(6)**:** R2029-2036.

Ikuta T, Eguchi H, Tachibana T, Yoneda Y, Kawajiri K (1998). Nuclear localization and export signals of the human aryl hydrocarbon receptor. *J Biol Chem* **273**(5)**:** 2895-2904.

Imai Y, Tsukahara S, Ishikawa E, Tsuruo T, Sugimoto Y (2002). Estrone and 17beta-estradiol reverse breast cancer resistance protein-mediated multidrug resistance. *Japanese journal of cancer research : Gann* **93**(3)**:** 231-235.

Imaoka S, Hashizume T, Funae Y (2005). Localization of rat cytochrome P450 in various tissues and comparison of arachidonic acid metabolism by rat P450 with that by human P450 orthologs. *Drug metabolism and pharmacokinetics* **20**(6)**:** 478-484.

Imig JD (2012). Epoxides and soluble epoxide hydrolase in cardiovascular physiology. *Physiological reviews* **92**(1)**:** 101-130.

Imig JD, Zhao X, Capdevila JH, Morisseau C, Hammock BD (2002). Soluble epoxide hydrolase inhibition lowers arterial blood pressure in angiotensin II hypertension. *Hypertension* **39**(2 Pt 2)**:** 690-694.

Inoue M, Kishimoto A, Takai Y, Nishizuka Y (1977). Studies on a cyclic nucleotide-independent protein kinase and its proenzyme in mammalian tissues. II. Proenzyme and its activation by calcium-dependent protease from rat brain. *The Journal of biological chemistry* **252**(21)**:** 7610-7616.

Inouye K, Sakaki T (2001). Enzymatic studies on the key enzymes of vitamin D metabolism; 1 alpha-hydroxylase (CYP27B1) and 24-hydroxylase (CYP24). *Biotechnology annual review* **7:** 179-194.

Ishihara Y, Hamaguchi A, Sekine M, Hirakawa A, Shimamoto N (2012). Accumulation of cytochrome P450 induced by proteasome inhibition during cardiac ischemia. *Archives of biochemistry and biophysics* **527**(1)**:** 16-22.

Issemann I, Green S (1990). Activation of a member of the steroid hormone receptor superfamily by peroxisome proliferators. *Nature* **347**(6294)**:** 645-650.

James J, Murry DJ, Treston AM, Storniolo AM, Sledge GW, Sidor C*, et al.* (2007). Phase I safety, pharmacokinetic and pharmacodynamic studies of 2-methoxyestradiol alone or in combination with docetaxel in patients with locally recurrent or metastatic breast cancer. *Investigational new drugs* **25**(1)**:** 41-48.

Jansson I, Stoilov I, Sarfarazi M, Schenkman JB (2001). Effect of two mutations of human CYP1B1, G61E and R469W, on stability and endogenous steroid substrate metabolism. *Pharmacogenetics* **11**(9)**:** 793-801.

Jenkins CM, Cedars A, Gross RW (2009). Eicosanoid signalling pathways in the heart. *Cardiovascular research* **82**(2)**:** 240-249.

Jennings BL, Anderson LJ, Estes AM, Fang XR, Song CY, Campbell WB*, et al.* (2012a). Involvement of cytochrome P-450 1B1 in renal dysfunction, injury, and inflammation associated with angiotensin II-induced hypertension in rats. *American journal of physiology. Renal physiology* **302**(4)**:** F408-420.

Jennings BL, Anderson LJ, Estes AM, Yaghini FA, Fang XR, Porter J*, et al.* (2012b). Cytochrome P450 1B1 contributes to renal dysfunction and damage caused by angiotensin II in mice. *Hypertension* **59**(2)**:** 348-354.

Jennings BL, Estes AM, Anderson LJ, Fang XR, Yaghini FA, Fan Z*, et al.* (2012c). Cytochrome P450 1B1 gene disruption minimizes deoxycorticosterone acetate-salt-

induced hypertension and associated cardiac dysfunction and renal damage in mice. *Hypertension* **60**(6)**:** 1510-1516.

Jennings BL, George LW, Pingili AK, Khan NS, Estes AM, Fang XR*, et al.* (2014a). Estrogen metabolism by cytochrome P450 1B1 modulates the hypertensive effect of angiotensin II in female mice. *Hypertension* **64**(1)**:** 134-140.

Jennings BL, Montanez DE, May ME, Jr., Estes AM, Fang XR, Yaghini FA*, et al.* (2014b). Cytochrome P450 1B1 contributes to increased blood pressure and cardiovascular and renal dysfunction in spontaneously hypertensive rats. *Cardiovascular drugs and therapy / sponsored by the International Society of Cardiovascular Pharmacotherapy* **28**(2)**:** 145-161.

Jennings BL, Sahan-Firat S, Estes AM, Das K, Farjana N, Fang XR*, et al.* (2010). Cytochrome P450 1B1 contributes to angiotensin II-induced hypertension and associated pathophysiology. *Hypertension* **56**(4)**:** 667-674.

Jin X, He Y, Zhu M, Lin X, Chen Q, Han Z*, et al.* (2010). The relationship between the polymorphism of SG13S114 A/T in ALOX5AP gene and the vulnerability of carotid atherosclerosis in Chinese Han population. *International journal of clinical and experimental medicine* **3**(1)**:** 28-32.

Jisaka M, Kim RB, Boeglin WE, Brash AR (2000). Identification of amino acid determinants of the positional specificity of mouse 8S-lipoxygenase and human 15S-lipoxygenase-2. *The Journal of biological chemistry* **275**(2)**:** 1287-1293.

Johnson FL (2014). Pathophysiology and etiology of heart failure. *Cardiology clinics* **32**(1)**:** 9-19, vii.

Kalay N, Basar E, Ozdogru I, Er O, Cetinkaya Y, Dogan A*, et al.* (2006). Protective effects of carvedilol against anthracycline-induced cardiomyopathy. *Journal of the American College of Cardiology* **48**(11)**:** 2258-2262.

Kandouz M, Nie D, Pidgeon GP, Krishnamoorthy S, Maddipati KR, Honn KV (2003). Platelet-type 12-lipoxygenase activates NF-kappaB in prostate cancer cells. *Prostaglandins & other lipid mediators* **71**(3-4)**:** 189-204.

Kang KH, Ling TY, Liou HH, Huang YK, Hour MJ, Liou HC*, et al.* (2013). Enhancement role of host 12/15-lipoxygenase in melanoma progression. *European journal of cancer* **49**(12)**:** 2747-2759.

Kang YJ, Chen Y, Epstein PN (1996). Suppression of doxorubicin cardiotoxicity by overexpression of catalase in the heart of transgenic mice. *The Journal of biological chemistry* **271**(21)**:** 12610-12616.

Kannel WB (1974). Role of blood pressure in cardiovascular morbidity and mortality. *Progress in cardiovascular diseases* **17**(1)**:** 5-24.

Kaplan ML, Cheslow Y, Vikstrom K, Malhotra A, Geenen DL, Nakouzi A*, et al.* (1994). Cardiac adaptations to chronic exercise in mice. *The American journal of physiology* **267**(3 Pt 2)**:** H1167-1173.

Karagiannis TC, Lin AJ, Ververis K, Chang L, Tang MM, Okabe J*, et al.* (2010). Trichostatin A accentuates doxorubicin-induced hypertrophy in cardiac myocytes. *Aging* **2**(10)**:** 659-668.

Katoh T, Lakkis FG, Makita N, Badr KF (1994). Co-regulated expression of glomerular 12/15-lipoxygenase and interleukin-4 mRNAs in rat nephrotoxic nephritis. *Kidney international* **46**(2)**:** 341-349.

Kaur-Knudsen D, Nordestgaard BG, Tybjaerg-Hansen A, Bojesen SE (2009). CYP1B1 genotype and risk of cardiovascular disease, pulmonary disease, and cancer in 50,000 individuals. *Pharmacogenetics and genomics* **19**(9)**:** 685-694.

Kauser K, Clark JE, Masters BS, Ortiz de Montellano PR, Ma YH, Harder DR*, et al.* (1991). Inhibitors of cytochrome P-450 attenuate the myogenic response of dog renal arcuate arteries. *Circulation research* **68**(4)**:** 1154-1163.

Kawamoto T, Sueyoshi T, Zelko I, Moore R, Washburn K, Negishi M (1999). Phenobarbital-responsive nuclear translocation of the receptor CAR in induction of the CYP2B gene. *Molecular and cellular biology* **19**(9)**:** 6318-6322.

Kawano S, Kubota T, Monden Y, Kawamura N, Tsutsui H, Takeshita A*, et al.* (2005). Blockade of NF-kappaB ameliorates myocardial hypertrophy in response to chronic infusion of angiotensin II. *Cardiovascular research* **67**(4)**:** 689-698.

Kayama Y, Minamino T, Toko H, Sakamoto M, Shimizu I, Takahashi H*, et al.* (2009). Cardiac 12/15 lipoxygenase-induced inflammation is involved in heart failure. *The Journal of experimental medicine* **206**(7)**:** 1565-1574.

Kennedy SW, Lorenzen A, James CA, Collins BT (1993). Ethoxyresorufin-O-deethylase and porphyrin analysis in chicken embryo hepatocyte cultures with a fluorescence multiwell plate reader. *Anal Biochem* **211**(1)**:** 102-112.

Kerzee JK, Ramos KS (2001). Constitutive and inducible expression of Cyp1a1 and Cyp1b1 in vascular smooth muscle cells: role of the Ahr bHLH/PAS transcription factor. *Circ Res* **89**(7)**:** 573-582.

Khan SR, Baghdasarian A, Nagar PH, Fahlman R, Jurasz P, Michail K*, et al.* (2015). Proteomic profile of aminoglutethimide-induced apoptosis in HL-60 cells: Role of myeloperoxidase and arylamine free radicals. *Chemico-biological interactions* **239:** 129-138.

Kikuta Y, Kusunose E, Kusunose M (2000). Characterization of human liver leukotriene B(4) omega-hydroxylase P450 (CYP4F2). *Journal of biochemistry* **127**(6)**:** 1047-1052.

Kikuta Y, Kusunose E, Sumimoto H, Mizukami Y, Takeshige K, Sakaki T*, et al.* (1998). Purification and characterization of recombinant human neutrophil leukotriene B4 omega-hydroxylase (cytochrome P450 4F3). *Archives of biochemistry and biophysics* **355**(2)**:** 201-205.

Kim HJ, Lee SB, Park SK, Kim HM, Park YI, Dong MS (2005). Effects of hydroxyl group numbers on the B-ring of 5,7-dihydroxyflavones on the differential inhibition of human CYP 1A and CYP1B1 enzymes. *Archives of pharmacal research* **28**(10)**:** 1114-1121.

Kimes BW, Brandt BL (1976). Properties of a clonal muscle cell line from rat heart. *Experimental cell research* **98**(2)**:** 367-381.

Kirchheiner J, Henckel HB, Meineke I, Roots I, Brockmoller J (2004). Impact of the CYP2D6 ultrarapid metabolizer genotype on mirtazapine pharmacokinetics and adverse events in healthy volunteers. *Journal of clinical psychopharmacology* **24**(6)**:** 647-652.

Kiriazis H, Kranias EG (2000). Genetically engineered models with alterations in cardiac membrane calcium-handling proteins. *Annual review of physiology* **62:** 321-351.

Kliewer SA, Goodwin B, Willson TM (2002). The nuclear pregnane X receptor: a key regulator of xenobiotic metabolism. *Endocrine reviews* **23**(5)**:** 687-702.

Kodama S, Negishi M (2006). Phenobarbital confers its diverse effects by activating the orphan nuclear receptor car. *Drug metabolism reviews* **38**(1-2)**:** 75-87.

Koeners MP, Wesseling S, Ulu A, Sepulveda RL, Morisseau C, Braam B*, et al.* (2011). Soluble epoxide hydrolase in the generation and maintenance of high blood pressure in spontaneously hypertensive rats. *American journal of physiology. Endocrinology and metabolism* **300**(4)**:** E691-698.

Koganti S, Snyder R, Thekkumkara T (2012). Pharmacologic effects of 2-methoxyestradiol on angiotensin type 1 receptor down-regulation in rat liver epithelial and aortic smooth muscle cells. *Gender medicine* **9**(2)**:** 76-93.

Kohli S, Ahuja S, Rani V (2011). Transcription factors in heart: promising therapeutic targets in cardiac hypertrophy. *Current cardiology reviews* **7**(4)**:** 262-271.

Kong EK, Huang Y, Sanderson JE, Chan KB, Yu S, Yu CM (2010). Baicalein and Wogonin inhibit collagen deposition in SHR and WKY cardiac fibroblast cultures. *BMB reports* **43**(4)**:** 297-303.

Kong EK, Yu S, Sanderson JE, Chen KB, Huang Y, Yu CM (2011). A novel anti-fibrotic agent, baicalein, for the treatment of myocardial fibrosis in spontaneously hypertensive rats. *European journal of pharmacology* **658**(2-3)**:** 175-181.

Kopf PG, Huwe JK, Walker MK (2008). Hypertension, cardiac hypertrophy, and impaired vascular relaxation induced by 2,3,7,8-tetrachlorodibenzo-p-dioxin are associated with increased superoxide. *Cardiovascular toxicology* **8**(4)**:** 181-193.

Korashy HM, Al-Suwayeh HA, Maayah ZH, Ansari MA, Ahmad SF, Bakheet SA (2014). Mitogen-Activated Protein Kinases Pathways Mediate the Sunitinib-Induced Hypertrophy in Rat Cardiomyocyte H9c2 Cells. *Cardiovascular toxicology*.

Korashy HM, El-Kadi AO (2005). Regulatory mechanisms modulating the expression of cytochrome P450 1A1 gene by heavy metals. *Toxicological sciences : an official journal of the Society of Toxicology* **88**(1)**:** 39-51.

Korashy HM, El-Kadi AO (2006). The role of aryl hydrocarbon receptor in the pathogenesis of cardiovascular diseases. *Drug metabolism reviews* **38**(3)**:** 411-450.

Korashy HM, El-Kadi AO (2006a). The Role of aryl hydrocarbon receptor in the pathogenesis of cardiovascular diseases. *Drug Metab Rev* **38**(3)**:** 411-450.

Kriska T, Cepura C, Magier D, Siangjong L, Gauthier KM, Campbell WB (2012). Mice lacking macrophage 12/15-lipoxygenase are resistant to experimental hypertension. *American journal of physiology. Heart and circulatory physiology* **302**(11)**:** H2428-2438.

Kroll J, Epting D, Kern K, Dietz CT, Feng Y, Hammes HP*, et al.* (2009). Inhibition of Rho-dependent kinases ROCK I/II activates VEGF-driven retinal neovascularization and sprouting angiogenesis. *American journal of physiology. Heart and circulatory physiology* **296**(3)**:** H893-899.

Krotz F, Riexinger T, Buerkle MA, Nithipatikom K, Gloe T, Sohn HY*, et al.* (2004). Membrane-potential-dependent inhibition of platelet adhesion to endothelial cells by epoxyeicosatrienoic acids. *Arteriosclerosis, thrombosis, and vascular biology* **24**(3)**:** 595-600.

Kuhn H, Banthiya S, van Leyen K (2015). Mammalian lipoxygenases and their biological relevance. *Biochimica et biophysica acta* **1851**(4)**:** 308-330.

Kumar AP, Garcia GE, Orsborn J, Levin VA, Slaga TJ (2003). 2-Methoxyestradiol interferes with NF kappa B transcriptional activity in primitive neuroectodermal brain tumors: implications for management. *Carcinogenesis* **24**(2)**:** 209-216.

Kumar S, Prasad S, Sitasawad SL (2013). Multiple antioxidants improve cardiac complications and inhibit cardiac cell death in streptozotocin-induced diabetic rats. *PloS one* **8**(7)**:** e67009.

Kunert MP, Roman RJ, Alonso-Galicia M, Falck JR, Lombard JH (2001). Cytochrome P-450 omega-hydroxylase: a potential O(2) sensor in rat arterioles and skeletal muscle cells. *American journal of physiology. Heart and circulatory physiology* **280**(4)**:** H1840-1845.

Kwak HJ, Park KM, Choi HE, Lim HJ, Park JH, Park HY (2010). The cardioprotective effects of zileuton, a 5-lipoxygenase inhibitor, are mediated by COX-2 via activation of PKC delta. *Cellular signalling* **22**(1)**:** 80-87.

Lacape G, Daret D, Crockett R, Rigaud M, Larrue J (1992). Dual metabolic pathways of 12-HETE in rat aortic smooth muscle cells. *Prostaglandins* **44**(3)**:** 167-176.

Ladas EJ, Jacobson JS, Kennedy DD, Teel K, Fleischauer A, Kelly KM (2004). Antioxidants and cancer therapy: a systematic review. *Journal of clinical oncology : official journal of the American Society of Clinical Oncology* **22**(3)**:** 517-528.

Lakhani NJ, Sparreboom A, Xu X, Veenstra TD, Venitz J, Dahut WL*, et al.* (2007). Characterization of in vitro and in vivo metabolic pathways of the investigational anticancer agent, 2-methoxyestradiol. *Journal of pharmaceutical sciences* **96**(7)**:** 1821-1831.

Lal H, Ahmad F, Zhou J, Yu JE, Vagnozzi RJ, Guo Y*, et al.* (2014). Cardiac fibroblast glycogen synthase kinase-3beta regulates ventricular remodeling and dysfunction in ischemic heart. *Circulation* **130**(5)**:** 419-430.

Lamba JK, Lamba V, Yasuda K, Lin YS, Assem M, Thompson E*, et al.* (2004). Expression of constitutive androstane receptor splice variants in human tissues and their functional consequences. *The Journal of pharmacology and experimental therapeutics* **311**(2)**:** 811-821.

Lavigne JA, Goodman JE, Fonong T, Odwin S, He P, Roberts DW*, et al.* (2001). The effects of catechol-O-methyltransferase inhibition on estrogen metabolite and oxidative DNA damage levels in estradiol-treated MCF-7 cells. *Cancer research* **61**(20)**:** 7488-7494.

Lawrence T (2009). The nuclear factor NF-kappaB pathway in inflammation. *Cold Spring Harbor perspectives in biology* **1**(6)**:** a001651.

Lebrecht D, Geist A, Ketelsen UP, Haberstroh J, Setzer B, Walker UA (2007). Dexrazoxane prevents doxorubicin-induced long-term cardiotoxicity and protects myocardial mitochondria from genetic and functional lesions in rats. *British journal of pharmacology* **151**(6)**:** 771-778.

Lee AJ, Cai MX, Thomas PE, Conney AH, Zhu BT (2003). Characterization of the oxidative metabolites of 17beta-estradiol and estrone formed by 15 selectively expressed human cytochrome p450 isoforms. *Endocrinology* **144**(8)**:** 3382-3398.

Lee CA, Neul D, Clouser-Roche A, Dalvie D, Wester MR, Jiang Y*, et al.* (2010). Identification of novel substrates for human cytochrome P450 2J2. *Drug metabolism and disposition: the biological fate of chemicals* **38**(2)**:** 347-356.

Lemieux H, Hoppel CL (2009). Mitochondria in the human heart. *Journal of bioenergetics and biomembranes* **41**(2)**:** 99-106.

Levick SP, Loch DC, Taylor SM, Janicki JS (2007). Arachidonic acid metabolism as a potential mediator of cardiac fibrosis associated with inflammation. *Journal of immunology* **178**(2)**:** 641-646.

Levy D, Anderson KM, Savage DD, Kannel WB, Christiansen JC, Castelli WP (1988). Echocardiographically detected left ventricular hypertrophy: prevalence and risk factors. The Framingham Heart Study. *Annals of internal medicine* **108**(1)**:** 7-13.

Lewis DF (2004). 57 varieties: the human cytochromes P450. *Pharmacogenomics* **5**(3)**:** 305-318.

Leychenko A, Konorev E, Jijiwa M, Matter ML (2011). Stretch-induced hypertrophy activates NFkB-mediated VEGF secretion in adult cardiomyocytes. *PloS one* **6**(12)**:** e29055.

Li-Weber M (2009). New therapeutic aspects of flavones: the anticancer properties of Scutellaria and its main active constituents Wogonin, Baicalein and Baicalin. *Cancer treatment reviews* **35**(1)**:** 57-68.

Li H, Dou W, Padikkala E, Mani S (2013). Reverse yeast two-hybrid system to identify mammalian nuclear receptor residues that interact with ligands and/or antagonists. *Journal of visualized experiments : JoVE*(81)**:** e51085.

Li S, E M, Yu B (2008). Adriamycin induces myocardium apoptosis through activation of nuclear factor kappaB in rat. *Molecular biology reports* **35**(4)**:** 489-494.

Li T, Yu RT, Atkins AR, Downes M, Tukey RH, Evans RM (2012). Targeting the pregnane X receptor in liver injury. *Expert opinion on therapeutic targets* **16**(11)**:** 1075-1083.

Li Y, Cai X, Guan Y, Wang L, Wang S, Li Y*, et al.* (2016). Adiponectin Upregulates MiR-133a in Cardiac Hypertrophy through AMPK Activation and Reduced ERK1/2 Phosphorylation. *PloS one* **11**(2)**:** e0148482.

Libby RT, Smith RS, Savinova OV, Zabaleta A, Martin JE, Gonzalez FJ*, et al.* (2003). Modification of ocular defects in mouse developmental glaucoma models by tyrosinase. *Science* **299**(5612)**:** 1578-1581.

Lieber CS (1997). Cytochrome P-4502E1: its physiological and pathological role. *Physiological reviews* **77**(2)**:** 517-544.

Lin HS, Choo QY, Ho PC (2010). Quantification of oxyresveratrol analog trans-2,4,3',5'-tetramethoxystilbene in rat plasma by a rapid HPLC method: application in a pre-clinical pharmacokinetic study. *Biomedical chromatography : BMC* **24**(12)**:** 1373-1378.

Lindenfeld J, Masoudi FA (2007). Fluid retention with thiazolidinediones: does the mechanism influence the outcome? *Journal of the American College of Cardiology* **49**(16)**:** 1705-1707.

Lindpaintner K, Kreutz R, Ganten D (1992). Genetic variation in hypertensive and 'control' strains. What are we controlling for anyway? *Hypertension* **19**(5)**:** 428-430.

Lindsey SH (2014). Importance of estrogen metabolites. *Hypertension* **64**(1)**:** 21-22.

Lipshultz SE, Rifai N, Dalton VM, Levy DE, Silverman LB, Lipsitz SR*, et al.* (2004). The effect of dexrazoxane on myocardial injury in doxorubicin-treated children with acute lymphoblastic leukemia. *The New England journal of medicine* **351**(2)**:** 145-153.

Liu B, Khan WA, Hannun YA, Timar J, Taylor JD, Lundy S*, et al.* (1995). 12(S)-hydroxyeicosatetraenoic acid and 13(S)-hydroxyoctadecadienoic acid regulation of protein kinase C-alpha in melanoma cells: role of receptor-mediated hydrolysis of inositol phospholipids. *Proceedings of the National Academy of Sciences of the United States of America* **92**(20)**:** 9323-9327.

Liu Q, Chen X, Macdonnell SM, Kranias EG, Lorenz JN, Leitges M*, et al.* (2009). Protein kinase C{alpha}, but not PKC{beta} or PKC{gamma}, regulates contractility and heart failure susceptibility: implications for ruboxistaurin as a novel therapeutic approach. *Circulation research* **105**(2)**:** 194-200.

Liu Y, Peterson DA, Kimura H, Schubert D (1997). Mechanism of cellular 3-(4,5-dimethylthiazol-2-yl)-2,5-diphenyltetrazolium bromide (MTT) reduction. *Journal of neurochemistry* **69**(2)**:** 581-593.

Livak KJ, Schmittgen TD (2001). Analysis of relative gene expression data using real-time quantitative PCR and the 2(-Delta Delta C(T)) Method. *Methods* **25**(4)**:** 402-408.

Lo SN, Chang YP, Tsai KC, Chang CY, Wu TS, Ueng YF (2013). Inhibition of CYP1 by berberine, palmatine, and jatrorrhizine: selectivity, kinetic characterization, and molecular modeling. *Toxicology and applied pharmacology* **272**(3)**:** 671-680.

Locher MR, Razumova MV, Stelzer JE, Norman HS, Moss RL (2011). Effects of low-level α-myosin heavy chain expression on contractile kinetics in porcine myocardium. *American journal of physiology. Heart and circulatory physiology* **300**(3)**:** H869-878.

Lopaschuk GD, Ussher JR, Folmes CD, Jaswal JS, Stanley WC (2010). Myocardial fatty acid metabolism in health and disease. *Physiological reviews* **90**(1)**:** 207-258.

Lopez-Lazaro M (2009). Distribution and biological activities of the flavonoid luteolin. *Mini reviews in medicinal chemistry* **9**(1)**:** 31-59.

Lorenzen A, Kennedy SW (1993). A fluorescence-based protein assay for use with a microplate reader. *Anal Biochem* **214**(1)**:** 346-348.

Low RL, Orton S, Friedman DB (2003). A truncated form of DNA topoisomerase IIbeta associates with the mtDNA genome in mammalian mitochondria. *European journal of biochemistry* **270**(20)**:** 4173-4186.

Lu C, Liu Y, Tang X, Ye H, Zhu D (2006a). Role of 15-hydroxyeicosatetraenoic acid in phosphorylation of ERK1/2 and caldesmon in pulmonary arterial smooth muscle cells. *Canadian journal of physiology and pharmacology* **84**(10)**:** 1061-1069.

Lu T, Ye D, Wang X, Seubert JM, Graves JP, Bradbury JA*, et al.* (2006b). Cardiac and vascular KATP channels in rats are activated by endogenous epoxyeicosatrienoic acids through different mechanisms. *The Journal of physiology* **575**(Pt 2)**:** 627-644.

Lu Y, Cederbaum AI (2008a). CYP2E1 and oxidative liver injury by alcohol. *Free radical biology & medicine* **44**(5)**:** 723-738.

Lu Z, Xu X, Hu X, Zhu G, Zhang P, van Deel ED*, et al.* (2008b). Extracellular superoxide dismutase deficiency exacerbates pressure overload-induced left ventricular hypertrophy and dysfunction. *Hypertension* **51**(1)**:** 19-25.

Ma C, Li Y, Ma J, Liu Y, Li Q, Niu S*, et al.* (2011). Key role of 15-lipoxygenase/15-hydroxyeicosatetraenoic acid in pulmonary vascular remodeling and vascular angiogenesis associated with hypoxic pulmonary hypertension. *Hypertension* **58**(4)**:** 679-688.

Ma J, Liang S, Wang Z, Zhang L, Jiang J, Zheng J*, et al.* (2010). ROCK pathway participates in the processes that 15-hydroxyeicosatetraenoic acid (15-HETE) mediated the pulmonary vascular remodeling induced by hypoxia in rat. *Journal of cellular physiology* **222**(1)**:** 82-94.

Ma YH, Harder DR, Clark JE, Roman RJ (1991). Effects of 12-HETE on isolated dog renal arcuate arteries. *The American journal of physiology* **261**(2 Pt 2)**:** H451-456.

Maayah ZH, Abdelhamid G, El-Kadi AO (2015a). Development of cellular hypertrophy by 8-hydroxyeicosatetraenoic acid in the human ventricular cardiomyocyte, RL-14 cell line, is implicated by MAPK and NF-kappaB. *Cell biology and toxicology* **31**(4-5)**:** 241-259.

Maayah ZH, Abdelhamid G, El-Kadi AO (2015b). Development of cellular hypertrophy by 8-hydroxyeicosatetraenoic acid in the human ventricular cardiomyocyte, RL-14 cell line, is implicated by MAPK and NF-kappaB. *Cell biology and toxicology*.

Maayah ZH, Abdelhamid G, Elshenawy OH, El-Sherbeni AA, Althurwi HN, McGinn E*, et al.* (2017). The Role of Soluble Epoxide Hydrolase Enzyme on Daunorubicin-Mediated Cardiotoxicity. *Cardiovascular toxicology*.

Maayah ZH, Althurwi HN, Abdelhamid G, Lesyk G, Jurasz P, El-Kadi AO (2016a). CYP1B1 inhibition attenuates doxorubicin-induced cardiotoxicity through a mid-chain HETEs-dependent mechanism. *Pharmacological research*.

Maayah ZH, Althurwi HN, Abdelhamid G, Lesyk G, Jurasz P, El-Kadi AO (2016b). CYP1B1 inhibition attenuates doxorubicin-induced cardiotoxicity through a mid-chain HETEs-dependent mechanism. *Pharmacol Res* **105:** 28-43.

Maayah ZH, Ansari MA, El Gendy MA, Al-Arifi MN, Korashy HM (2014). Development of cardiac hypertrophy by sunitinib in vivo and in vitro rat cardiomyocytes is influenced by the aryl hydrocarbon receptor signaling pathway. *Archives of toxicology* **88**(3)**:** 725-738.

Maayah ZH, El-Kadi AO (2015c). 5-, 12- and 15-Hydroxyeicosatetraenoic acids induce cellular hypertrophy in the human ventricular cardiomyocyte, RL-14 cell line, through MAPK- and NF-kappaB-dependent mechanism. *Archives of toxicology*.

Maayah ZH, El-Kadi AO (2015d). The role of mid-chain hydroxyeicosatetraenoic acids in the pathogenesis of hypertension and cardiac hypertrophy. *Archives of toxicology*.

Maayah ZH, El-Kadi AO (2016c). The role of mid-chain hydroxyeicosatetraenoic acids in the pathogenesis of hypertension and cardiac hypertrophy. *Archives of toxicology* **90**(1)**:** 119-136.

Maayah ZH, El Gendy MA, El-Kadi AO, Korashy HM (2013). Sunitinib, a tyrosine kinase inhibitor, induces cytochrome P450 1A1 gene in human breast cancer MCF7 cells through

ligand-independent aryl hydrocarbon receptor activation. *Archives of toxicology* **87**(5)**:** 847-856.

Maayah ZH, Elshenawy OH, Althurwi HN, Abdelhamid G, El-Kadi AO (2015e). Human fetal ventricular cardiomyocyte, RL-14 cell line, is a promising model to study drug metabolizing enzymes and their associated arachidonic acid metabolites. *Journal of pharmacological and toxicological methods* **71:** 33-41.

Maayah ZH, Levasseur J, Siva Piragasam R, Abdelhamid G, Dyck JRB, Fahlman RP*, et al.* (2018). 2-Methoxyestradiol protects against pressure overload-induced left ventricular hypertrophy. *Scientific reports* **8**(1)**:** 2780.

Mabjeesh NJ, Escuin D, LaVallee TM, Pribluda VS, Swartz GM, Johnson MS*, et al.* (2003). 2ME2 inhibits tumor growth and angiogenesis by disrupting microtubules and dysregulating HIF. *Cancer cell* **3**(4)**:** 363-375.

Makinen J, Frank C, Jyrkkarinne J, Gynther J, Carlberg C, Honkakoski P (2002). Modulation of mouse and human phenobarbital-responsive enhancer module by nuclear receptors. *Molecular pharmacology* **62**(2)**:** 366-378.

Malik KU, Jennings BL, Yaghini FA, Sahan-Firat S, Song CY, Estes AM*, et al.* (2012). Contribution of cytochrome P450 1B1 to hypertension and associated pathophysiology: a novel target for antihypertensive agents. *Prostaglandins & other lipid mediators* **98**(3-4)**:** 69-74.

Mammen JS, Kleiner HE, DiGiovanni J, Sutter TR, Strickland PT (2005). Coumarins are competitive inhibitors of cytochrome P450 1B1, with equal potency for allelic variants. *Pharmacogenetics and genomics* **15**(3)**:** 183-188.

Manyike PT, Kharasch ED, Kalhorn TF, Slattery JT (2000). Contribution of CYP2E1 and CYP3A to acetaminophen reactive metabolite formation. *Clinical pharmacology and therapeutics* **67**(3)**:** 275-282.

Marcus AJ, Broekman MJ, Safier LB, Ullman HL, Islam N, Sherhan CN*, et al.* (1982). Formation of leukotrienes and other hydroxy acids during platelet-neutrophil interactions in vitro. *Biochemical and biophysical research communications* **109**(1)**:** 130-137.

Marcus AJ, Safier LB, Ullman HL, Broekman MJ, Islam N, Oglesby TD*, et al.* (1984). 12S,20-dihydroxyicosatetraenoic acid: a new icosanoid synthesized by neutrophils from 12S-hydroxyicosatetraenoic acid produced by thrombin- or collagen-stimulated platelets.

Proceedings of the National Academy of Sciences of the United States of America **81**(3)**:** 903-907.

Masferrer JL, Rios AP, Schwartzman ML (1990). Inhibition of renal, cardiac and corneal (Na(+)-K+)ATPase by 12(R)-hydroxyeicosatetraenoic acid. *Biochemical pharmacology* **39**(12)**:** 1971-1974.

Maskrey BH, Bermudez-Fajardo A, Morgan AH, Stewart-Jones E, Dioszeghy V, Taylor GW*, et al.* (2007). Activated platelets and monocytes generate four hydroxyphosphatidylethanolamines via lipoxygenase. *The Journal of biological chemistry* **282**(28)**:** 20151-20163.

Matsui Y, Jia N, Okamoto H, Kon S, Onozuka H, Akino M*, et al.* (2004). Role of osteopontin in cardiac fibrosis and remodeling in angiotensin II-induced cardiac hypertrophy. *Hypertension* **43**(6)**:** 1195-1201.

Maulik SK, Kumar S (2012). Oxidative stress and cardiac hypertrophy: a review. *Toxicology mechanisms and methods* **22**(5)**:** 359-366.

McFadyen MC, Cruickshank ME, Miller ID, McLeod HL, Melvin WT, Haites NE*, et al.* (2001a). Cytochrome P450 CYP1B1 over-expression in primary and metastatic ovarian cancer. *Br J Cancer* **85**(2)**:** 242-246.

McFadyen MC, McLeod HL, Jackson FC, Melvin WT, Doehmer J, Murray GI (2001b). Cytochrome P450 CYP1B1 protein expression: a novel mechanism of anticancer drug resistance. *Biochem Pharmacol* **62**(2)**:** 207-212.

McHowat J, Swift LM, Arutunyan A, Sarvazyan N (2001). Clinical concentrations of doxorubicin inhibit activity of myocardial membrane-associated, calcium-independent phospholipase A(2). *Cancer research* **61**(10)**:** 4024-4029.

Meszaros J, Levai G (1990). Ultrastructural and electrophysiological alterations during the development of catecholamine-induced cardiac hypertrophy and failure. *Acta biologica Hungarica* **41**(4)**:** 289-307.

Michaud V, Frappier M, Dumas MC, Turgeon J (2010). Metabolic activity and mRNA levels of human cardiac CYP450s involved in drug metabolism. *PloS one* **5**(12)**:** e15666.

Minamiyama Y, Takemura S, Akiyama T, Imaoka S, Inoue M, Funae Y, *et al.* (1999). Isoforms of cytochrome P450 on organic nitrate-derived nitric oxide release in human heart vessels. *FEBS letters* **452**(3)**:** 165-169.

Minoda Y, Kharasch ED (2001). Halothane-dependent lipid peroxidation in human liver microsomes is catalyzed by cytochrome P4502A6 (CYP2A6). *Anesthesiology* **95**(2)**:** 509-514.

Minotti G, Menna P, Salvatorelli E, Cairo G, Gianni L (2004). Anthracyclines: molecular advances and pharmacologic developments in antitumor activity and cardiotoxicity. *Pharmacological reviews* **56**(2)**:** 185-229.

Mitchell MD, Koenig JM (1991). Increased production of 15-hydroxyeicosatetraenoic acid by placentae from pregnancies complicated by pregnancy-induced hypertension. *Prostaglandins, leukotrienes, and essential fatty acids* **43**(1)**:** 61-62.

Mitra MS, Donthamsetty S, White B, Latendresse JR, Mehendale HM (2007). Mechanism of protection of moderately diet restricted rats against doxorubicin-induced acute cardiotoxicity. *Toxicology and applied pharmacology* **225**(1)**:** 90-101.

Modesti PA, Serneri GG, Gamberi T, Boddi M, Coppo M, Lucchese G, *et al.* (2008). Impaired angiotensin II-extracellular signal-regulated kinase signaling in failing human ventricular myocytes. *Journal of hypertension* **26**(10)**:** 2030-2039.

Molkentin JD, Lu JR, Antos CL, Markham B, Richardson J, Robbins J, *et al.* (1998). A calcineurin-dependent transcriptional pathway for cardiac hypertrophy. *Cell* **93**(2)**:** 215-228.

Monostory K, Pascussi JM, Kobori L, Dvorak Z (2009). Hormonal regulation of CYP1A expression. *Drug metabolism reviews* **41**(4)**:** 547-572.

Morgan ET (2001). Regulation of cytochrome p450 by inflammatory mediators: why and how? *Drug metabolism and disposition: the biological fate of chemicals* **29**(3)**:** 207-212.

Mross K, Maessen P, van der Vijgh WJ, Gall H, Boven E, Pinedo HM (1988). Pharmacokinetics and metabolism of epidoxorubicin and doxorubicin in humans. *Journal of clinical oncology : official journal of the American Society of Clinical Oncology* **6**(3)**:** 517-526.

Muga SJ, Thuillier P, Pavone A, Rundhaug JE, Boeglin WE, Jisaka M, *et al.* (2000). 8S-lipoxygenase products activate peroxisome proliferator-activated receptor alpha and induce differentiation in murine keratinocytes. *Cell growth & differentiation : the molecular biology journal of the American Association for Cancer Research* **11**(8)**:** 447-454.

Mulugeta S, Suzuki T, Hernandez NT, Griesser M, Boeglin WE, Schneider C (2010). Identification and absolute configuration of dihydroxy-arachidonic acids formed by oxygenation of 5S-HETE by native and aspirin-acetylated COX-2. *Journal of lipid research* **51**(3)**:** 575-585.

Murdter TE, Sperker B, Kivisto KT, McClellan M, Fritz P, Friedel G, *et al.* (1997). Enhanced uptake of doxorubicin into bronchial carcinoma: beta-glucuronidase mediates release of doxorubicin from a glucuronide prodrug (HMR 1826) at the tumor site. *Cancer research* **57**(12)**:** 2440-2445.

Murray GI, Melvin WT, Greenlee WF, Burke MD (2001). Regulation, function, and tissue-specific expression of cytochrome P450 CYP1B1. *Annu Rev Pharmacol Toxicol* **41:** 297-316.

Murray GI, Taylor MC, McFadyen MC, McKay JA, Greenlee WF, Burke MD, *et al.* (1997). Tumor-specific expression of cytochrome P450 CYP1B1. *Cancer research* **57**(14)**:** 3026-3031.

Muthalif MM, Benter IF, Karzoun N, Fatima S, Harper J, Uddin MR, *et al.* (1998). 20-Hydroxyeicosatetraenoic acid mediates calcium/calmodulin-dependent protein kinase II-induced mitogen-activated protein kinase activation in vascular smooth muscle cells. *Proceedings of the National Academy of Sciences of the United States of America* **95**(21)**:** 12701-12706.

Nadler JL, Natarajan R, Stern N (1987). Specific action of the lipoxygenase pathway in mediating angiotensin II-induced aldosterone synthesis in isolated adrenal glomerulosa cells. *The Journal of clinical investigation* **80**(6)**:** 1763-1769.

Nakamura K, Fushimi K, Kouchi H, Mihara K, Miyazaki M, Ohe T, *et al.* (1998). Inhibitory effects of antioxidants on neonatal rat cardiac myocyte hypertrophy induced by tumor necrosis factor-alpha and angiotensin II. *Circulation* **98**(8)**:** 794-799.

Nakao J, Ooyama T, Ito H, Chang WC, Murota S (1982). Comparative effect of lipoxygenase products of arachidonic acid on rat aortic smooth muscle cell migration. *Atherosclerosis* **44**(3)**:** 339-342.

Natarajan R, Bai W, Rangarajan V, Gonzales N, Gu JL, Lanting L*, et al.* (1996). Platelet-derived growth factor BB mediated regulation of 12-lipoxygenase in porcine aortic smooth muscle cells. *Journal of cellular physiology* **169**(2)**:** 391-400.

Natarajan R, Gonzales N, Lanting L, Nadler J (1994). Role of the lipoxygenase pathway in angiotensin II-induced vascular smooth muscle cell hypertrophy. *Hypertension* **23**(1 Suppl)**:** I142-147.

Natarajan R, Gu JL, Rossi J, Gonzales N, Lanting L, Xu L*, et al.* (1993). Elevated glucose and angiotensin II increase 12-lipoxygenase activity and expression in porcine aortic smooth muscle cells. *Proceedings of the National Academy of Sciences of the United States of America* **90**(11)**:** 4947-4951.

Nazarewicz RR, Zenebe WJ, Parihar A, Parihar MS, Vaccaro M, Rink C*, et al.* (2007). 12(S)-hydroperoxyeicosatetraenoic acid (12-HETE) increases mitochondrial nitric oxide by increasing intramitochondrial calcium. *Archives of biochemistry and biophysics* **468**(1)**:** 114-120.

Nebert DW, Dalton TP, Okey AB, Gonzalez FJ (2004). Role of aryl hydrocarbon receptor-mediated induction of the CYP1 enzymes in environmental toxicity and cancer. *J Biol Chem* **279**(23)**:** 23847-23850.

Nebert DW, Russell DW (2002). Clinical importance of the cytochromes P450. *Lancet* **360**(9340)**:** 1155-1162.

Nelson DR (2006). Cytochrome P450 nomenclature, 2004. *Methods Mol Biol* **320:** 1-10.

Newbold RR, Liehr JG (2000). Induction of uterine adenocarcinoma in CD-1 mice by catechol estrogens. *Cancer research* **60**(2)**:** 235-237.

Newton AC (2001). Protein kinase C: structural and spatial regulation by phosphorylation, cofactors, and macromolecular interactions. *Chemical reviews* **101**(8)**:** 2353-2364.

Ni L, Zhou C, Duan Q, Lv J, Fu X, Xia Y*, et al.* (2011). beta-AR blockers suppresses ER stress in cardiac hypertrophy and heart failure. *PLoS One* **6**(11)**:** e27294.

Nieves D, Moreno JJ (2006). Hydroxyeicosatetraenoic acids released through the cytochrome P-450 pathway regulate 3T6 fibroblast growth. *Journal of lipid research* **47**(12)**:** 2681-2689.

Nissen SE, Wolski K (2007). Effect of rosiglitazone on the risk of myocardial infarction and death from cardiovascular causes. *The New England journal of medicine* **356**(24)**:** 2457-2471.

Nithipatikom K, Grall AJ, Holmes BB, Harder DR, Falck JR, Campbell WB (2001). Liquid chromatographic-electrospray ionization-mass spectrometric analysis of cytochrome P450 metabolites of arachidonic acid. *Analytical biochemistry* **298**(2)**:** 327-336.

Nithipatikom K, Gross ER, Endsley MP, Moore JM, Isbell MA, Falck JR*, et al.* (2004). Inhibition of cytochrome P450omega-hydroxylase: a novel endogenous cardioprotective pathway. *Circulation research* **95**(8)**:** e65-71.

Node K, Huo Y, Ruan X, Yang B, Spiecker M, Ley K*, et al.* (1999). Anti-inflammatory properties of cytochrome P450 epoxygenase-derived eicosanoids. *Science* **285**(5431)**:** 1276-1279.

Node K, Ruan XL, Dai J, Yang SX, Graham L, Zeldin DC*, et al.* (2001). Activation of Galpha s mediates induction of tissue-type plasminogen activator gene transcription by epoxyeicosatrienoic acids. *The Journal of biological chemistry* **276**(19)**:** 15983-15989.

Nozawa K, Tuck ML, Golub M, Eggena P, Nadler JL, Stern N (1990). Inhibition of lipoxygenase pathway reduces blood pressure in renovascular hypertensive rats. *The American journal of physiology* **259**(6 Pt 2)**:** H1774-1780.

O'Flaherty JT, Rogers LC, Chadwell BA, Owen JS, Rao A, Cramer SD*, et al.* (2002). 5(S)-Hydroxy-6,8,11,14-E,Z,Z,Z-eicosatetraenoate stimulates PC3 cell signaling and growth by a receptor-dependent mechanism. *Cancer research* **62**(23)**:** 6817-6819.

O'Flaherty JT, Wykle RL, Redman J, Samuel M, Thomas M (1986). Metabolism of 5-hydroxyicosatetraenoate by human neutrophils: production of a novel omega-oxidized derivative. *Journal of immunology* **137**(10)**:** 3277-3283.

Obara K, Koide M, Nakayama K (2002). 20-Hydroxyeicosatetraenoic acid potentiates stretch-induced contraction of canine basilar artery via PKC alpha-mediated inhibition of KCa channel. *British journal of pharmacology* **137**(8)**:** 1362-1370.

Octavia Y, Tocchetti CG, Gabrielson KL, Janssens S, Crijns HJ, Moens AL (2012). Doxorubicin-induced cardiomyopathy: from molecular mechanisms to therapeutic strategies. *Journal of molecular and cellular cardiology* **52**(6)**:** 1213-1225.

Okita RT, Okita JR (2001). Cytochrome P450 4A fatty acid omega hydroxylases. *Current drug metabolism* **2**(3)**:** 265-281.

Ottewell PD, Woodward JK, Lefley DV, Evans CA, Coleman RE, Holen I (2009). Anticancer mechanisms of doxorubicin and zoledronic acid in breast cancer tumor growth in bone. *Molecular cancer therapeutics* **8**(10)**:** 2821-2832.

Owan TE, Hodge DO, Herges RM, Jacobsen SJ, Roger VL, Redfield MM (2006). Trends in prevalence and outcome of heart failure with preserved ejection fraction. *The New England journal of medicine* **355**(3)**:** 251-259.

Oyama K, Takahashi K, Sakurai K (2009). Cardiomyocyte H9c2 Cells Exhibit Differential Sensitivity to Intracellular Reactive Oxygen Species Generation with Regard to Their Hypertrophic vs Death Responses to Exogenously Added Hydrogen Peroxide. *Journal of clinical biochemistry and nutrition* **45**(3)**:** 361-369.

Pandey A, Mann M (2000). Proteomics to study genes and genomes. *Nature* **405**(6788)**:** 837-846.

Parmentier JH, Muthalif MM, Saeed AE, Malik KU (2001). Phospholipase D activation by norepinephrine is mediated by 12(s)-, 15(s)-, and 20-hydroxyeicosatetraenoic acids generated by stimulation of cytosolic phospholipase a2. tyrosine phosphorylation of phospholipase d2 in response to norepinephrine. *The Journal of biological chemistry* **276**(19)**:** 15704-15711.

Patricia MK, Kim JA, Harper CM, Shih PT, Berliner JA, Natarajan R*, et al.* (1999). Lipoxygenase products increase monocyte adhesion to human aortic endothelial cells. *Arteriosclerosis, thrombosis, and vascular biology* **19**(11)**:** 2615-2622.

Patten RD, Hall-Porter MR (2009). Small animal models of heart failure: development of novel therapies, past and present. *Circulation. Heart failure* **2**(2)**:** 138-144.

Pearson G, Robinson F, Beers Gibson T, Xu BE, Karandikar M, Berman K*, et al.* (2001). Mitogen-activated protein (MAP) kinase pathways: regulation and physiological functions. *Endocrine reviews* **22**(2)**:** 153-183.

Pertegal M, Fenoy FJ, Bonacasa B, Mendiola J, Delgado JL, Hernandez M*, et al.* (2015). 2-methoxyestradiol plasma levels are associated with clinical severity indices and biomarkers of preeclampsia. *Reproductive sciences* **22**(2)**:** 198-206.

Petit T (2004). [Anthracycline-induced cardiotoxicity]. *Bulletin du cancer* **91 Suppl 3:** 159-165.

Phaneuf S, Leeuwenburgh C (2002). Cytochrome c release from mitochondria in the aging heart: a possible mechanism for apoptosis with age. *American journal of physiology. Regulatory, integrative and comparative physiology* **282**(2)**:** R423-430.

Piao L, Fang YH, Cadete VJ, Wietholt C, Urboniene D, Toth PT*, et al.* (2010). The inhibition of pyruvate dehydrogenase kinase improves impaired cardiac function and electrical remodeling in two models of right ventricular hypertrophy: resuscitating the hibernating right ventricle. *Journal of molecular medicine* **88**(1)**:** 47-60.

Picot D, Loll PJ, Garavito RM (1994). The X-ray crystal structure of the membrane protein prostaglandin H2 synthase-1. *Nature* **367**(6460)**:** 243-249.

Pingili AK, Kara M, Khan NS, Estes AM, Lin Z, Li W*, et al.* (2015). 6beta-hydroxytestosterone, a cytochrome P450 1B1 metabolite of testosterone, contributes to angiotensin II-induced hypertension and its pathogenesis in male mice. *Hypertension* **65**(6)**:** 1279-1287.

Pingili AK, Thirunavukkarasu S, Kara M, Brand DD, Katsurada A, Majid DS*, et al.* (2016). 6beta-Hydroxytestosterone, a Cytochrome P450 1B1-Testosterone-Metabolite, Mediates Angiotensin II-Induced Renal Dysfunction in Male Mice. *Hypertension* **67**(5)**:** 916-926.

Pluim BM, Zwinderman AH, van der Laarse A, van der Wall EE (2000). The athlete's heart. A meta-analysis of cardiac structure and function. *Circulation* **101**(3)**:** 336-344.

Plum SM, Park EJ, Strawn SJ, Moore EG, Sidor CF, Fogler WE (2009). Disease modifying and antiangiogenic activity of 2-methoxyestradiol in a murine model of rheumatoid arthritis. *BMC musculoskeletal disorders* **10:** 46.

Poulos TL (2005). Intermediates in P450 catalysis. *Philos Transact A Math Phys Eng Sci* **363**(1829)**:** 793-806; discussion 1035-1040.

Powell WS, Gravelle F, Gravel S (1992). Metabolism of 5(S)-hydroxy-6,8,11,14-eicosatetraenoic acid and other 5(S)-hydroxyeicosanoids by a specific dehydrogenase in human polymorphonuclear leukocytes. *The Journal of biological chemistry* **267**(27)**:** 19233-19241.

Powell WS, Rokach J (2015). Biosynthesis, biological effects, and receptors of hydroxyeicosatetraenoic acids (HETEs) and oxoeicosatetraenoic acids (oxo-ETEs) derived from arachidonic acid. *Biochimica et biophysica acta* **1851**(4)**:** 340-355.

Prato M, Gallo V, Giribaldi G, Aldieri E, Arese P (2010). Role of the NF-kappaB transcription pathway in the haemozoin- and 15-HETE-mediated activation of matrix metalloproteinase-9 in human adherent monocytes. *Cellular microbiology* **12**(12)**:** 1780-1791.

Prossnitz ER, Arterburn JB, Sklar LA (2007). GPR30: A G protein-coupled receptor for estrogen. *Molecular and cellular endocrinology* **265-266:** 138-142.

Purcell NH, Wilkins BJ, York A, Saba-El-Leil MK, Meloche S, Robbins J*, et al.* (2007). Genetic inhibition of cardiac ERK1/2 promotes stress-induced apoptosis and heart failure but has no effect on hypertrophy in vivo. *Proceedings of the National Academy of Sciences of the United States of America* **104**(35)**:** 14074-14079.

Qi G, Jia L, Li Y, Bian Y, Cheng J, Li H*, et al.* (2011). Angiotensin II infusion-induced inflammation, monocytic fibroblast precursor infiltration, and cardiac fibrosis are pressure dependent. *Cardiovascular toxicology* **11**(2)**:** 157-167.

Quintana LF, Guzman B, Collado S, Claria J, Poch E (2006). A coding polymorphism in the 12-lipoxygenase gene is associated to essential hypertension and urinary 12(S)-HETE. *Kidney international* **69**(3)**:** 526-530.

Rajkumar SV, Richardson PG, Lacy MQ, Dispenzieri A, Greipp PR, Witzig TE*, et al.* (2007). Novel therapy with 2-methoxyestradiol for the treatment of relapsed and plateau phase multiple myeloma. *Clinical cancer research : an official journal of the American Association for Cancer Research* **13**(20)**:** 6162-6167.

Ramana KV, Kohli KK (1998). Gene regulation of cytochrome P450--an overview. *Indian J Exp Biol* **36**(5)**:** 437-446.

Rao GN, Baas AS, Glasgow WC, Eling TE, Runge MS, Alexander RW (1994). Activation of mitogen-activated protein kinases by arachidonic acid and its metabolites in vascular smooth muscle cells. *The Journal of biological chemistry* **269**(51)**:** 32586-32591.

Ravi D, Das KC (2004). Redox-cycling of anthracyclines by thioredoxin system: increased superoxide generation and DNA damage. *Cancer chemotherapy and pharmacology* **54**(5)**:** 449-458.

Reddy MA, Thimmalapura PR, Lanting L, Nadler JL, Fatima S, Natarajan R (2002). The oxidized lipid and lipoxygenase product 12(S)-hydroxyeicosatetraenoic acid induces hypertrophy and fibronectin transcription in vascular smooth muscle cells via p38 MAPK and cAMP response element-binding protein activation. Mediation of angiotensin II effects. *The Journal of biological chemistry* **277**(12)**:** 9920-9928.

Reiser PJ, Portman MA, Ning XH, Schomisch Moravec C (2001). Human cardiac myosin heavy chain isoforms in fetal and failing adult atria and ventricles. *American journal of physiology. Heart and circulatory physiology* **280**(4)**:** H1814-1820.

Revermann M, Mieth A, Popescu L, Paulke A, Wurglics M, Pellowska M*, et al.* (2011). A pirinixic acid derivative (LP105) inhibits murine 5-lipoxygenase activity and attenuates vascular remodelling in a murine model of aortic aneurysm. *British journal of pharmacology* **163**(8)**:** 1721-1732.

Ritter JK, Sheen YY, Owens IS (1990). Cloning and expression of human liver UDP-glucuronosyltransferase in COS-1 cells. 3,4-catechol estrogens and estriol as primary substrates. *The Journal of biological chemistry* **265**(14)**:** 7900-7906.

Robert J, Vrignaud P, Nguyen-Ngoc T, Iliadis A, Mauriac L, Hurteloup P (1985). Comparative pharmacokinetics and metabolism of doxorubicin and epirubicin in patients with metastatic breast cancer. *Cancer treatment reports* **69**(6)**:** 633-640.

Rockman HA, Chien KR, Choi DJ, Iaccarino G, Hunter JJ, Ross J, Jr.*, et al.* (1998). Expression of a beta-adrenergic receptor kinase 1 inhibitor prevents the development of myocardial failure in gene-targeted mice. *Proceedings of the National Academy of Sciences of the United States of America* **95**(12)**:** 7000-7005.

Roger VL (2013). Epidemiology of heart failure. *Circulation research* **113**(6)**:** 646-659.

Roman RJ (2002). P-450 metabolites of arachidonic acid in the control of cardiovascular function. *Physiological reviews* **82**(1)**:** 131-185.

Rothermel BA, McKinsey TA, Vega RB, Nicol RL, Mammen P, Yang J*, et al.* (2001). Myocyte-enriched calcineurin-interacting protein, MCIP1, inhibits cardiac hypertrophy in vivo. *Proceedings of the National Academy of Sciences of the United States of America* **98**(6)**:** 3328-3333.

Sadik CD, Sies H, Schewe T (2003). Inhibition of 15-lipoxygenases by flavonoids: structure-activity relations and mode of action. *Biochemical pharmacology* **65**(5)**:** 773-781.

Sadoshima J, Izumo S (1995). Rapamycin selectively inhibits angiotensin II-induced increase in protein synthesis in cardiac myocytes in vitro. Potential role of 70-kD S6 kinase in angiotensin II-induced cardiac hypertrophy. *Circulation research* **77**(6)**:** 1040-1052.

Sahan-Firat S, Jennings BL, Yaghini FA, Song CY, Estes AM, Fang XR*, et al.* (2010). 2,3',4,5'-Tetramethoxystilbene prevents deoxycorticosterone-salt-induced hypertension: contribution of cytochrome P-450 1B1. *American journal of physiology. Heart and circulatory physiology* **299**(6)**:** H1891-1901.

Saito F, Hori MT, Ideguchi Y, Berger M, Golub M, Stern N*, et al.* (1992). 12-Lipoxygenase products modulate calcium signals in vascular smooth muscle cells. *Hypertension* **20**(2)**:** 138-143.

Sambrook J, Fritsch EF, Maniatatis T (1989). In: Ford, N. (Ed.), Molecular Cloning. A Laboratory Manual. Cold Spring Harbour Laboratory Press, Plainview, NY.

Sasaki M, Hori MT, Hino T, Golub MS, Tuck ML (1997). Elevated 12-lipoxygenase activity in the spontaneously hypertensive rat. *American journal of hypertension* **10**(4 Pt 1)**:** 371-378.

Schinkel AH, Jonker JW (2003). Mammalian drug efflux transporters of the ATP binding cassette (ABC) family: an overview. *Advanced drug delivery reviews* **55**(1)**:** 3-29.

Schlessinger J (2000). Cell signaling by receptor tyrosine kinases. *Cell* **103**(2)**:** 211-225.

Schluter KD, Schreiber D (2005). Adult ventricular cardiomyocytes: isolation and culture. *Methods Mol Biol* **290:** 305-314.

Schmidt JV, Bradfield CA (1996a). Ah receptor signaling pathways. *Annu Rev Cell Dev Biol* **12:** 55-89.

Schmidt JV, Su GH, Reddy JK, Simon MC, Bradfield CA (1996b). Characterization of a murine Ahr null allele: involvement of the Ah receptor in hepatic growth and development. *Proc Natl Acad Sci U S A* **93**(13)**:** 6731-6736.

Schwartzman ML, Balazy M, Masferrer J, Abraham NG, McGiff JC, Murphy RC (1987). 12(R)-hydroxyicosatetraenoic acid: a cytochrome-P450-dependent arachidonate metabolite that inhibits Na+,K+-ATPase in the cornea. *Proceedings of the National Academy of Sciences of the United States of America* **84**(22)**:** 8125-8129.

Schwartzman ML, da Silva JL, Lin F, Nishimura M, Abraham NG (1996). Cytochrome P450 4A expression and arachidonic acid omega-hydroxylation in the kidney of the spontaneously hypertensive rat. *Nephron* **73**(4)**:** 652-663.

Seeger H, Mueck AO, Lippert TH (1997). Effect of estradiol metabolites on the susceptibility of low density lipoprotein to oxidation. *Life sciences* **61**(9)**:** 865-868.

Sehgal N, Kumawat KL, Basu A, Ravindranath V (2012). Fenofibrate reduces mortality and precludes neurological deficits in survivors in murine model of Japanese encephalitis viral infection. *PloS one* **7**(4)**:** e35427.

Serhan CN (2005). Lipoxins and aspirin-triggered 15-epi-lipoxins are the first lipid mediators of endogenous anti-inflammation and resolution. *Prostaglandins, leukotrienes, and essential fatty acids* **73**(3-4)**:** 141-162.

Seubert J, Yang B, Bradbury JA, Graves J, Degraff LM, Gabel S*, et al.* (2004). Enhanced postischemic functional recovery in CYP2J2 transgenic hearts involves mitochondrial ATP-sensitive K+ channels and p42/p44 MAPK pathway. *Circulation research* **95**(5)**:** 506-514.

Shen T, Ma J, Zhang L, Yu X, Liu M, Hou Y*, et al.* (2013). Positive feedback-loop of telomerase reverse transcriptase and 15-lipoxygenase-2 promotes pulmonary hypertension. *PloS one* **8**(12)**:** e83132.

Shimada T, Fujii-Kuriyama Y (2004). Metabolic activation of polycyclic aromatic hydrocarbons to carcinogens by cytochromes P450 1A1 and 1B1. *Cancer Sci* **95**(1)**:** 1-6.

Shimada T, Hayes CL, Yamazaki H, Amin S, Hecht SS, Guengerich FP*, et al.* (1996). Activation of chemically diverse procarcinogens by human cytochrome P-450 1B1. *Cancer research* **56**(13)**:** 2979-2984.

Shimizu I, Minamino T (2016). Physiological and pathological cardiac hypertrophy. *Journal of molecular and cellular cardiology* **97:** 245-262.

Shimizu Y, Nagamine Y, Onuma T (1988). [Calcified chronic subdural hematoma in a young child]. *Neurologia medico-chirurgica* **28**(2)**:** 190-194.

Shioi T, Kang PM, Douglas PS, Hampe J, Yballe CM, Lawitts J*, et al.* (2000). The conserved phosphoinositide 3-kinase pathway determines heart size in mice. *The EMBO journal* **19**(11)**:** 2537-2548.

Shishehbor MH, Zhang R, Medina H, Brennan ML, Brennan DM, Ellis SG*, et al.* (2006). Systemic elevations of free radical oxidation products of arachidonic acid are associated with angiographic evidence of coronary artery disease. *Free radical biology & medicine* **41**(11)**:** 1678-1683.

Shizukuda Y, Matoba S, Mian OY, Nguyen T, Hwang PM (2005). Targeted disruption of p53 attenuates doxorubicin-induced cardiac toxicity in mice. *Molecular and cellular biochemistry* **273**(1-2)**:** 25-32.

Shmueli O, Horn-Saban S, Chalifa-Caspi V, Shmoish M, Ophir R, Benjamin-Rodrig H*, et al.* (2003). GeneNote: whole genome expression profiles in normal human tissues. *Comptes rendus biologies* **326**(10-11)**:** 1067-1072.

Sibonga JD, Lotinun S, Evans GL, Pribluda VS, Green SJ, Turner RT (2003). Dose-response effects of 2-methoxyestradiol on estrogen target tissues in the ovariectomized rat. *Endocrinology* **144**(3)**:** 785-792.

Siddiq T, Richardson PJ, Trotter SE, Preedy VR (1996). Protein synthesis during regression of left ventricular hypertrophy with lisinopril in abdominal aortic constriction model of hypertension. *Biochemical and molecular medicine* **57**(1)**:** 19-24.

Silvestre JS, Robert V, Heymes C, Aupetit-Faisant B, Mouas C, Moalic JM*, et al.* (1998). Myocardial production of aldosterone and corticosterone in the rat. Physiological regulation. *The Journal of biological chemistry* **273**(9)**:** 4883-4891.

Sim SC, Ingelman-Sundberg M (2006). The human cytochrome P450 Allele Nomenclature Committee Web site: submission criteria, procedures, and objectives. *Methods Mol Biol* **320:** 183-191.

Simpson AE (1997). The cytochrome P450 4 (CYP4) family. *General pharmacology* **28**(3)**:** 351-359.

Smith SJ, Towers N, Saldanha JW, Shang CA, Mahmood SR, Taylor WR*, et al.* (2016). The cardiac-restricted protein ADP-ribosylhydrolase-like 1 is essential for heart chamber outgrowth and acts on muscle actin filament assembly. *Developmental biology* **416**(2)**:** 373-388.

Song X, Qian X, Shen M, Jiang R, Wagner MB, Ding G*, et al.* (2015a). Protein kinase C promotes cardiac fibrosis and heart failure by modulating galectin-3 expression. *Biochimica et biophysica acta* **1853**(2)**:** 513-521.

Song YS, Kim MS, Lee DH, Oh DK, Yoon DY (2015b). 15-Hydroxyeicosatetraenoic acid inhibits phorbol-12-myristate-13-Acetate-induced MUC5AC expression in NCI-H292 respiratory epithelial cells. *Journal of microbiology and biotechnology*.

Sopontammarak S, Aliharoob A, Ocampo C, Arcilla RA, Gupta MP, Gupta M (2005). Mitogen-activated protein kinases (p38 and c-Jun NH2-terminal kinase) are differentially regulated during cardiac volume and pressure overload hypertrophy. *Cell biochemistry and biophysics* **43**(1)**:** 61-76.

Souders CA, Bowers SL, Baudino TA (2009). Cardiac fibroblast: the renaissance cell. *Circulation research* **105**(12)**:** 1164-1176.

Spanbroek R, Grabner R, Lotzer K, Hildner M, Urbach A, Ruhling K*, et al.* (2003). Expanding expression of the 5-lipoxygenase pathway within the arterial wall during human atherogenesis. *Proceedings of the National Academy of Sciences of the United States of America* **100**(3)**:** 1238-1243.

Spector AA, Norris AW (2007). Action of epoxyeicosatrienoic acids on cellular function. *American journal of physiology. Cell physiology* **292**(3)**:** C996-1012.

Stenson WF, Parker CW (1979). Metabolism of arachidonic acid in ionophore-stimulated neutrophils. Esterification of a hydroxylated metabolite into phospholipids. *The Journal of clinical investigation* **64**(5)**:** 1457-1465.

Stern N, Golub M, Nozawa K, Berger M, Knoll E, Yanagawa N*, et al.* (1989). Selective inhibition of angiotensin II-mediated vasoconstriction by lipoxygenase blockade. *The American journal of physiology* **257**(2 Pt 2)**:** H434-443.

Stern N, Kisch ES, Knoll E (1996). Platelet lipoxygenase in spontaneously hypertensive rats. *Hypertension* **27**(5)**:** 1149-1152.

Stoltz RA, Abraham NG, Laniado-Schwartzman M (1996). The role of NF-kappaB in the angiogenic response of coronary microvessel endothelial cells. *Proceedings of the National Academy of Sciences of the United States of America* **93**(7)**:** 2832-2837.

Su T, Ding X (2004). Regulation of the cytochrome P450 2A genes. *Toxicology and applied pharmacology* **199**(3)**:** 285-294.

Sueyoshi T, Kawamoto T, Zelko I, Honkakoski P, Negishi M (1999). The repressed nuclear receptor CAR responds to phenobarbital in activating the human CYP2B6 gene. *The Journal of biological chemistry* **274**(10)**:** 6043-6046.

Sutter TR, Tang YM, Hayes CL, Wo YY, Jabs EW, Li X*, et al.* (1994). Complete cDNA sequence of a human dioxin-inducible mRNA identifies a new gene subfamily of cytochrome P450 that maps to chromosome 2. *The Journal of biological chemistry* **269**(18)**:** 13092-13099.

Suzuki H, Kayama Y, Sakamoto M, Iuchi H, Shimizu I, Yoshino T*, et al.* (2015). Arachidonate 12/15-lipoxygenase-induced inflammation and oxidative stress are involved in the development of diabetic cardiomyopathy. *Diabetes* **64**(2)**:** 618-630.

Sweeney C, Liu G, Yiannoutsos C, Kolesar J, Horvath D, Staab MJ*, et al.* (2005). A phase II multicenter, randomized, double-blind, safety trial assessing the pharmacokinetics, pharmacodynamics, and efficacy of oral 2-methoxyestradiol capsules in hormone-refractory prostate cancer. *Clinical cancer research : an official journal of the American Association for Cancer Research* **11**(18)**:** 6625-6633.

Swift LP, Cutts SM, Nudelman A, Levovich I, Rephaeli A, Phillips DR (2008). The cardio-protecting agent and topoisomerase II catalytic inhibitor sobuzoxane enhances doxorubicin-DNA adduct mediated cytotoxicity. *Cancer chemotherapy and pharmacology* **61**(5)**:** 739-749.

Szekeres CK, Tang K, Trikha M, Honn KV (2000). Eicosanoid activation of extracellular signal-regulated kinase1/2 in human epidermoid carcinoma cells. *The Journal of biological chemistry* **275**(49)**:** 38831-38841.

Tacconelli S, Patrignani P (2014). Inside epoxyeicosatrienoic acids and cardiovascular disease. *Frontiers in pharmacology* **5:** 239.

Tak PP, Firestein GS (2001). NF-kappaB: a key role in inflammatory diseases. *The Journal of clinical investigation* **107**(1)**:** 7-11.

Takai S, Jin D, Kirimura K, Fujimoto Y, Miyazaki M (2001). 12-Hydroxyeicosatetraenoic acid potentiates angiotensin II-induced pressor response in rats. *European journal of pharmacology* **418**(1-2)**:** R1-2.

Takemura G, Fujiwara H (2007). Doxorubicin-induced cardiomyopathy from the cardiotoxic mechanisms to management. *Progress in cardiovascular diseases* **49**(5)**:** 330-352.

Takewaki S, Kuro-o M, Hiroi Y, Yamazaki T, Noguchi T, Miyagishi A*, et al.* (1995). Activation of Na(+)-H+ antiporter (NHE-1) gene expression during growth, hypertrophy and proliferation of the rabbit cardiovascular system. *Journal of molecular and cellular cardiology* **27**(1)**:** 729-742.

Tan C, Tasaka H, Yu KP, Murphy ML, Karnofsky DA (1967). Daunomycin, an antitumor antibiotic, in the treatment of neoplastic disease. Clinical evaluation with special reference to childhood leukemia. *Cancer* **20**(3)**:** 333-353.

Tanaka K, Honda M, Takabatake T (2001). Redox regulation of MAPK pathways and cardiac hypertrophy in adult rat cardiac myocyte. *Journal of the American College of Cardiology* **37**(2)**:** 676-685.

Tang DG, Renaud C, Stojakovic S, Diglio CA, Porter A, Honn KV (1995). 12(S)-HETE is a mitogenic factor for microvascular endothelial cells: its potential role in angiogenesis. *Biochemical and biophysical research communications* **211**(2)**:** 462-468.

Tang Y, Scheef EA, Wang S, Sorenson CM, Marcus CB, Jefcoate CR*, et al.* (2009). CYP1B1 expression promotes the proangiogenic phenotype of endothelium through decreased intracellular oxidative stress and thrombospondin-2 expression. *Blood* **113**(3)**:** 744-754.

Taniyama Y, Walsh K (2002). Elevated myocardial Akt signaling ameliorates doxorubicin-induced congestive heart failure and promotes heart growth. *Journal of molecular and cellular cardiology* **34**(10)**:** 1241-1247.

Tebbi CK, London WB, Friedman D, Villaluna D, De Alarcon PA, Constine LS*, et al.* (2007). Dexrazoxane-associated risk for acute myeloid leukemia/myelodysplastic syndrome and other secondary malignancies in pediatric Hodgkin's disease. *Journal of clinical oncology : official journal of the American Society of Clinical Oncology* **25**(5)**:** 493-500.

Tejera N, Boeglin WE, Suzuki T, Schneider C (2012). COX-2-dependent and -independent biosynthesis of dihydroxy-arachidonic acids in activated human leukocytes. *Journal of lipid research* **53**(1)**:** 87-94.

Testa M, Yeh M, Lee P, Fanelli R, Loperfido F, Berman JW*, et al.* (1996). Circulating levels of cytokines and their endogenous modulators in patients with mild to severe congestive heart failure due to coronary artery disease or hypertension. *Journal of the American College of Cardiology* **28**(4)**:** 964-971.

Tevaarwerk AJ, Holen KD, Alberti DB, Sidor C, Arnott J, Quon C*, et al.* (2009). Phase I trial of 2-methoxyestradiol NanoCrystal dispersion in advanced solid malignancies. *Clinical cancer research : an official journal of the American Association for Cancer Research* **15**(4)**:** 1460-1465.

Theken KN, Deng Y, Kannon MA, Miller TM, Poloyac SM, Lee CR (2011). Activation of the acute inflammatory response alters cytochrome P450 expression and eicosanoid metabolism. *Drug metabolism and disposition: the biological fate of chemicals* **39**(1)**:** 22-29.

Thomas CP, Morgan LT, Maskrey BH, Murphy RC, Kuhn H, Hazen SL*, et al.* (2010). Phospholipid-esterified eicosanoids are generated in agonist-activated human platelets and enhance tissue factor-dependent thrombin generation. *The Journal of biological chemistry* **285**(10)**:** 6891-6903.

Thorburn J, McMahon M, Thorburn A (1994). Raf-1 kinase activity is necessary and sufficient for gene expression changes but not sufficient for cellular morphology changes associated with cardiac myocyte hypertrophy. *The Journal of biological chemistry* **269**(48)**:** 30580-30586.

Thorn CF, Oshiro C, Marsh S, Hernandez-Boussard T, McLeod H, Klein TE*, et al.* (2011). Doxorubicin pathways: pharmacodynamics and adverse effects. *Pharmacogenetics and genomics* **21**(7)**:** 440-446.

Thum T, Borlak J (2000a). Cytochrome P450 mono-oxygenase gene expression and protein activity in cultures of adult cardiomyocytes of the rat. *British journal of pharmacology* **130**(8)**:** 1745-1752.

Thum T, Borlak J (2000b). Gene expression in distinct regions of the heart. *Lancet* **355**(9208)**:** 979-983.

Thum T, Borlak J (2002). Testosterone, cytochrome P450, and cardiac hypertrophy. *FASEB journal : official publication of the Federation of American Societies for Experimental Biology* **16**(12)**:** 1537-1549.

Tofovic SP, Dubey RK, Jackson EK (2001). 2-Hydroxyestradiol attenuates the development of obesity, the metabolic syndrome, and vascular and renal dysfunction in obese ZSF1 rats. *The Journal of pharmacology and experimental therapeutics* **299**(3)**:** 973-977.

Tofovic SP, Jones TJ, Bilan VP, Jackson EK, Petrusevska G (2010). Synergistic therapeutic effects of 2-methoxyestradiol with either sildenafil or bosentan on amelioration of monocrotaline-induced pulmonary hypertension and vascular remodeling. *Journal of cardiovascular pharmacology* **56**(5)**:** 475-483.

Tran DT, Ohinmaa A, Thanh NX, Howlett JG, Ezekowitz JA, McAlister FA*, et al.* (2016). The current and future financial burden of hospital admissions for heart failure in Canada: a cost analysis. *CMAJ open* **4**(3)**:** E365-E370.

Tse MM, Aboutabl ME, Althurwi HN, Elshenawy OH, Abdelhamid G, El-Kadi AO (2013). Cytochrome P450 epoxygenase metabolite, 14,15-EET, protects against isoproterenol-induced cellular hypertrophy in H9c2 rat cell line. *Vascular pharmacology* **58**(5-6)**:** 363-373.

Tsuchiya Y, Nakajima M, Takagi S, Taniya T, Yokoi T (2006). MicroRNA regulates the expression of human cytochrome P450 1B1. *Cancer research* **66**(18)**:** 9090-9098.

Ueda A, Hamadeh HK, Webb HK, Yamamoto Y, Sueyoshi T, Afshari CA*, et al.* (2002). Diverse roles of the nuclear orphan receptor CAR in regulating hepatic genes in response to phenobarbital. *Molecular pharmacology* **61**(1)**:** 1-6.

Vakili BA, Okin PM, Devereux RB (2001). Prognostic implications of left ventricular hypertrophy. *American heart journal* **141**(3)**:** 334-341.

van Acker SA, Kramer K, Voest EE, Grimbergen JA, Zhang J, van der Vijgh WJ*, et al.* (1996). Doxorubicin-induced cardiotoxicity monitored by ECG in freely moving mice. A new model to test potential protectors. *Cancer chemotherapy and pharmacology* **38**(1)**:** 95-101.

van Empel VP, Bertrand AT, Hofstra L, Crijns HJ, Doevendans PA, De Windt LJ (2005). Myocyte apoptosis in heart failure. *Cardiovascular research* **67**(1)**:** 21-29.

Vanezis A, Thaitirarot C, Butt M, Squire I, Samani N, Rodrigo G (2014). 208 The PKC Epsilon/AMPK ALPHA/ENOS Pathway is Implicated as a Mechanism by which Remote Ischaemic Conditioning Attenuates Endothelin-1 Mediated Cardiomyocyte Hypertrophy. *Heart* **100 Suppl 3:** A114.

Varga ZV, Ferdinandy P, Liaudet L, Pacher P (2015). Drug-induced mitochondrial dysfunction and cardiotoxicity. *American journal of physiology. Heart and circulatory physiology* **309**(9)**:** H1453-1467.

Vasile VC, Edwards WD, Ommen SR, Ackerman MJ (2006). Obstructive hypertrophic cardiomyopathy is associated with reduced expression of vinculin in the intercalated disc. *Biochemical and biophysical research communications* **349**(2)**:** 709-715.

Vasiliou V, Gonzalez FJ (2008). Role of CYP1B1 in glaucoma. *Annual review of pharmacology and toxicology* **48:** 333-358.

Verenich S, Gerk PM (2010). Therapeutic promises of 2-methoxyestradiol and its drug disposition challenges. *Molecular pharmaceutics* **7**(6)**:** 2030-2039.

Vieira I, Sonnier M, Cresteil T (1996). Developmental expression of CYP2E1 in the human liver. Hypermethylation control of gene expression during the neonatal period. *European journal of biochemistry* **238**(2)**:** 476-483.

Volkova M, Palmeri M, Russell KS, Russell RR (2011). Activation of the aryl hydrocarbon receptor by doxorubicin mediates cytoprotective effects in the heart. *Cardiovascular research* **90**(2)**:** 305-314.

Vonach C, Viola K, Giessrigl B, Huttary N, Raab I, Kalt R*, et al.* (2011). NF-kappaB mediates the 12(S)-HETE-induced endothelial to mesenchymal transition of lymphendothelial cells during the intravasation of breast carcinoma cells. *British journal of cancer* **105**(2)**:** 263-271.

Wahli W, Braissant O, Desvergne B (1995). Peroxisome proliferator activated receptors: transcriptional regulators of adipogenesis, lipid metabolism and more. *Chemistry & biology* **2**(5)**:** 261-266.

Walisser JA, Glover E, Pande K, Liss AL, Bradfield CA (2005). Aryl hydrocarbon receptor-dependent liver development and hepatotoxicity are mediated by different cell types. *Proc Natl Acad Sci U S A* **102**(49)**:** 17858-17863.

Wallukat G, Morwinski R, Kuhn H (1994). Modulation of the beta-adrenergic response of cardiomyocytes by specific lipoxygenase products involves their incorporation into phosphatidylinositol and activation of protein kinase C. *The Journal of biological chemistry* **269**(46)**:** 29055-29060.

Wang AW, Song L, Miao J, Wang HX, Tian C, Jiang X*, et al.* (2015). Baicalein Attenuates Angiotensin II-Induced Cardiac Remodeling via Inhibition of AKT/mTOR, ERK1/2, NF-kappaB, and Calcineurin Signaling Pathways in Mice. *American journal of hypertension* **28**(4)**:** 518-526.

Wang B, Zhou SF (2009). Synthetic and natural compounds that interact with human cytochrome P450 1A2 and implications in drug development. *Current medicinal chemistry* **16**(31)**:** 4066-4218.

Wang G, Li W, Lu X, Bao P, Zhao X (2012). Luteolin ameliorates cardiac failure in type I diabetic cardiomyopathy. *Journal of diabetes and its complications* **26**(4)**:** 259-265.

Wang MH, Zhang F, Marji J, Zand BA, Nasjletti A, Laniado-Schwartzman M (2001). CYP4A1 antisense oligonucleotide reduces mesenteric vascular reactivity and blood pressure in SHR. *American journal of physiology. Regulatory, integrative and comparative physiology* **280**(1)**:** R255-261.

Wang X, Ni L, Yang L, Duan Q, Chen C, Edin ML*, et al.* (2014). CYP2J2-derived epoxyeicosatrienoic acids suppress endoplasmic reticulum stress in heart failure. *Molecular pharmacology* **85**(1)**:** 105-115.

Wang Y, Lyu YL, Wang JC (2002). Dual localization of human DNA topoisomerase IIIalpha to mitochondria and nucleus. *Proceedings of the National Academy of Sciences of the United States of America* **99**(19)**:** 12114-12119.

Wassmann S, Laufs U, Baumer AT, Muller K, Konkol C, Sauer H*, et al.* (2001). Inhibition of geranylgeranylation reduces angiotensin II-mediated free radical production in vascular smooth muscle cells: involvement of angiotensin AT1 receptor expression and Rac1 GTPase. *Molecular pharmacology* **59**(3)**:** 646-654.

Watanabe T, Medina JF, Haeggstrom JZ, Radmark O, Samuelsson B (1993). Molecular cloning of a 12-lipoxygenase cDNA from rat brain. *European journal of biochemistry / FEBS* **212**(2)**:** 605-612.

Weiss RB (1992). The anthracyclines: will we ever find a better doxorubicin? *Seminars in oncology* **19**(6)**:** 670-686.

Welch WJ (2008). Angiotensin II-dependent superoxide: effects on hypertension and vascular dysfunction. *Hypertension* **52**(1)**:** 51-56.

Wen Y, Gu J, Liu Y, Wang PH, Sun Y, Nadler JL (2001). Overexpression of 12-lipoxygenase causes cardiac fibroblast cell growth. *Circulation research* **88**(1)**:** 70-76.

Wen Y, Gu J, Peng X, Zhang G, Nadler J (2003). Overexpression of 12-lipoxygenase and cardiac fibroblast hypertrophy. *Trends in cardiovascular medicine* **13**(4)**:** 129-136.

Wetsel WC, Khan WA, Merchenthaler I, Rivera H, Halpern AE, Phung HM*, et al.* (1992). Tissue and cellular distribution of the extended family of protein kinase C isoenzymes. *The Journal of cell biology* **117**(1)**:** 121-133.

Whitelaw ML, Gottlicher M, Gustafsson JA, Poellinger L (1993). Definition of a novel ligand binding domain of a nuclear bHLH receptor: co-localization of ligand and hsp90 binding activities within the regulable inactivation domain of the dioxin receptor. *Embo J* **12**(11)**:** 4169-4179.

Whitelaw ML, Gustafsson JA, Poellinger L (1994). Identification of transactivation and repression functions of the dioxin receptor and its basic helix-loop-helix/PAS partner factor Arnt: inducible versus constitutive modes of regulation. *Mol Cell Biol* **14**(12)**:** 8343-8355.

Wong SC, Fukuchi M, Melnyk P, Rodger I, Giaid A (1998). Induction of cyclooxygenase-2 and activation of nuclear factor-kappaB in myocardium of patients with congestive heart failure. *Circulation* **98**(2)**:** 100-103.

Wu CC, Cheng J, Zhang FF, Gotlinger KH, Kelkar M, Zhang Y*, et al.* (2011a). Androgen-dependent hypertension is mediated by 20-hydroxy-5,8,11,14-eicosatetraenoic acid-induced vascular dysfunction: role of inhibitor of kappaB Kinase. *Hypertension* **57**(4)**:** 788-794.

Wu CC, Schwartzman ML (2011b). The role of 20-HETE in androgen-mediated hypertension. *Prostaglandins & other lipid mediators* **96**(1-4)**:** 45-53.

Xie HJ, Yasar U, Lundgren S, Griskevicius L, Terelius Y, Hassan M*, et al.* (2003). Role of polymorphic human CYP2B6 in cyclophosphamide bioactivation. *The pharmacogenomics journal* **3**(1)**:** 53-61.

Xie Z, Kometiani P, Liu J, Li J, Shapiro JI, Askari A (1999). Intracellular reactive oxygen species mediate the linkage of Na+/K+-ATPase to hypertrophy and its marker genes in cardiac myocytes. *The Journal of biological chemistry* **274**(27)**:** 19323-19328.

Xu D, Li N, He Y, Timofeyev V, Lu L, Tsai HJ*, et al.* (2006). Prevention and reversal of cardiac hypertrophy by soluble epoxide hydrolase inhibitors. *Proceedings of the National Academy of Sciences of the United States of America* **103**(49)**:** 18733-18738.

Xu X, Persson HL, Richardson DR (2005). Molecular pharmacology of the interaction of anthracyclines with iron. *Molecular pharmacology* **68**(2)**:** 261-271.

Xu ZG, Yuan H, Lanting L, Li SL, Wang M, Shanmugam N*, et al.* (2008). Products of 12/15-lipoxygenase upregulate the angiotensin II receptor. *Journal of the American Society of Nephrology : JASN* **19**(3)**:** 559-569.

Yaghini FA, Li F, Malik KU (2007). Expression and mechanism of spleen tyrosine kinase activation by angiotensin II and its implication in protein synthesis in rat vascular smooth muscle cells. *The Journal of biological chemistry* **282**(23)**:** 16878-16890.

Yamamoto S (1992). Mammalian lipoxygenases: molecular structures and functions. *Biochimica et biophysica acta* **1128**(2-3)**:** 117-131.

Yan L, Huang H, Tang QZ, Zhu LH, Wang L, Liu C*, et al.* (2010). Breviscapine protects against cardiac hypertrophy through blocking PKC-alpha-dependent signaling. *Journal of cellular biochemistry* **109**(6)**:** 1158-1171.

Yang F, Teves SS, Kemp CJ, Henikoff S (2014a). Doxorubicin, DNA torsion, and chromatin dynamics. *Biochimica et biophysica acta* **1845**(1)**:** 84-89.

Yang H, Wang H (2014b). Signaling control of the constitutive androstane receptor (CAR). *Protein & cell* **5**(2)**:** 113-123.

Yasumoto A, Tokuoka SM, Kita Y, Shimizu T, Yatomi Y (2017). Multiplex quantitative analysis of eicosanoid mediators in human plasma and serum: Possible introduction into clinical testing. *Journal of chromatography. B, Analytical technologies in the biomedical and life sciences* **1068-1069:** 98-104.

Yen HC, Oberley TD, Vichitbandha S, Ho YS, St Clair DK (1996). The protective role of manganese superoxide dismutase against adriamycin-induced acute cardiac toxicity in transgenic mice. *The Journal of clinical investigation* **98**(5)**:** 1253-1260.

Yiu SS, Zhao X, Inscho EW, Imig JD (2003). 12-Hydroxyeicosatetraenoic acid participates in angiotensin II afferent arteriolar vasoconstriction by activating L-type calcium channels. *Journal of lipid research* **44**(12)**:** 2391-2399.

Yokoyama C, Shinjo F, Yoshimoto T, Yamamoto S, Oates JA, Brash AR (1986). Arachidonate 12-lipoxygenase purified from porcine leukocytes by immunoaffinity chromatography and its reactivity with hydroperoxyeicosatetraenoic acids. *The Journal of biological chemistry* **261**(35)**:** 16714-16721.

Yorifuji T, Uchida T, Abe H, Toyofuku Y, Tamaki M, Fujitani Y*, et al.* (2011). 2-Methoxyestradiol ameliorates glucose tolerance with the increase in beta-cell mass in db/db mice. *Journal of diabetes investigation* **2**(3)**:** 180-185.

Yoshida H, Karmazyn M (2000). Na(+)/H(+) exchange inhibition attenuates hypertrophy and heart failure in 1-wk postinfarction rat myocardium. *American journal of physiology. Heart and circulatory physiology* **278**(1)**:** H300-304.

Yoshida M, Shiojima I, Ikeda H, Komuro I (2009). Chronic doxorubicin cardiotoxicity is mediated by oxidative DNA damage-ATM-p53-apoptosis pathway and attenuated by pitavastatin through the inhibition of Rac1 activity. *Journal of molecular and cellular cardiology* **47**(5)**:** 698-705.

Yousif MH, Benter IF, Roman RJ (2009). Cytochrome P450 metabolites of arachidonic acid play a role in the enhanced cardiac dysfunction in diabetic rats following ischaemic reperfusion injury. *Autonomic & autacoid pharmacology* **29**(1-2)**:** 33-41.

Yu AM, Tian Y, Tu MJ, Ho PY, Jilek JL (2016). MicroRNA Pharmacoepigenetics: Posttranscriptional Regulation Mechanisms behind Variable Drug Disposition and Strategy to Develop More Effective Therapy. *Drug metabolism and disposition: the biological fate of chemicals* **44**(3)**:** 308-319.

Yu S, Reddy JK (2007). Transcription coactivators for peroxisome proliferator-activated receptors. *Biochimica et biophysica acta* **1771**(8)**:** 936-951.

Yu Z, Xu F, Huse LM, Morisseau C, Draper AJ, Newman JW*, et al.* (2000). Soluble epoxide hydrolase regulates hydrolysis of vasoactive epoxyeicosatrienoic acids. *Circulation research* **87**(11)**:** 992-998.

Yuan W, Yu Y, Li J, Singh P, Li D, Gui Y*, et al.* (2013). Estrogen metabolite 2-methoxyestradiol prevents hypertension in deoxycorticosterone acetate-salt rats. *Cardiovascular drugs and therapy / sponsored by the International Society of Cardiovascular Pharmacotherapy* **27**(1)**:** 17-22.

Yue TL, Bao W, Jucker BM, Gu JL, Romanic AM, Brown PJ*, et al.* (2003). Activation of peroxisome proliferator-activated receptor-alpha protects the heart from ischemia/reperfusion injury. *Circulation* **108**(19)**:** 2393-2399.

Zhang L, Li Y, Chen M, Su X, Yi D, Lu P*, et al.* (2014). 15-LO/15-HETE mediated vascular adventitia fibrosis via p38 MAPK-dependent TGF-beta. *Journal of cellular physiology* **229**(2)**:** 245-257.

Zhang S, Liu X, Bawa-Khalfe T, Lu LS, Lyu YL, Liu LF*, et al.* (2012a). Identification of the molecular basis of doxorubicin-induced cardiotoxicity. *Nature medicine* **18**(11)**:** 1639-1642.

Zhang W, Elimban V, Nijjar MS, Gupta SK, Dhalla NS (2003). Role of mitogen-activated protein kinase in cardiac hypertrophy and heart failure. *Experimental and clinical cardiology* **8**(4)**:** 173-183.

Zhang Y, Cao Y, Duan H, Wang H, He L (2012b). Imperatorin prevents cardiac hypertrophy and the transition to heart failure via NO-dependent mechanisms in mice. *Fitoterapia* **83**(1)**:** 60-66.

Zhang Y, El-Sikhry H, Chaudhary KR, Batchu SN, Shayeganpour A, Jukar TO*, et al.* (2009a). Overexpression of CYP2J2 provides protection against doxorubicin-induced cardiotoxicity. *American journal of physiology. Heart and circulatory physiology* **297**(1)**:** H37-46.

Zhang Y, Nuglozeh E, Toure F, Schmidt AM, Vunjak-Novakovic G (2009b). Controllable expansion of primary cardiomyocytes by reversible immortalization. *Human gene therapy* **20**(12)**:** 1687-1696.

Zhao Y, Sorenson CM, Sheibani N (2015). Cytochrome P450 1B1 and Primary Congenital Glaucoma. *Journal of ophthalmic & vision research* **10**(1)**:** 60-67.

Zhou S, Starkov A, Froberg MK, Leino RL, Wallace KB (2001). Cumulative and irreversible cardiac mitochondrial dysfunction induced by doxorubicin. *Cancer research* **61**(2)**:** 771-777.

Zhu BT, Conney AH (1998). Functional role of estrogen metabolism in target cells: review and perspectives. *Carcinogenesis* **19**(1)**:** 1-27.

Zhu W, Shou W, Payne RM, Caldwell R, Field LJ (2008). A mouse model for juvenile doxorubicin-induced cardiac dysfunction. *Pediatric research* **64**(5)**:** 488-494.

Zong J, Zhang DP, Zhou H, Bian ZY, Deng W, Dai J*, et al.* (2013). Baicalein protects against cardiac hypertrophy through blocking MEK-ERK1/2 signaling. *Journal of cellular biochemistry* **114**(5)**:** 1058-1065.

Zordoky BN, Aboutabl ME, El-Kadi AO (2008). Modulation of cytochrome P450 gene expression and arachidonic acid metabolism during isoproterenol-induced cardiac hypertrophy in rats. *Drug metabolism and disposition: the biological fate of chemicals* **36**(11)**:** 2277-2286.

Zordoky BN, Anwar-Mohamed A, Aboutabl ME, El-Kadi AO (2010a). Acute doxorubicin cardiotoxicity alters cardiac cytochrome P450 expression and arachidonic acid metabolism in rats. *Toxicology and applied pharmacology* **242**(1)**:** 38-46.

Zordoky BN, El-Kadi AO (2010b). 2,3,7,8-Tetrachlorodibenzo-p-dioxin and beta-naphthoflavone induce cellular hypertrophy in H9c2 cells by an aryl hydrocarbon receptor-dependant mechanism. *Toxicology in vitro : an international journal published in association with BIBRA* **24**(3)**:** 863-871.

Zordoky BN, El-Kadi AO (2010c). Effect of cytochrome P450 polymorphism on arachidonic acid metabolism and their impact on cardiovascular diseases. *Pharmacology & therapeutics* **125**(3)**:** 446-463.

Zou J, Le K, Xu S, Chen J, Liu Z, Chao X*, et al.* (2013). Fenofibrate ameliorates cardiac hypertrophy by activation of peroxisome proliferator-activated receptor-alpha partly via preventing p65-NFkappaB binding to NFATc4. *Molecular and cellular endocrinology* **370**(1-2)**:** 103-112.